UNIVERSITÉ D'ORLÉANS

SANTE, SCIENCES BIOLOGIQUES ET CHIMIE DU VIVANT

Centre de Biophysique Moléculaire (CBM, UPR 4301)

Equipe Biologie Cellulaire, Cibles Moléculaires et Thérapies Innovantes

THÈSE présentée par :

Pinpin WANG

Soutenue le : **20 février 2020**

Pour obtenir le grade de : **Docteur de l'Université d'Orléans**

Discipline/ Spécialité : Biologie Moléculaire, Thérapie génique

Evaluation de l'activité de NS1, une protéine non structurale dérivée du virus de l'influenza A pour une traduction améliorée de l'ARNm de BMP2 pour la régénération osseuse

Evaluation of Influenza A derived nonstructural protein NS1 to enhance BMP2 mRNA translation for bone regeneration

THÈSE DIRIGÉE PAR :

PICHON Chantal	Professeure, Université d'Orléans

RAPPORTEURS :

GUICHEUX Jérôme	Directeur de Recherches INSERM, Université De Nantes
MONTIER Tristan	Professeur-Praticien Hospitalier, Université de Bretagne

---

JURY :

PICHON Chantal	Professeure, Université d'Orléans
GUICHEUX Jérôme	Directeur de Recherches INSERM, Université De Nantes
MONTIER Tristan	Professeur-Praticien Hospitalier, Université de Bretagne
ROCHET Nathalie	Chargé de recherche, Université Côte d'Azur
PERCHE Fédérico	Chargé de recherche CNRS, Center de Biophysique Moléculaire
COUILLIN Isabelle	Directrice de Recherches CNRS, Université d'Orléans

PRÉSIDENT DU JURY :

COUILLIN Isabelle Directrice de Recherches CNRS, Université d'Orléans

Contents

Acknowledgment

Three years ago, Prof. Chantal Pichon provided me the chance to join her team. From then on, my life turned to a new page. The time in France is precious to me. I explored deeper self-awareness and self-motivation as never before! I am very grateful to all the people who have helped me, directly or indirectly, during the past three years.

I express my sincere thanks and gratitude to my major supervisor Dr. Chantal Pichon and my co-supervisor Dr. Federico Perche, for their constant guidance and advice, which were vital for the completion of the thesis. They have been patient and kind all the way along, and I thank them for everything. I am very delighted to be a part of the “Biologie Cellulaire, Cibles Moléculaires et Thérapies Innovantes” team. It has been a massive learning experience.

I am very grateful for the financial support from the China Scholarship Council (CSC) that has helped me pursue my degree abroad.

Without the contributions of our close collaborators, much of the work in this thesis would not have been possible. Thank you to Dr. Delphine Logeart-Avramoglou (Université de Paris, CNRS, INSERM, B3OA) for providing cells, collecting and interpreting radiography and histology results. Thank you to Dr. Kyle K.L. Phua (National University of Singapore) for providing NS1 gene, and to Dr. Ilídio J. Correiad and Catia S.D. Cabrald (Universidade da Beira Interior) for performing mechanical tests of various scaffolds.

I thank all the members in Dr. Pichon’s lab: Dr. Patrick Midoux, Dr. Patrick Baril, Dr. Anthony Delalande, Fatma Elleuch, Elodie Henriet, Vinodini Vijayarangan, Caroline Girardin, Dr. Cristine Goncalvez, Virginie Malard, Yoan Laurent, Amandine Suet, Delphine Maze. Everyone has been very encouraging, supportive. It has been a pleasure working with them.

I also thank Dr. Jérôme Guicheux, Dr. Tristan Montier, Dr. Nathalie Rochet and Dr. Isabelle Couillin for their time and effort while serving on my thesis defense committee.

I give my thanks to Hao Li, FengFeng Zhang, Qian Li, YanGang Ren, Min Cai, ChaoYang Xue. I have always enjoyed the company of these friends and shall always remember the good times that we all have spent together.

My wife YuXiao Li deserves a special mention here. Without her love, support and encouragement all throughout my study, I will not go through the hard times. Thank you, my love!

My parents, my brother, my sister in law, my cute nieces, thank you for your invaluable support and prayer! Each message, phone call from you warm my heart and give me strength!

Despite my best intentions, I know that I am unable to acknowledge all the people who made this thesis possible. For those mentioned above, and for all those who should have been mentioned, I offer another sincere THANK YOU! Thank you for your company!

List of Abbreviations

BTE: Bone tissue engineering

B18R: Soluble interferon α/β receptor B18

BMP2: Bone Morphogenetic Protein 2

NS1: Non-structural protein 1

IAV: Influenza A virus

IVT: In vitro transcription

TLR: Toll-like receptor

IFN: Interferon

PKR: Interferon-induced, double-stranded RNA-dependent protein kinase PKR

RIG-1: Retinoic acid-inducible gene I

OAS1: 2'-5'-oligoadenylate synthetase 1

IFIT1: Interferon-induced protein with tetratricopeptide repeats 1

rhBMP2: Recombinant human BMP-2

ALP: Alkaline phosphatase

Runx2: Runt-related transcription factor 2

Coll1α1: Collagen type 1 alpha chain 1

OCN: Osteocalcin

OPN: Osteopontin

GFP: Enhanced green fluorescence protein

Fluc: Firefly luciferase

Gluc: Gaussia luciferase

ARS: Alizarin red S

CPC: cetylpyridinium chloride

UTR: Untranslated region

ORF: Open reading frame

Ψ: pseudouridine

cmRNA: Chemical modified mRNA

BRE: BMP-2 response element

LFM: LipofectamineTM MessengerMax

β-GP: beta-glycerophosphate

As2P: ascorbic acid-2-phosphate

MSC: Mesenchymal stem cell

LPR: lipopolyplex

RAM: RNA-activated matrix

GAM: gene-activated matrix

Lip100: imidazole/imidazolium binary liposome

His-lPEI: histidylated linear polyethyleneimine

CoLL-nHA: collagen-nanohydroxyapatite scaffold

VEGF: Vascular endothelial growth factor

VEE: Venezuelan equine encephalitis

RepRNA: Self-replicating mRNA

Smurf: Smad-specific E3 ubiquitin ligase

NF-kB: Nuclear factor kappa B

TNF: Tumor necrosis factor

List of Figures and Tables

Figures and Tables in part I: Review of the Literature

Figures and Tables in Part II: Influenza A derived NS1 enhances *in vitro* transcribed BMP-2 mRNA translation in multipotent stem cells leading to an improved osteogenic differentiation

Figures and Tables in Part III: BMP2 mRNA and NS1 mRNA activated collagen-hydroxyapatite matrix for bone regeneration

Figures in Part IV: Conclusions and perspectives

Introduction of the PhD Thesis

1. Project hypothesis

These last years, there is an increasing interest in the use of *in vitro* transcribed (IVT) mRNA for bone regeneration as novel therapeutic modality (Elangovan, Khorsand et al. 2015); (Balmayor, Geiger et al. 2016). However, although IVT mRNAs allow *in situ* expression of protein in native state, it triggers an immune response resulting in its translation inhibition and degradation (Kariko, Ni et al. 2004). This is due to the presence of RNA sensors that can detect the presence of exogenous RNA including mRNA inside the cytosol as part of the immune system. In addition, the inflammation associated with this immune response could be suboptimal for bone formation (Osta, Benedetti et al. 2014). Accordingly, a successful application of IVT mRNA for bone regeneration should modulate such responses to maximize protein expression and improve osteogenic commitment of osteoprogenitors (e.g. mesenchymal stem cells).

To date, IVT mRNA can be produced with modified nucleosides to evade the RNA sensors recognition (Kariko, Buckstein et al. 2005). The limitation of this strategy is not only its high cost but also the need of a large screening to identify the right modified nucleosides; hence there is a dependency as function of cell types and RNA sequences (Uchida, Kataoka et al. 2015).

RNA viruses have evolved sophisticated strategies to avoid the activation of RNA sensors in the cells during the infection (Alcami and Koszinowski 2000). They express proteins that minimize viral infection induced RNA sensors activation and allow viral RNA translation and replication. Amongst them, the nonstructural protein-1 (NS1) from Influenza A virus (IAV) decreases the intracellular recognition of viral RNA and the immune response against viral RNA, therefore favoring its translation and replication (Hale, Randall et al. 2008); (Ruckle, Haasbach et al. 2012).

Thus, we hypothesize that a co-delivery of NS1 mRNA with mRNA coding osteogenic factor, such as bone morphogenetic protein-2 (BMP-2), will allow an improved expression of osteogenic protein in mesenchymal stem cells (MSCs) and promotes MSCs osteogenic differentiation. Subsequently, the dual mRNAs will be used to functionalize bone tissue engineering (BTE) matrices for *in vivo* bone regeneration application.

2. Thesis Outline

The manuscript is organized in four main chapters: the first one is dedicated to the review of the literature; the second and the third chapters are related to obtained results presented in two articles; and in the last chapter, I gave conclusions and perspectives of this work.

The first part of this thesis reviewed the main results obtained so far in relevant fields (part I), including:

i. Bone fracture related principles of bone biology.

ii. Principles and progresses of bone tissue engineering;

iii. Advances and challenges of using IVT mRNA for osteogenesis;

iiii. Mechanisms of viral immune evasion proteins against host cell immune responses.

The second part of the thesis reported the NS1 function in suppressing exogeneous mRNA induced immune responses, and in favoring the osteogenic differentiation of murine multipotent stem cells (part II):

i. The NS1 from influenza A/Texas/36/1991 was reported to inhibit IVT mRNA induced immune responses (Phua, Liu et al. 2017). Therefore, the first goal of this study is to confirm such function in an osteoprogenitor cell (i.e., murine multipotent stem cell line C3H10T1/2). Then we intended at maximizing BMP-2 expression by co-delivering BMP2 mRNA with the NS1 mRNA. Finally, we explored the impact of dual mRNA system (BMP2/NS1 mRNAs) on osteogenesis of C3H10T1/2.

The third part of the thesis is related to the function of the dual mRNA system in inducing osteogenesis of human bone marrow-derived mesenchymal stem cells (hMSCs), and the preparation of mRNA activated matrix served as BTE graft for *in vivo* application (part III):

i. In this part, we aimed at exploring the efficacy of administration of the BMP2/NS1 mRNAs to hMSCs, in order to verify its eligibility to be translated to human application;

ii. Meanwhile, the dual mRNA system was loaded into the nanohydroxyapatite reinforced collagen scaffold to check its potential of *in vivo* osteoinduction.

The last part of the thesis summarized the main finds through this project, and perspectives for further studies.

Part I

Review of the Literature

1.1 Bone Biology and Fracture Healing

Bone regeneration is a complex, well-regulated physiological process of bone formation. Understanding of bone biology and normal fracture healing process is imperative for designing impactful strategies to accelerate bone regeneration.

1.1.1 Bone structure: an overview

The bone tissue is a type of connective tissue of vertebrates. Human mature skeletal system is composed of 206 individual bones, responsible for the support, movement, and protection of human body, and as calcium 'bank' for mineral homeostasis.

According to the shape, human bones can be divided into long bones (leverage function, e.g. femur, tibia, radius, ulna), short bones (provide stability, support, while allowing for some motion, e.g. carpus and tarsus), flat bones (provide muscles attachment points, and protect internal organs, e.g. shoulder blade, skull, rib), sesamoid bones (protect tendons from compressive forces, e.g. patella), and irregular bones (protect internal organs, e.g. vertebra, pelvis).

Corresponding to the two main stages of bone formation, there is primary bone (woven bone known as fibrous bone) followed by secondary bone (lamellar bone) (Buckwalter 1995). Primary bone contains small (10-20 nm in diameter), irregularly organized collagen fibril bundles, and osteocytes lying in lacunae (Bonucci 1992); (Buckwalter 1995). The mineralization within a primary bone is relatively rapid and unorganized, forming a 'woven' bone microstructure, wherein the mineralized crystals are not closely associated with the collagen, but, within the proteoglycan matrix, referred to as extrafibrillar mineralization (Olszta, Cheng et al. 2007). The woven bone is then replaced by lamellar bone, the main type of bone in mature skeleton (Fig. 1A). In lamellar bone, the collagen fibrils are larger than those in woven bone (~78 nm in diameter), and assemble into highly organized, close-packed lamellae sheets (Bonucci 1992). Mineral crystals form, embedded within the fibril (intrafibrillar mineralization), and grow along the fibril long axis. Lamellar bone is categorized to

cortical/compact bone and trabecular/cancellous bone. Cortical bone forms the dense hard external layer of bone tissue whereas the cancellous bone forms the inner layer containing sponge-like structure with interconnecting cavities. Cortical bone is composed of osteons or Haversian systems, which are formed by highly organized concentric lamellae sheets surrounding a central canal (Haversian canal). Haversian canal contains the bone's blood vessels and nerves. Osteons in cortical bone tissues are aligned parallel to the long axis of the bone and help the bone resist axis lining stress and bending. Cancellous bone does not contain osteons, instead, it consists of trabeculae, which is lamellae assembled rods or plates. The 3D porous lattice structure of trabeculae in cancellous bone enables bone tissue resistance against multidirectional forces (Lopes, Martins-Cruz et al. 2018).

Within the cancellous bone is bone marrow, a semi-solid tissue, which is the source of blood cells (hematopoietic stem cells) and osteogenic cells (stromal stem cells) (Krebsbach, Kuznetsov et al. 1999). On the external surface of cortical bone is periosteum, a fibrous connective tissue, with strong osteogenic potential, as it embeds mesenchymal stem cells, osteoprogenitor cells, and osteoblasts (Dwek 2010).

The structure mentioned above lies at the foundation of bones. It should be kept in mind that the macro-structure of bone tissue could vary between bone types, and also, bone is a dynamic tissue, thus the macro/nano-structure slightly changes in response to applied loads, immobilization, and other factors (Frost 1990).

1.1.2 Bone composition

In molecular and cellular level, bone tissue is comprised of the bone cells as well as the bone extracellular matrix (Fig. 1B). All components functionalize synergistically to maintain the structure and function of bone tissue.

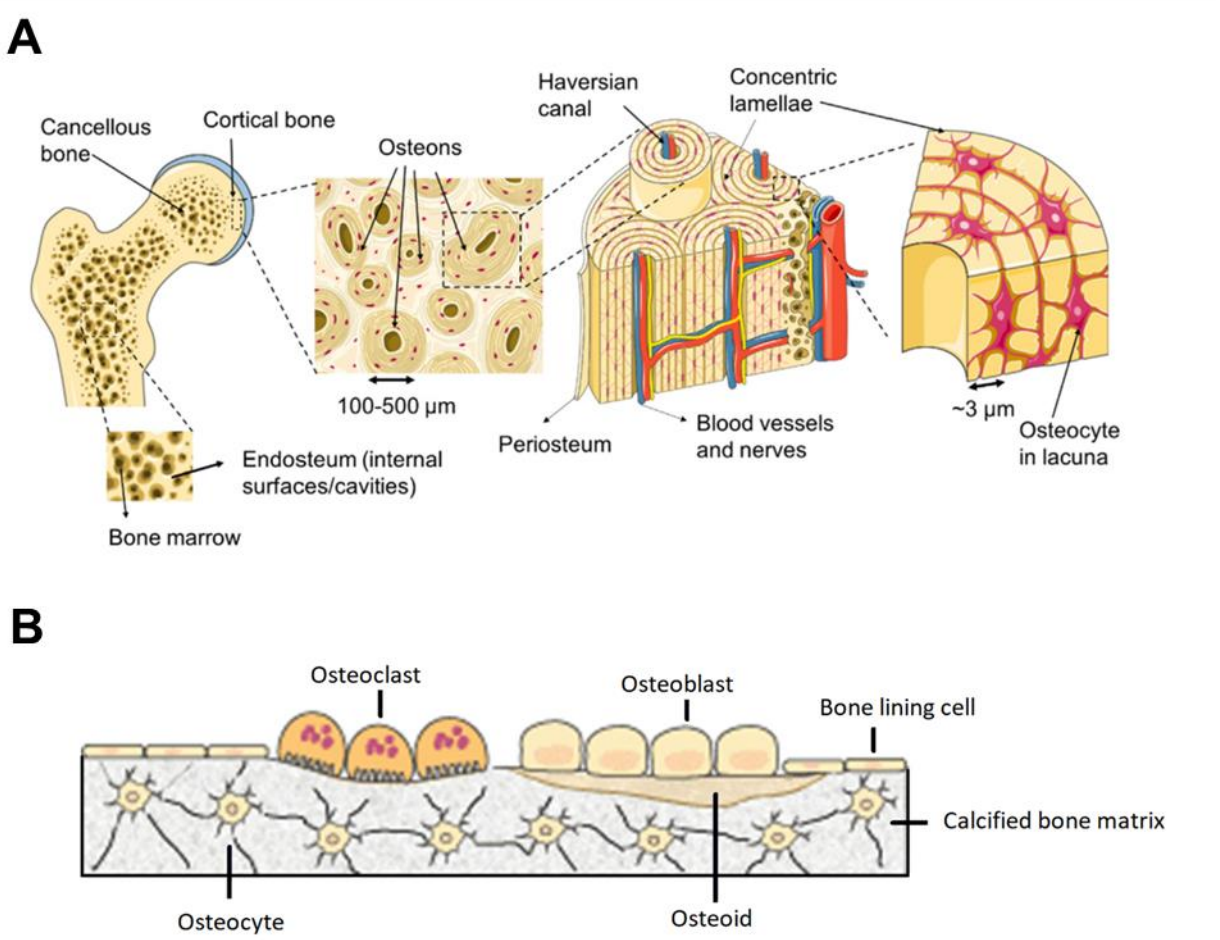

Fig. 1. Interscale representation of bone. (**A**) A macroscopic-to-microscopic view of cancellous and cortical bone. Bone marrow lies in the cavities of cancellous bone, which are lined by the endosteum structure. Tightly packed osteons integrate cortical tissue, which is covered by the periosteum membrane. Osteons are formed by Harversian canals, which contain blood vessels and nerve tissue, surrounded by concentric lamellae that show thicknesses of circa 3 µm. Osteocytes reside in the osteon inside lacuna structures. Adapted from (Lopes, Martins-Cruz et al. 2018) with permission (**B**) bone resident cells. Modified from https://www.iofbonehealth.org/introduction-bone-biology-all-about-our-bones (accessed on 09/27/2019).

As shown in Fig. 1B, there are four types of resident cells in bone tissue: osteoblasts, osteocytes, bone lining cells, and osteoclasts. Osteoblasts originate from mesenchymal stem cells and vascular pericytes, which proliferate and differentiate into osteoblasts under stimulation, such as fracture. They lie on the surface of the bone and synthesize organic matrix (osteoid) (Buckwalter 1995); (Lopes, Martins-Cruz et al. 2018). When the bone formation process finishes, cuboidal active osteoblasts become quiescent flat-shaped osteoblasts named bone lining cells, or embed themselves into the bone matrix and become osteocytes. Osteocytes are the most abundant cells in bone tissue (90-95%). Osteocytes have long, branched cytoplasmic processes, which, *via* the canaliculi, extend throughout the bone matrix, enabling to contact with other cells (Buckwalter 1995); (Bonewald 2011). Osteoclasts originate from hematopoietic stem cells. Under the signaling of bone resorption, these stem cells differentiate to osteoclast precursors, then proliferate and fuse to form active multinucleated osteoclasts. Through secreting protons and acid proteases toward the adhered bone, osteoclasts could efficiently degrade the calcified bone matrix (Baron, Neff et al. 1985); (Blair, Teitelbaum et al. 1989).

Bone matrix contains organic phase and inorganic phase, which correspond to approximately 25 wt.% and 65 wt.%, respectively. Water contributes the rest 10 wt.% (Buckwalter 1995); (Eastoe and Eastoe 1954). Collagen type I is the dominant organic component in bone matrix, approximately 90%, and others components include glycoproteins (e.g. fibronectin, osteonectin, and bone sialoprotein), γ-Carboxy Glutamic Acid (Gla)-Containing proteins (e.g. osteocalcin, osteopontin), proteoglycans (e.g. decorin, lumican and biglycan), and growth factors (e.g. morphogenetic proteins) (Bilezikian, Raisz et al. 2008); (Florencio-Silva, Sasso et al. 2015).

The repeat amino acid sequence, which is $–(Gly\text{-}X\text{-}Y\text{-})_n-$, where X and Y are frequently proline and hydroxyproline, allows the of type I collagen molecules to assemble into a triple helical structure, named as tropocollagen. Tropocollagen is the unit that forms collagen fibrils, in a quarter-staggered manner, leaving periodic gaps for crystallization (Eastoe and Eastoe 1954). During lamellar bone formation, tropocollagens direct the mineral growth such that crystals grow in the direction along the long axis of the collagen fibril. The non-collagen proteins also play a crucial role in bone matrix mineralization as evidenced by abnormal skeleton formation in collagen knock-out animal models (Bassuk, Birkebak et al. 1999); (Ducy, Desbois et al. 1996), and

dystrophic calcification foci upon over expression (Bellahcene and Castronovo 1997); (Waltregny, Bellahcene et al. 1998).

Hydroxyapatite (HA) is the main inorganic materials. Significant amounts of carbonate, bicarbonate, fluorite, zinc, barium, sodium, magnesium, and strontium are also present (Morgan, Barnes et al. 2013). Although the bone structure is reasonably well defined, its formation remains unclear. There are two argued mechanisms of hydroxyapatite crystals formation. One is the crystals are formed *via* traditional solution crystallization process, i.e. nucleation and growth (Glimcher, Bonar et al. 1981); (Landis, Song et al. 1993), and another is the crystals' formation initiates from the deposition of an amorphous calcium phosphate precursor (Termine and Posner 1966); (Olszta, Cheng et al. 2007).

1.1.3 Fracture healing mechanisms

Bone fracture is a common injury where the continuity of the bone tissue is broken. It can be caused by various reasons, mostly high force impact or stress. Under optimal conditions, bone has self-healing capacity allowing it to restore the damaged area to pre-injury structure and function.

Regarding the histologic features, fracture healing can be divided into primary fracture healing and secondary fracture healing (Einhorn 1998). In primary healing, *via* rigid internal fixation, the fracture surfaces tightly unit to each other with minimal displacement (anatomic reduction) and inter-fragmentary strain (McKibbin 1978). Under this mechanical continuity, osteoclasts adjacent to the fracture line resorb cortical bone matrix, forming 'cutting cones', followed by osteoblasts-mediated refill. Reestablished Harversian cannels provide pathways for blood vessel penetration (Dimitriou, Tsiridis et al. 2005); (Loi, Cordova et al. 2016). The primary fracture healing resembles the normal bone remodeling process, with no callus formation (Einhorn 1998).

Instead of primary fracture healing, majority of fracture healing undergoes secondary fracturing healing resulted from intramembranous ossification and endochondral ossification. The rigid stabilization or anatomical reduction is not necessary during secondary fracturing healing, and on the contrary, the healing is enhanced by micro-motion and weight bearing. Typically, secondary fracture healing includes several

stages that occur in a sequential manner: 1) hematoma and inflammation, 2) soft and hard callus formation, and 3) bone remodeling (Claes, Recknagel et al. 2012); (Einhorn and Gerstenfeld 2015) (Fig. 2).

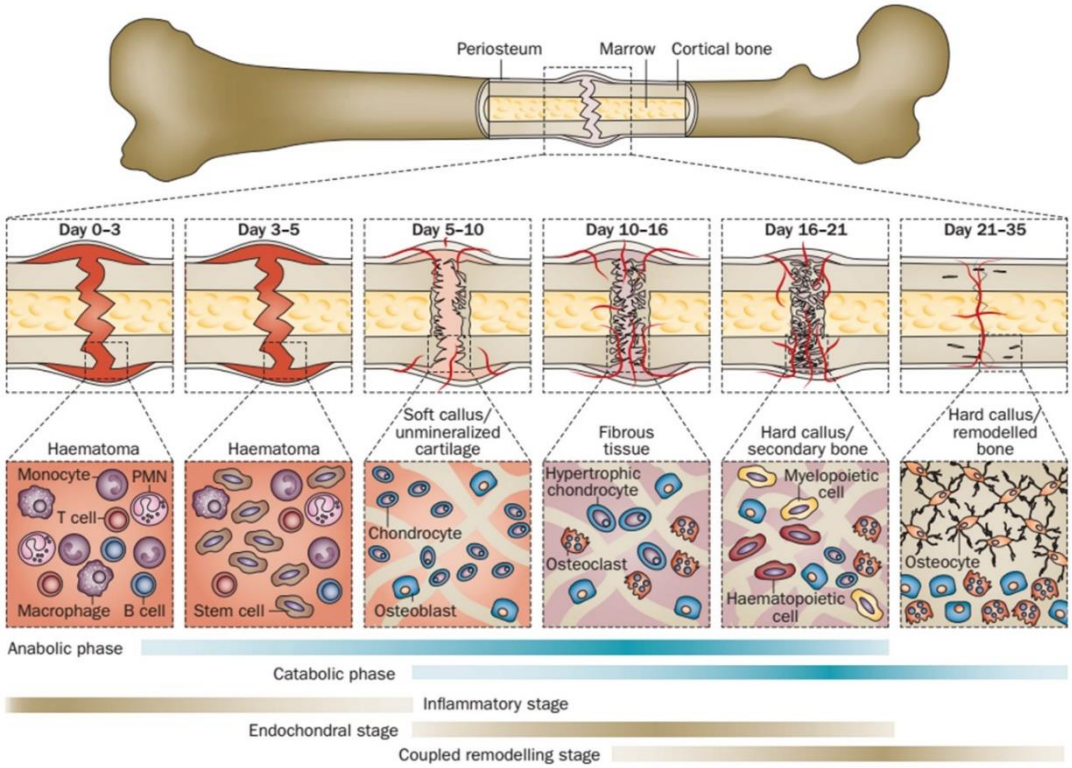

Fig. 2. An overview of femur fracture healing process. The healing of a mouse closed femur fracture fixed with an intramedullary rod. The major metabolic phases (blue bars) and biological stages (brown bars) of fracture healing are labeled; The primary cells involved in each stage, and the time spans of their prevalence are denoted. Abbreviations: BMP, bone morphogenetic protein; BMPR, bone morphogenetic protein receptor; DKK1, Dickkopf-related protein 1; LRP, LDL-receptor-related protein; MSC, mesenchymal stem cell; PMN, polymorphonuclear leukocyte; PTH, parathyroid hormone; PTHrP, parathyroid-hormone-related protein; RANKL, receptor activator of nuclear factor κB ligand. Adapted from (Einhorn and Gerstenfeld 2015) with permission.

1.1.3.1. Hematoma and inflammation

Hematoma and the associated acute inflammation are the first phase of fracture healing and are critical to initiate the cascades of repair events. Immediately following the fracture, vascular disruption results in clot formation due to activation of platelets and conversion of fibrinogen to fibrin. The fibrin-rich clot between and around the fracture ends, and within the medulla serves as a provisional matrix for cellular recruitment under stimulation of signaling molecules (such as PDGF) and template for later callus formation (Bolander 1992).

The inflammatory phase is mediated by neutrophils, lymphocytes, macrophages, and eosinophils (Claes, Recknagel et al. 2012). The neutrophils are the first inflammatory cells that infiltrate to the fracture site during the acute inflammation period (first 24h after injury) (Loi, Cordova et al. 2016), which recruit a second wave of inflammatory cell ingress by secreting inflammatory and chemotactic factors (such as IL-6 and CCL2) (Hurst, Wilkinson et al. 2001); (Xing, Lu et al. 2010). Recent studies showed that macrophages present throughout the whole healing process (Alexander, Chang et al. 2011), while in this early stage, their main function is to remove the clot, cellular debris, and possible pathogens through phagocytosis (Leibovich and Ross 1975).

1.1.3.2. Soft and hard callus formation:

After several days to a week, the hematoma and acute inflammation are cleared and replaced by granulation tissue rich in proliferating mesenchymal stem cells and developing neovasculature embedded in an unorganized extracellular collagen matrix (Lopes, Martins-Cruz et al. 2018).

Mesenchymal stem cells (MSCs) recruitment, proliferation, and osteogenic differentiation are crucial for bone regeneration. The exact source of MSCs in the fracture site is still not fully understood. Early studies demonstrate that the MSCs are recruited locally, i.e., from adjacent periosteum, soft tissue, bone marrow, while recent data show a circulation source of MSCs. Stromal cell-derived factor-1 (SDF-1), also called C-X-C motif chemokine 12 (CXCL12) and its receptor CXCR4 is considered as a key regulator for CXCR4 positive MSCs homing to facture site *via* chemotaxis (Granero-Molto, Weis et al. 2009).

From 7 to 10 days of fracture healing, periosteum undergoes intramembranous bone formation (hard callus) at the edges of the fracture (Einhorn 1998). Intramembranous bone formation is achieved by direct transformation of mesenchymal cells into osteoblasts, and secretion of bone matrix.

At the same time, the facture gap containing the granulation tissue is subsequently replaced by fibrous tissue, fibrocartilage and later cartilage (soft callus). Concurrent with cartilage tissue development, nascent blood vessel formation cells are recruited and differentiate in the surrounding muscle sheath (Kurdy, Weiss et al. 1996); (Einhorn and Gerstenfeld 2015). As the chondrocyte differentiation progresses, the soft callus undergoes ossification (endochondral ossification) mediated by osteoblasts, differentiated from mesenchymal stem cells or osteoprogenitor cells (Lee, Choi et al. 1998).

1.1.3.3. Bone remodeling

Finally, bone remodeling takes over the end-stage. The intramembranous and endochondral ossification formed bone matrix is resorbed by osteoclasts, and filled with new mature bony tissue by osteoblasts (Einhorn and Gerstenfeld 2015); (Loi, Cordova et al. 2016). Vascular remodeling takes place as well (Melnyk, Henke et al. 2008). During this prolonged period, the original cortical structure, bone marrow space, and blood flow are reestablished to the pre-injury level.

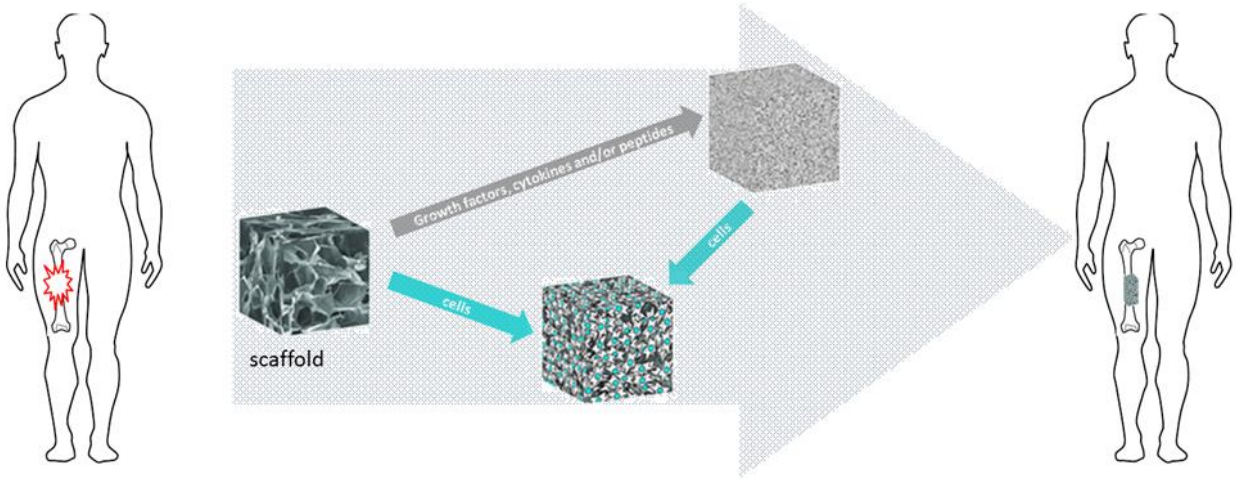

Fig. 3. Schematic illustration of bone tissue engineering (BTE) grafts construction and application. In the traditional 3D scaffold-based BTE grafts, growth factors, peptides, cytokines and/or cells are utilized as building blocks to create a functionalized 3D scaffold that is ultimately used either with or without pre-seeded cells for engineering bone tissue. Modified from (Kesireddy and Kasper 2016) with permission.

1.2 Bone Tissue Engineering

Although bone is one of the tissues that display capacity of regeneration, massive bone defects are great challenges to the self-healing. In this case, therapeutic intervention is needed. Moreover, bone lesions (e.g., critical-sized bone defects) still have great chance to become scared rather than regenerated, leading to nonunion (Petite, Viateau et al. 2000).

Using bone grafts to fill and bridge the defect is a common clinical strategy to augment bone repair and regeneration. Two hundred years ago, autologous bones (autografts) had been used for bone repair (White 1998).To data, autografts remain considered as gold standard for bone grafts due to the histocompatibility and non-immunogenicity, and most importantly, they contain all the essential elements for bone repair: osteoconductivity (i.e. three-dimensional porous structure and blood vessel), osteoinductivity (i.e. growth factors and signaling molecules), and osteogenesis (i.e. osteogenic and osteoprogenitor cells) (Amini, Laurencin et al. 2012). However, the autologous bone harvesting results in additional trauma and expenses to the patient, and risk of donor site morbidity, deformity, scarring and infection (Laurie, Kaban et al. 1984), especially for elders. Moreover, the autologous bone cannot meet the requirement when large volume of grafts is needed. Allogeneic transplantation can be adapted under this situation. First usage of allografts has been reported in 1915, which were retrieved from a cadaver (White 1998). Even though, allografts have good histocompatibility, osteoconductivity, the osteoinductivity are not fully conserved since cellular components are removed. Allografts are available in various forms (e.g. demineralized bone matrix, cancellous chips, cortical grafts) that can be easily processed to required sizes and shapes. Although underwent decellularization and

irradiation processes, allografts are still associated with risk of immunoreaction and infection transmissions (O'Keefe and Mao 2011); (Amini, Laurencin et al. 2012).

Globally, there are millions of patients who receive bone defect repairs each year. Therefore, autografts and allografts are far for being enough to cover the demand. This number is expected to increase because of various reasons, including increased population number and life expectancy. According to a recent investigation, “the global bone grafts and substitutes market was valued at $2,690 million in 2017, and is expected to reach $3,912 million by 2025, registering a CAGR of 4.8% during the forecast period” (Allied Market Research: https://www.alliedmarketresearch.com/bone-graft-substitutes-market).

The emergence of bone tissue engineering (BTE) gives the chance to fill the gap of the demand. BTE is a multidisciplinary field, combining biology, material science, chemistry, engineering, etc., with an ultimate goal to create bone grafts for bone repair and regeneration (O'Keefe and Mao 2011). A conventional BTE graft is composed of a biocompatible and biodegradable scaffold to support cell growth and functionalize, and bioactive components for osteogenesis and vascularization (Fig. 3).

Ideally, the BTE grafts could possess the advantages of autografts, while avoiding the drawbacks. So, it is projected that the BTE grafts will replace autografts and allografts for bone repair and regeneration. To fulfill this aim, the biological events (described in **section 1.1**) of bone repair need to be well understood, and choose/develop appropriate materials and methods to fabricate the BTE grafts.

1.2.1 BTE Scaffolds

1.2.1.1. Biomaterials of BTE Scaffold

The biomaterials are the basis to construct a BTE graft, which should be biocompatible, biodegradable and osteoconductive, and ideally, bioactive, osteoinductive:

Although the definition remains debated, the most important factor refers to the biocompatibility is not causing an unacceptable degree of harm to the body when contacting with tissues of the human body. With reference of the mechanism behind biocompatibility got from experiments and clinical experience, Williams redefined the

biocompatibility of biomaterials as follows: "*Biocompatibility refers to the ability of a biomaterial to perform its desired function with respect to a medical therapy, without eliciting any undesirable local or systemic effects in the recipient or beneficial of that therapy, but generating the most appropriate beneficial cellular or tissue response in that specific situation, and optimizing the clinically relevant performance of that therapy*" (Williams 2008). Biodegradability means that the material can be degraded in the physiological environment. As bone is a dynamic tissue, unbiodegradable material will influence bone remodeling. Bioactive materials could stimulate bone tissue formation by directly bound to the bone to form a unique strong biomaterial-bone interface. In contrary, bioinert materials stimulate the formation of fibrous tissue instead of bone. Osteoconductivity, when referring to biomaterials, is the ability of the material to serve as a scaffold or template to guide the formation of the newly forming bone along their surfaces. Osteoinductivity is the ability of a material to induce *de novo* bone formation without the presence of osteogenic factors, which usually demonstrated by bone formation after implantation in non-osseous sites (e.g., subcutaneously or in intramuscular sites).

These properties can be inherent in the raw materials or engineered. Generally, depending on the chemical composition, biomaterials for fabricating BTE scaffold can be classified into organic (natural or synthetic polymers) and inorganic (synthetic ceramics and coral-derives) materials (Pountos and Giannoudis 2016).

A. Calcium Phosphate-based materials:

Calcium phosphate (CaP)-based biomaterials are the major components of inorganic scaffold materials, others, including calcium carbonate, calcium sulfates, and silica-based bioglass.

Several CaP materials have been used to fabricate bone substitutes, including hydroxyapatite (HA, $Ca_{10}(PO_4)_6(OH)_2$) (Denissen and Groot 1979, Yamasaki and Sakai 1992); (Yuan, Kurashina et al. 1999), tricalcium phosphate (TCP, $Ca_3(PO_4)_2$) (Klein, de Groot et al. 1994); (Kondo, Ogose et al. 2006), biphasic calcium phosphates (BCP, HA+TCP) (Kurashina, Kurita et al. 2002); (LeGeros, Lin et al. 2003), and coral-derives (Ripamonti 1991);(Petite, Viateau et al. 2000). The rationale for developing CaP materials is their similarity to the bone mineral composition that gives them

excellent biocompatibility, bioactivity, biodegradability, and osteoconductivity (LeGeros 2008).

Biodegradability: The CaP biomaterials can be degraded in acidic environment, which is generated *in vivo* during osteoclast-mediated bone resorption (Ghayor and Weber 2016). Their degradation rate is dependent on the chemical composition and the preparation conditions. Generally, the amorphous TCP has a higher degradation rate than crystal HA (unsintered HA > sintered HA). Thus, the BCP degradation depends on the ratio of TCP-to-HA, which can be adjusted to match the clinical usages (LeGeros 2008).

Bioactivity and osteoconductivity: The CaP implants can form direct interaction with host bone, instead of encapsulated by fibroblast tissue (Daculsi, Passuti et al. 1990). This bone-CaP bonding is suggested intermediated by carbonate apatite (CHA), a thin layer at the bone-CaP interface (Anderson 1992). *In vivo*, the CHA layer adsorbs proteins from the surrounding milieu on which bone cells attach, migrate, proliferate, and differentiate, leading to matrix production and mineralization.

Osteoinductivity: Despite the promising clinical success of CaP implants, no conclusive evidence about its osteoinductive mechanism has been presented yet. Some believe that CaP is an intrinsic osteoinductive material (Ripamonti 1996); (Yuan, Fernandes et al. 2010), others consider that the physical properties of CaP-scaffold play more roles in its osteoinductivity (Yamasaki and Sakai 1992)(Yamasaki and Sakai 1992); (Yuan, Kurashina et al. 1999). Yuan et al. evaluated the bone formation properties of two types of hydroxyapatite ceramic rods (i.e., J-HA with average pore size of 200 μm, a porosity of 70%, and was sintered at 1200 ℃; S-HA with average pore size 400 μm, porosity 60-70%, sintered at 1100℃) in the dog dorsal muscle model (Yuan, Kurashina et al. 1999). Although with same chemical composition, bone formation was found in all S-HA implants, but not in any of J-HA implants, in which only fibrous tissues and blood vessels were observed. The sintering temperature and micropores in the wall may contribute to the osteoinduction of S-HA. It was demonstrated that the apatite crystals sintered at lower temperature have lower crystallinity and were more active in bone formation. Apatite crystals of J-HA aligned orderly and fused together leaving dense wall, while in S-HA, apatite crystals distributed irregularly, and less fused leaving many interconnected submicropores.

This submicrostructure could also affect osteogenic cell behaviors (Lee, Choi et al. 2004); (Sheridan, Gil et al. 2008).

B. Collagen-based materials

The polymers used to fabricate scaffolds can be biological origin or synthetic. Biological polymers are interesting candidates for tissue engineering and provide innate biological informational guidance to cells that favor cell attachment and promotes chemotactic responses. Although, concerns exist over their immunogenicity, the potential risk of disease transmission, sourcing, poor handling, and weak mechanical properties (Stevens 2008).

Collagen is the most abundant protein in mammals, and to date, 28 types of collagens are identified (Zhang, Wu et al. 2018). Type I collagen is most investigated for biomedical applications (such as bone regeneration, spinal fusion, skin regeneration) (Yannas, Lee et al. 1989), due to several advantages listed below.

Bioresorbility (Krane 1982);(Laurent 1987): *In vivo* degradation of extracellular collagen is initially mediated by collagenases which cleave collagen fiber at specific sites, then by neutral proteases cutting the collagen into fragments. These fragments may be uptaken by cells before extracellular degradation, and undergo intracellular degradation within lysosome or endoplasmic reticulum or Golgi apparatus. Fibroblasts are known to be involved in the degradation pathways by expressing collagenases. Other cells, such as macrophages and neutrophils, capable of phagocytosing collagen as well as releasing proteases, also play a role in collagen degradation. Collagen degradation rate varies in different tissues;

Low antigenicity: Generally, the macromolecular features of a protein that are not common to the host species are more likely to trigger an immune response, and thus the antigenicity of collagen is intimately linked with the self-tolerance and interspecies variation. The triple-helical region of the collagen shows a high degree of consistency between mammalian species (only a few percent difference) (Fietzek and Kuhn 1976). The variation in the nonhelical terminal regions contributes to the major antigenic determinants (Michaeli, Martin et al. 1969). The most persuasive evidence comes from clinical application (Lynn, Yannas et al. 2004): In clinic, all collagen products are extracted from animals (i.e. bovine and porcine dermal), and to date, they have been

used for more than 50 years. Immunological studies showed of 2-4% patients have preexisting hypersensitivity to injectable collagen from calfskin, and an additional 1% of subjects got postoperative allergy. Rare incidence of adverse reactions, such as granuloma and localized inflammation, have been observed and they were generally resolved within a few months. No collagen-triggered adverse immunological responses were documented from patients accepting animal origin dermal substitutes for wound cover and closure.

Modulating cell behaviors (i.e., adhesion, migration, proliferation): The function of collagen substrate in regulating cell behaviors was studied as early as 1970s (Elsdale and Bard 1972). The morphology, adhesion, and growth of human fibroblasts and HeLa cells on and within hydrated collagen lattices have been studied. However, they were just observational studies, the mechanisms behind were not revealed. In the following decades, the molecular biology behind collagen-cell interactions were discovered. Collagen can regulate cell function through the engagement and activation of specific cell surfaces receptors, including integrins, discoidin domain receptors (DDRs), glycoprotein VI, and immune receptors (Leitinger and Hohenester 2007, Farndale, Lisman et al. 2008). For instance, glycoprotein VI and collagen interaction mediates platelets adhesion and activation, which is important to form hemostatic clot at the sites of vascular injury (Kato, Kanaji et al. 2003). Additional to the direct interaction, collagen can also regulate cell behaviors *via* intermediates, such as fibronectin, secreted protein acidic and rich in cysteine (SPARC), decorin, and transforming growth factor-beta (TGF-β). For instance, in collagen deficient mouse, although the intracellular synthesis of SPARC was not affected, the extracellular SPARC accumulation was significantly reduced. This phenomenon is caused by lack of incorporation of SPARC by fibroblasts from collagen-deficient mouse (Iruela-Arispe, Vernon et al. 1996).

Modification: Collagen can be easily modified due to the abundance of functional groups (amine and carboxyl groups), introducing crosslinks to enhance its mechanical and enzymatic resistance properties, or grafting biological molecules to create a wide variety of collagen-based biomaterials with tailored biological properties (Weadock, Miller et al. 1995); (O'Leary, Fallas et al. 2011).

Several methods are available to crosslink collagen scaffolds: physical, chemical, and enzymatic crosslinking. UV irradiation and dehydrothermal (DHT) treatment represent the physical crosslinking methods. The physical treatments increase collagen tensile strength, meanwhile fragment the collagen to some extent (Weadock, Miller et al. 1995). Many chemicals are used to crosslink collagen materials, including aldehydes (e.g. formaldehyde and glutaraldehyde), carbodiimide family (e.g. dicyclohexylcarbodiimide and 1-Ethyl-3-(3-dimethylaminopropyl)carbodiimide), and isocyanate family (e.g. hexamethylene diisocyanate). After crosslinking, the chemicals and byproducts should be thoroughly washed out to avoid to toxicity. The protein posttranslational covalent modification is a common process in organisms, which is mostly catalyzed by specific enzyme(s). For instance, eukaryotic transglutaminases generate protein networks by introducing glutamyl-lysyl isopeptide bonds between target proteins (Heck, Faccio et al. 2013). Lysyl oxidases crosslink the collagen and elastin chains in the extracellular matrix (Lucero and Kagan 2006). These enzymes can be applied *in vitro* to crosslink collagen materials (O'Leary, Fallas et al. 2011). Unlike chemicals, enzyme-mediated crosslinking does not introduce toxic residues.

Easy processing: Collagen can be processed into different physical forms (e.g. micro-/nanospheres, porous scaffolds, and films) to adapt to the wide variety of applications.

Emulsification is the conventional technique to fabricate collagen microspheres (Nagai, Kumasaka et al. 2010). The sizes of the microspheres can be adjusted by controlling the molecular weight of the collagen (Rossler, Kreuter et al. 1995), and surfactant concentration and rotating speed during emulsification process (Nagai, Kumasaka et al. 2010). Collagen nanoparticles can be obtained using a high-voltage electrostatic field system. Series of nanosized collagen particles are able to be prepared by setting the processing conditions, including temperature, collagen concentration, and voltage intensity (Kuo, Chang et al. 2008). The collagen microspheres have been applied to deliver therapeutics, such as antibacterial drugs, BMPs, and VEGF. The collagen nanoparticles can direct the growth and osteogenic differentiation of bone marrow mesenchymal stem cells (BMSCs) (Chen, Chung et al. 2009).

Free-drying and electrospinning are suitable to prepare collagen membranes (Law, Liau et al. 2017). Several commercially available collagen membranes (e.g. EZ

Cure™, BiCON™, Cytoplast™) have been developed using type I collagen as their major component for guided bone regeneration and guided tissue regeneration procedures in dental surgery.

Over the years, a series of processing techniques, such as solvent casting, phase inversion, freeze-drying, and rapid prototyping techniques have been developed to produce scaffolds with adequate properties for bone tissue engineering (Ferreira, Gentile et al. 2012).

1.2.1.2. Physical properties of BTE Scaffold

For functional tissue engineering, the scaffold not only serves as a support substrate for preloading cells or ingressive cells from surrounding tissue but also to provide instructional cues in regulating their behaviors, including adhesion, migration, proliferation, and differentiation (Huang, Hagar et al. 2004); (Peyton and Putnam 2005); (Khatiwala, Peyton et al. 2007); (Khetan, Guvendiren et al. 2013).

Many physical properties of the scaffold influence the performance of BTE grafts:

A. Mechanical strength

Several studies have reported that the scaffold mechanical strength (i.e. softness and stiffness) participates in modulating ingrowth cells' behaviors by transferring an intrinsic and extrinsic mechanical signal to the attached cells (Engler, Sen et al. 2006); (Khatiwala, Peyton et al. 2007).

Substrate rigidity directs cell fate: Cells have the ability to sense the stiffness of the substrate surface by pulling against the substrate, and then cellular mechanotransducers generate signals that induce downstream reactions (Khatiwala, Peyton et al. 2006). The substrate stiffness directly influences the focal-adhesion structure and the cytoskeleton, consequently modulating the cells' fate. Using elastically tunable gel systems, researchers demonstrated that cells respond to different substrate/ matrix rigidity.

Such studies first started with two-dimensional (2D) culture. Polyacrylamide gel coated with collagen is a well-defined model, in which the concentration of bis-acrylamide crosslinking controls the elasticity and the type I collagen coating supports cell adhesion. Khatiwala et al. cultured pre-osteoblastic MC3T3-E1 cells on the

polyacrylamide gels functionalized with different density of collagen (i.e. 5μg/cm^2 and 50μg/cm^2), and found that on soft substrates (E=11.78KPa) the cellular F-actin network was disorganized and poorly defined, along with small focal adhesions. Whilst on hard substrates (E=38.98 kPa), the actin filaments were assembled into a robust stress fiber network that terminated in well-defined vinculin-containing focal adhesions (Khatiwala, Peyton et al. 2006). The assembling of these structures was enhanced on substrates with higher collagen densities. Consequently, the cell migration speed was increased on surfaces coated with low density of collagen as the gel stiffness increase. On surfaces coated with high density of collagen, the migration speed exhibited biphasic dependence on the substrate compliance. Specifically, cells on medium rigid gels (E=21.6 KPa) had maximum speed, whereas cells on soft and hard gels had lower migration speed. The high-stress actin cytoskeleton may contribute to the motility decrease, as the cell movement is enhanced when the actin-mediated traction stresses are optimally balanced. The authors further measured the cell proliferation and osteoblastic differentiation on gel substrates with low collagen density. Similar to the cell migration, the proliferation and the differentiation were also enhanced on more rigid substrates. The enhancement is associated with activation of mitogen-activated protein kinase (MAPK) family (Khatiwala, Peyton et al. 2007). In addition, it is worth to note that the optimal stiffness of substrates is cell type-dependent, as evidenced by the migration difference between MC3T3-E1 cells and smooth muscle cells (Peyton and Putnam 2005).

In 2006, Engler and colleagues reported that the matrix rigidity could direct mesenchymal stem cell lineage specification in the absence of any other induction cues (Engler, Sen et al. 2006). By controlling the bis-acrylamide crosslinking level, they produced polyacrylamide gels with different elasticities similar to the brain (E=0.1-1KPa), muscle (E=8-17KPa), and collagenous osteoid precursors of bone (E=25-40KPa). On the softest gels, MSCs showed an increasingly branched, filopodia-rich morphology, which is similar to primary neurons cultured on Matrigel-coated gels; On moderately stiff matrices, MSCs exhibited spindle-shipped morphology similar to C2C12 myoblasts; On the stiffest matrices, MSCs yielded polygonal shape similar to the morphology of osteoblasts. The non-muscle myosin IIs (NMM IIs), especially NMM IIB, responded to generate force leading to cell morphology change. NMM IIB expression was upregulated on stiff matrices, while downregulated on soft matrices.

Inhibition of NMM IIs blocked the cellular sensitivity to matrices elasticity. The matrix elasticity-driven differentiation was further proved from transcriptional profiles of neurogenic, myogenic, and osteogenic markers—from early commitment markers through mid/late development markers, which were consistent with indications from morphology observations.

Recent developments in materials science have enabled the development of more physiologically relevant three-dimensional (3D) culture systems to help further decouple the role of cell shape, substrate stiffness and cytoskeletal tension in regulating MSC fate (Pek, Wan et al. 2010); (Huebsch, Arany et al. 2010); (Parekh, Chatterjee et al. 2011); (Khetan, Guvendiren et al. 2013). Unlike 2D culture, the embedded cells show more complex responses to the surrounding milieu.

Clonally derived murine mesenchymal stem-cell (mMSC), encapsulated in 3D hydrogel (formed by alginate polymers that present integrin-binding RGD peptides) for 1 week, showed different phenotypes relating to the matrix rigidity: osteogenic commitment occurring primarily at intermediate (E=11–30 kPa) and adipogenic lineage predominating in softer (E=2.5–5 kPa) microenvironments (Huebsch, Arany et al. 2010). This phenomenon was matrix composition independent as evidenced by the similar differentiation of mMSCs in RGD-modified agarose and poly(ethylene glycol dimethacrylate) hydrogels. As the matrices are not susceptible to enzymatic degradation by mammalian cells, their mechanical properties are expected to remain constant throughout differentiation studies. Thus, the cell phenotype difference can be distinguished from indirect effects stemming from matrix degradation, which by itself has been linked to cell fate in previous work. In contrast with previous 2D studies, matrices rigidity had no significant effects on gross mMSCs morphology in 3D matrices either at a short time or at later time-points, and cells appeared to be grossly spherical. By investigating the binding of integrin (α_5) and its substrate RGD, the authors found that the matrices stiffness drove cell fate, at least partially, by directly regulating integrin/RGD bond formation. In another study, the human bone marrow stromal cells (hBMSCs) underwent osteogenic differentiation in poly (ethylene glycol) hydrogels regardless the modulus (from 0.2KPa to 59KPa) (Parekh, Chatterjee et al. 2011).

The above results are based on non-degradable hydrogels. Khetan et al. measured hMSCs fate in degradable methacrylate and maleimide groups modified hyaluronic

acid (MeMaHA) hydrogels (Khetan, Guvendiren et al. 2013). Interestingly, hMSCs committed to osteoblastic differentiation in soft MeMaHA hydrogels (E = 4.30 ± 0.11 kPa) and rigid hydrogel (2.5–5 kPa) commited mMSCs to adipogenesis (Huebsch, Arany et al. 2010). The osteogenic differentiation was inhibited by switching the degradable matrices to non-degradable matrices, and by treating with Y-27632, an inhibitor of ROCK, the RhoA effector that induces non-muscle myosin-mediated contractility as well. This finding is contradictory with that reported by Parekh and colleagues who reported that the disruption of mechanosensing myosin II contraction and RhoA kinase did not abrogate hMSCs osteogenic differentiation in 3D poly(ethylene glycol) hydrogels (Parekh, Chatterjee et al. 2011).

These inconsistent results demonstrate that controlling MSCs fate by substrate rigidity highly depends on environment dimension (2D or 3D), substrate biodegradability, and cell type. Accordingly, all these factors need to be considered when designing matrix/scaffold for MSCs culture. Moreover, more research must be performed to identify the mechanisms involved.

Scaffold transfer extrinsic mechanical stimuli to cells: It is known that exercise, such as running and weight training, could increase bone density, muscle fiber diameter, etc., due to the mechanical stimulation (compression, stretch, and torsion). From micro-level, cells generate responses to the biomechanical stimuli, which are essential to maintain the normal activity of cells, structure and function of tissues/organs. In contrast, relief from the mechanical stimulation antagonizes the physical activity. For instance, bone fracture-fixation associated stress shielding, which refers to the reduction of bone density as a result of removal of typical stress from the bone, and consequently a decrease of bone remodeling.

Dynamic compression loading to the 3D constructs stimulates the encapsulated MSCs to undergo chondrogenic differentiation in the absence of exogenous growth factors (Huang, Hagar et al. 2004); (Li, Kupcsik et al. 2010). The compression stimulation upregulated TGF-β1 gene expression suggesting that it may activate similar pathways as exogenous TGF- β stimulation.

Applying cyclic stretch to MSCs within porous scaffolds (e.g. collagen scaffold, collagen–glycosaminoglycan scaffold) has been shown to enhance endogenous BMP-2 expression, osteogenic marker expression, and mineralization (Sumanasinghe,

Bernacki et al. 2006); (Byrne, Farrell et al. 2008). The osteogenic differentiation was, at least in part, due to the activation of mitogen-activated protein kinases (MAPK) pathway (Ward, Salasznyk et al. 2007). In another study, MSCs synthesized more proteoglycans in collagen-GAG scaffolds that underwent cyclic tensile strain, implying that the tensile stimulation can also lead to a pro-chondrogenic response (McMahon, Campbell et al. 2008).

The results from mechanical stimulation of 3D constructs are, at some extent, hard to interpret, as the compression and stretching also increase the fluid flow within 3D constructs, causing fluid shear stress to cells, which have consistently been found to promote the expression of osteogenic markers in murine mesenchymal stem cell line (C3H10T1/2) (Arnsdorf, Tummala et al. 2009), adipo-derived MSCs (Knippenberg, Helder et al. 2005), and bone marrow-derived MSCs (Li, Batra et al. 2004); (Riddle, Taylor et al. 2006). Meanwhile, associated with increase of fluid flow, the nutrient and gas transfer within the 3D constructs increased as well.

Recently, Steinmetz and colleagues made a comprehensive study revealing the synergistic influence of matrices stiffness and mechanical stimulation on MSCs differentiation (Steinmetz, Aisenbrey et al. 2015). hMSCs were embedded in a triple layer poly(ethylene glycol)-based hydrogels, including a soft cartilage-like layer with chondroitin sulfate and low RGD concentrations, a stiff bone-like layer with high RGD concentrations, and an intermediate interfacial layer. Dynamic compression led to differentially high expression of collagen II in the cartilage-like layer, collagen X in the interfacial layer and collagen I in the bone-like layer, and mineral deposits localized to the bone layer.

Optimization of the scaffold mechanical strength: Overall, stiff scaffolds are more suitable for bone tissue engineering. Despite the MSCs fate conduction ability, high rigidity enables scaffolds to retain origin structure (e.g. pore size and interconnectivity) that influences cell ingrowth and nutrient diffusion, and provides temporary mechanical integrity at the defect site until the bone tissue is regenerated, and normal biomechanical function restored.

The material composition of a scaffold largely influences its mechanical properties. For instance, ceramic (HA, TCP, and BCP) scaffolds have high elastic modulus, which is useful in maintaining its porous structure and *in vivo* mechanical integrity of bone

lesion. However, the low toughness leads to fracture under force apply. On the other hand, the polymer-based scaffolds display high toughness, while weak mechanical property. The ceramic and polymer hybrid scaffolds (ceramic reinforced polymer scaffolds or polymer reinforced ceramic scaffolds) have been extensively investigated, since they can be tailored to the particular mechanical demands of the host tissue by effectively controlling volume fraction of the inorganic and organic phases.

Being dominant components of bone ECM, collagen and HA composite is often used for bone tissue engineering scaffolds. The collagen/HA scaffolds can be prepared by directly mixing the two materials (Cunniffe, Dickson et al. 2010), or coating one to another (Zhang, Wu et al. 2018); (Castillo, Montelongo et al. 2016). Compared to pure collagen scaffolds, mixing HA nanoparticles (nHA) to collagen slurry before lyophilization significantly increased the compressive strength (5.50 ± 1.70 kPa vs. 0.30 ± 0.09 kPa), with no effect on scaffold porosity (98.9% vs. 99.5%) (Cunniffe, Dickson et al. 2010). Immersing collagen scaffold in a nHA suspension has similar effects, but less reproducible. Besides direct absorbance of nHA onto the scaffolds surface, nHA can form *in situ* by immersing collagen scaffold in calcium and phosphate rich liquid (Zhang, Wu et al. 2018). Castillo *et al.,* tested the mechanical performance of collagen-coated HA scaffolds, and found the ultimate stress and toughness increased after collagen coating, particularly when using 0.05% (w/v) collagen slurry (Castillo, Montelongo et al. 2016).

Crosslinking could also enhance the mechanical strength for scaffolds containing exposed reactive groups. Collagen–glycosaminoglycan (CG) scaffolds treated with dehydrothermal, 1-ethyl-3-3-dimethyl aminopropyl carbodiimide or glutaraldehyde showed increased compressive modulus, up to fourfold compared to nontreated CG scaffolds. Higher cell (MC3T3-E1) proliferation and distribution were observed in crosslinked CG scaffolds (Haugh, Murphy et al. 2011).

In addition, different scaffold stiffness can be achieved by adjusting the pore size, connectivity and porosity: the smaller the pore size, the lower the porosity, the higher the stiffness. For instance, the compressive modulus of foams made with Poly Lactic and Glycolic acid (PLGA) with pore size of 110 µm (PLGA-110) was 297 MPa, and 232 MPa for PLGA foams with a pore size of 210 µm (PLGA-210). The two PLGA foams had similar porosity (Borden, El-Amin et al. 2003). Increasing the porosity of

poly(d,l-lactide) (PDLLA) scaffolds from 58% to 80% resulted in decrease of compressive strength from 11.0 to 2.7 MPa, and of modulus from 168.3 to 43.5 MPa (Lin, Barrows et al. 2003). However, it is worth to note that these microstructural factors also influence cellular performance inside the scaffold, so their relationship needs to be well balanced.

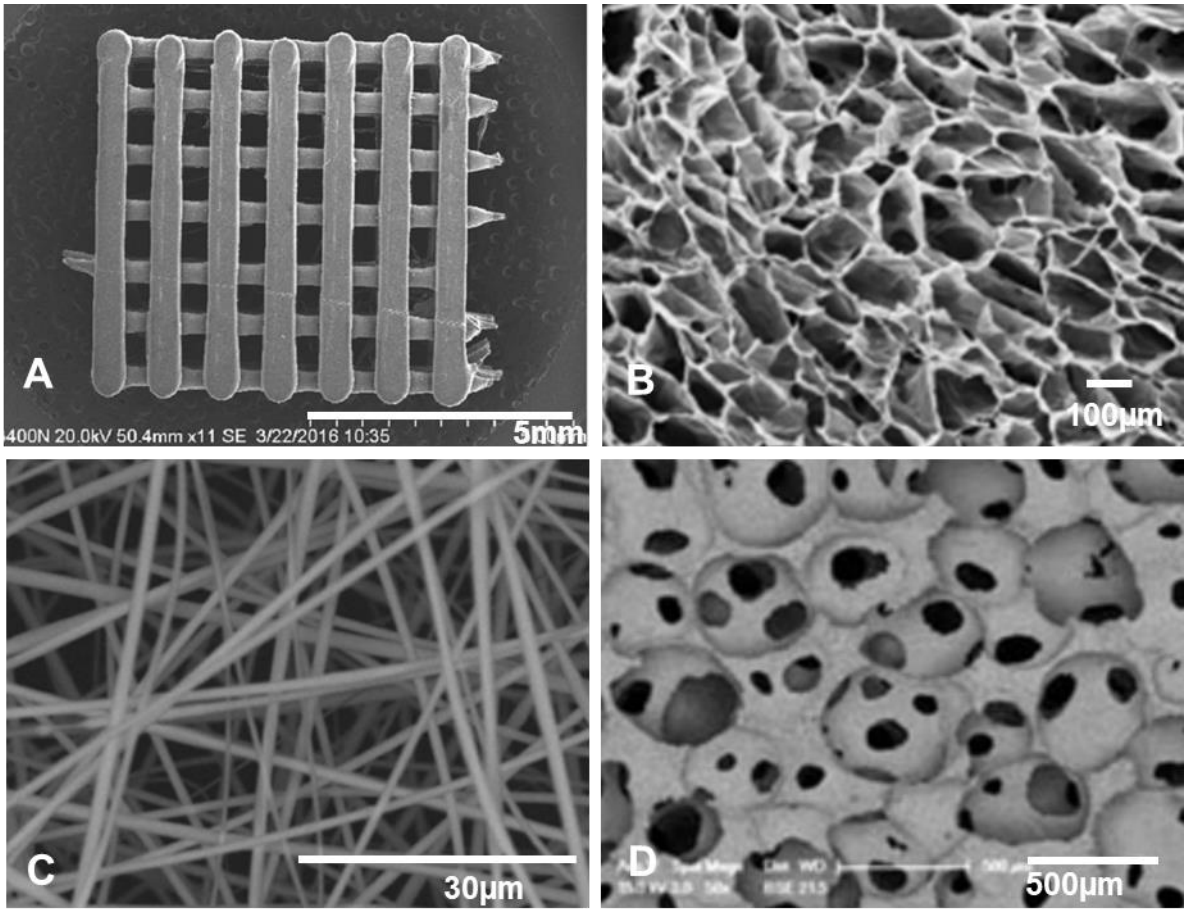

Fig. 4. Scaffolds built by different methods. (A): 3D printed poly(lactic acid) scaffold (Teixeira, Aprile et al. 2019). (**B**): freeze-dried collagen scaffold (Offeddu, Ashworth et al. 2015). (**C**): Electrospun Silica nonwoven fabrics (Iijima, Ishikawa et al. 2018). (**D**): Gas foaming fabricated Biphasic Calcium Phosphate scaffold (Kim, Park et al. 2012).

B. Micro-/Nano-structure

Porosity and pore size: Scaffold pore structure (Fig. 4), i.e., pore size, porosity, and interconnectivity, is an essential consideration for proper *in vitro* osteogenesis and *in vivo* bone formation (Karageorgiou and Kaplan 2005);(Amini, Laurencin et al. 2012).

The porosity of a scaffold is the percentage of void space, which is a morphological property independent of the material. Numerous studies have demonstrated that high porosity results in an enhanced osteogenesis. Dental implants coated with cancellous structured titanium with high porosity (48%) induced more bone ingrowth in canine mandibles and femora than that with low porosity (44%) (Story, Wagner et al. 1998). Lewandrowski et al. developed a poly(propylene fumarate) scaffold containing soluble calcium filler salts. Scaffolds with higher percentage of salts, which subsequently generate high porosity *in vivo* after implantation, showed greater and deeper bone ingrowth in rat tibias defect model (Lewandrowski, Gresser et al. 2000).

Pores are necessary for bone tissue formation as they allow osteogenic cells penetration and proliferation, nutrients exchange, as well as vascularization (Amini, Laurencin et al. 2012). For most bone ingrowth settings, the pore size used is between 150 and 500 µm, large enough to support ingrowth of vascular tissues, depending on the depth of penetration required (Muschler, Nakamoto et al. 2004). *In vitro* studies of seeding rat osteoblasts onto the PolyHIPE polymer foams with different pore sizes (40, 60, and 100µm) demonstrated that the cells had faster inward penetration in 100µm-foams, however the final penetration depth (approximately 1.4 mm) and mineralization level were not affected (Akay, Birch et al. 2004). Their results about the cell inward migration are consistent with other findings that scaffolds with small pore sizes (less than 200 µm) display peripheral cellular activity, due to decreased oxygen and nutrient diffusion throughout the scaffolds (Muschler, Nakamoto et al. 2004); (Murphy and O'Brien 2010). While, scaffolds with a mean pore size of 300 µm displayed increased osteoblast infiltration, proliferation and differentiation throughout the entire scaffold (Murphy and O'Brien 2010); (Amini, Laurencin et al. 2012).

In addition to affecting cell activity, the porous surface improves mechanical interlocking between the implant and the surrounding tissues, providing greater interfacial mechanical stability (Story, Wagner et al. 1998); (Gotz, Muller et al. 2004). Under this consideration, the large pore size is not preferred. Laser-textured titanium

alloy implants with pore sizes of 100, 200, and 300 µm were transcortically implanted into rabbit femora (Gotz, Muller et al. 2004). 12 weeks post-implantation, implants with 200 µm pores resulted in a more profound osseointegration than that with 300 µm pores.

Several traditional scaffold fabrication techniques, such as particulate leaching (Hutmacher 2000), gas foaming (Stevens 2008), freeze-drying (Ferreira, Gentile et al. 2012), and phase separation (Karageorgiou and Kaplan 2005), are available to fabricate highly porous scaffolds with isotropic distributed voids and connecting pores. Recently developed solid free-form fabrication methods (e.g., stereolithography, fused deposition modeling, and three-dimensional printing), allows the production of more precise hierarchical microstructures (mimic of bone structure) from a variety of materials (Lee, Kim et al. 2010).

Topography: Cells are inherently sensitive to their surroundings. Topographic reaction (i.e. reaction to the surface landscape) of cells to grooves, ridges, walls, and other features of the substrates at the micron-scale (Leven, Virdi et al. 2004); (Lee, Choi et al. 2004) and, more recently, the nanoscale is now well established (Dalby, Gadegaard et al. 2007); (Stevens 2008).

Leven and colleagues evaluated the cellular response of rat bone marrow stromal cells (bMSCs) to substratum surface roughness (Leven, Virdi et al. 2004). Titanium alloy discs with different surfaces roughness (i.e. Ra=0.14 µm and Ra=5.8 µm) were applied. The bMSCs cultured on the Ra/0.14 µm surface showed typical fibroblastic morphology, whereas cells on the Ra/5.8 µm surface showed a more epithelial appearance. Osteogenic-relevant genes expression assay demonstrated that: at 24h, alkaline phosphatase, and osteonectin were more upregulated on Ra/5.8 µm surface than on Ra/0.14µm. At 48h, the genes expressions were similar on the two surfaces except for osteopontin which was more expressed on Ra/1.4 µm surface. Their results clearly showed that the substratum surface topography affects cellular morphology and gene expression. However, the influence on osteogenesis was not conclusive, due to the short culture time.

Dalby and colleagues evaluated the long-term effects of a nano-topographical surface on the osteogenic differentiation of human mesenchymal stem cells (hMSCs) (Dalby, Gadegaard et al. 2007). They created polymethylmethacrylate (PMMA) substratum

embossed with regularly arranged or disordered nanopits. After 21 days culture, more hMSCs differentiated towards osteoblasts on PMMA substratum with disordered nanopits. Unlike microscale roughness system, the nanotopographical featured surfaces, produced *via* electron beam lithography (EBL), are ultra-precise and reproducible. Thus, the MSCs from different donors showed highly consistent results.

Scaffolds made from nanofibers with controlled alignments were shown to direct cell orientation and migration (Shin, Yoshimoto et al. 2004); (Wang, Ding et al. 2013). Through introducing P-containing anionic functional groups to induce the nucleation and deposition of hydroxyapatite, these scaffolds may even be directly mineralized (Stevens 2008). Various processing techniques, such as thermally induced phase separation (Nam and Park 1999), molecular self-assembly (Whitesides, Mathias et al. 1991), and electrospinning (Li, Laurencin et al. 2002), have been developed to fabricate nanofibrous scaffolds to be used as ECM substitutes.

Traditional methods (e.g. freeze-frying and gas foaming) fabricated scaffolds usually contain open micron pores and submicron pores on the wall. These submicron pores were shown to influence cellular behaviors (Lee, Choi et al. 2004); (Sheridan, Gil et al. 2008). The adhesion and proliferation of MG63 human osteosarcoma cells were progressively inhibited as the substrate polycarbonate (PC) containing increased size of micropores (from 0.2 to 8.0 μm) (Lee, Choi et al. 2004). This phenomenon probably caused by surface discontinuities. Interestingly, cells protein synthesis showed reversed trend, including two osteogenic markers (alkaline phosphatase early marker and osteocalcin late marker).

In fact, as previously described in the bone biology section, the native bone tissue ECM contains micro-and nano-scale architectures. Thus, developing new techniques to mimic the native multi-scale hierarchical structure will undoubtedly benefit bone tissue engineering.

1.2.2 BTE scaffolds functionalization

In addition to providing a matrix with favorable physical-chemical properties, the functional BTE grafts with additional cues for bone regeneration is well investigated. The functional modification can take on different levels of complexity, from peptides, full-size proteins to cells, and combinations.

1.2.2.1. Peptides

Cell adhesion: Adhesive interactions with extracellular matrix play critical roles in osteoblast survival, proliferation, differentiation, and matrix mineralization, as well as in bone formation (Khatiwala, Peyton et al. 2006); (Globus, Doty et al. 1998). Furthermore, adhesive interactions are also important for osteoclast function and bone resorption (Fisher, Caulfield et al. 1993). Thus, various mimetic peptide sequences, such as Arg-Gly-Asp (RGD) peptides (Yoon, Song et al. 2004), P-15 peptide (Mobbs, Maharaj et al. 2014), PHSRN (Feng and Mrksich 2004, Aye, Li et al. 2018), are incorporated into scaffolds to mediate cells adhesion and spreading, specifically for scaffolds lacking cell recognition signals (synthetic polymer made scaffolds). Such scaffolds have ultimately demonstrated enhanced osteogenesis and osteointegration *in vivo* (Visser, Rico-Llanos et al. 2016).

Cell adhesion to extracellular matrix ligands is primarily mediated by integrins, a widely expressed family of transmembrane receptors. As described before, the integrin-ligands binding is important to regulate mesenchymal stem cell commitment and osteoblastic differentiation. RGD sequence, which presents in many bone ECM molecules (e.g. fibronectin, bone sialoprotein-1, osteopontin), is recognized by cellular integrin receptors. The RGD is probably the most commonly adopted peptide motif to modify BTE scaffolds (e.g. PLGA-RGD (Yoon, Song et al. 2004); PCL-RGD (Zhang, Lin et al. 2009); PLLA-RGD (Ho, Hou et al. 2006); PLA/starch-RGD (Gutierrez-Sanchez, Escobar-Barrios et al. 2019); poly(propylene fumarate-co-ethylene glycol)-RGD (Behravesh and Mikos 2003). RGD motifs functionalized BTE scaffolds exhibit enhanced *in vitro* osteogenic cell adhesion, proliferation, differentiation, and *in vivo* bone formation. In addition, the RGD-integrin interaction specificity, especially RGD-α5β1, could be improved by inclusion of flanking residues and constraining the conformation of the RGD motif to a loop *via* cyclization (Scarborough, Naughton et al. 1993); (Mould, Askari et al. 2000).

Osteogenic ability: To stimulate stem cells toward osteoblastic differentiation, peptides with osteogenic function are incorporated into BTE grafts (Bab and Chorev 2002); (Jabbari 2013); (Visser, Rico-Llanos et al. 2016). Most of the osteogenic peptides are derived from BMPs, especially BMP-2, such as NSVNSKIPKACCVPTELSAI (Suzuki, Tanihara et al. 2000),

KIPKA***SS***VPTELSAIS***T***LYL (Saito, Suzuki et al. 2003), KIPKA***SS***VPTELSAIS***T***LYLD***DD*** (Niu, Feng et al. 2009). Additionally, synthetic peptides from human type I collagen (i.e. NGLPGPIGP), parathyroid hormone (i.e. PTH1–34) were shown to enhance BTE grafts *in vivo* function as well (Wang, Misra et al. 2008); (Takahata, Schwarz et al. 2012). Osteogenic growth peptide (OGP) is a naturally occurring 14-mer peptide in serum. Proteolytic cleavage of OGP yields a C-terminal YGFGG pentapeptide, known as OGP10–14, which activates an intracellular G_i-mitogen-activated protein (MAP) kinases signaling pathway, and then downstream osteogenic response (Gabarin, Gavish et al. 2001);(Bab and Chorev 2002).

Angiogenic feature: QK peptide (K***LTWQEL***YQ***LK***Y***KGI***) derived from angiogenic endothelial growth factor (VEGF) has been described to help BTE grafts vascularization(D'Andrea, Iaccarino et al. 2005); (Finetti, Basile et al. 2012).

Immune-modulating: Thrombin peptide 508 (TP508, aa 508-530 of thrombin), was recently shown to have an immune-modulating function on bone regeneration. It activates the same signaling pathways stimulated by TNF-α, IL-1, and other pro-inflammatory cytokines during fracture healing (Wang, Li et al. 2005). Delivery of TP508 from PLGA microspheres to critically sized ulnar defects of New Zealand White rabbits significantly accelerated defects restoration (Sheller, Crowther et al. 2004).

1.2.2.2 Growth factors and signaling molecules

Bone regeneration is a complex physical process, dozens of growth factors and signaling molecules are involved in recruiting cells, and stimulating their proliferation and differentiation (Dimitriou, Tsiridis et al. 2005); (Herrmann, Verrier et al. 2015). Local delivery of these growth factors and signaling molecules that accelerate osteogenesis and vascularization from an implanted graft certainly benefits bone regeneration. The exogenous proteins can be incorporated into the BTE scaffolds by simply soaking for subsequent fast release, by encapsulation in scaffolds, or by covalent immobilization for controlled and extended-release (reviewed in (Amini, Laurencin et al. 2012)).

To restore the defect bone tissue, the bone-forming cells (e.g. MSCs) and blood vessel forming cells (e.g. EPCs) are needed. They can be pre-seeded or recruited into the implanted graft. Stromal derived factor-1 (SDF-1, also referred to as CXCL12) is one

of the chemokines that have critical role in the recruitment of MSCs. CXCR4, the receptor of SDF-1, positive MSCs homing to the bone lesion site under chemotaxis toward SDF-1 (Granero-Molto, Weis et al. 2009). Numbers of *in vivo* studies have shown local delivery of SDF-1 promote bone healing. For instance, collagen scaffolds loaded with SDF-1 effectively promoted cartilage regeneration in rabbit osteochondral defects when compared with empty collagen scaffolds (Chen, Tao et al. 2015).

Later, the incoming MSCs differentiate to bone-forming osteoblasts or cartilage forming chondrocytes, which mediate the intramembranous ossification and endochondral ossification. Bone morphogenetic proteins (BMPs) mediated signaling is the most well-studied bone regeneration pathway (Fig. 5). BMPs are members of the TGF-β superfamily. There are a number of osteogenic BMPs, in which BMP-2, BMP-4, and BMP-7 are the most characterized BMPs. Since 1992, Yasko and colleagues demonstrated the successful union of segmental bone defects of rat femora using recombinant human BMP2 (rhBMP2) (Yasko, Lane et al. 1992), numerous studies develop rhBMPs-based strategies for bone regeneration. In 2002, rhBMP2 (INFUSE® Bone Graft) was approved by the American Food and Drug Administration (FDA) for clinical usage in United States followed by rhBMP7 (Osigraft®) in 2004 approved by European Medicines Agency (EMA).

Concurrent with MSC expansion and preceding bone formation callus, tissue must undergo angiogenesis for proper healing to occur (Hankenson, Dishowitz et al. 2011). It was shown that the highest amount of new bone formation occurs in the most vascularized areas. In contrast, inadequate vascularization leads to decreased bone tissue repair and regeneration, and has been identified as the major pitfall to successful BTE. Vessels not only provide oxygen, but also are a conduit for additional osteoblasts, play a positive-signaling role for promoting cell differentiation, and are required for endochondral ossification.

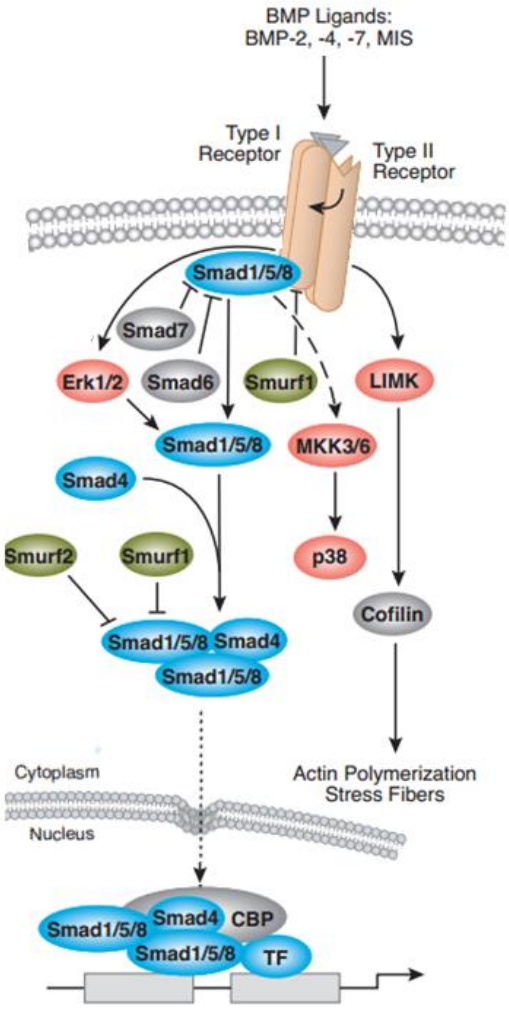

Fig. 5. BMPs signaling. BMP signaling is initiated by the ligand binding to type I and type II BMP receptors which are serine/threonine kinase receptors complexing into transmembrane heterodimer. Upon binding of BMPs to their receptors, the activated receptors initiate two intracellular transduction pathways: the canonical Smad pathway and non-canonical mitogen-activated protein kinase (MAPK) pathway. In the canonical pathway, activated receptor recruits and phosphorylates Smad 1/5/8, which then translocate to the nucleus associated with Smad 4. The Smads complex together with Runx2 activate the expression of downstream osteogenic genes such as alkaline phosphatase (ALP), osteocalcin (OCN), osteopontin (OPN). The MAPK pathway is Smad independent and includes the activation of extracellular signal-regulated kinase 1/2 (ERK1/2), p38, and c-Jun NH2-terminal kinase (JNK1/2) resulting in Runx2 expression upregulation. Modified from Cell Signaling of TGF-β Signaling: https://www.cellsignal.com/contents/science-cst-pathways-developmental-biology/tgf-signaling/pathways-tgfb (accessed on 1/2/2020).

SDF-1 mediates endothelial progenitor cell mobilization and homing, as well as vascular endothelial growth factor (VEGF), and thus directly promotes angiogenesis (Herrmann, Verrier et al. 2015). Wernike *et al.,* investigated the effects of incorporation of VEGF into biphasic calcium phosphate (BCP) ceramics on bone healing (Wernike, Montjovent et al. 2010). The VEGF promoted BCP grafts vascularization, osseointegration, and bone formation in critical-size cranial defects in Balb/c mice. The authors mentioned that the sustained release of low concentration of VEGF is important for the promotion of bone grafts vascularization and bone formation, as burst release of VEGF leads to the formation of abnormal, nonfunctional vessels.

Multiple growth factors delivery along spatial and temporal gradients may results in enhanced results, as physical bone tissue development is controlled by the interaction of multiple growth factors. Studies have shown that combinations of BMP with VEGF obtain a robust success (Zhang, Zhu et al. 2014); (Lv, Xiu et al. 2015). Silk scaffolds loaded with VEGF and BMP2 accelerated rabbit skull defects (Zhang, Zhu et al. 2014). It was hypothesized that local release of VEGF and BMP-2 facilitated the mobilization of endogenous stem cells and directed the differentiation of these cells into endothelial and osteogenic lineages. The incorporation of SDF-1 and BMP-2 also resulted in accelerated bone regeneration (Herberg, Susin et al. 2014).

Local delivery of growth factors is either driven by passive diffusion (absorbed proteins) or coupled to the rate of biomaterial degradation (encapsulated and covalently linked proteins). The growth factors release in tune with the actual healing process and cellular demand is critical and can be altered by the varying the amount of growth factor added or the degradation rate of the material. It has been demonstrated that uncontrolled VEGF release arose malformed and malfunctioned vasculature. Hence, the key obstacle that limits rhBMP-2 clinical application is the supraphysiological dose induced complications, such as ectopic bone formation, cancer induction, and inflammation. The controlled release will address the dose-related adverse effects.

1.2.2.3. Cells

Cellular-based approaches in BTE primarily benefits the early stages of bone repair when the recruitment of skeletal progenitors may be impaired. The mechanisms behind could be: 1) early release of key osteogenic and vasculogenic growth factors

and signaling molecules; 2) recruit host osteogenic and vasculogenic cells; 3) actively laying down bone matrix and vascularizing the bone construct.

Several cell types have been assessed for their abilities to promote bone repair and regeneration: mesenchymal stem cells (MSCs), embryonic stem cells (ESCs), and induced pluripotent stem cells (iPSCs).

Mesenchymal stem cells (MSCs) are recognized for their potential in engineering bone grafts because they differentiate and form bone during the natural bone development process. MSCs have been isolated from a number of adult sources, mainly bone marrow (Bianco, Riminucci et al. 2001), peripheral blood (Kuznetsov, Mankani et al. 2001), dental pulp (Shi and Gronthos 2003), adipose tissue (Zuk, Zhu et al. 2002).

The incorporation of MSCs into BTE scaffolds is a widely studied strategy for accelerated bone formation through osteogenic differentiation and stimulation of the migration and differentiation of host osteoprogenitors. In addition, pre-differentiating MSCs towards the osteogenic lineage before implantation has been shown to further accelerate defect repair and osteointegration of the construct *in vivo* by delivering a more mature osteogenic population capable of immediate bone formation. Pre-clinical trials with MSC-seeded constructs have proven effective in accelerating bone repair in various scenarios, including critical-size femoral defects, cranio-maxillofacial deformities, and spinal fusions (Mauney, Volloch et al. 2005).

Also, MSCs have been shown to have the immune-suppressive ability (i.e., immune-privileged). Specifically, MSCs do not induce the proliferation of lymphocytes, and they suppress the proliferation of T cells and cytokine production in response to alloantigens or insignificant mitogens, as well as inhibiting the function of B cells, dendritic cells, and the natural killer cells. These data greatly pushed up the therapeutical appeal of MSCs in BTE.

Although MSCs seem to represent a great cellular option to functionalize BTE, several issues with their use have been identified. First, the lack of knowledge about common markers for MSCs isolated from different sources makes it difficult to define MSCs. Second, the low proliferation ability (with senescence-associated growth arrest after 24–40 population doublings). Third, osteogenic differentiation potential *in vitro* and

bone-forming efficiency *in vivo* significantly decreases with increasing donor age and systemic disease.

Adipose-derived mesenchymal stem cells (ADMSCs) represent an easily accessible, widely available, and abundant source of autologous osteogenic cells. Lipoaspirates house a relatively high frequency of ADSCs (1 to 5% of isolated cells), in comparison to MSCs in bone marrow (0.001% to 0.1% of isolated cells) (Amini, Laurencin et al. 2012).

Unlike MSCs, EPCs have very relatively high and long-term proliferative potential (more than 1,000 population doublings), and maybe quickly expanded for clinical use. When cultured on and within Matrigel, EPCs display complex and intricate network showing the angiogenic ability (Nukavarapu and Amini 2011). Delivery of EPCs to a bone defect in rats, did result in an increased angiogenesis in the bone calluses compared to rats that did not receive EPCs (Hankenson, Gagne et al. 2015).

Combination of angiogenic cells and osteogenic cells in BTE constructs is proved to have better function in accelerating bone regeneration. For instance, the *in vitro* formed premature vessels by the endothelial cells may later mature and anastomose with the host vasculature upon implantation. (Amini, Laurencin et al. 2012); (Fedorovich, Haverslag et al. 2010). Yu et al. also noted that central necrosis is avoided when scaffolds are seeded with EPCs and MSC derived osteoblasts, which is not the case when only osteoblasts are seeded alone and implanted (Yu, Vandevord et al. 2008).

Tissue regeneration is the result of an interplay between cells and growth factors. Growth factors/signaling molecules regulate cell migration, proliferation, and tissue formation and morphogenesis. As discussed before, multiple cell types and a number of signaling molecules are involved in bone repair processes. To recapitulate some of these events, the functionality of BTE grafts could be further improved through the combination of multiple levels of modification. Kanczler *et al.,* evaluated the function of VEGF/rhBMP2/hBMSCs incorporated into alginate/PDLLA grafts to repair mice critical-sized femur defect (Kanczler, Ginty et al. 2010). The alginate/PDLLA-VEGF/rhBMP2/hBMSCs group showed a significant increase in the quantity of regenerated bone compared to the alginate/PDLLA-VEGF/rhBMP2 and alginate/PDLLA group.

Bone marrow aspirate concentrate (BMAC) as natural sources of the autologous cells and factor cocktails was used to functionalize BTE scaffolds (e.g. Collagen sponge and Hydroxyapatite scaffold) as well (Jager, Herten et al. 2011). The BMACs are commonly harvested from the patient's iliac crest to yield a rich source of osteogenic stem cells (e.g. MSCs, EPCs, HSCs, platelets, lymphocytes, and granulocytes) and osteoinductive growth factors (e.g. PDGF, SDF-1) (Chahla, Mannava et al. 2017). Incorporated in allografts, the BMACs has proven to be a safe alternative method to promote bone unions in clinic, with effects similar to autologous bone grafting (Thua, Bui et al. 2015).

1.3. *In vitro* transcribed (IVT) mRNA for Osteogenesis

The contents of this section was adapted from part of our published review (Wang, Perche et al. 2019). The full article was listed as annex at the end of the thesis.

Despite the promising results for bone reparation in clinical studies of BTE bone substitutes, many crucial hurdles remain, such as side effects related to the supraphysiological dose of implanted osteogenic proteins (Shimer, Oner et al. 2009). Gene therapy is an alternative to conventional protein- and cell-based therapy for bone regeneration (Franceschi, Yang et al. 2004);(Evans and Huard 2015). This approach enables local expression of osteogenic factors to modulate osteogenic cells. Gene therapy is based on usage of plasmid DNA (pDNA) or RNAs (Naldini 2015). Although pDNA has been extensively studied for decades with encouraging preclinical and clinical results, side effects and low efficiency associated with nuclear trafficking are hard to bypass. Unlike pDNA, messenger RNA (mRNA) exert their function in the cytoplasm, thereby being safer and more efficient.

1.3.1. Eukaryotic mRNA and *in vitro* transcription

mRNAs are the intermediate between the genetic information stored in DNA and proteins. DNA is first transcribed into mRNA in the nucleus before mRNA exports and translation into proteins by the ribosomes in the cytoplasm. All mature eukaryotic mRNA consists of five moieties, which are the 5' methylated guanosine cap (m^7Gp3N), the 5' and 3' untranslated region (5'-UTR and 3'-UTR) flank the open reading frame

(ORF), and the 50-250 adenosine residues (poly(A) tail) (Jackson 1993); (Banerjee 1980) (Fig. 6). ORF stores protein information in the codon sequence while the rest moieties responsible for regulation of mRNA translocation, translation, and stability. Understanding the mechanisms behind mRNA translation and stability regulation has been useful to guide the design of *in vitro* transcribed (IVT) mRNA and increase the efficacy of mRNA therapy.

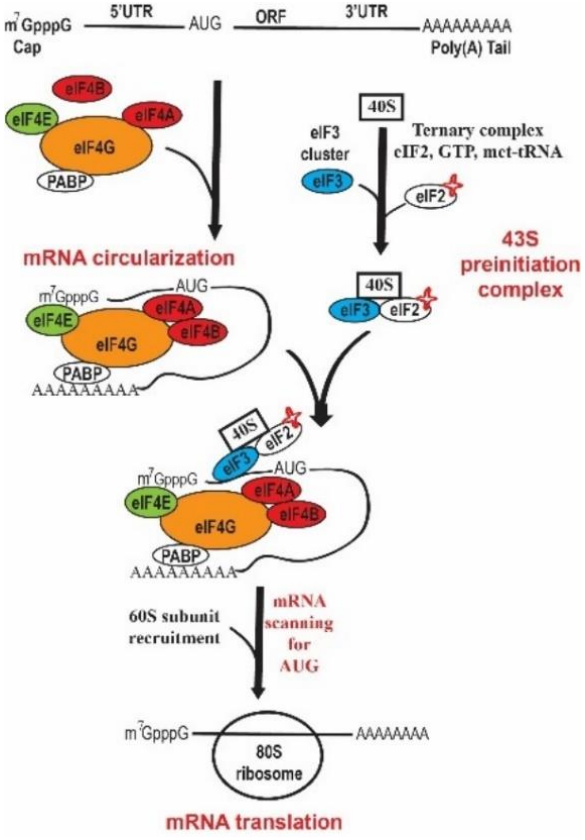

Fig. 6. Eukaryotic mRNA structure and translation initiation. Mature eukaryotic mRNA consists the 5' methylated guanosine cap (m^7Gp3N), the 5' and 3' untranslated region (5'-UTR and 3'-UTR) flank the open reading frame (ORF), and the 50-250 adenosine residues (poly(A) tail). During translation, eukaryotic translation initiation factor 4E (eIF4E) binds to the m^7Gp3N cap, and polyadenylate-binding protein 1 (PABP1) binds to the 3´ poly(A) tail, followed by recruitment of eIF4G and eIF4A, leading to mRNA circularization. The translation initiation factor 4F complex (eIF4E, eIF4G, and eIF4A) recruits 43S preinitiation complex and associated translation factors to the 5'-UTR. Next, $tRNA^{met}$ recognizes the initiation codon (AUG), and large ribosome subunit (80S) locks the ORF and starts polypeptide synthesis.

The 5’ m^7G cap is an evolutionarily conserved modification of eukaryotic mRNA with an N^7 methylated guanosine covalent to the first nucleotide of the pre-mRNA *via* a reversed 5’ to 5’ triphosphate linkage. Additional to N^7 methylation in 5’m7G cap (m7GpppN, Cap 0), in higher eukaryotes, methylation also occurs at the 2’-O position of the +1 ribonucleotide (m^7GpppNm, Cap 1) and +2 ribonucleotide (m^7GpppNmNm, Cap 2), respectively (Wei, Gershowitz et al. 1975);(Langberg and Moss 1981). The cap structure and properties were revealed in the 1970s, due to the technical development of purification mRNA based on the poly(A) structure (Edmonds, Vaughan et al. 1971); (Mendecki, Lee et al. 1972). The majority of cellular mRNA translation is initiated in a cap-dependent manner. The cap acts as an anchor for recruiting eukaryotic translation initiation factor 4F complex (eIF4F complex), including eIF4E, eIF4G, and eIF4A, which is responsible for the recruitment of 43S complex of the small ribosomal subunit and associated translation factors to form the 48S pre-initiation complex (McCormick and Khaperskyy 2017). mRNA lacks m^7G cap exhibited at least ten folds protein expression reduction (Horikami, De Ferra et al. 1984); (Lo, Huang et al. 1998). Cap analogs, such as GpppG, m^7GpppG and m^7GpppGm, are incorporated into RNAs during IVT (Konarska, Padgett et al. 1984); (Contreras, Cheroutre et al. 1982). However, one-third of the IVT mRNA is improperly capped thus poorly recognized by the translation initiation machinery (Matsuo, Li et al. 1997); (Cai, Jankowska-Anyszka et al. 1999). To address this problem, the Jemielity group developed the anti-reverse cap analog (ARCA) in which the hydroxyl group in C2 or C3 position of the m^7G is removed or substituted with methoxy group (Stepinski, Waddell et al. 2001); (Jemielity, Fowler et al. 2003). The ARCA-capped mRNA resulting in increased as well as prolonged protein expression (Mockey, Goncalves et al. 2006); (Zohra, Chowdhury et al. 2007). A further improvement in synthetic cap analogs has been achieved using sulfur to substitute a nonbridging oxygen in either the α, β, or γ-position of the triphosphate. This substitution leads to an inhibition of pyrophosphatase Dcp1p/Dcp2p mediated mRNA decapping degradation (Grudzien-Nogalska, Jemielity et al. 2007). Another option is to replace the triphosphate with tetraphosphate to increase the affinity to translation initiation factor eIF4E to the cap analog (Strenkowska, Kowalska et al. 2010).

5’ and 3’ UTRs play crucial roles in mRNA regulation of translocation (Jansen 2001), translation (van der Velden and Thomas 1999) and stabilization (Bashirullah,

Cooperstock et al. 2001). 5'-UTR regulates mRNA translation efficiency through its structure features, i.e., length, secondary structure, nucleotide sequence (Mignone, Gissi et al. 2002). The best context for translation initiation is when the starting methionine codon (AUG) is in a Kozak sequence context (GCC^{A}/$_{G}$CCAUGG) with a purine at the -3 position and a guanine at the +4 position (Kozak 1987) (Kozak 2005). Yang et al. found that mRNAs with longer 3'-UTR (>1Kb) decayed at a significantly faster rate than shorter 3'-UTR (Yang, van Nimwegen et al. 2003). Additionally, the exosome complex destructs transcripts bearing AU-rich motifs (Chen, Gherzi et al. 2001); (Mukherjee, Gao et al. 2002), especially when the AU-rich motif is located in the 3'-UTR (Yang, van Nimwegen et al. 2003).

Poly (A) tail is also essential to improve mRNA intracellular stability and for successful translation initiation. Initiation of translation requires the formation of a pre-initiation complex (PIC) which is Poly(A) tail binds to polyadenylate-binding protein 1 (PABP) then interacts with eIF4G leading to mRNA circulation (Gallie 1998). The length of the poly(A) tail is essential for mRNA stability. Eukaryotic mRNA undergoes progressive deadenylation leading to decapping followed by 5'-3' exonucleolytic degradation (Coller and Parker 2004). Transcripts with a short poly(A) tail are shown more vulnerable to decapping (Couttet, Fromont-Racine et al. 1997). In parallel, translation efficient of administered IVT mRNA is positively correlated with poly(A) tail length (Mockey, Goncalves et al. 2006); (Peng, Murray et al. 2008). The poly(A) tail could be either put on the template or added post IVT by enzymatic polyadenylation; the former strategy resulting in less polydisperse mRNA with higher translational activity (Grier, Burleigh et al. 2016).

In summary, the IVT mRNA should at least contains a cap structure, a poly(A) tail longer than 12 A residues which is the minimum poly(A) length for PABP binding (Sachs, Davis et al. 1987). For optimal expression and stability, the 5' and 3' UTR with designed sequence can be added.

1.3.2 mRNA therapy and immunogenicity

Introducing exogenous mRNA into cells to express protein of interest started three decades ago. In 1989, Malone and colleagues transfected tissue cultured NIH3T3 cells with IVT *P. pyralis* luciferase mRNA using a synthetic cationic lipid (Malone, Felgner et al. 1989). The following year, Wolff and colleagues first demonstrated the

feasibility of IVT mRNA mediated protein expression *in vivo* by direct injection of naked IVT mRNAs into mouse skeletal muscle (Wolff, Malone et al. 1990). In 1992, arginine vasopressin IVT mRNA was used to treat genetic mutation of vasopressin-induced diabetes insipidus in rat (Jirikowski, Sanna et al. 1992). The diabetes insipidus was temporarily reversed for up to 5 days. Since then, extensive studies were focused on mRNA therapy (Tavernier, Andries et al. 2011);(Schlake, Thess et al. 2018). Although mRNA design, synthesis, and delivery methods gained remarkable progress, the use of mRNA has been so far limited to vaccination because of its instability and immunogenicity (Pascolo 2008); (Schlake, Thess et al. 2018). After internalization, mRNA is mainly accumulated into endosomes, where the IVT mRNAs are recognized by Toll-like receptors (TLRs), specifically TLR3, 7, and 8, located in the endosome membrane (Kariko, Buckstein et al. 2005); (Alexopoulou, Holt et al. 2001); (Heil, Hemmi et al. 2004). Binding of RNA to TLR results in the induction of an antiviral response resulting in RNA degradation and translational shutoff. TLR3 recognizes double-stranded RNA, and TLR7/8 recognize single-stranded RNA. The TLRs stimulation induces type I interferon (INFα/β) expression and associated anti-viral responses resulting in IVT mRNA translation suppression and degradation, and even host cell apoptosis (Kariko, Ni et al. 2004); (Dan, Zheng et al. 2012). The comprehensive immune responses induced by IVT mRNA is shown in Fig. 7.

In the last 10 years, the discovery that incorporation of naturally modified nucleotides, such as pseudouridine, 5-methylcytidine, N6-methyladenosine, 5-methyluridine, or 2-thiouridine, suppressed IVT mRNA induced TLR3/7/8 activation in human DCs revitalized mRNA-based therapies (Kariko, Buckstein et al. 2005); (Freund, Eigenbrod et al. 2019). Further, Kariko and colleagues compared the influence of each modified nucleotides in mRNA translation (Kariko, Muramatsu et al. 2008). Interestingly, although pseudouridine is primarily found in tRNA, rRNA, and small nuclear RNA (Anderson, Muramatsu et al. 2010), incorporation of pseudouridine into mRNA showed the highest translation enhancement *in vitro*, because pseudouridine incorporation changed the mRNA structure motifs which can active RNA-dependent protein kinase (PKR) leading to inhibition of translation initiation by eIF2α phosphorylation (Zheng and Bevilacqua 2004). In addition to the nucleotides mentioned above, other modified nucleotides also exhibited the ability to increase mRNA translation and stability (Li, Luo et al. 2016). Svitkin and colleagues showed N1-methyl-pseudouridine modified

luciferase mRNA yield 7.4-fold luciferase expression compared to non-modified mRNA, which was higher than the 5-methylcytidine modification and their combination. In addition, they described the enhanced translation was partially contributed by suppressed eIF2α phosphorylation and increased ribosome pausing and density on the mRNA (Svitkin, Cheng et al. 2017).

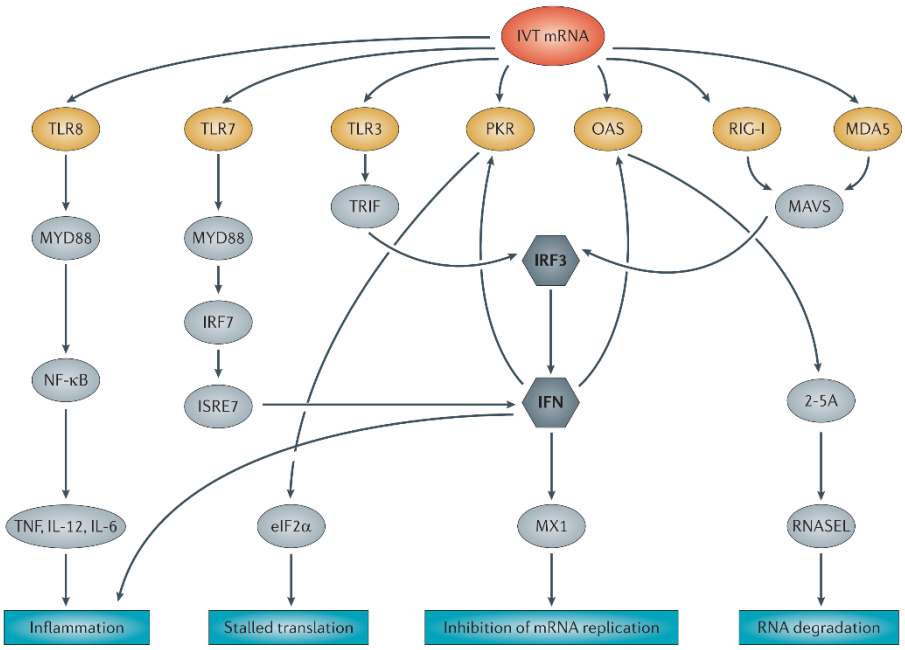

Fig. 7. Immune responses to synthetic mRNA. In vitro transcribed (IVT) mRNA is recognized by various endosomal innate immune receptors (toll-like receptor3/7/8 (TLR3/7/8)) and cytoplasmic innate immune receptors (RNA-activated protein kinase (PKR), retinoic acid-inducible gene I protein (RIG-I), melanoma differentiation associated protein 5 (MDA5) and 2′–5′-oligoadenylate synthase (OAS)). The activation of these RNA sensors results in IVT mRNA translation and replication inhibition, and degradation promotion. IFN, interferon; TNF, tumor necrosis factor; IL, interleukin; eIF2α, eukaryotic translation initiation factor 2α; RNASEL, ribonuclease L; IRF, interferon regulatory factor; ISRE7, interferon-stimulated response element; MAVS, mitochondrial antiviral signaling protein; MDA5, melanoma differentiation-associated protein 5; MYD88, myeloid differentiation primary response protein 88; MX1, myxovirus (influenza) resistance 1; NF-κB, nuclear factor-κB; TRIF, Toll-IL-1 receptor domain-containing adapter protein inducing IFNβ. Adapted from (Sahin, Kariko et al. 2014) with permission.

mRNA obtained by IVT is not uniform in length and structure. They can contain contaminants such as short RNAs generated from abortive transcription and double-stranded RNAs generated from RNA-primed transcription from RNA templates, self-complementary 3' extension, transcription runoffs and, RNA-dependent RNA polymerase activity (Milligan, Groebe et al. 1987); (Triana-Alonso, Dabrowski et al. 1995); (Arnaud-Barbe, Cheynet-Sauvion et al. 1998); (Nacheva and Berzal-Herranz 2003); (Mu, Greenwald et al. 2018). These contaminants are potent inducers of immune responses and their removal requires mRNA purification after IVT (Kariko, Muramatsu et al. 2008); (Kariko, Muramatsu et al. 2011). The purification is mostly done using chromatography to separate appropriately-sized mRNA from free nucleoside triphosphates, short RNA and DNA template (Kim, McKenna et al. 2007); (McKenna, Kim et al. 2007). The elimination of double-stranded RNA requires high-performance liquid chromatography (HPLC) purification (Kariko, Muramatsu et al. 2011); (Weissman, Pardi et al. 2013). These procedures are now used by most of mRNA-producing companies.

1.3.4 mRNA-based therapeutic for osteogenesis

mRNA as a potential therapeutic extends from vaccination to protein replacement therapy once modified mRNA was shown to facilitate *in vivo* exogenous mRNA-mediated protein expression with no or low immunogenicity (Kariko, Muramatsu et al. 2008); (Kormann, Hasenpusch et al. 2011). Zangi et al. injected modified RNA encoding human VEGF-A into mouse heart with myocardial infarction (Zangi, Lui et al. 2013). The VEGF-A expressed from modified mRNA significantly decreased the infarct size and enhanced the survival rate of recipients.

1.3.4.1 BMPs replacement therapy

For bone regeneration, recombinant BMPs have been used in therapy for over 40 years (Urist and Strates 2009). As dominant osteoinductive factors, BMPs have been delivered into the site that needs bone regeneration in the form of recombinant protein (McKay, Peckham et al. 2007) or *via* plasmid encoding BMP gene used as naked or vectorized form (Fang, Zhu et al. 1996); (Khorsand, Nicholson et al. 2017). The outcomes were promising, and the drawbacks were also apparent, as mentioned previously. Elangovan et al. employed modified mRNA encoding BMP-2 to enhance bone regeneration *in vitro* and *in vivo* (Elangovan, Khorsand et al. 2015). Using IFNα

as a marker, combined modification of pseudouridine and 5-methylcytidine almost entirely circumvented unmodified mRNA induced immune response. They compared the osteoblastic differentiation induction between the modified BMP2 mRNA and its pDNA counterpart. Bone Marrow-derived Stem Cells (BMSCs) transfected with polyethylenimine (PEI)-complexed modified mRNA (branched PEI, mol. wt. 25 kDa) yielded three times more BMP2 in the cell culture medium than cells transfected with pDNA. The osteogenic differentiation markers expression, such as alkaline phosphatase (ALP), osteocalcin (OCN), were also higher in the modified mRNA group. As a result, implanting a collagen scaffold containing modified mRNA polyplexes into rat calvarial defects showed 3.94-fold higher BV/TV (mineralized bone volume as a fraction of the total tissue volume of interest) in defect site compared to empty scaffold control. This study, for the first time, verified the safety and efficacy of using modified mRNA coding an osteogenic factor for bone regeneration. It also demonstrated the potential of modified mRNA-loaded scaffold as a novel bone graft substitute. Similarly, BMP-2 mRNA bearing methylcytidine and 2-thiouridine modification exhibited greater bone formation capacity (Balmayor, Geiger et al. 2016); (Badieyan, Berezhanskyy et al. 2016); (Balmayor, Geiger et al. 2017). Balmayor et al. prepared modified mRNA coding human BMP-2 by replacing 25% cytidine and 25% uridine with methylcytidine and 2-thiouridine. Adipo-derived mesenchymal stem cells (AMSCs) showed osteogenic differentiation once transfected with this modified BMP-2 mRNA through lipofection or magnetofection (Badieyan, Berezhanskyy et al. 2016). Interestingly, AMSCs osteogenic differentiation was dose-dependent. For *in vivo* osteogenesis, liposomal formulation of modified BMP-2 mRNA mixed with a fibrin matrix was implanted into rat femur hole model. Two weeks post-operation, rats treated with modified BMP-2 mRNA obtained ~2-fold more callus tissue than fibrin matrix alone.

Most of studies on bone regeneration have been based on the use of BMP2 since it is considered as one of the most osteogenic factors. A recent study highlighted that BMP-9 could be also used as an alternative. The efficiency of modified mRNA coding BMP-2 or BMP-9 to induce i*n vitro* osteogenic induction and *in vivo* bone regeneration have been compared in a recent report (Khorsand, Elangovan et al. 2017). BMSCs transfected with PEI-complexed modified BMP-9 had a significant increase in ALP gene expression and calcium deposition compared to modified BMP-2 mRNA, but not in Runx2 and OCN genes expression. Implanting collagen matrices containing

modified BMP-9 mRNA or BMP-2 into rat calvarial defect resulted in a similar ratio of bone volume to tissue volume. However, modified BMP-9 groups had 2-fold more density in connective tissue than BMP-2 groups, which is consistent with the *in vitro* observation.

Table 1: Summary of published studies using mRNA for *in vivo* bone regeneration.

Gene	Nucleotides modification in IVT mRNA	vector	Scaffold/cells	In vivo model	Ref.
BMP-2	$\psi_{(1)}^{*}$ and $m5C_{(1)}$	Branched PEI (25 kDa)	Collagen sponge containing 25 µg mRNA polyplexes	Rat calvarial defect-5 mm diameter	(Elangovan, Khorsand et al. 2015)
BMP-2	$s2U_{(0.25)}$ and $m5C_{(0.25)}$	cationic lipid C12-EPE with helper lipids DOPE, cholesterol, and DMPE-PEG 2k	Fibrin gel loaded with 2.5 µg mRNA lipoplexes	Rat femur diaphysis transcortical bone defect-2mm diameter	(Balmayor, Geiger et al. 2016)
BMP-2	$s2U_{(0.25)}$ and $m5C_{(0.25)}$	cationic lipid C12-EPE with helper DPPC and cholesterol, and DMG-PEG2K	Collagen sponge containing 2.5 µg mRNA lipoplexes	Rat femur diaphysis transcortical bone defect-2mm diameter	(Badieyan, Berezhanskyy et al. 2016)
BMP-2/9	$\psi_{(1)}$ and $m5C_{(1)}$	Branched PEI (mol. wt. 25 kDa)	Freeze dried collagen scaffold containing 50 µg mRNA polyplexes	Rat calvarial defect-5 mm diameter	(Khorsand, Elangovan et al. 2017)
BMP-9	$\psi_{(1)}$ and $m5C_{(1)}$	Branched PEI (mol. wt. 25 kDa)	Freeze dried collagen membrane containing 10 µg mRNA polyplexes	Rat calvarial defect-5 mm diameter	(Khorsand, Elangovan et al. 2018)
BMP-2	$5IU_{(0.35)}5IC_{(0.075)}$	cationic lipid C12-(2-3-2) with helper lipids DPPC, cholesterol,	Vacuum dried collagen sponge containing 2.5 µg or 5 µg mRNA lipoplexes	Rat femoral segmental bone defect-5mm diameter	(Zhang, De La Vega et al. 2018)

		and DMG-PEG 2k			

*, the subscripted value represents the proposition of modified nucleotides in the IVT mRNA;

Ψ, pseudouridine; m5C, 5-methylcytosine; 5IU, 5-iodo-uridine; 5IC, 5-iodo-cytidine; s2U, 2-thiouridine; C12-EPE: DOPC, 1,2-Dioleoyl-sn-Glycero-3-Phosphocholine; DPPC, 1,2-dipalmitoyl-sn-glycero-3-phosphocholine; DMG-PEG2K, 1,2-dimyristoyl-rac-glycero-3-methoxypolyethylene glycol-2000; DMPE-PEG2K, 1,2-distearoyl-sn-glycero-3-phosphoethanolamine-N-[amino(polyethylene glycol)-2000;

1.3.4.2 Reprogramming proteins replacement

Stem cells with osteogenic differentiation capacity have great applications in engineering bone substitutes with biocompatible scaffolds for bone regeneration (Amini, Laurencin et al. 2012). Mesenchymal stem cells are good candidates due to their bispecific differentiation toward osteogenic lineages. However, their limited proliferation in elderly patients and multi-passage induced senescence limit their clinical applications (Jones and Yang 2011). On the contrary, iPSCs (induced pluripotent stem cells) derived from somatic cells, typically fibroblast reprogramming, have the potential to circumvent this obstacle, with a lower rate of iPSCs senescence after expansion, both *in vitro* and *in vivo*. (Takahashi and Yamanaka 2006); (Takahashi, Tanabe et al. 2007). iPSCs showed osteogenic differentiation under stimulation of osteogenic factors (Teng, Liu et al. 2014); (Csobonyeiova, Polak et al. 2017).

Warren et al., reprogrammed fibroblasts to iPSCs by transfecting them with a mix of pseudouridine and 5-methylcytidine containing IVT mRNAs encoding reprogramming transcription factors which are KLF4/ c-MYC/ OCT4/ SOX2 (KMOS) or KLF4/ c-MYC/ OCT4/ SOX2/ LIN28 (KMOSL), respectively (Warren, Manos et al. 2010). The KMOSL mRNAs mix induced ESC-like colonies almost ten days earlier than the KMOS mRNAs mix, consistent with the previous report that LIN28 facilitated reprogramming (Yu, Jin et al. 2017); (Hanna, Saha et al. 2009).

1.4. Viral Immune Evasion Proteins Enhance IVT mRNA Performance

One of the main obstacles for developing IVT mRNAs for protein replacement related applications (e.g. somatic cell reprogramming, tissue regeneration) is the IVT mRNAs induced cellular innate immune responses.

The strong and detrimental immune responses against foreign RNAs are conserved mechanisms of cells to defend against RNA virus infection. However, during the millions of years of coexisting with their hosts, viruses have learned how to manipulate host immune control mechanisms (Alcami and Koszinowski 2000); (Katze, He et al. 2002).

Viruses express various immune evasion proteins (e.g. K3L, E3L, B18R, NS1) which directly interact with innate immunity proteins (e.g. IFNs, RIG-I, PKR), and impair the triggering of antiviral responses.

Mimicking this viral immune-evasion process could, therefore, be an interesting strategy to bypass the mRNA-triggered immune responses and increase the transfection efficiency of IVT mRNA based gene delivery systems (Devoldere, Dewitte et al. 2016). The viral derived immune evasion protein(s) could be introduced either in form of protein or in form of IVT mRNA. B18R (from DNA virus) and NS1 (from RNA virus) are two represent viral proteins that proved to enhance IVT mRNA administration.

1.4.1 B18R

B18R is a secreted protein with three immunoglobulin domains encoded by Vaccinia Virus Western Reserve gene B18R. B18R exerts its function as a soluble receptor for type I IFNs (IFNα/β) with high affinity and broad species specificity (Fig. 8). It protect cells from the antiviral reactions induced by IFNα/β (Alcamí, Symons et al. 2000).

Recombinant B18R is broadly used as cell culture medium supplement during *in vitro* IVT mRNA transfection helping to maintain cell viability and IVT mRNA translation (Warren, Manos et al. 2010); (Yoshioka, Gros et al. 2013); (Zangi, Lui et al. 2013). The incorporation of B18R interferon inhibitor is especially useful for cell reprogramming, as multi-transfection usually needed.

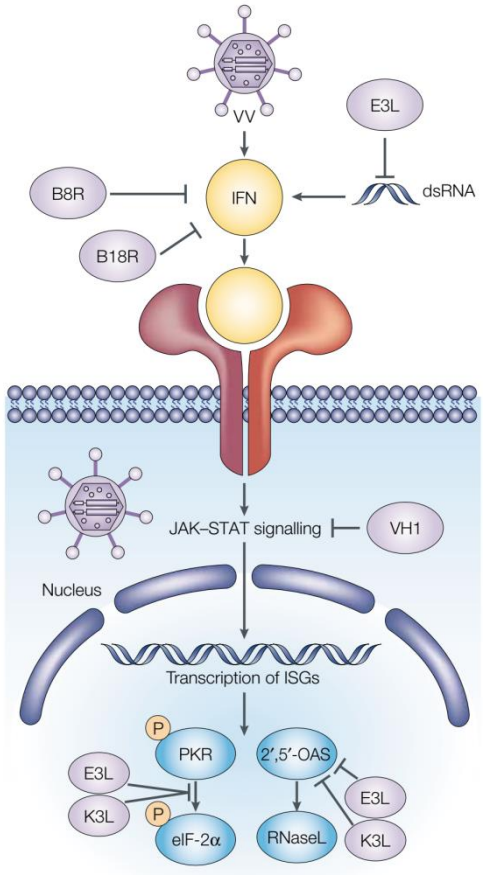

Fig. 8. Interplay between the IFN pathways and vaccinia virus. Vaccinia virus and other poxviruses encode soluble interferon (IFN) receptors (B8R and B18R) that block the binding of IFNs to their cell-surface receptors. The vaccinia virus E3L gene product is a double-stranded (ds) RNA-binding protein that inhibits activation of the protein kinase PKR and blocks IFN responses by sequestering dsRNA molecules. The vaccinia virus K3L gene encodes a eukaryotic initiation factor 2, α-subunit (eIF-2α) homologue that interferes with PKR function by acting as a pseudosubstrate. Both E3L and K3L gene products have also been proposed to block the IFN-induced 2′,5′-oligoadenylate synthetase (OAS) antiviral pathway. The vaccinia virus VH1 phosphatase, a virion component, intercepts the IFN signaling pathway through dephosphorylation of signal transducer and activator of transcription 1 (STAT1). JAK, Janus kinase. Adapted from (Katze, He et al. 2002) with permission.

The addition of recombinant B18R is efficient to inhibit IFNs response, while only suitable for *in vitro* application. Michel and colleagues tested the effects of B18R

translated from administered synthetic B18R-coding mRNA (Michel, Golombek et al. 2019). The co-delivery of enhanced green fluorescent protein (eGFP) mRNA with B18R encoding mRNA to fibroblasts over 7-days resulted in comparable cell viability and eGFP protein expression as in the cells transfected with eGFP mRNA and incubated with B18R protein.

Although IFNα/β are the most critical factors in cellular innate immune responses, blocking the engagement of IFNs with their receptors is not sufficient to inhibit the immune responses. Thus, the DNA viruses, e.g., vaccinia viruses, encode VH1 phosphatase to block IFN signaling transduction, and E3L and K3L to block the activation of IFN-induced effectors (Fig. 8). It is impractical to incorporate all these immune evasion proteins during synthetic mRNA administration.

1.4.2. Influenza A virus (IAV) nonstructural protein 1 (NS1)

Unlike the single function of B18R, IAV nonstructural protein 1 (NS1) is a multifunctional protein helping influenza virus genome replication and virulence (Katze, He et al. 2002); (Hale, Randall et al. 2008) (Fig. 9, 10). The proteins encoded by RNA viruses are usually multifunctional, as the genome size of RNA viruses is limited; thus, there is little room in the genome to allow immune defenses to be encoded by individual genes (Alcami and Koszinowski 2000).

1.4.2.1. NS1 structure

The NS1 protein is encoded from viral RNA segment eight, containing a strain-specific length of 215–237 amino acids (aa), and an approximate molecular mass of 26 kDa (Krug and García‐Sastre 2013) (Fig. 9). From the functional perspective, NS1 is divided into two domains connected by a short linker: an N-terminal RNA-binding domain (RBD, residues 1–73), which binds to several RNA species, and a C-terminal effector domain (ED, residues 88 – end), which predominantly mediates interactions with host-cell proteins, but also functionally stabilizes the RNA-binding domain. Full-length NS1 exists as a homodimer, with both the RNA-binding and effector domains contributing to multimerization. The RNA-binding domain alone is a symmetrical homodimer with each monomer consisting of three α-helices (Liu, Lynch et al. 1997); (Chien, Tejero et al. 1997). Dimerization is essential for binding dsRNA (Wang, Riedel et al. 1999). The C-terminal effector domain of both human and avian NS1 protein

(residues 88–230) can independently homodimerize, with each monomer consisting of seven β-strands and three α-helices (Bornholdt and Prasad 2006). The sequence of NS1 proteins from different virus strains is largely conserved. The most abundant sequence variations occur in the C-terminal region of the ED (Hale, Randall et al. 2008).

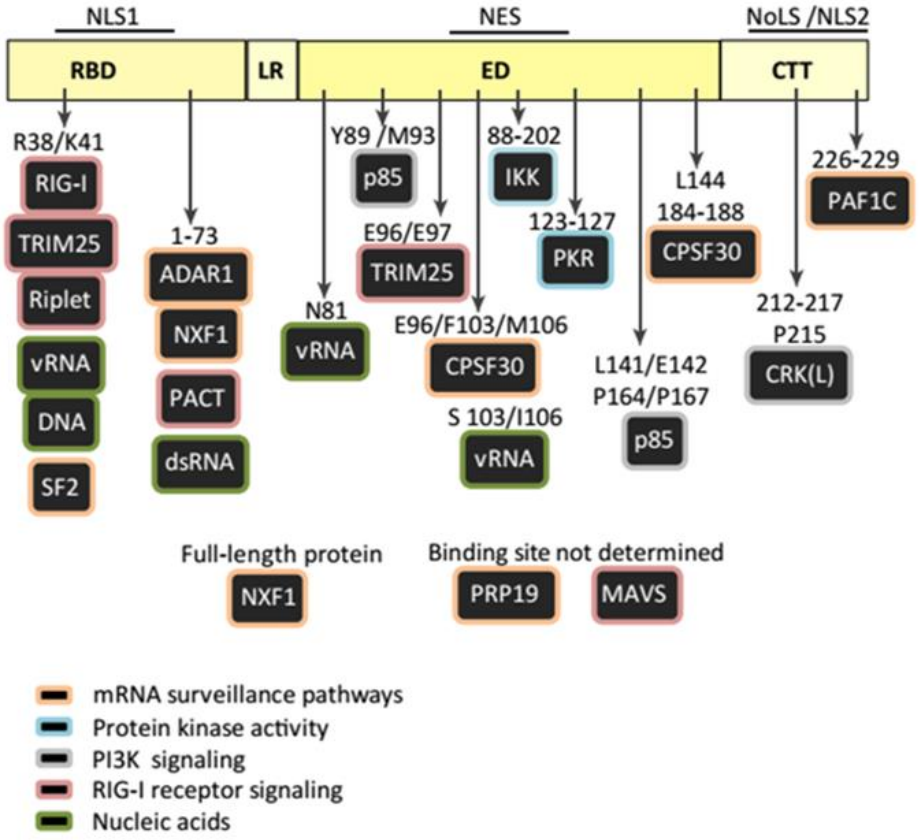

Fig. 9. Schematic representation of the NS1 protein, together with its known interactors. Full-length NS1 encompasses 202–237 amino acids (aa). The RNA binding domain (RBD) is located withinthe first 73 aa, followed by a linker domain (LR), an effector domain (ED), which is formed by residues 88–202, and a Cterminal tail (CTT). Two nuclear localisation signals (NLSs) are located in the RBD (NLS1) and at the C terminus (NLS2). Depending on the strain, an additional nucleolar localisation signal (NoLS) is associated with NLS2. The ED harbours a nuclear export signal (NES). Residues R38 and K41 of the RBD interact with RIG-I, TRIM25, Riplet, viral mRNA (vRNA), cellular DNA, and SF2. Furthermore, ADAR1, PACT, NXF1, and double-stranded RNA can bind the RBD. The ED harbours binding sites for vRNA, p85, TRIM25, CPSF30, IKK, and PKR. Within the CTT, CRK(L) and PAF1C can bind.

Interactions with PRP19 and MAVS-NS1 have been reported but the binding sites have not yet been determined. Functional clustering of interaction partners is represented by different border colours. Adapted from (Klemm, Boergeling et al. 2018) with permission.

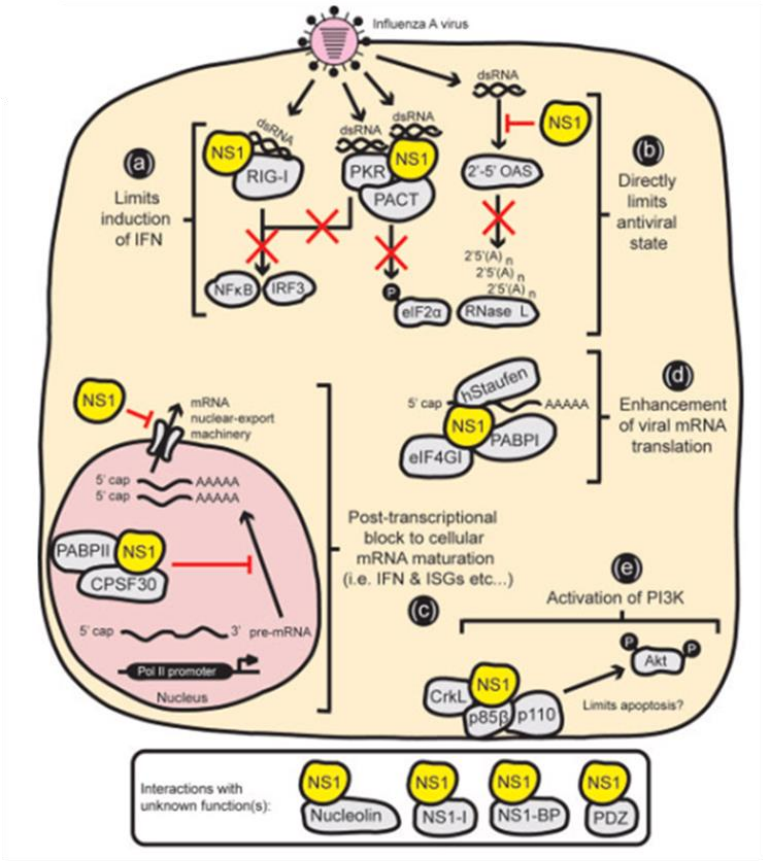

Fig. 10. Schematic diagram of the multiple functions of NS1 within infected cells. (a) Pre-transcriptional limitation of IFN-b induction. (b) Inhibition of the antiviral properties of PKR and OAS/RNase L. (c) Post-transcriptional block to processing and nuclear export of all cellular mRNAs. (d) Enhancement of viral mRNA translation. (e) Activation of PI3K. Interactions with unknown consequences and/or localizations are detailed in the lower box. Adapted from (Hale, Randall et al. 2008) with permission.

1.4.2.2. NS1 and the host innate immune response

Upon influenza virus infection, the virus compounds are recognized by patterns recognization receptors (PRRs), including endosome membrane located Toll-like receptors (TLRs) and cytoplasmic retinoic acid-induced gene I (RIG-I)-like receptors (RLRs). Influenza virus double-stranded RNAs (dsRNAs) or single-stranded RNAs (ssRNAs) are recognized by the TLR3 or TLR7 and 8, respectively, and by the RIG-I that detect dsRNAs and 5'- triphosphates bearing ssRNAs. The virus RNA-PRRs interaction actives downstream transcription factors (i.e. IFN regulatory factor 3/7 (IRF3/7), nuclear factor kappa B (NF-κB), and activator protein 1 (AP-1)), leading to the transcription of type I and type III IFNs and pro-inflammatory cytokines. Secreted type I and III IFNs bind to their transmembrane receptors to induce the expression of IFN-stimulated genes (ISGs), many of which display antiviral activity, such as myxovirus resistance (Mx), IFN-induced transmembrane (IFITM), dsRNA-dependent protein kinase R (PKR), and 2'-5' oligoadenylate synthetase (OAS). NS1 plays a key role in IAV counteracting host antiviral activities (Fig. 10).

A. Inhibition of IFNs production

Plenty of studies showed that NS1 proteins could limit IFNs production *via* multi-strategies, from pre-transcriptional initiation to post-transcriptional modification.

Upon influenza virus infection, the regulation of IRF3/7 is the most important for IFNs expression. In one mechanism, the NS1 protein blocks RIG-I to inhibits the activation of the IRF3/7 transcription factors that are required for the activation of IFNs transcription (Mibayashi, Martinez-Sobrido et al. 2007); (Gack, Albrecht et al. 2009); (Rajsbaum, Albrecht et al. 2012); (Tawaratsumida, Phan et al. 2014); (Feng, Sun et al. 2017) (Fig. 11).

RIG-I is composed of two N-terminal caspase activation and recruitment domains (CARD1 and CARD2), ATPase containing DEAD box helicase (DEAD helicase), and a regulatory C-terminal domain (CTD). Binding to foreign RNAs possessing 5'-triphosphate groups or 5'-diphosphate groups (Schlee and Hartmann 2010); (Goubau, Schlee et al. 2014) induces a structural change in RIG-I that exposes the CARDs (Myong, Cui et al. 2009). This transformation allows CARD2 to be ubiquitinated at Lys172 by tripartite motif-containing protein 25 (TRIM25) (Gack, Albrecht et al. 2009)

and at Lys154, 164 and 172 by Riplet (also known as RNF135 or REUL) (Oshiumi, Matsumoto et al. 2009). The ubiquitinated CARD2 then bind to the CARD domain of the mitochondrial membrane-associated protein (MAVS: mitochondrial antiviral signaling protein; also known as IPS-1: interferon-beta promoter stimulator 1). This ultimately leads to the nuclear translocation of the transcription factors IRF3/7, AP-1 (c-Jun/ATF-2), and NF-κB, which drive transcription of the type I IFN genes, thereby stimulating the innate antiviral response to influenza infection (Loo and Gale 2011).

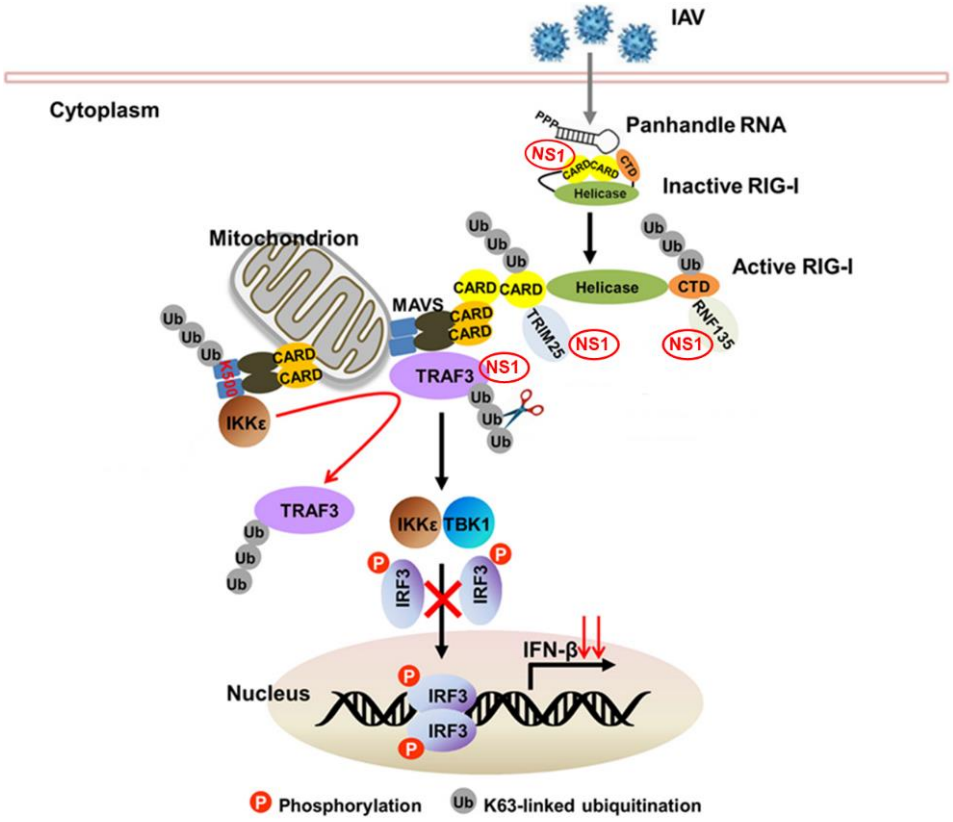

Fig. 11. Scheme of TRAF3-dependent regulation of RIG-I signaling pathway by NS1. The NS1 protein of IAV inhibits host IFN-β production by binding to RIG-I CARD2 domain, TRIM25 and/or RIPLET proteins required for RIG-I activation. In addition, the NS1 associates with TRAF3 leading to remove of the Lys63-polyubiquitin and disruption of the MAVS–TRAF3 complex. The release of TRAF3 from the mitochondria, further decreasing the level of K63-linked ubiquitination and impairing IRF3 phosphorylation. Modified from (Qian, Wei et al. 2017) with permission.

Data of co-immunoprecipitation experiments demonstrated that NS1 formed complexes with RIG-I to inhibit RIG-I activation (Mibayashi, Martinez-Sobrido et al. 2007); (Opitz, Rejaibi et al. 2007); (Guo, Chen et al. 2007). Jureka and colleagues found the A/Brevig Mission/1918 NS1-RIG-I interaction is made directly through NS1-RBD and RIG-I-CARD2 binding, instead of mediated by other intermediates (Jureka, Kleinpeter et al. 2015). The RBD-CARD2 binding is strain-specific, as A/Udorn/1972 NS1-RBD did not bind to CRRD2. Further assessment revealed the Arg21 residue in A/Brevig Mission/1918 NS1-RBD (Gln21 in A/Udorn/1972 NS1-RBD) is necessary, but not sufficient, for the RBD and CARD2 binding.

Moreover, NS1 proteins inhibit RIG-I by interacting with ubiquitin E3 ligases TRIM25 and Riplet, which ubiquitin and activate RIG-I (Gack, Albrecht et al. 2009); (Rajsbaum, Albrecht et al. 2012). The R38/K41 in NS1-RBD and E96/E97 residues in NS1-ED (from A/PR/8/34, A/Texas/36/, A/New Caledonia/20/99, A/Wyoming/3/2003, and A/Panama/2007/99) mediate its interaction with the coiled-coil domain of TRIM25, thus blocking TRIM25 oligomerization and subsequent RIG-I CARD domain ubiquitination (Gack, Albrecht et al. 2009). The R38A/K41A mutation hindered the interaction of NS1-TRIM25 and NS1-Riplet, however E96A/E97A mutation only affected NS1-TRIM25 interaction (Rajsbaum, Albrecht et al. 2012).

Besides, the protein activator of the interferon-induced protein kinase (PACT) is another NS1 binding partner (Kok, Lui et al. 2011); (Tawaratsumida, Phan et al. 2014). PACT is a dsRNA binding protein containing three dsRNA binding domains that mediate protein-protein interactions among different dsRNA binding proteins. PACT actives RIG-I *via* its interaction with the CTD of RIG-I (Brisse and Ly 2017). NS1 (A/PR/8/34, A/laughing gull/Delaware bay/42/2006, A/Perth/16/2009, and A/quail/California/D113023808/2012) binds PACT during virus replication and blocks PACT/RIG-I-mediated activation of IFN-I (Tawaratsumida, Phan et al. 2014). The NS1-RBD is important for this protein-protein interaction, evidenced by R38A/K41A mutation significantly reduced, albeit not completely abolished, NS1-PACT binding.

Moreover, NS1 indirectly regulates RIG-I signaling by induction of the ubiquitin-editing protein A20 (also known as TNFAIP3) upon infection (Feng, Sun et al. 2017). A20, acting as a negative feedback regulator of inflammation and immunity, has been shown to mediate suppression of RIG-I-induced innate antiviral state following viral

infection. Cells (A549) transfected with NS1 (A/Goose/Guangdong/3/97, A/FPV/Rostock/34, A/WSN/1933, A/Puerto Rico/8/34, A/Puerto Rico/8/34/Mount Sinai, A/bar-headed goose/Qinghai/3/2005) coding plasmids showed increased A20 expression, however, the mechanism behind this A20 induction is yet to be revealed.

Recent studies demonstrate that NS1 blocks RIG-I/MAVS downstream signaling pathway as well (Gao, Song et al. 2012); (Qian, Wei et al. 2017). The NS1-ED (126-225) (A/duck/Hubei/hangmei01/2006) but not the NS1-RBD, binds TNF receptor-associated factor 3 (TRAF3), a key component in RIG-I/MAVS downstream signaling pathway. Further analysis showed that NS1/126-225 binds to TRAF3 through the TRAF domain, subsequently decreasing TRAF3 K63-linked ubiquitination. NS1/126-225-TRAF3 binding also disrupted the formation of the MAVS–TRAF3 complex, increasing the recruitment of IKKε to MAVS, ultimately shutting down the RIG-I-mediated signal transduction and cellular antiviral responses.

NS1 targets the NF-κB pathway by blocking inhibitor of kappa B (IκB) kinase (IKK) to prevent NF-κB activation and nuclear translocation (Wang, Li et al. 2000); (Ruckle, Haasbach et al. 2012); (Gao, Song et al. 2012). NS1-ED (A/Qinghai/12/05, A/WSN/33) could directly bind the N-terminal kinase domain of IKKα/β, thus reduce IκB phosphorylation and classic NF-κB activation (Gao, Song et al. 2012). IKKα is required for activation of the alternative NF-κB pathway through the phosphorylation and processing of p100 to p52 (Lawrence 2009). NS1-IKKα interaction significantly decreased the p52 level in host cells.

The nuclear localization sequence (NLS) enables NS1 not only exert its function in the cytoplasm but also in nucleus (Hale, Randall et al. 2008).

The NS1 protein from H3N2 strains possesses a ARSK sequence (amino acids 226–229) that is chemically analogous to the ARTK4 sequence that comprises the lysine 4 site (H3K4) of histone H3, which leads to directing binding to the human RNA polymerase associated factor 1 (hPAF1) complex (hPAF1C) (Marazzi, Ho et al. 2012). PAF1C attracts particular interest because it has been implicated in transcription elongation (Kim, Guermah et al. 2010). The NS1-hPAF1C interaction reduces virus- and type I interferon-induced gene expression.

Through binding to the two zinc-finger regions in the 30 kDa subunit of cleavage and polyadenylation specificity factor (CPSF30) (Nemeroff, Barabino et al. 1998); (Noah, Twu et al. 2003) and poly(A)-binding protein II (PABPII) (Chen, Li et al. 1999), NS1 inhibits nuclear pre-mRNA maturation (i.e. cleavage and polyadenylation of the 3'-end of pre-mRNAs) (Fig. 10C). Several residues in NS1-ED were claimed necessary for the NS1-CPSF30 binding: L144 and residues 184–188 (A/Udorn/72) (Noah, Twu et al. 2003);(Twu, Noah et al. 2006); F103 and M106 (Kochs, Garcia-Sastre et al. 2007). The NS1 protein of the H7N9 virus, an avian virus that has recently caused substantial human deaths, contains I rather than M at position 106. I106M enhanced virus replication *in vivo* (Ayllon, Domingues et al. 2014). The NS1-PABPII interaction requires NS1 residues 223–237 (A/Udorn/72) (Li, Chen et al. 2001).

Furthermore, NS1 has also been reported to block the antiviral gene expression by direct interaction with host cell DNA preventing the loading of transcriptional machinery to the DNA (Anastasina, Le May et al. 2016). The authors revealed the NS1 (A/WSN/33)-dsDNA interaction was mediated by NS1-RBD, and R38A/K41A mutation eliminated this interaction.

B. Inhibition of IFN-signaling transduction

IAV disrupt JAK/STAT signaling, at least in part, by reducing the expression of the IFN receptors (IFNAR1 and IFNAR2) and phosphorylation of STAT (Fig. 12) (Klemm, Boergeling et al. 2018).

NS1 (A/Vietnam/3046/04, A/HK/483/97, A/HK/54/98, and A/Ca/04/09) coding plasmids transfected HeLa cells showed reduced cell membrane IFNAR1, but not IFNAR2 (Jia, Rahbar et al. 2010). In further disease-relevant tests, human monocyte-derived macrophages were infected with H5N1 or H1N1 virus, and both IFNAR1 and IFNAR2 exhibited biphasic expression: first shortly upregulated, then downregulated. The NS1-mediated host gene transcription, maturation, and export may be involved in the IFN receptor expression regulation. The authors also demonstrated that human lung epithelial A549 cells had notably higher STAT2 phosphorylation level than NS1 expressing A549 cells. Tomas et al. transfected 293 cells with plasmids coding avian, human or aa mutant NS1 proteins, then treated the cells with IFNα (Thomas, Kranjec et al. 2011). IFNα strongly induced STAT1 phosphorylation, which was markedly

inhibited in the presence of avian NS1, and weakly by human NS1 and the aa mutant. The STAT1 phosphorylation inhibition was believed to be mediated by NS1-hScrib interaction (Werme, Wigerius et al. 2008), and the inhibition level consistent with the binding affinity of NS1s to hScrib protein. *Via* large-scale sequencing of influenza A viral genomes, a PDZ (PSD95/Dlg 1/zo-1) domain-binding motif (PDM) at the C terminus (amino acids 227 to 230) of most NS1 proteins was identified (Obenauer, Denson et al. 2006). This motif is recognized by cellular PDZ domain containing proteins, such as Scrib protein, postsynaptic density protein (PSD95), Drosophila disc large tumor suppressor (Dlg1), and zonula occludens-1 protein (zo-1), playing essential roles in trafficking, signaling, apoptosis (Harris and Lim 2001). Most avian influenza virus NS1 proteins possess a PDM with the sequence ESEV, which is RSKV for human influenza virus NS1. The avian NS1-ESEV showed high affinity to 30 different human PDZ domains, whereas the human NS1-RSKV proteins bind at a very low level or not at all (Obenauer, Denson et al. 2006).

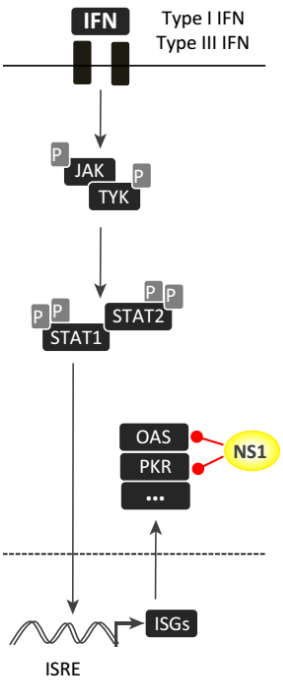

Fig. 12. NS1 regulates IFN signaling transduction. Secreted IFN binds to IFN receptors in a paracrine and autocrine manner, which activates the JAK/STAT signalling pathway. Phosphorylated STAT dimers translocate to the nucleus and stimulate the expression of IFN-stimulated genes (ISGs), such as dsRNA-dependent serine/threonine protein kinase R (PKR) and 2'-5'-oligoadenylate synthetase (OAS).

The STAT phosphorylation and, OAS and PKR activation are blocked by NS1. Adapted from (Klemm, Boergeling et al. 2018).

C. Inhibition of the activity of IFN-induced anti-viral effectors

PKR and OAS are two major IFN-induced anti-viral effectors (Fig. 12). PKR is activated by dsRNA, then phosphorylate eukaryotic translation initiation factor 2α (eIF2α) leading to cytoplasmic mRNA (virus and host) translation inhibition. dsRNA also binds to and actives OAS. Activated OAS polymerizes ATP into 2'-5' oligoadenylate chains, which then dimerizes and actives latent RNase (RNase L) causing general degradation of RNA.

Data from Min and colleagues indicate that a predominant function of the NS1-RBD is to out-compete OAS for interaction with dsRNA, thereby benefiting viral RNA replication (Min and Krug 2006). Residues in NS1-RBD that mediate this interaction, either directly or *via* improving complex stability, include T5, P31, D34, R35, R38, K41, G45, R46 and T49 (Wang, Riedel et al. 1999); (Yin, Khan et al. 2007). H3N2 influenza A/Udorn/72 virus encoding a NS1 protein with a R38A mutation resulted in a 1000-fold attenuation of virus replication during multiple cycle growth (Min and Krug 2006).

The RNA-binding defective NS1 protein efficiently limited PKR activation in response to dsRNA or PACT, a protein activator of PKR, and also NS1 interacted with PKR in a dsRNA-independent manner (Li, Min et al. 2006). Thus, NS1 blocks dsRNA-induced PKR activation mainly *via* directly binding to PKR, instead of sequestering dsRNA, which require NS1 residues 123–127. This conclusion was further confirmed by the lack of PKR activation in NS1 mutant (R38A) A/Udorn/72 infected cells (Min and Krug 2006).

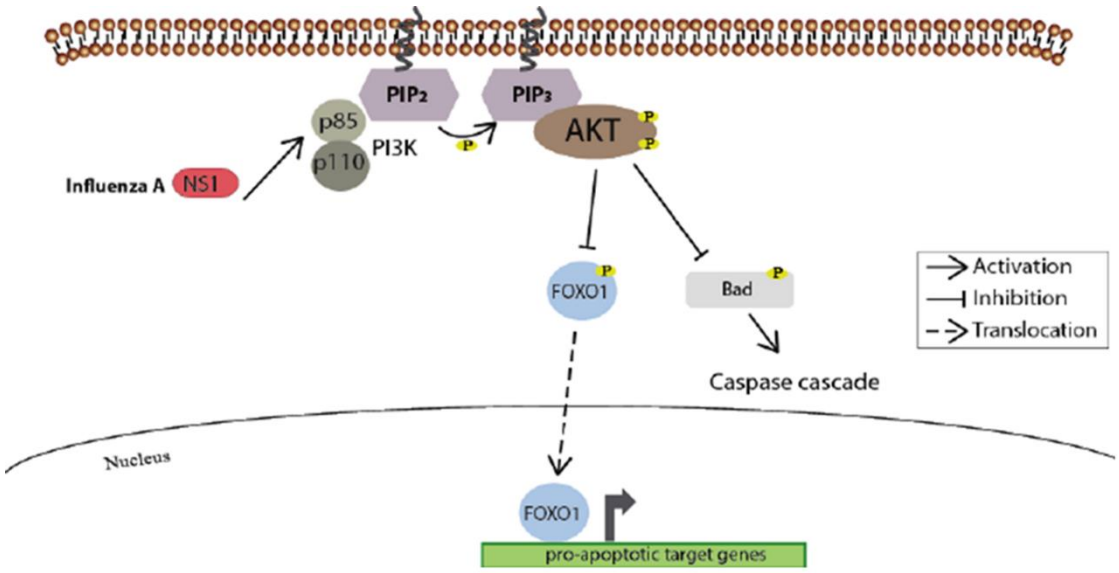

Fig. 13. Schematic of NS1 actives the PI3K/Akt signaling pathway to regulate cellular survival. Upon incoming survival signals, the Akt-mediated inhibitory phosphorylation of pro-apoptotic molecules such as BAD prevents the induction of the caspase cascade. Besides, the inhibitory phosphorylation of the transcription factor FOXO1 by Akt blocks its translocation into the nucleus and thus prevents the expression of pro-apoptotic genes. Modified from (Diehl and Schaal 2013) with permission.

1.4.2.3. NS1 and the host apoptotic response

Activation of PKR and OAS/RNase L leading to virus and host RNA translation stalling and RNA degradation, which causes host cell apoptosis. Limiting IFNs production and downstream effects, NS1 displays an anti-apoptotic function to promote viral genome replication and protein expression. Additionally, NS1 affects host cell viability through activation of the phosphatidylinositol 3-kinase (PI3K)/Akt pathway (Fig. 13) (Hale, Jackson et al. 2006); (Ehrhardt, Wolff et al. 2007); (Fan, Macken et al. 2013).

The PI3K/Akt pathway regulates many different cellular events, including apoptosis, cell metabolism, and proliferation (Ehrhardt and Ludwig 2009). The PI3K is a heterodimeric protein/lipid kinase consisting of a regulatory subunit (p85α, p85β, P55α, p55γ, or p50α), and a catalytic subunit (p110α, β, γ, or δ) (Vanhaesebroeck, Ali et al. 2005). When growth factors or cytokines are sensed by their receptor tyrosine

kinases (RTKs) or G protein-coupled receptors (GPCRs), PI3K phosphorylates the 3-hydroxyl group of the inositol ring of membrane bound phosphatidylinositol (PtdIns) lipid substrates, generating phosphatidylinositol-3,4,5-trisphosphates (PIP_3), which subsequently serve as docking stations for proteins that harbor lipid binding domains, mainly the serine/threonine kinase AKT. After binding of its pleckstrin homology (PH) domain to PIP_3, Akt becomes phosphorylated at Thr308 and Ser473. Finally, several downstream targets like tuberous sclerosis protein 2 (TSC2; translation), glycogen synthase kinase 3 (GSK3; cell growth), or Bcl-2-associated death promoter (BAD; cell survival) and forkhead box protein (FOXO; cell survival) are altered in their function through the Akt-mediated phosphorylation (Diehl and Schaal 2013).

Hale and colleagues reported that NS1 (PR8/NS1, Ud/NS1, and Vic/NS1) binds directly to p85β, and subsequently activates P13K signaling and promotes virus replication. The highly conserved Y89 residue in the NS1 ED is vital for the NS1- p85β interaction (Hale, Jackson et al. 2006). The NS1-Y89F mutant Ud virus was clearly attenuated. However, the WSN NS1-Y89F did not appear to exhibit an attenuated phenotype under tissue culture conditions, which, demonstrated the NS1 function is strain-dependent. In another study, Ehrhardt et al. found, besides p85β, NS1 interacted with p85α as well, although at a somewhat lower level. The critical residues for the NS1-p85 interaction was extended to D125 and 181-185(LIGGL) (Ehrhardt, Wolff et al. 2007), E229 and F138 (Fan, Macken et al. 2013).

1.4.2.4. Proof of concept studies

Considering the promising function of NS1 in suppressing antiviral responses, Phua's team did several proof-of-concept studies of co-delivering NS1 mRNA with gene of interest, which shown NS1 was able to inhibit IVT mRNA induced immune responses and enhance IVT mRNA translation (Phua, Liu et al. 2017); (Liu, Chia et al. 2018). They have compared several NS1 proteins from different strains (A/Hong Kong/156/1997; A/Vietnam/1203/2004; A/Puerto Rico/8/1934; A/Texas/36/1991; A/California/04/2009; A/Shanghai/2013), and found that NS1 from A/Texas/36/1991 (NS1/Tx91) had the best performance. This was, attributed to the consensus amino acids (e.g. R38, K41, F103, M106, I123, M124) that gave NS1/Tx91 the most comprehensive function from blocking the pre-transcriptional initiation to post-transcription modification of antiviral genes (Fig. 14). The finding consistent with

previous studies that NS1 function is highly strain-dependent. In some cell types, the NS1/Tx91 mediated enhancement of transfection efficiency exceeded modified IVT mRNA (Phua, Liu et al. 2017).

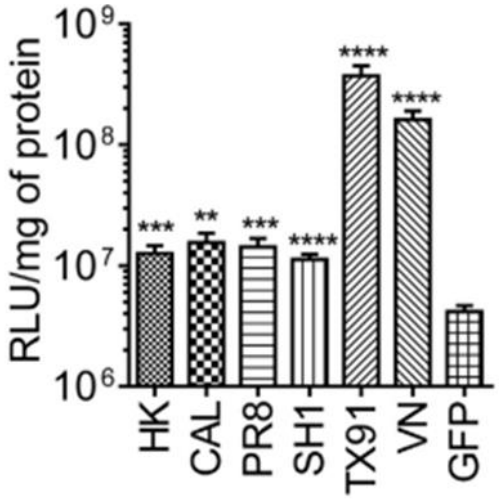

Fig. 14. IAV derived NS1 enhances *in vitro* mRNA transfection. Low passage (p4-5) human BJ fibroblasts were co-transfected with mRNAs encoding luciferase and, respectively as indicated, NS1 derived from different influenza A virus strains. Luciferase expression normalized to total protein was assayed 18 h post transfection. Footnote: HK: A/Hong Kong/156/1997; CAL: A/California/04/2009; PR8: A/Puerto Rico/8/1934; SH1: A/Shanghai/1/2003; TX91: A/Texas/36/1991; VN: A/Vietnam/1203/2004. Adapted from (Phua, Liu et al. 2017) with permission.

Part II

Influenza A Derived NS1 protein Enhances *in vitro* Transcribed BMP2 mRNA Translation in Multipotent Stem Cells Leading to an Improved Osteogenic Differentiation

La protéine NS1 dérivée du virus de la grippe Influenza A améliore la traduction des ARNm codant la protéine BMP-2 dans les cellules souches multipotentes conduisant à une différenciation ostéogénique améliorée

La protéine NS1 dérivée du virus de la grippe Influenza A améliore la traduction des ARNm codant la protéine BMP-2 dans les cellules souches multipotentes conduisant à une différenciation ostéogénique améliorée

L'application de l'ARN messager (ARNm) pour la régénération osseuse est une alternative prometteuse à l'ADN, aux protéines recombinantes et aux peptides. Cependant, l'utilisation d'un ARNm obtenu par transcription *in vitro* (ARNm IVT) déclenche une réponse immunitaire innée entraînant une dégradation de l'ARNm et une inhibition de sa traduction. En s'inspirant de la capacité des protéines virales à inhiber les réponses immunitaires des cellules hôtes contre l'ARN viral, nous avons exploité la protéine 1 non structurelle (NS1) du virus de la grippe A (A / Texas / 36/1991) pour améliorer la traduction in cellulo d'ARNm IVT.

Dans un premier temps, nous avons validé l'action bénéfique de l'expression de l'ARNm codant NS1 sur l'expression d'ARNm de différents gènes rapporteurs dans différents types cellulaires. Nos résultats ont mis en évidence un blocage dose-dépendant des senseurs immuns d'ARN par l'expression de la protéine NS1. La co-délivrance de l'ARNm de NS1 avec l'ARNm de la luciferase de Firefly, la GFP et la luciferase de Renilla a considérablement augmenté l'efficacité de leur traduction. Fait intéressant, contrairement à l'utilisation de la modification des nucléosides, l'amélioration de la traduction de l'ARNm médiée par NS1 ne dépend pas du type de cellule.

Dans un second temps, nous avons effectué une double administration d'ARNm NS1 et d'ARNm de la protéine ostéo-inductive BMP-2 aux cellules souches multipotentes murines (C3H10T1/2). La combinaison des deux ARNms a favorisé la différenciation ostéogénique mise en évidence par une expression accrue des marqueurs ostéoblastiques (par exemple, la phosphatase alcaline, le collagène de type I, l'ostéopontine et l'ostéocalcine) et la minéralisation extracellulaire en comparaison avec la délivrance de l'ARNm BMP-2 seul.

L'ensemble de nos résultats confirment la potentialité adjuvante de NS1 pour les thérapies régénératives à base d'ARNm.

Le manuscrit relatif à ce travail a été soumis à Acta Biomaterialia.

Influenza A Derived NS1 protein Enhances *in vitro* Transcribed BMP2 mRNA Translation in Multipotent Stem Cells Leading to an Improved Osteogenic Differentiation

Pinpin Wang[a], Delphine Logeart-Avramoglou[c], Hervé Petite[c], Cristine Goncalves[a], Patrick Midoux[a], Federico Perche[a], Chantal Pichon[a, b]*

a. Centre de Biophysique Moléculaire, UPR 4301 CNRS, Rue Charles Sadron, 45071 Orléans, France

b. Faculty of Sciences and Techniques, University of Orléans

c. Université de Paris, CNRS, INSERM, B3OA, 10 Avenue de Verdun, 75010 Paris, France

* Corresponding author

Graphical abstract

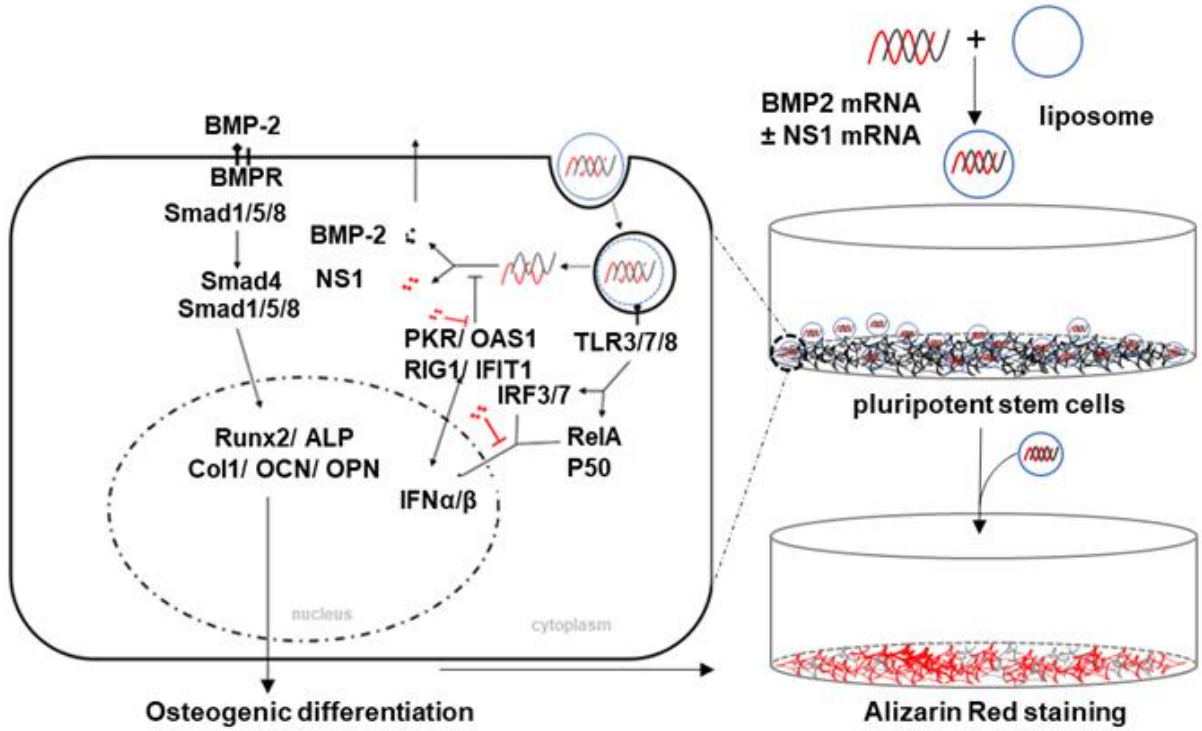

2.1. Abstract

Application of messenger RNA (mRNA) for bone regeneration is a promising alternative to DNA, recombinant proteins and peptides. However, exogenous *in vitro* transcribed mRNA (IVT mRNA) triggers innate immune response resulting in mRNA degradation and translation inhibition. Inspired by the ability of viral immune evasion proteins to inhibit host cell responses against viral RNA, we applied non-structural protein-1 (NS1) from *Influenza A* virus (A/Texas/36/1991) as an IVT mRNA enhancer. We evidenced a dose-dependent blocking of RNA sensors by NS1 expression. The co-delivery of NS1 mRNA with mRNA of reporter genes significantly increased the translation efficiency. Interestingly, unlike the use of nucleosides modification, NS1-mediated mRNA translation enhancement does not dependent to cell type. Dual delivery of NS1 mRNA and BMP-2 mRNA to murine multipotent stem cells (C3H10T1/2), promoted osteogenic differentiation evidenced by enhanced expression of osteoblastic markers (e.g. alkaline phosphatase, type I collagen, osteopontin, and osteocalcin), and extracellular mineralization. Overall, these results support the adjuvant potentiality of NS1 for mRNA-based regenerative therapies.

Keywords: mRNA delivery, non-structural protein 1, RNA sensors, bone morphogenetic protein 2, osteogenesis

2.2. Introduction

Bone defects affect millions of people every year (Lopes, Martins-Cruz et al. 2018). The treatment of large bone defects resulting from trauma, nonunion fractures, tumor resections or craniofacial malformations remains challenging. The situation is more severe with the increase of aging population.

Many strategies have been proposed to improve the regeneration of damaged bone tissue. Among them, the delivery of osteoinductive growth factors (or derivatives), mostly bone morphogenetic protein-2 (BMP-2), to the lesion site remains a promising approach to promote bone healing (Niu, Feng et al. 2009, Lv, Xiu et al. 2015). However, delivery of supraphysiological dose induced deleterious side effects,

including significant inflammation, swelling, and heterotopic ossification, that had limited the extent of their clinical use (Shimer, Oner et al. 2009).

DNA and messenger RNA (mRNA)-based gene therapies represent alternative approaches for locally delivering growth factors (Wang, Perche et al. 2019). They allow an *in situ* expression of growth factors in host cells, and undergo precise post-translational modifications required for optimal activity. Furthermore, gene therapy is preferable for delivering products that exert their function intracellularly, such as transcription factors and signaling transduction molecules (Evans and Huard 2015).

DNA delivery to produce osteogenic proteins has demonstrated an enhancement of osteogenesis both *in vitro* and *in vivo,* proving the great potential of this strategy for bone healing and regeneration (Lee, Kang et al. 2010, Raftery, Mencia-Castano et al. 2018). The main limitation of DNA delivery, however, is the requirement of nuclear transport of the transgene for its transcription leading to low transfection efficiency and risk of genome insertion. In contrast, mRNA molecules are directly translated inside the cytoplasm, making this technology more efficient, and suitable in non-dividing cells. This aspect is especially useful when inducing cell differentiation since terminal differentiation usually coincides with proliferation arrest (Ruijtenberg and van den Heuvel 2016). Although mRNA therapy demonstrates clear advantages, its broad application has been so far limited to vaccination because of its instability and immunogenicity (Pascolo 2008, Schlake, Thess et al. 2018). After internalization, IVT mRNA molecules mainly accumulate into endosomes, where they are recognized by Toll-like receptors (TLRs), specifically TLR3, 7, and 8, located in the endosome membrane (Alexopoulou, Holt et al. 2001, Heil, Hemmi et al. 2004, Kariko, Buckstein et al. 2005). TLRs engagement induces type I interferon (INFα/β) expression and associated anti-viral responses resulting in IVT mRNA translation suppression and degradation, and even host cell apoptosis (Kariko, Ni et al. 2004, Dan, Zheng et al. 2012). To reduce such immune effects, chemically modified nucleotides have been developed; the synthesis of such nucleotides, however, is expensive and the type and percentage of modified nucleotides in the mRNA sequence must be tuned as function of mRNA and cell type for maximum activity (Uchida, Kataoka et al. 2015). Recently, other strategies have been developed based on RNA-virus mimicry (Phua, Liu et al. 2017, Liu, Chin et al. 2019).

During millions of years of coexisting with their hosts, viruses have acquired the ability to manipulate host immune mechanisms (Alcami and Koszinowski 2000, Katze, He et al. 2002). Viruses express various immune evasion proteins (e.g. protein K3 (K3L), protein E3 (E3L), soluble interferon α/β receptor B18 (B18R), NS1) which sequester the host immune-mediating proteins (e.g. interferons (IFNs), retinoic acid-inducible gene I protein (RIG-I), interferon-induced, double -stranded RNA-activated protein kinase (PKR) induced by detecting immune triggers (e.g. dsRNA). Mimicking this viral immune-evasion process could, therefore, be an interesting strategy to bypass the IVT mRNA-triggered immune responses and, therefore to increase the transfection efficiency (Devoldere, Dewitte et al. 2016). Specifically, B18R is a secreted protein that exerts its function as a soluble receptor for type I IFNs (Alcamí, Symons et al. 2000); the use of recombinant B18R from Western Reserve strain of vaccinia virus as cell culture medium supplement during *in vitro* transfection is known to maintain cell viability and to enhance the IVT mRNA translation efficacy (Warren, Manos et al. 2010, Yoshioka, Gros et al. 2013, Zangi, Lui et al. 2013). In contrast to B18R, NS1 is a multifunctional viral protein that participates in every step of host immune reaction (Hale, Randall et al. 2008). During the viral replication cycle, NS1 completely interacts with dsRNA, thereby inhibiting 2'-5'-oligoadenylate synthase (OAS)/RNase L-mediated RNA degradation, and PKR-mediated protein synthesis reduction (Garcia, Gil et al. 2006, Min and Krug 2006). NS1 forms a complex with RIG-1 that blocks the activation of NF-κB (nuclear factor kappa B) and IRF3 (interferon regulatory factor 3) and, subsequently, reduces IFN α/β expression (Talon, Horvath et al. 2000, Wang, Li et al. 2000). Co-delivery of NS1 mRNA with mRNA of interest was able to enhance mRNA translation to an extent superior to the incorporation of modified nucleotides (Phua, Liu et al. 2017, Liu, Chin et al. 2019). In addition, unlike chemical modified mRNA which could have contrary effects (Uchida, Kataoka et al. 2015, Li, Luo et al. 2016), we found the NS1-mediated gene expression enhancement is general regardless cell type.

Here, we propose to combine NS1 mRNA with BMP-2 mRNA to improve the efficiency of mRNA therapy for bone regeneration. The hypothesis is that the co-delivery of both NS1 mRNA and BMP2 mRNA into osteoprogenitor cells enhances the BMP-2 expression and ultimately promotes osteogenesis. In this study, a murine multipotent stem cell line (C3H10T1/2) was used to evaluate the *in vitro* osteogenic potential of

this novel strategy. The stem cells transfected with the dual mRNAs, under optimized mass ratio, expressed significantly higher BMP-2 than cells transfected with BMP2 mRNA alone, which led to increased induction of osteogenic genes and extracellular calcium deposits.

Through this proof-of-concept study, we successfully validated the application of NS1 mRNA as supplement for enhanced therapeutic mRNA transfection. To the best of our knowledge, this is the first study demonstrating therapeutic potential of non-modified mRNAs in regeneration medicine. We hope that through this strategy, a new horizon of mRNA therapy could be developed.

2.3. Materials and Methods

2.3.1. Preparation of plasmids and mRNAs

Mouse BMP-2 ORF was PCR amplified from pCMV3-mBMP2-GFPSpark (Sino Biologicals) with 5'-TATGGATCCACTTAAGATGGTGGCCGGGACCCGCTGT-3' as forward primer and 5'-TATTGCGGCCGCTTAACGACACCCGCAGCCCTC-3'as reverse primer (Eurogentec). NS1 (A/Texas/36/1991) ORF was PCR amplified from pUC57-NS1 (Genscript) with 5'-tgtacggatcctcctatggattccaacactgtgtc-3' and 5'-atttgcggccgctcaaacttctgacct-3' as the forward primer and reverse primer (Eurogentec), respectively. The BMP2 and NS1 segments were inserted into the previously described pGEM4Z-luc-A64 plasmid (Perche, Benvegnu et al. 2011), between BamHI and NotI, respectively. All plasmid DNAs were extracted, purified with NucleoBond® Xtra Maxi EF kit (Macherey-Nagel) and verified by sequencing (Eurofins).

The plasmids were linearized for mRNA preparation with a mMessage mMachine T7 kit (Ambion) according to the manufacturer's instructions. The poly(A) tail was extended with PolyA polymerase (Ambion) to generate at least 150nt guaranteed by the manufacturer. To produce chemically modified mRNAs (cmRNAs), 50% uridine-5'-triphosphate were replaced with pseudouridine-5'-triphosphate (TriLink). Synthesized mRNAs were purified with phenol: chloroform and isopropanol precipitation. Sizes and integrity of the mRNAs were verified by denatured agarose gel electrophoresis (Supplementary Fig. 1).

2.3.2. Cell culture

C2C12 murine myoblasts, 4T1 murine breast cancer cells, A549 human lung cancer cells, U87-MG human glioblastoma cells, HepG2 human hepatocellular carcinoma cells and, C3H10T1/2 murine multipotent stem cells were purchased from the American Type Culture Center (ATCC). Murine DC 2.4 cells were a kind gift from Pr. Kenneth Rock (Shen, Reznikoff et al. 1997). C2C12-BRE/Luc cells, which contain a BMP-2 sensitive reporter gene were obtained after stably transfection with the BMP-responsive element (BRE) fused to the luciferase gene as previously described (D. Logeart-Avramoglou 2006). Cells were grown at 37°C in a humidified atmosphere containing 5% CO2. Cells were mycoplasma-free as evidenced by MycoAlert Mycoplasma Detection Kit (Lonza).

2.3.3. *In vitro* transfection

All transfections were mediated by Lipofectamine MessengerMax (LFM) (ThermoFisher) transfection reagent according to the manufacturer's protocol.

2.3.4. Evaluation of translation of BMP2 and NS1 mRNAs containing different 3' UTR

The day before transfection, C2C12-BRE/Luc cells were seeded at 5×10^4 cells/well in 24-well plate. The next day, 0.5 µg BMP2-NotI mRNA (transcribed from NotI linearized BMP2 plasmid) or 0.5 µg BMP2-XbaI mRNA (transcribed from XbaI linearized BMP2 plasmid) both complexed with LFM were delivered to C2C12-BRE/LUC cells. One day post-transfection, cells were lysed, and the luciferase activity was quantified as previously reported (Perche, Benvegnu et al. 2011).Luminescence from cell lysates was measured with the LB9075 illuminometer (Biorad) and, expressed as relative light unit (RLU) per mg of proteins.

NS1-NotI and NS1-XbaI mRNA were delivered using the same procedure as BMP2 mRNAs, and semi-quantified by Western blot.

2.3.5. Assessment of NS1 cytocompatibility

C3H10T1/2 cells (5×10^4 cells/well in 24-well plate) were transfected with increasing doses of NS1 mRNA (0 .1µg, 0.3µg, and 0.5µg per well which correspond to 2pg, 6pg, and 10pg per cell, respectively) complexed with LFM. Same amount of GFP mRNA

was used as control. 24h and 48h later, cytotoxicity level was evaluated by an XTT assay (Cell Proliferation Kit II, Sigma-Aldrich) following the manufacturer's instruction.

2.3.6. Validation of NS1-mediated IVT mRNA translation enhancement

One day after cell plating, 0.2µg GFP mRNA was co-delivered with either 0.1µg, or 0.3µg, or 0.5µg NS1 mRNA into C3H10T1/2 cells. Twelve hours post-transfection, the GFP expression was evaluated by flow cytometry (FACSort, Becton Dickinson), and the intracellular NS1 from each condition tested was semi-quantified by Western-blot.

To measure the kinetic of GFP expression, 0.2µg GFP mRNA was co-delivered with either 0.2µg Gluc mRNA or 0.2µg NS1 mRNA. The GFP expression was measured from 6h to 168 h post-transfection.

To study the immune activation post-transfection, C3H10T1/2 cells were transfected with 1 µg/well of total mRNA comprising different weight ratios of GFP mRNA and NS1 mRNA: 1µg GFP mRNA (1 GFP); 0.75µg GFP mRNA and 0.25µg NS1 mRNA (0.75 GFP/0.25 NS1); 0.5µg GFP mRNA and 0.5µg NS1 mRNA (0.5 GFP/0.5 NS1); 0.25µg GFP mRNA and 0.75µg NS1 mRNA (0.25 GFP/0.75 NS1); 1µg NS1 mRNA (1 NS1) Cells transfected with Ψ-modified GFP mRNA (GFP(50%ψ)) were set as controls. Interferon alpha (IFN α) secreted in the supernatant was measured by enzyme-linked immunosorbent assay (ELISA, PBL Assay Science) according to the manufacturer's instructions. Gene expression level of IFN α/β, PKR, RIG-1, OAS1, Interferon-induced protein with tetratricopeptide repeats 1 (IFIT1) were determined by real-time quantitative reverse-transcription polymerase chain reaction (RT-qPCR) according to a previous report (Lin, Perche et al. 2016). Briefly, total RNA were extracted using RNeasy Mini kit (Qiagen), RNA concentration and purity was measured using Nanodrop (ThermoFisher). First strand cDNA synthesis kit (Thermo Scientific) was used for reverse transcription following manufacturer's protocol. qPCR was performed using the Luna qPCR Master mix (NEB) with a Light Cycler© 480 PCR system (Roche). The qPCR data were analyzed by the comparative ΔΔCt method using the GAPDH RT-qPCR signal as the internal control for normalization. Primers for RT-qPCR were listed in Supplementary Table 2.

2.3.7. Screening of NS1 function as function of mRNA and cell context

C3H10T1/2, C2C12, DC 2.4, 4T1, A549, U87MG, HepG2 cells were seeded and cultured into 24-well plate in order to obtain 70-80% confluence at the time of transfection. These cells were transfected with lipoplexes containing 0.25 µg mRNA of reporter genes (i.e., GFP, Fluc, and Gluc) with either 0.25 µg NS1 mRNA or 0.25 µg noncoding mRNA. The GFP and Fluc expression were evaluated as described before. Gluc expression, both secreted and intracellular, was evaluated with the Pierce Gaussia Luciferase Glow assay kit (ThermoScientific). The luminescence obtained from secreted and intracellular Gluc were normalized to total cellular protein and per mg cellular protein, respectively.

2.3.8. Optimization of BMP2 mRNA and NS1 mRNA ratio

C2C12-BRE/LUC cells were seeded into 24-well plate at the density of $1x10^5$ cells/well. One day later, cells were transfected with 1 µg/well total mRNA with different weight ratio of BMP2 mRNA and NS1 mRNA: 1µg BMP2 mRNA (1 BMP2); 0.75µg BMP2 mRNA and 0.25µg NS1 mRNA (0.75 BMP2/0.25 NS1); 0.5µg BMP2 mRNA and 0.5µg NS1 mRNA (0.5 BMP2/0.5 NS1); 0.25µg BMP2 mRNA and 0.75µg NS1 mRNA (0.25 BMP2/0.75 NS1). Luciferase activity was measured one day later as described above.

2.3.9. Quantification of BMP2 secreted by transfected C3H10T1/2

C3H10T1/2 cells were seeded into 4-well plate at a density of 5×10^4 cells/well and cultured until confluency. Then, 1 µg total mRNA with optimized BMP2 and NS1 mRNA ratio were used to transfect the cells. Every 12 h, half of the culture medium was collected and replaced with fresh medium. Collected media were stored at -80°C before BMP2 content quantification. BMP2 contents were determined by ELISA (Abcam) following the manufacturer's instruction. The absorbance was measured at 450 nm and BMP2 contents were calculated based on a standard curve (range: 0-4000 pg/ml mouse BMP2).

2.3.10. *In vitro* osteogenesis

C3H10T1/2 cells were seeded as indicated in 2.9. Prior to transfection, cells were cultured in osteogenic medium containing 25ng/ml rhBMP2 (R&D system), 50µg/ml

ascorbic acid-2-phosphate (Sigma) and 10mM β-glycerophosphate (Sigma) for seven days and half of the medium was changed every other day. Then, cells were transfected twice with 1 µg/well mRNA at day 0 and day 7 (experimental scheme shown in Fig. 7A), and maintained in osteogenic medium (without rhBMP2) throughout the whole osteogenic induction process. From day 0, half of the medium was changed every 3 days during the first 10 days and then every 2 days.

At day 3, 7, and 14 post-transfection, ALP activity was quantified with ALP activity colorimetric assay kit (Biovision) following the manufacturer's protocol. Intracellular ALP expression was visualized by Nitro Blue Tetrazolium (NBT)/5-Bromo-4-chloro-3-indolyl phosphate disodium salt (BCIP) (Sigma) staining as previously reported (Cui, Sun et al. 2017) with slight modification. Briefly, at day 14 post-transfection, cells were washed with PBS and then fixed in 4% formaldehyde for 2 min. BCIP/NBT solution was added to react with ALP for 30 min in dark at RT. The staining solution was washed out with PBS.

At day 1, 3, 5, 7, 14, and 21 post-transfection, the expression of Runx2, ALP, collagen type 1, OCN, OPN were quantified by RT-qPCR. The process was the same as described before, except that total RNA was isolated and purified by TRIzol (Life technology)-chloroform method. Primers for RT-qPCR were listed in Supplementary Table 2.

Alizarin Red staining was performed 28 days post-transfection to evaluate calcium deposition. Cells were washed with D-PBS and then fixed in 4% p-formaldehyde for 30 min at room temperature (RT) followed by 2 times washes with distilled water (dH_2O). Extracellular calcium was stained by incubating the cell layers in alizarin red S (Sigma) solution (saturated in dH_2O, pH 4.1). Nonspecific staining was removed by washing the wells with dH_2O five times under gentle agitation. To quantify the mineralization, the alizarin red dye was subsequently extracted with cetylpyridinium chloride (Sigma) solution (10% in 10mM sodium phosphate) for 30 min at RT. Absorbance was then measured at 560nm using the Victor ^{3}V spectrophotometer (PerkinElmer).

2.3.11. Statistical analysis

Unless otherwise indicated, each experiment was performed in triplicates with two independent repeats. All numerical data are expressed as mean ± standard deviation. Statistical analysis was performed using GraphPad Prism version 6.07 (GraphPad software). Any p-value less than 0.05 was considered statistically significant. Specifically, * and # represent $P < 0.05$; ** and ## represent $P < 0.01$; *** and ### represent $P < 0.001$; **** and #### represent $P < 0.0001$.

2.4. Results

2.4.1. 3' UTR affects IVT mRNA translation efficiency

The production of mRNA by *in vitro* transcription requires the linearization of the plasmid DNA template. In our construction, this linearization was done by digesting the template with either NotI or XbaI endonuclease enzymes, resulting in the production of mRNAs with different 3' UTRs (Fig. 1A).

We first assessed which of those two mRNA types has the best translation efficiency. As shown in Fig. 1B, the amount of NS1 produced from NS1-NotI mRNA was 1.5-fold higher than that obtained with NS1-XbaI mRNA. The same observation was made with BMP-2 mRNA, which was evaluated in C2C12-BRE/LUC cells that express the luciferase reporter gene upon BMP2 activation. These data indicate that mRNA-NotI gave a higher protein expression than mRNA-XbaI regardless of the gene type. The mRNA-NotI was chosen for the next experiments.

2.4.2. NS1 promotes IVT mRNA translation by suppressing cellular innate immune responses

We first checked the impact of NS1 expression on cell viability. Results shown in Fig. 2 indicate that the cell viability decreased in a dose-dependent manner. The highest cytotoxic effect was observed with 10pg/cell, which results in 70% of viable cells compared to untreated cells 48h post-transfection. No effect on the viability of cells transfected with 2pg/cell of either NS1 or GFP mRNAs was observed. At 6 and 10pg/cell, we found that NS1 mRNA expression did not lead to a significant cell viability decrease at 24h post-transfection, whilst GFP mRNA did. For the next 24h, the trend

was reversed. No significant difference either between GFP and NS1 transfected cells or between 24h and 48h post-transfection time points were observed.

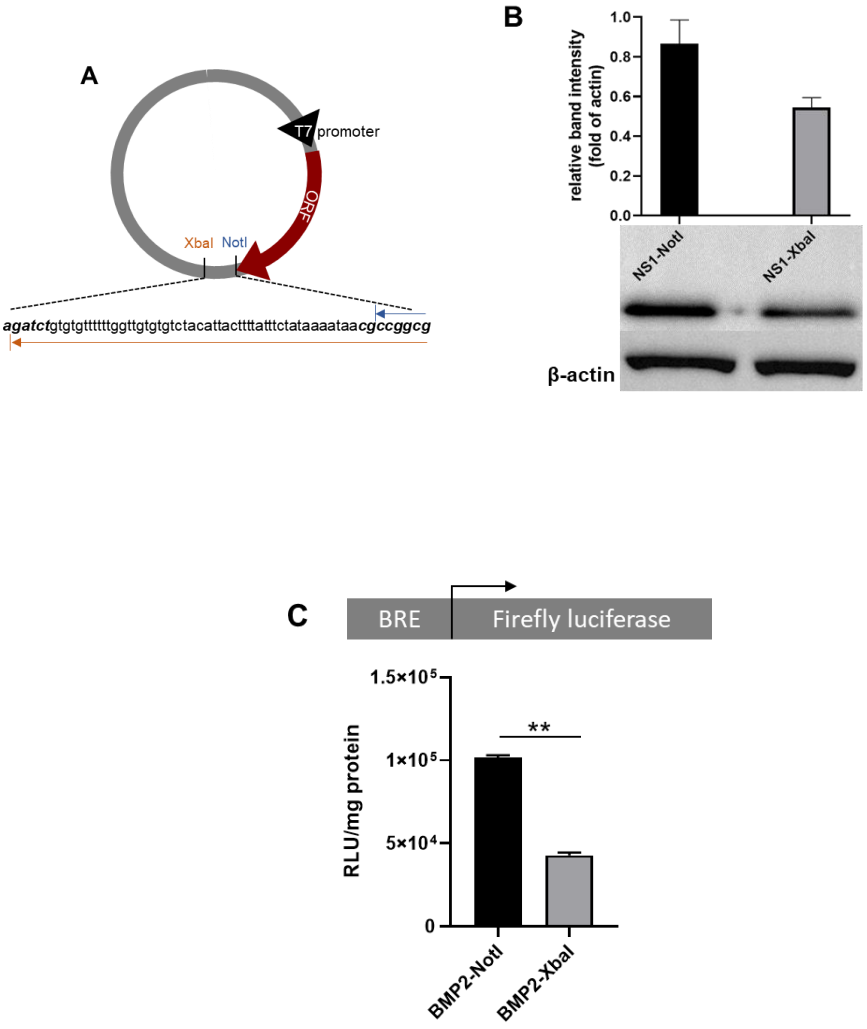

Fig. 1. Impact of 3' UTR on mRNAs translation efficiency. (**A**) To produce BMP2 and NS1 IVT mRNAs, DNA templates were linearized by either NotI or XbaI, which gave the IVT mRNAs different 3' UTR. (**B**) C2C12-BRE/LUC cells were transfected either with NS1-NotI or NS1-XbaI mRNAs formulated with Lipofectamine MessengerMax. One day later, NS1 and β-actin expressions in cell lysates were semi-quantified by Western-blots. (**C**) As for B, C2C12-BRE/LUC cells that stably express the luciferase gene under BMP2-responsive elements were transfected either with BMP2-NotI and BMP2-XbaI mRNAs. One day later the luciferase activity reflecting the BMP2 expression was evaluated by luminescence assay. Paired t test was used for the statistical analysis.

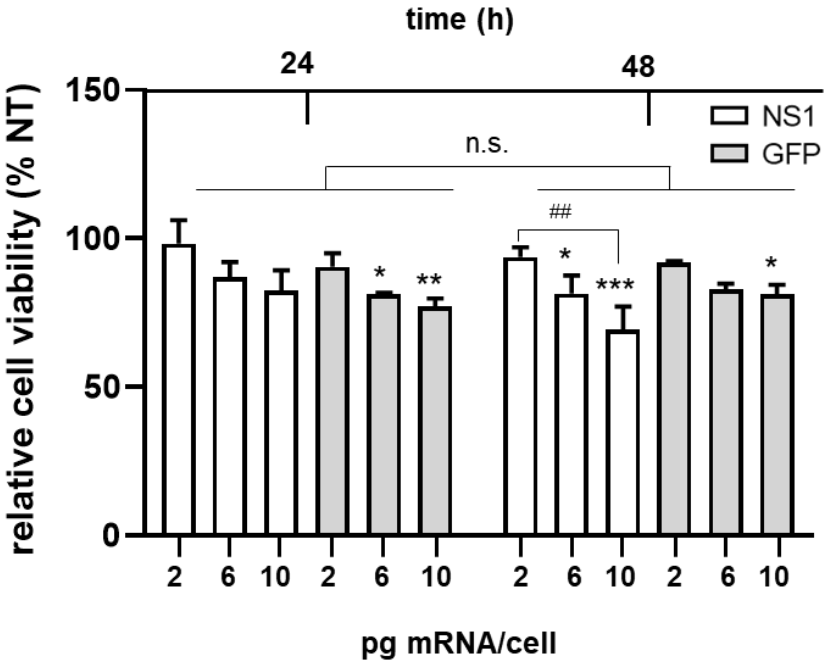

Fig. 2. Cytocompatibility of NS1. C3H10T1/2 cells were transfected with indicated amount of NS1 mRNA and GFP mRNA, respectively. 24h and 48h post-transfection, cell viability was measured via XTT assay, and normalized to non-transfected cells. *, **, *** compared to non-transfected cells. 2way ANOVA, Tukey's multiple comparisons test, was used for the statistical analysis.

Next, we validated the positive effect of NS1 expression on the translation of GFP mRNA (Fig. 3). Different amounts of NS1 mRNA (0.1µg to 0.5µg/well) were co-delivered with a fixed amount of GFP mRNA (0.2µg/well). Compared to cells transfected with GFP mRNA alone, the co-delivery with NS1 mRNA resulted in a significant dose-dependent enhancement of GFP expression. By contrast, cells co-transfected with GLuc mRNA did not lead to an improved GFP translation. Note that the percentage of GFP positive cells in each group remains the same. Fig. 3B confirmed the increased amount of NS1 proteins produced as a function of mRNA used for the transfection. The kinetic profiles of GFP produced in cells transfected with either GFP mRNA/NS1 mRNA or GFP mRNA/Gluc mRNA were similar with a peak of expression occurring between 12- and 24-hours post-transfection, and followed by a dramatic drop of the protein expression after 72 hours in both conditions. However, in the presence of NS1, the number of produced GFP copies was increased as

evidenced by the 1.4-fold increase of the MFI. Such NS1-mediated enhancement lasted for 72h.

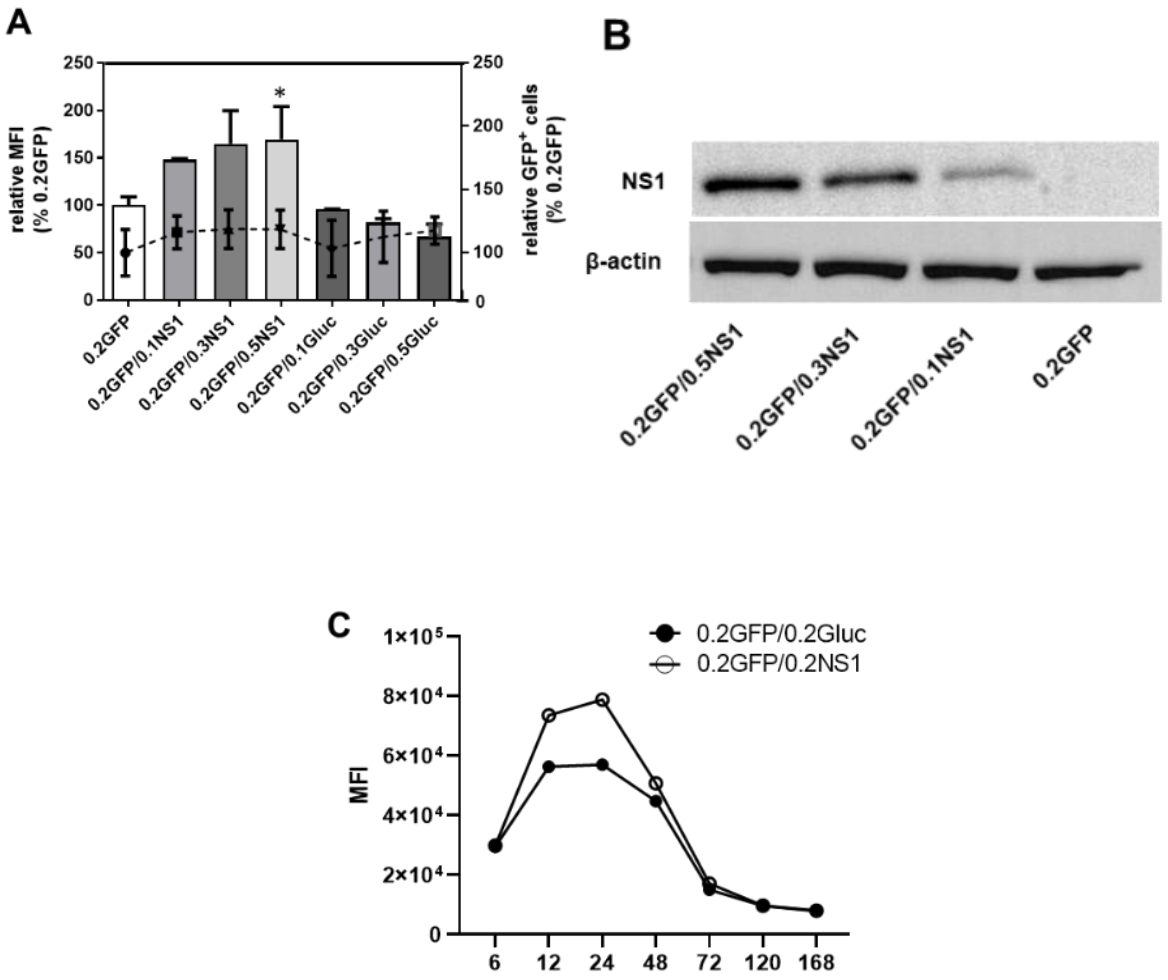

Fig. 3. Improved GFP mRNA translation when co-delivered with NS1 mRNA. (**A, B**) 0.2µg GFP mRNA was co-delivered with either 0 .1µg, or 0.3µg, or 0.5µg NS1 mRNA into C3H10T1/2 cells. Gluc mRNA was used as control to balance the total mRNA amount. (**A**) 12h post transfection, the GFP expression was evaluated by flow cytometry. (**B**) The amount of NS1 translated from the different conditions was confirmed by Western-blot. (**C**) The kinetic of GFP expression was assessed by transfecting C3H10T1/2 cells with either 0.2µg GFP mRNA and 0.2µg Gluc mRNA or 0.2µg GFP mRNA and 0.2µg NS1 mRNA. The mean fluorescence intensity (MFI) was measured by flow cytometry. *, compared to 0.2µg GFP transfected cells. Ordinary one-way ANOVA, Dunnett's multiple comparisons test, was used for the statistical analysis.

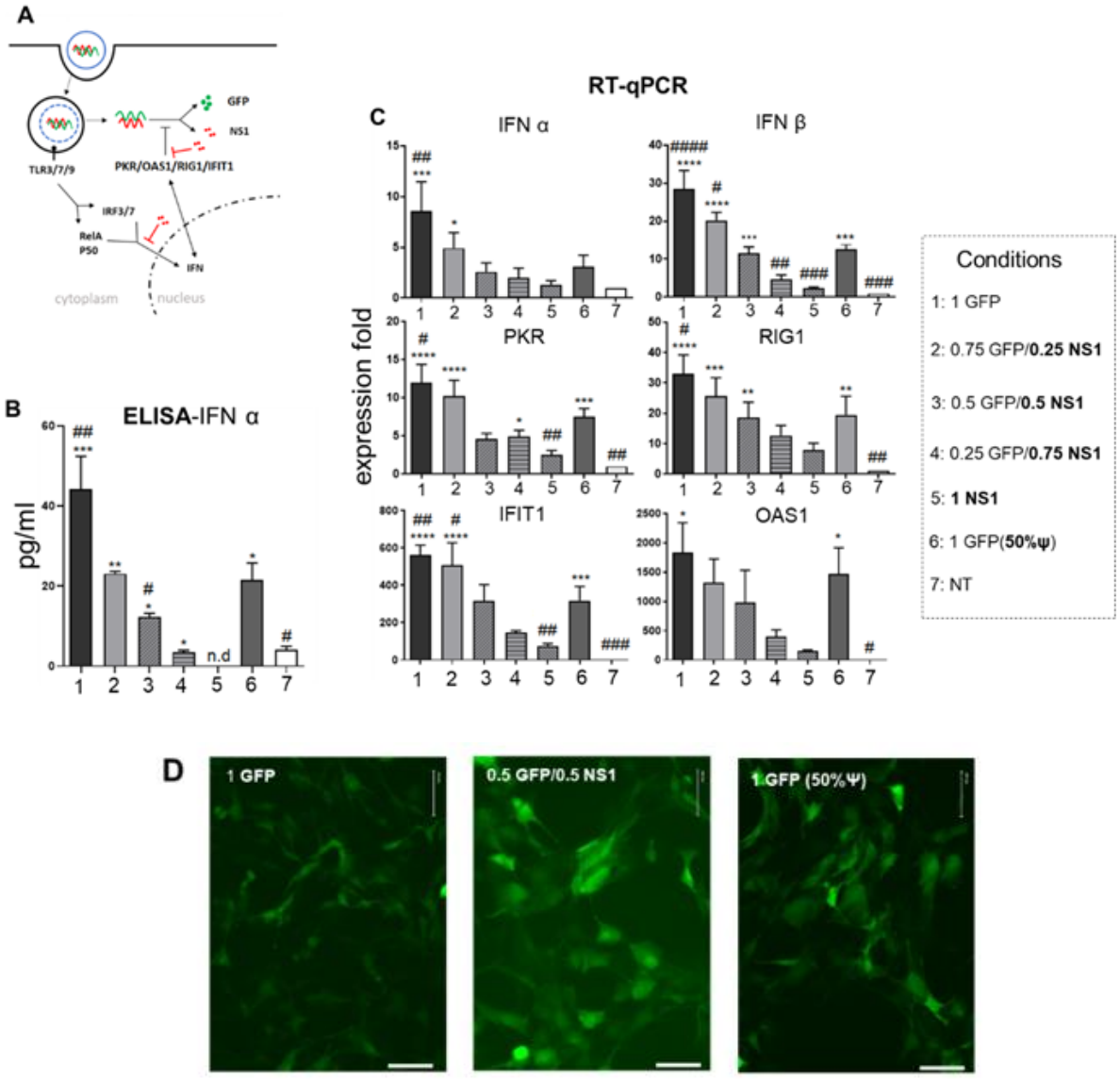

Fig. 4. NS1 regulates GFP translation by inhibiting RNA sensors. GFP mRNA was co-delivered with various amounts of NS1 mRNA into C3H10T1/2 cells (i.e. 1µg GFP mRNA (1 GFP); 0.75µg GFP mRNA and 0.25µg NS1 mRNA (0.75 GFP/0.25 NS1); 0.5µg GFP mRNA and 0.5µg NS1 mRNA (0.5 GFP/0.5 NS1); 0.25µg GFP mRNA and 0.75µg NS1 mRNA (0.25 GFP/0.75 NS1); 1µg NS1 mRNA (1 NS1)). 50% pseudouridine modified GFP mRNA (GFP(50%Ψ)) transfected cells and non-treated cells (NT) were set as controls. (**A**) Scheme of NS1 intracellular functions (Phua, Liu et al. 2017). (**B**) IFNα content in culture medium was quantified by ELISA. (**C**) Transcript levels of RNA sensors (i.e. IFN α/β, PKR, RIG 1, IFIT 1, and OAS 1 were measured by RT-qPCR. *, **, ***, **** compared to NT cells; #, #, ##, ###, ####, compared to GFP (50%Ψ). Ordinary one-way ANOVA, Dunnett's multiple

comparisons test, was used for the statistical analysis. (**D**) Representative images of cells transfected with indicated mRNAs. Scale bar, 125 µm.

Cell transfection with non-chemical modified IVT mRNA is known to active host cell immune response. Therefore, we assessed the effect of NS1 expression on the IVT mRNA-induced host immune responses in comparison with the use of chemically modified mRNA (GFP (50%ψ)) (Fig. 4). As expected, non-modified GFP mRNA (1 GFP) transfection significantly induced IFNα expression as well as other RNA sensors, i.e. IFNβ, PKR, RIG 1, IFIT 1, and OAS 1, whereas the presence of NS1 led to opposite effects (Fig. 4B and C). It is worth to note that the NS1 mRNA was non-modified as well. In addition, when cells were transfected with mRNA mix comprising of 75% GFP and 25% NS1 mRNA (0.75 GFP/0.25 NS1), the expression level of RNA sensors were comparable to that obtained from GFP (50%ψ) transfection. Consequently, the co-delivery with NS1 mRNA enhanced GFP expression as observed in Fig. 4D.

2.4.3. NS1 promotes IVT mRNA translation regardless gene context and cell type

GFP, Fluc and Gluc reporter mRNAs were co-delivered with equal amount of NS1 mRNA in 4 murine (i.e. C2C12, 4T1, DC 2.4, C3H10T1/2) and 3 human (A549, U87-MG, HepG2) cell types (Fig. 5). The translation of GFP mRNA was enhanced only 1.2-fold in DC 2.4 and HepG2 cells, and 4.2-fold in A549 cells (Fig. 5A), while the translation of Fluc mRNA was higher increased i.e. 10.5-fold in DC 2.4 cells and 175.3-fold in HepG2 cells (Fig. 5B). The effect on Gluc mRNA translation was evaluated by measuring the Gluc activity both in the medium and inside the cells. The improvement ranged from 1.2-fold (A549 cells) to 3-fold (4T1, U87MG, C3H10T1/2 and C2C12 cells) for Gluc released in the medium (Fig. 5C). Concerning Gluc activity inside the cells, the range of enhancement was from 2.0-fold (A549 and HepG2 cells) to 21.1-fold (C2C12 cells) (Fig.5D). Overall, those data indicated that the co-delivery of NS1 mRNA enhanced the level of translation of all the reporter genes tested and no inhibition was observed; the level of enhancement, however, was dependent on the cell type.

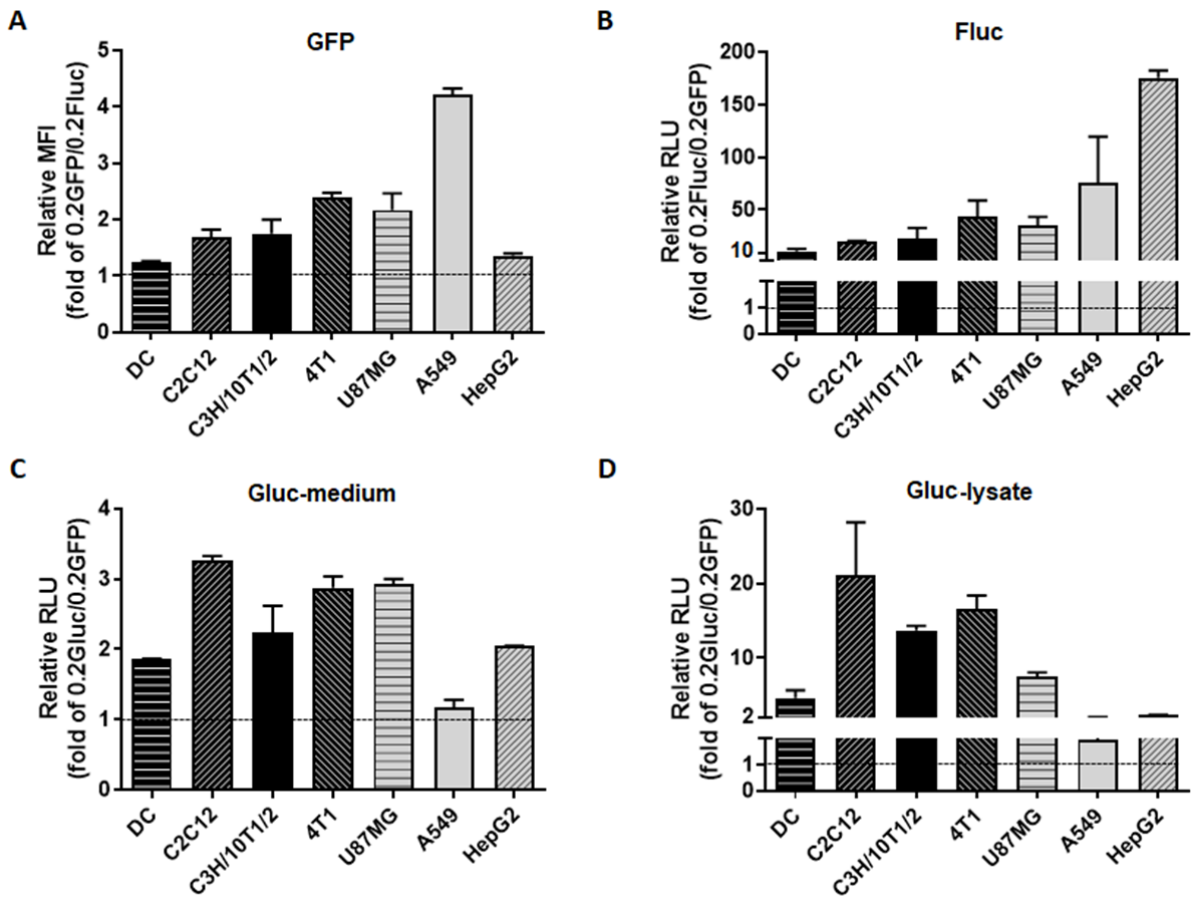

Fig. 5. NS1 mediated translation enhancement of different IVT mRNAs in different cell types. GFP, Fluc, and Gluc mRNAs were co-transfected to indicated cell types with NS1 mRNA at 1:1 mass ratio (0.2µg: 0.2µg). As controls, eGFP, FLuc and GLuc mRNA were codelivered with 0.2 µg FLuc mRNA, 0.2 µg eGFPmRNA, 0.2µg eGFP mRNA, respectively. (**A**) Fluorescence and (**B, C, D**) luminescence assays were performed one day post-transfection. For Gluc transfection, both (**C**) secreted and (**D**) intracellular Gluc productions were evaluated. All results were normalized to that obtained from controls.

2.4.4. Co-delivery of BMP-2 mRNA with NS1 mRNA generates a high level of BMP-2

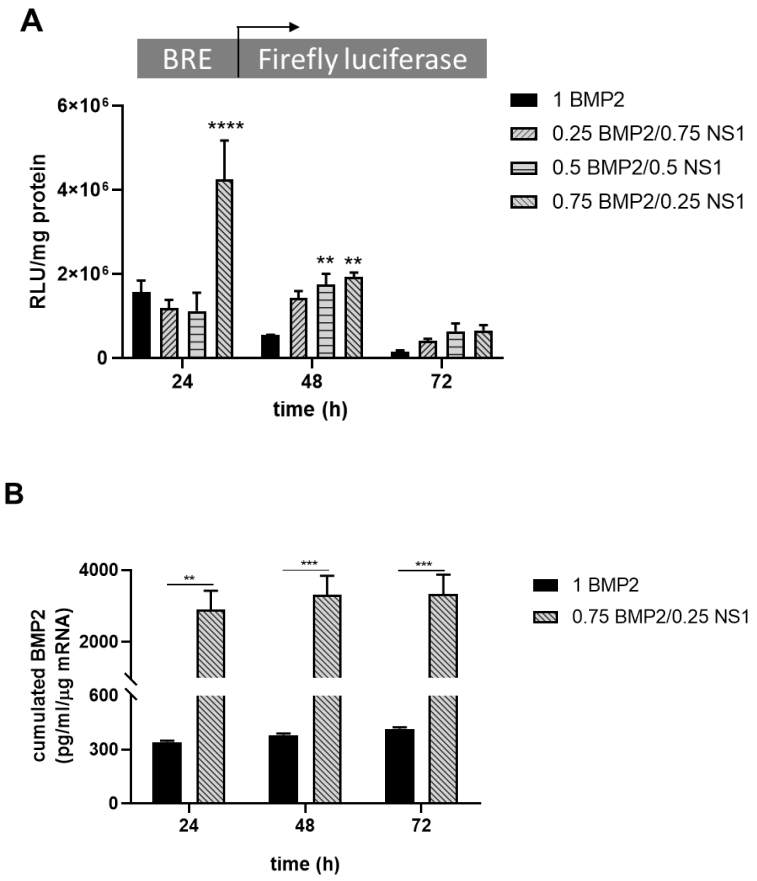

Fig. 6. BMP-2 expression from transfected cells. (**A**) Optimization of BMP2 and NS1 mRNAs ratio to give the best BMP2 activity. C2C12-BRE/LUC cells that stably express luciferase reporter gene under BMP-2 responsive elements (BRE-luciferase) were transfected with 1µg of total mRNA with varied amounts of BMP-2 and NS1 mRNA: 1µg BMP-2 mRNA, 0.75µg BMP2 mRNA + 0.25µg NS1 mRNA (25%), 0.5µg BMP2 mRNA + 0.5µg NS1(50%), 0.25µg BMP2 mRNA+ 0.75µg NS1 mRNA (75%). At indicated times, cells were lysed, and luciferase activity was measured to evaluate BMP2 expression. *, **, ****, compared to 1 BMP2 group within each time point. 2way ANOVA, Dunnett's multiple comparisons test, was used for the statistical analysis. (B) **Enhanced BMP2 mRNA translation when co-delivered with NS1 mRNA in C3H10T1/2 multipotent stem cells.** C3H10T1/2 cells were transfected with either 1 µg BMP2 mRNA (1 BMP2) or mRNA mix containing 0.75 µg BMP2 mRNA and 0.25 µg NS1 mRNA (0.75 BMP2/0.25 NS1). The BMP2 production in culture medium was analyzed by ELISA, and accumulated BMP2 amounts after indicated times are

presented. 2way ANOVA, Sidak's multiple comparisons test, was used for the statistical analysis.

C2C12-BRE/Luc cells were transfected with both BMP2 and NS1 mRNAs at different ratio (1 BMP2, 0.75 BMP2/0.25 NS1, 0.5 BMP2/0.5 NS1, 0.25 BMP2/0.75 NS1), and the luciferase activity, which can be correlated with the production of BMP-2, was measured after 24, 48 and 72 hours post-transfection. Fig. 6A shows a clear benefit of 25% NS1 mRNA substitution (0.75 BMP2/0.25 NS1) throughout the measuring time. The luciferase activity from cells transfected with 0.75 BMP2/0.25 NS1 was significantly higher (2.7-fold at 24h; 3.5-fold at 48h; 4.7-fold at 72h) than in cells transfected with BMP2 mRNA alone (1 BMP2). The decay of luciferase activity obtained from the BMP2 group was quite drastic after 48h (65%) and 72h (91%) which was not the case for 0.75 BMP2/0.25 NS1 group (48h-54%; 72h-85%). Notably, even at one-third BMP2 mRNA dose (0.25 BMP2/0.75 NS1), the luciferase expression remained higher than full dose of BMP2 mRNA alone at 48h and 72h post-transfection. Thus, the BMP2 mRNA to NS1 mRNA mass ratio of 3: 1 was used in further BMP-2 quantification and osteogenesis experiments.

Fig. 6B shows the quantification of BMP-2 production from C3H10T1/2 multipotent cells transfected with either BMP2 mRNA or BMP2/NS1 mRNAs. For both groups, BMP2 was extensively secreted in the first 24h post-transfection. Compared to BMP2 mRNA alone, BMP2/NS1 mRNAs generated 8.5-fold higher BMP2 production in the first 24h, and further to 10.5-fold in the next 48 h.

2.4.5. Dual delivery of BMP2 mRNA with NS1 mRNA favors osteogenic commitment of C3H10T1/2 multipotent stem cells

The osteogenic differentiation of C3H10T1/2 cells was evaluated from multiple aspects, i.e. osteoblastic gene expression, alkaline phosphatase (ALP) activity, and extracellular mineralization. For osteogenic induction, the C3H10T1/2 cells were transfected twice (Fig. 7A), as single transfection did not induce the cells differentiate toward osteoblasts (data not shown). As shown in Fig. 7C, cellular ALP activity gradually increased with time compared to non-transfected cells (NTrans). In cells transfected with NS1 mRNA, the increase was more significant at day 7 and day 14

compared to cells transfected with BMP2 mRNA alone. The ALP staining by BCIP/NBT at day 14 revealed that BMP2/NS1 transfected cells exhibited more intense blue-violet color than BMP2 mRNA transfected cells and NTrans cells confirming ALP quantification results (Fig. 7B). Twenty-eight days after the first transfection, the deposited calcium was stained with Alizarin red S (ARS). BMP2/NS1 mRNA transfected cells exhibited more calcium nodules than BMP2 mRNA transfected cells (Fig. 7D). These qualitative images were validated with the quantification of ARS-stained calcium following dissolution of aggregates (Fig. 7E). Both transfected groups showed a significantly higher calcium deposition in comparison to NTrans group.

From the gene expression aspect, the osteogenic-related transcripts were quantified at different time points by RT-qPCR (Fig. 7F). Compared to NTrans group, BMP2/NS1 mRNAs transfection induced Runx2 and ALP expressions peaked at day 7, which were significantly higher than that induced by BMP2 mRNA transfection (Fig. 7F-a and b). On day 14, ALP in BMP2/NS1 group still maintained a high expression and in line with the results shown in Fig. 7C. For Runx2, no significant difference was observed at day 14 and day 21. In contrary to Runx2 and ALP transcripts, the transcripts of Collagen type 1 started only to increase on day 7, and were steady up to day 21 (Fig. 7F-c). For OPN transcripts, the expression trend was similar to that of Runx2 and ALP (Fig. 7F-d). OCN expression gradually increased over time but the difference between BMP2/NS1 and BMP2 transfected cells was not significant despite.

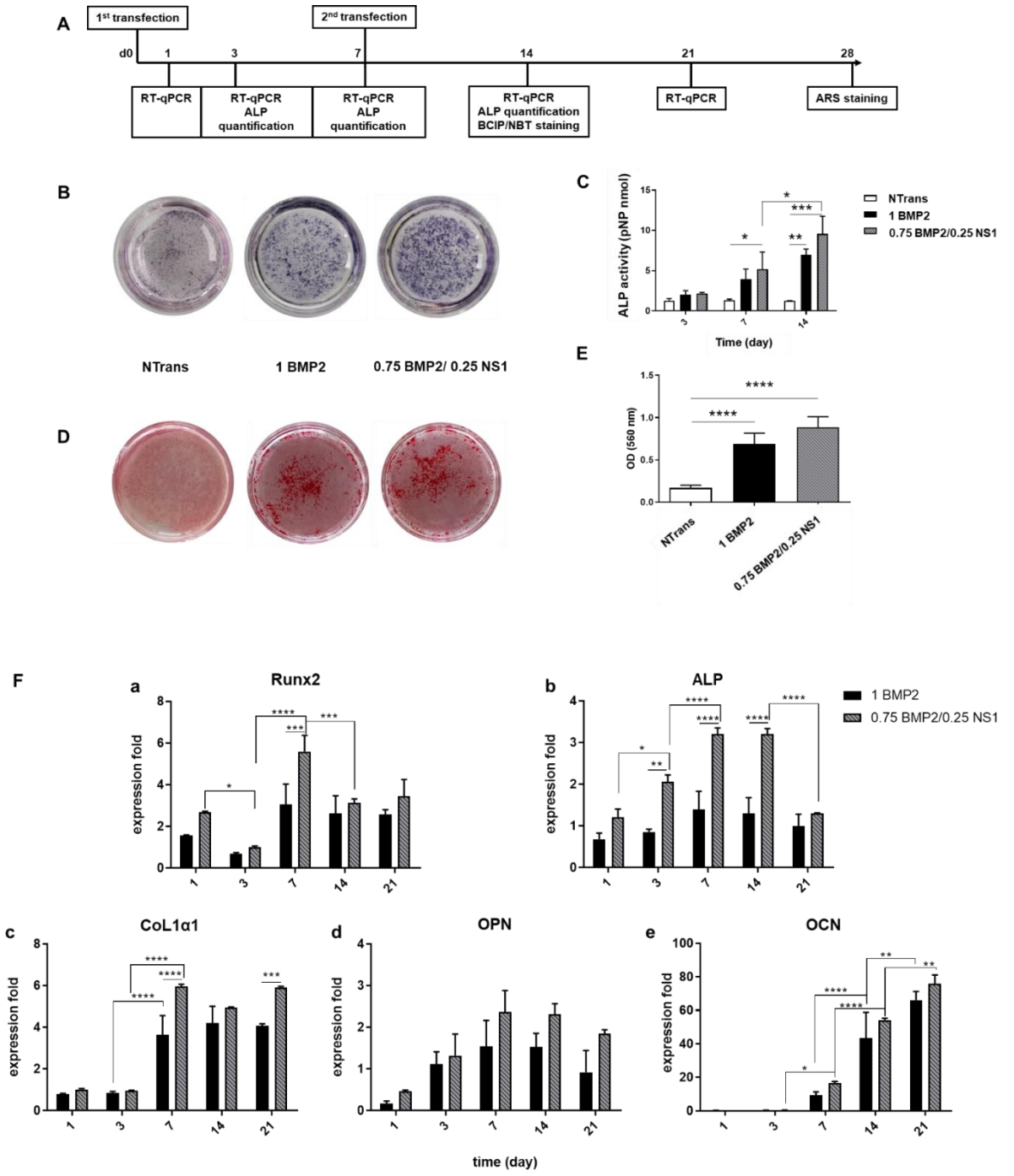

Fig. 7. Osteogenic differentiation of C3H10T1/2 multipotent stem cells. (A) Schematic illustration of protocol performed for osteogenic induction and quantification. (**B**) At 3, 7 and 14 days post 1st transfection, the ALP activity in C3H10T1/2 cells was quantified, and presented as nmol of *p*-Nitrophenol (pNP). 28 days post 1st transfection, **(C**) Representative ALP staining with BCIP/NBT solution, 14 days after 1st transfection. 2way ANOVA, Tukey's multiple comparisons test, was used for the statistical analysis. (**D**) Extracellular mineralization was observed upon alizarin red S (ARS) staining, and

(**E**) quantified by dissolving the stained ARS-aggregates into 10% cetylpyridinium chloride, followed by an optical density (OD) measurement at 560nm. Ordinary one-way ANOVA, Tukey's multiple comparisons test, was used for the statistical analysis. (**F**) At 1, 3, 7, 14 and 21 days following the 1st transfection, the transcripts of (**a**) Runx2, (**b**) ALP, (**c**) CoL1α1, (**d**) OPN and (**e**) OCN were quantified by RT-qPCR, and normalized to non-transfected cells. $2^{\wedge-\Delta\Delta Ct}$ method was used in the calculation. 2way ANOVA, Tukey's multiple comparisons test, was used for the statistical analysis.

2.5. Discussion

Different reports have shown the use of mRNA as a potent therapeutic for improving osteogenesis, but only using chemically modified equivalents (Elangovan, Khorsand et al. 2015, Balmayor, Geiger et al. 2016, Zhang, De La Vega et al. 2018, Wang, Perche et al. 2019). The goal of our study is to demonstrate that non-modified mRNA can promote osteogenic effects when combined with NS1 mRNA, encoding for an immune evasion protein derived from influenza A virus. Here, we adopted NS1 from A/Texas/36/1991 strain as IVT mRNA translation enhancer, which was proved to be the most potent than NS1 from other strains, i.e. A/Hong Kong/156/1997; A/Vietnam/1203/2004; A/Puerto Rico/8/1934; A/Texas/36/1991; A/California/04/2009; A/Shanghai/2013) (Phua, Liu et al. 2017).

Building the mRNA structure is one of the critical steps for mRNA therapy. A classical eukaryotic mRNA contains the 5' methylated guanosine cap, the 5' and 3' untranslated region (5'- and 3'-UTR), the open reading frame (ORF), and the poly(A) tail. It was shown that all parts of this structure have an impact on mRNA translation efficiency to some extent (Babendure, Babendure et al. 2006, Wang, Perche et al. 2019). For instance, we and other groups reported that mRNA containing longer poly(A) (e.g. 120nt) showed higher translation efficiency than that containing shorter ploy(A) tail (e.g. 67nt) (Holtkamp, Kreiter et al. 2006, Mockey, Goncalves et al. 2006, Grier, Burleigh et al. 2016). In line with this, we observed that BMP2-A150 mRNA resulted in higher protein expression than BMP2-A64 mRNA (data not shown). To optimize the protein expression, we generated mRNAs with different 3' UTRs (Fig. 1A), and found that the mRNA with shorter 3' UTR resulted in higher protein expression (Fig. 1B and C). This phenomenon was probably caused by differences in the stability of mRNA

secondary structures. Indeed, *via* computation (RNAfold 2.4.13), BMP2-NotI mRNA forms a secondary structure different from BMP2-XbaI (not shown).

As NS1 is a virus-derived protein, we explored whether its expression could induce a cytotoxic effect (Fig. 2). We did not find significant cell viability differences between NS1 mRNA transfected cells and GFP mRNA transfected cells with the dose range used during this study. Interestingly, XTT results indicated that GFP mRNA-transfected cells started to recover at 48h post-transfection, while getting worse for NS1 mRNA transfected cells. However, we did not observe significant increase of detached cells in NS1-treated wells. It was reported that during virus infection, NS1 could arrest the host cell at G0/G1 cycle to benefit virus replication (Jiang, Wang et al. 2013). Thus, we hypothesized that the reverse trend of XTT data could be due to NS1 cytostatic effect. Subsequently, we checked the cell cycle of treated cells, and found that the cell population in G0/G1 state was greater in NS1 mRNA transfected cells than in GFP mRNA transfected cells (Supplementary Fig. 2). So, the significant cell viability decrease in NS1 transfected cells could be caused, at least partly, by this cytostatic activity.

The co-delivery of NS1 mRNA with GFP mRNA into C3H10T1/2 cells resulted in enhanced protein expression, thanks to RNA sensors inhibition (Fig. 3 and Fig. 4). The incorporation of chemically modified nucleosides is also known to abrogate the IVT mRNA-induced immunogenicity. However, the effect is highly depending on modification type/ratio, mRNA context, and cell type (Kariko, Muramatsu et al. 2008, Uchida, Kataoka et al. 2015). For instance, Li *et al.*, reported that, in THP-1 macrophages, 5meC/ψ modified Fluc mRNA resulted in significantly higher Fluc expression, while 5meC/ψ modified eGFP mRNA resulted in a decreased GFP expression; me1ψ modified Fluc in THP-1 cells generated 8-fold more Fluc than that in hepatocellular carcinoma Hep 3B cells (Li, Luo et al. 2016). To check if NS1 mRNA could act as a versatile enhancer of mRNA translation, we co-delivered NS1 mRNA with different well-known reporter genes into several cell types (Fig. 5). By contrast to chemically modified mRNA, no negative effect was found in all tested conditions. Nevertheless, there was still variations in the translation efficacy depending on the gene of interest and the cell type. Specifically, Firefly luciferase mRNA expression was the most sensitive to the NS1 effect and, dendritic cells seemed to be more refractory likely because of its immune feature. For the majority of cell types tested including

mesenchymal cells, the enhancement was at least 2-fold which is already significant in terms of the amount of proteins produced.

The opportunity cost of replacing BMP2 mRNA with NS1 mRNA was measured (Fig. 6). The mass ratio of 3 to 1 of BMP2 mRNA to NS1 mRNA resulted in the highest BMP2 expression. As for gene delivery, the mRNA dose is correlated with the amount of carrier, and to avoid the cytotoxicity, a dose limit of the carrier must be respected. In this strategy, the replacement of part of mRNA of interest with NS1 gave a higher transgene expression indicating no opportunity cost as described previously (Phua, Liu et al. 2017).

In our study, NS1 increased BMP-2 expression for up to 8-fold. Interestingly, even the expression of BMP-2 mRNA alone was higher (10 times more) in this study compared to studies based on chemical modified BMP-2 mRNA (Elangovan, Khorsand et al. 2015, Balmayor, Geiger et al. 2016). This phenomenon could be explained by the type of cell, the transfection reagents used and the difference in BMP2 mRNA sequences, i.e. UTRs and length of poly(A) tail, which could also dramatically influence mRNA performance (Thess, Grund et al. 2015). The level of secreted BMP-2, however, remarkably decreased within 3 days due to the transient expression of mRNA. This finding is aligned with the data reported in the literature (Zangi, Lui et al. 2013, Sultana, Magadum et al. 2017).

As expected, secreted BMP-2 induced the expression of osteogenesis-related genes since this molecule is a potent osteogenic growth factor. The expressions of both early and late osteogenic genes were significantly enhanced following BMP-2 mRNA transfection and were further improved when cells were co-transfected with both BMP2 mRNA and NS1 mRNA. Our data indicated that Runx2, the master osteoblastic transcriptional factor, was firstly upregulated under BMP-2 stimulation with a peak of expression at day 7 post-transfection (Fig. 7F-a). Then, there is a production of bone matrix proteins expressed at middle-to-late stages of osteoblastic maturation, i.e. ALP, Col1α1, OPN, and OCN (Fig. 7F-b, c, d, e), all of them regulated by Runx2 through binding to their gene promoters (Ducy, Starbuck et al. 1999). Notably, osteocalcin was continuously expressed after 14 days (Fig. 7F-e), which is known to promote the deposition of mineral substance (Fig. 7D-E) due to the presence of calcium-binding residues (di-carboxylic glutamyl (gla)). Outcomes from this study were comparable to

those reported previously by others using chemically modified BMP-2 mRNA in terms of expression kinetics of osteogenic genes. It worth to note the osteogenic commitment of C3H10T1/2 stem cells could benefit from the cytostatic effect of NS1 expression. We are aware that the calcium deposits obtained were not as high as expected (Fig. 7D-E), indicating that the transient BMP2 enhancement was not sufficient to generate significantly higher osteogenesis. However, these results are valuable considering the fact that they were obtained with C3H10T1/2 cells. Indeed, it is known that C3H10T1/2 hardly differentiate toward osteoblasts compared to tissue derived primary mesenchymal stem cells which could spontaneously differentiate toward osteoblasts when cultured under osteogenic medium (Lotfy, Salama et al. 2014). Our effort is now focused on developing mRNA enabling long-term BMP-2 expression and, applying this strategy *in vivo* to heal non-union bone fracture, which is a challenging public health issue with the aging of human population.

2.6. Conclusion

Overall, results from this study demonstrated for the first time that dual delivery of non-modifed BMP-2 mRNA with NS1 mRNA as translation enhancer is a potential therapeutic since it allows a high expression of BMP-2 that results in the improvement of osteogenic genes expression. The strategy could be used as an alternative of chemically modified mRNA as the production of BMP-2 is higher than obtained with reported previously.

2.7. Supplementary Data

S. Table 1. Primers for RT-qPCR.

Gene (mouse)	Primer		Reference
ALP	F	AACCCAGACACAAGCATTCC	10.1073/pnas.0704360104
	R	GAGACATTTTCCCGTTCACC	
OCN	F	GCAGCTTGGTGCACACCTAG	
	R	GGAGCTGCTGTGACATCCATAC	
OPN	F	CTTTCACTCCAATCGTCCCTA	
	R	GCTCTCTTTGGAATGCTCAAGT	
Runx2	F	AGGGACTATGGCGTCAAACA	Self-design
	R	GGCTCACGTCGCTCATCTT	
Coll1α1	F	ACGCCATCAAGGTCTACTGC	
	R	ACTCGAACGGGAATCCATCG	
GAPDH	F	GCACAGTCAAGGCCGAGAAT	10.1016/j.jconrel.2016.08.037
	R	GCCTTCTCCATGGTGGTGAA	
IFN α	F	AAGCCATCCTTGTGCTAAGAGA	PrimerBank
	R	AGCAAGTTGGTTGAGGAAGAGA	
IFN β	F	AGCTCCAAGAAAGGACGAACA	
	R	GCCCTGTAGGTGAGGTTGAT	
IFIT1	F	GCCTATCGCCAAGATTTAGATGA	
	R	TTCTGGATTTAACCGGACAGC	
OAS1	F	GGGCCTCTAAAGGGGTCAAG	
	R	TCAAACTTCACTCCACAACGTC	
PKR	F	ATGCACGGAGTAGCCATTACG	
	R	TGACAATCCACCTTGTTTTCGT	
RIG-1	F	CAGATCCGAGACACTAAAGGGA	
	R	TCCTCATCAGCCTTGCTTTCA	

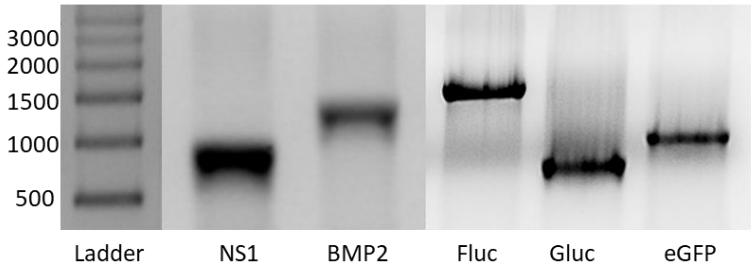

S. Fig. 1. Denatured agarose electrophoresis of IVT mRNAs. 2µg of indicating IVT mRNAs were run in 1% denatured agarose gel. The size and integrity of IVT mRNA bands were observed *via* a gel documentation system (GeneFlash, Syngene).

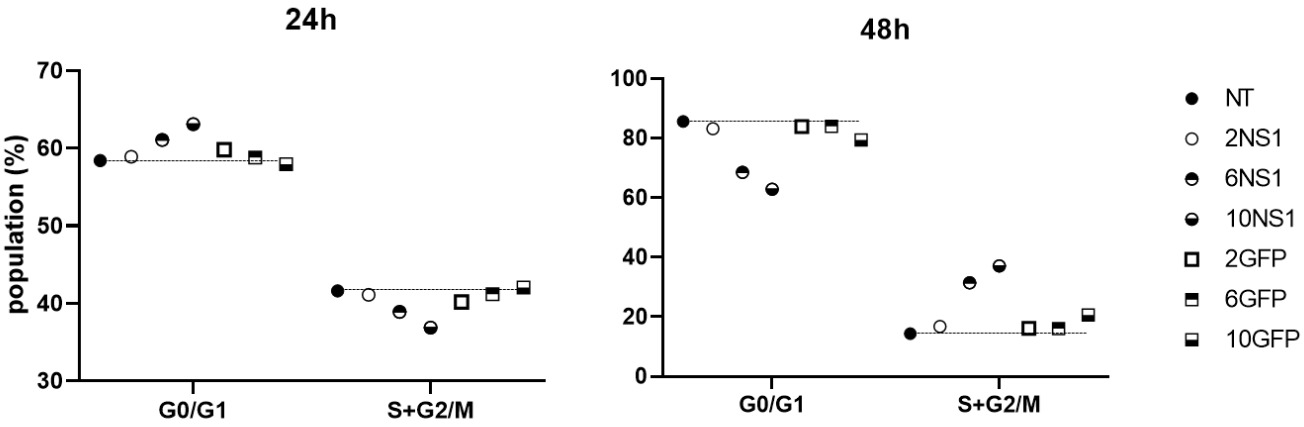

S. Fig. 2. Cell cycle of C3H10T1/2 cells. C3H10T1/2 cells were transfected with NS1 mRNA or GFP mRNA with the concentration of 2pg mRNA/cell (2NS1 or 2 GFP), 6pg mRNA/cell (6NS1 or 6GFP), or 10pg mRNA/cell (10 NS1 or 10GFP). 24h and 48h post-transfection, the cell cycle was determined by flow cytometry (BD Fortessa X20, BD Biosciences) after staining the genome DNA with propidium iodide (PI, Becton Dickinson). Briefly, cells were harvested, and fixed in ethanol (70%) for 30min on ice; then, cells were labeled in dark with staining buffer, containing 50µg/ml PI, 100µg/ml RNase A in PBS, for 30min at room temperature (RT).

Part III

BMP2 mRNA and NS1 mRNA Activated Collagen-nanoHydroxyapatite Matrix for Bone Regeneration

Evaluation des matrices de collagène renforcées par de l'hydroxyapatite chargées en ARNm codant la protéine BMP2 mRNA et l'ARNm codant la protéine NS1 pour la régénération osseuse

Ces dernières années, les biomatériaux utilisés comme support physique sur lequel des cellules peuvent adhérer, migrer, proliférer et se différencier et dans lesquels on peut charger des molécules ostéoinductrices sont intéressants pour la régénération osseuse. Les matrices activées en ARN messager (RAM : RNA-Activated Matrix) font actuellement l'objet d'évaluation pour la régénération osseuse, pour permettre une expression *in-situ* et soutenue de protéines ostéogéniques. Dans l'étude précédente, nous avons démontré que la co-délivrance de l'ARNm de BMP2 et de l'ARNm de la protéine 1 non structurelle 1 (NS1) du virus de la grippe A capable d'inhiber efficacement les senseurs d'ARN intracellulaires, améliore considérablement l'expression de la protéine BMP-2. Dans la présente étude, nous avons exploité cette stratégie avec des cellules souches mésenchymateuses dérivées de la moelle osseuse humaine (hMSC) pour favoriser leur différenciation ostéogénique. Ces ARNm formulés avec des liposomes ont induit la différenciation ostéogénique des hMSC, comme en témoigne l'expression accrue des gènes ostéoblastiques et la calcification extracellulaire. Ensuite, ces ARNm ont été formulés en complexes ternaires de liposome/polymère/ARNm appelés lipopolyplexes (LPR ont été incorporés dans une matrice de collagène-nano hydroxyapatite pour préparer les RAM. Ces LPR sont connus pour délivrer efficacement les ARNm. L'imagerie par microscopie électronique à balayage et les tests mécaniques ont démontré que la charge en ARNm n'influençait pas la microstructure de la matrice alors que la résistance à la compression était augmentée. Une libération des ARNm à partir des RAM a été observée jusqu'à 16 jours. Cette propriété a permis un doublement de la période d'expression des protéines par rapport à la transfection directe des cellules. Pour l'osteoinduction *in vivo*, les RAM ont été implantées par voie sous-cutanée sur le dos des souris. Les analyses de leur effet osteoinductif sont en cours d'évaluation. L'ensemble de nos résultats montrent que la matrice RAM pourrait être un produit standard de chirurgie orthopédique.

BMP2 mRNA and NS1 mRNA Activated Collagen-nanoHydroxyapatite Matrix for Bone Regeneration

Pinpin Wang[a], Federico Perche[a], Rudy Clemençon[a], Catia S.D. Cabral[c], Virginie Malard[a], Ilídio J. Correia[c,d], Hervé Petite[b], Delphine Logeart-Avramoglou[b], Chantal Pichon[a]*

a. Centre de Biophysique Moléculaire (CBM), UPR 4301 CNRS, Orléans, France
b. Laboratory of osteoarticular biology, bioengineering and bioimaging (B3OA), UMR 7052 CNRS, Paris, France
c. Centro de Investigação em Ciências da Saúde (CICS), Universidade da Beira Interior, Av. Infante D. Henrique, 6200-506, Covilha, Portugal
d. Departamento Engenharia Química, Universidade de Coimbra, Rua Silvio Lima, 3030-790, Coimbra, Portugal

3.1. Abstract

Messenger RNA (mRNA) activated matrices (RAMs) are interesting for bone regeneration since they have the potentiality to produce *in-situ* and sustained expression of osteogenic proteins. In the previous study, we developed a dual mRNAs system for *in vitro* osteogenesis by co-delivering BMP2 mRNA and influenza A virus nonstructural protein 1 (NS1) mRNA. NS1 proteins efficiently inhibited cellular RNA sensors, and significantly enhanced BMP-2 expression. Here, we applied the dual mRNAs delivery to human bone marrow-derived mesenchymal stem cells (hMSCs) for osteoinduction. The two mRNAs were formulated with Lipofectamne MessengerMax and benefited hMSCs osteogenic differentiation as evidenced by enhanced osteoblastic genes expression and extracellular calcification. Then, the dual mRNAs, formulated as liposome/polymer/mRNA ternary complexes (termed lipopolyplexes: LPRs)- reported to be efficient *in vivo*- were incorporated into the collagen-nanohydroxyapatite scaffold to prepare RAMs. Scanning electron microscopy imaging and mechanical tests demonstrated that the mRNAs loading did not influence the scaffold's microstructure, whereas the compressive strength was increased. The mRNAs *in vitro* release from RAMs lasted for 16 days and resulted in a 2-fold prolonged protein expression period compared to direct one single transfection of cells (14 *versus* 7 days). Finally, RAMs were subcutaneously implanted onto mice back for *in vivo* osteoinduction. The evaluation of *in vivo* bone formation by radiography and histology analyses is in progress. Overall, our results demonstrate

that these free-dried RAMs could be promising off-the-shelf products for clinical orthopedic practice.

Keywords: mRNA delivery, BMP2, NS1, collagen-nanohydroxyapatite scaffold, lipopolyplex, *de novo* bone formation

3.2. Introduction

Nowadays, millions of patients require bone defect repairs each year, and both autografts and allografts are not sufficient to cover this demand (Amini, Laurencin et al. 2012, Campana, Milano et al. 2014). In the future, this number is expected to increase due to various reasons, including the increased life expectancy of human population. Bone tissue engineering (BTE) provides the chance to fill the gap of this demand. BTE is a multidisciplinary field, including biology, material science, chemistry, engineering, etc., with an ultimate goal to create bone grafts (BTE grafts) for bone repair and regeneration (Amini, Laurencin et al. 2012); (O'Keefe and Mao 2011). A classical BTE graft is composed of a biocompatible and biodegradable scaffold for supportive function, and bioactive components for osteogenesis and vascularization (Kesireddy and Kasper 2016).

The gene-activated matrices (GAMs) represent a novel type of BTE graft composed of genes (i.e. pDNA or mRNA, coding osteogenic proteins) instead of traditional recombinant proteins and cells (D'Mello, Atluri et al. 2017). The GAMs are designed for long-term *in situ* growth factors expression with proper post-translational modifications at physiological tolerated dose. The feasibility of GAMs as a therapeutic for bone defect repair was fist demonstrated by Fang et al. in 1996 (Fang, Zhu et al. 1996). In their study, the GAM contained two-plasmid DNAs encoding bone morphogenetic protein-4 (BMP-4) and parathyroid hormone fragment (PTH1-34: amino acids 1-34). It was implanted into the rat femoral osteotomy gap. The fibroblasts from invaded granulation tissue became transfected and expressed BMP-4 and PTH1-34. Gap bridging was observed as early as 4 weeks post GAM implantation. In the next decade, more GAMs were developed. They comprised various genes (e.g. vascular endothelial growth factor (VEGF), platelet-derived growth factor-B, BMP-2) delivered *via* either viral vectors (e.g. adenovirus and recombinant adeno-associated

virus) or non-viral vectors (e.g. polyethyleneimine, SuperFect^{TM} liposome, and calcium phosphate) (Ono, Yamashita et al. 2004); (Ito, Koefoed et al. 2005); (Chang, Cirelli et al. 2009); (Keeney, van den Beucken et al. 2010); (Elangovan, D'Mello et al. 2014).

To avoid the risk of genome integrity and low transfection efficiency inherent with pDNA delivery, Aliasger K. Salem group introduced *IVT* mRNA-activated matrices (RAMs) for bone regeneration (Elangovan, Khorsand et al. 2015). In a rat calvaria defect model, the RAM induced 2.03-fold and 3.94-fold more bone tissue when compared to GAM-pDNA and empty controls, respectively. Those encouraging *in vivo* outcomes have been followed by other studies based on RAM have been performed with chemically modified *IVT* mRNAs known to avoid induced immune response (Elangovan, Khorsand et al. 2015; Khorsand, Elangovan et al. 2017; Balmayor, Geiger et al. 2016; Zhang, De La Vega et al. 2018). Despite the improvement obtained with chemically modified mRNA, their main drawbacks are their cost and the dependency of the effect as function of gene context and cell type (Uchida, Kataoka et al. 2015).

Recently, Phua et al., has developed a strategy based on Influenza A virus derived non-structural protein 1 (NS1), an immune evasion protein, known to block cellular RNA sensors, thus improving the translation of non-modified *IVT* mRNA (Phua, Liu et al. 2017). In the same line, we co-delivered BMP2 mRNA with NS1 mRNA to murine multipotent stem cells (C3H10T1/2) to enhance BMP2 expression. NS1/BMP-2 mRNA (3:1 weight ratio) generated 10.5-fold more BMP-2 expression compared to single BMP2 mRNA delivery, and as a result, induced a higher level of osteogenic differentiation (Wang et al., under submission).

Besides the immunogenicity, an effective delivery, especially for *in vivo*, is another challenge for mRNA therapy. We have developed a lipopolyplex (Liposome/Polymer/RNA ternary complex, LPRs) platform capable of efficient *in vitro* and *in vivo* cell transfection with a negligible toxicity (Gonçalves, Berchel et al. 2014); (Van der Jeught, De Koker et al. 2018). The imidazole/imidazolium binary liposomes (Lip100) are made of cationic O,O-dioleyl-N-(3N-(N-methylimidazolium iodide) propylene) phosphoramidate (KLN25) and neutral O,O-dioleyl-N-histamine phosphoramidate (MM27), in a molar ratio of 1:1 (Mevel, Breuzard et al. 2008); (Mevel, Neveu et al. 2008). KLN25 possesses an N-methylimidazolium polar head conferring a permanent positive charge used for nucleic acids condensation. The imidazole group

of MM27 is not alkylated on the nitrogen atoms, which allowing it to acquire a cationic charge when the environmental pH below 6 favoring the endosome destabilization and nucleic acids release (endosome escape). The cationic polymer is a histidylated linear polyethyleneimine (His-lPEI) (Bertrand, Goncalves et al. 2011). Same as MM27, the protonation of imidazole groups from histidine increases endosome escape of trapped nucleic acids leading to higher transfection efficiency compared to lPEI.

Based on the previous studies, the objective of this study is to investigate if delivering the dual mRNAs (BMP2/NS1 mRNAs) could enhance *in vitro* osteogenic differentiation of hMSCs and prepare the dual mRNAs-activated matrices for *in vivo* bone tissue formation.

First, NS1 and BMP-2 mRNAs were transfected to hMSCs using Lipofectamine™ MessengerMax as gold standard vector. The BMP-2 production and the osteogenic derivation of transfected hMSCs were quantified. Second, we formulated NS1 and BMP-2 mRNAs as LPR nanoparticles (lip100/ His-lPEI /nucleic acid) and incorporated them into collagen-nanohydroxyapatite bone mimicking scaffolds to form mRNA-activated matrices (RAMs). *In vitro* LPRs release and activity were determined . Finally, the RAMs were implanted subcutaneously to assess the ability of the RAMs to induce *de novo* bone formation.

3.3. Materials and Methods

3.3.1. *IVT* mRNAs preparation

The pT7-GFP (Perche, Clemencon et al. 2019), pT7-BMP2 and pT7-NS1 (Wang et al., 2019 under submission) plasmids were linearized with either SpeI or NotI, for mRNAs production with the mMessage mMachine T7 kit (Ambion) according to the manufacturer's instructions. The poly(A) tail was added with PolyA polymerase (Ambion). Synthesized mRNAs were purified with phenol: chloroform and isopropanol precipitation. Purity, size and integrity of the mRNAs were verified by a UV spectrophotometer (NanoDrop One, Thermo Scientific) and denaturing agarose gel electrophoresis, respectively.

3.3.2. Cell culture

C2C12 cells were purchased from American Type Cell Collection (ATCC), and cultured in Dulbecco's modified eagle media (DMEM, Sigma) containing 10% heat-inactivated fetal bovine serum (FBS; Sigma) and 1% antibiotics (Sigma). C2C12-BRE/Luc cells, which contain a BMP-2 sensitive reporter gene were obtained after stably transfection with the BMP-responsive element (BRE) fused to the luciferase gene as previously described (D. Logeart-Avramoglou 2006). hMSCs were harvested from bone marrow obtained from discarded tissue during routine bone surgery from 3 donors (1 woman and 2 men; 15, 22, and 31 years old, respectively) at the Lariboisiere Hospital, Paris, France. The tissues were collected with the respective donor's consent in agreement with Lariboisiere Hospital regulations. hMSCs were isolated from each donor's bone marrow using a procedure as previously reported (Friedenstein, Piatetzky et al. 1966); (Moya, Larochette et al. 2018). Briefly, hMSCs were harvested by gently flushing the bone marrow using complete growth medium (specifically, alpha-Minimum Essential Medium (α-MEM, PAN Biotech) containing 10% heat-inactivated fetal bovine serum (FBS; Sigma) and 1% antibiotics (Sigma). These cells were characterized by expression of selected CD markers (specifically, positive for CD90, CD73, CD105 and negative for CD45; data not shown). At passage 1, hMSCs from each donor were pooled at an equal ratio, and used for experiments up to passage 8.

All cells were cultured at 37°C in a humidified atmosphere containing 5% CO_2, and mycoplasma-free as evidenced by MycoAlert Mycoplasma Detection Kit (Lonza).

3.3.3. Osteogenic commitment of hMSCs

3.3.3.1. Quantification of BMP-2 expression from transfected hMSCs

hMSCs were seeded in a 12-well plate at $1x10^5$ cells/well. The next day, cells were transfected with 1µg BMP2 mRNA or 0.75µg BMP2 mRNA/0.25µg NS1 formulated with Lipofectamine™ MessengerMax (LFM lipoplexes) according to the manufacturer's protocol. Every 12h, half culture medium was collected and the well was refilled with fresh growth medium. Collected media were stored at -80℃ before BMP-2 quantification. BMP-2 contents were determined by ELISA (Abcam) following the manufacturer's instruction. The absorbance was measured at 450nm (^{3}V

spectrophotometer, PerkinElmer) and BMP-2 contents were calculated based on a standard curve (range: 0-4000pg/ml human BMP-2).

3.3.3.2. In vitro osteoinduction

$5x10^4$ hMSCs were seeded into each well of 12-well plate, and cultured in growth medium for at least one week allowing cell confluence. Then 0.5µg BMP2 mRNA or 0.325µg BMP2 mRNA/0.125µg NS1 mRNA were delivered as lipoplexes to the cells. The cell culture medium was changed to osteogenic medium, which consisted of the growth medium plus 10 mM beta-glycerophosphate (β-GP, Sigma) and 150 µM ascorbic acid-2-phosphate (As2P, Sigma).

3.3.3.3. Osteoblastic genes expression

At day 1, 3, 5, 7, 14, and 21 post-transfection, the expression of Runx2, Alakine phosphatase (ALP), collagen type 1, osteocalcin (OCN), osteoprotegerin (OPN) were quantified by real-time quantitative reverse-transcription polymerase chain reaction (RT-qPCR) according to a previous report (Lin, Perche et al. 2016). Briefly, total RNA was isolated and purified by TRIzol (Life technology)-chloroform method. RNA concentration and purity were measured using Nanodrop (ThermoFisher). First-strand cDNA synthesis kit (Thermo Scientific) was used for reverse transcription following the manufacturer's protocol. qPCR was performed using the Luna qPCR Master Mix (NEB) with a Light Cycler© 480 PCR system (Roche). The qPCR data were analyzed by the comparative ΔΔCt method using the GAPDH RT-qPCR signal as an internal control for normalization. Primers for RT-qPCR were synthesized by Eurogentec, and the sequences were listed in Supplementary Table 1.

3.3.3.4. Evaluation of Alkaline phosphatase activity

At day 3, 7, and 14 post-transfection, ALP activity was visualized by Nitro Blue Tetrazolium (NBT)/5-Bromo-4-chloro-3-indolyl phosphate disodium salt (BCIP) (Sigma) staining as previously reported (Cui, Sun et al. 2017) with slight modification. Briefly, at day 14 post-transfection, cells were washed with PBS, and then fixed in 4% formaldehyde for 2 min. BCIP/NBT solution was added to react with ALP for 30 min in dark at RT. The staining solution was washed out with PBS.

3.3.3.5. Mineralization assessment

Alizarin Red staining was performed 28 days post-transfection to evaluate calcium deposition. Cells were washed with D-PBS and then fixed in 4% p-formaldehyde for 30 min at room temperature (RT) followed by 2 times washes with distilled water (dH2O). Extracellular calcium was stained by incubating the cells in Alizarin red S (Sigma) solution (saturated in dH_2O, pH 4.1). Nonspecific staining was removed by washing with dH_2O for five times under gentle agitation. To quantify the mineralization, the alizarin red dye was subsequently extracted with cetylpyridinium chloride (Sigma) solution (10% in 10mM sodium phosphate) for 30 min at RT. Absorbance was then measured at 560nm using the Victor ^{3}V spectrophotometer (PerkinElmer).

3.3.4. Collagen-nanohydroxyapatite scaffolds

The collagen-nanohydroxyapatite scaffolds (CoLL-nHA) were prepared as reported previously (Cunniffe, Dickson et al. 2010, Offeddu, Ashworth et al. 2015) with some modifications. Briefly, the collagen (Calf skin type I collagen, MP Biomedicals) was first hydrated in 0.1M acetic acid overnight at 4℃. The nano-sized hydroxyapatite (Sigma) was well dispersed in 0.1M acetic acid after two times sonication, each for 30min. Then, the hydroxyapatite suspension was dropped into the collagen slurry under vortexing (final collagen concentration was 0.75% w/v). The collagen-hydroxyapatite mix was further homogenized overnight at 4℃ using a roller mixer (Cat Ingenieurbuero™ RM540). After that, the collagen-hydroxyapatite mix was degassed under vacuum for 1min. Then, the mix was dispatched into polypropylene containers, which were frozen to -80℃ for 2h with a cooling rate of 1℃/min, followed by a sublimation step for at least 16h at -80℃ and 0.1mbar (Bioblock Scientific). The CoLL-nHA scaffolds were thencrosslinked by 1-ethyl-3-(3-dimethylaminopropyl) carbodiimide hydrochloride (EDC) and N-hydroxysuccinimide (NHS) (Olde Damink, Dijkstra et al. 1996) in 95% ethanol for 3h at room temperature followed by five times wash in distilled water for fifteen minutes each. Finally, freeze-drying the scaffolds using the same process as described above. The collagen scaffolds (0.75% w/v) were prepared as control.

3.3.4.1. Microstructure

The scaffolds' microstructures were observed with a scanning electron microscope (SEM) (Zeiss Ultra Plus, Carl Zeiss) after mounting on SEM stubs and coating gold-palladium.

3.3.4.2. Pore size and porosity

Pore size was measured using the ImageJ software (1.52a, National Institutes of Health) according to previously reported study (Bartos, Suchy et al. 2018). Briefly, 50 randomly selected pores from each of 8 SEM images (belong to two samples) were analyzed. The circularities were assumed as 1 for pore size calculation.

Porosity was assayed by the liquid displacement method (Karageorgiou and Kaplan 2005); (Nazarov, Jin et al. 2004). Briefly, the scaffold was immersed in 1ml (V1) distilled water in a cylindrical container, and a vacuum was applied for 1min allowing water fully infiltrate into the scaffold. After that, the total volume of water plus scaffold was defined as V2. Then, the water-impregnated scaffold was removed from the container, the remaining water volume was V3 and the porosity was calculated as follows:

$$\text{Porosity} = (V1-V3) / (V2-V3)$$

3.3.4.3. Mechanical strength

The mechanical measurements were performed at room temperature using a tensile testing machine (AG-X, Shimadzu) with a crosshead speed of 2 mm/min and a load cell of 5 kN. The compressive strength (Cs) was determined with the following Equation:

$$Cs=F/A$$

where F corresponds to the load strength (N) at the time of fracture and A represents the scaffold contact area (mm).

3.3.4.4. Cytocompatibility

$1x10^4$ C2C12 cells were suspended in 100 µl medium, and then drop onto a scaffold column (6mm × 2.5mm). Before adding culture medium, the scaffolds containing cells

termed as constructs were incubated for 2h in a humidified atmosphere with 5% CO2 at 37℃ to allow cells adhesion.

Cell proliferation inside the scaffolds was measured with Cell Proliferation Kit II (XTT) (Sigma-Aldrich) according to the manufacturer's instruction with modification. Briefly, at defined time points, constructs were washed twice with DPBS (Sigma), during which the constructs were gently pressed for complete medium and DPBS exchange. After removing the internal D-PBS with an absorbent tissue, the constructs were immerged into reaction mix, which contains 200 µl culture medium, 50 µl XTT solution, and 1 µl electron-coupling reagent. After 4h, 100 µl solution from each well was transferred into 96-well plate, and the absorbance was read at 450nm and 650nm with Victor ^{3}V spectrophotometer (PerkinElmer).

Cell density and morphology were observed with confocal laser scanning microscopy (LSM510, Zeiss). For that, the constructs were washed as described above, and then fixed with methanol (90%) for 30min at -20 ℃; next, the cells were blocked with PBS-1% BSA for 1h at RT followed by anti-actin antibody (Sigma) incubation (2h, RT); then, cells were incubated with Alexa Fluor® 488 conjugated secondary antibody (Invitrogen) for 2h at RT.

3.3.5 Lipopolyplex (LPR)

The His-lPEI grafted with 16% histidine residues was synthesized as previously described (Bertrand, Goncalves et al. 2011), and purchased from Polytheragene SAS (Genepole, Evry, France). KLN25 and MM27 were synthesized as previously described (Mevel, Breuzard et al. 2008); (Mevel, Neveu et al. 2008). The Lip100 containing an equal molar ratio of KLN25 and MM27 was prepared as previously described (Perche, Benvegnu et al. 2011); (Gonçalves, Berchel et al. 2014).

Lipopolyplexes were prepared according to (Gonçalves, Berchel et al. 2014) with some modifications (Fig. 3A). In brief, 15 µl HEPES (10mM, pH 7.4) containing 7.5 µg PTG1 (Polytheragene) was added into 37.5 µl HEPES containing 2.5 µg mRNA under vortex followed by 30 min incubation at RT to allow the polyplexes formation. Then, the polyplexes were added into liposome solution (3 µl 5.4mM Lip100 in 197 µl HEPES), and pipette up and down for 5 times followed by 15 min incubation at RT, allowing the LPRs formation.

3.3.5.1. LPR particle size and zeta potential

After diluting in HEPES buffer (10 mM, pH 7.4), the LPR particle sizes and zeta potential were measured by dynamic light scattering and electrophoretic mobility, respectively with nanoparticle analyzer SZ-100 (Horiba Scientific).

3.3.5.2. LPR morphology

LPR morphology was analyzed by transmission electron microscopy (TEM) using a Philips CM20/STEM electron microscope operating at 50 kV. TEM samples were prepared according to the technique of negative staining using uranyl acetate as reported by Perche et al. (Perche, Clemencon et al. 2019). The basis of the method is to surround the light atoms sample with a dense stain to create TEM contrast. 5 mL LPR solution in HEPES buffer was deposited on a carbon-coated copper grid for 5 min;and then adsorbed with filter paper. 5 mL uranyl acetate 2% in RNase-free water was then, deposited on the grid for 10 s. Samples were dried at room temperature for 20 min before TEM observation.

3.3.6. mRNA activated matrices (RAMs)

The LPRs were prepared as described above, except that the total volume was decreased 10-fold and containing 5% sucrose. Concentrated LPRs containing 20 µg mRNA were sucked into each scaffold disc (6mm × 2.5mm), which then undergoes the freeze-drying process as described in scaffold preparation. The mRNA activated matrices (RAMs) were stored at -20 ℃ for further usage.

The **SEM observation** and **mechanical test** of RAMs were performed as described in section 2.3.1 and 2.3.3.

3.3.6.1. LPRs release kinetics

The RAMs were immerged in 1ml RNase-free TE buffer (10 mM Tris-HCl, 1 mM EDTA, pH7.5) and incubated at 37℃. At scheduled time points, the 800µl TE buffer was collected and refilled with RNase-free TE buffer. All samples were stored at -80 ℃ for further measurement. The released LPRs were labeled with Quant-iT^{TM} RiboGreen (Invitrogen) following the manufacturer's instruction, and then quantified by a spectrophotometer (excitation: 490nm; emission: 525nm) (Victor ^{3}V, PerkinElmer).

3.3.6.2. In vitro LPRs release and transfection

$1x10^5$ C2C12-BRE/Luc cells/well were seeded in 24-well plate. The next day, RAMs either containing 20µg BMP2 mRNA or 15µg BMP2/ 5µg NS1 mRNAs were added into each well. At the defined time points, cells were lysed and stored at -80 ℃. Luciferase activity was measured as previously reported (Perche, Benvegnu et al. 2011). Cells transfected with 1µg BMP2 mRNA and 0.75µg BMP2/0.25µg NS1 mRNAs, which formulated into LPRs, were set as control.

3.3.7 *In vivo* de novo osteogenesis

Four-week-old male balb/c mice were purchased from JANVIER, and handled in accordance with the European Directive 2010/63/EU regarding the protection of animals used for scientific purposes. All animal experiments were performed with approval of the ministry of research. RAMs were subcutaneously implanted notp mice back (one RAM per mouse, n=8) as previously described (Moya, Larochette et al. 2018). Empty CoLL-1nHA scaffolds were set as control.

3.3.8 Statistical analysis

Unless otherwise indicated, the numerical data are expressed as mean ± standard deviation of three replicates. Statistical analysis was performed using GraphPad Prism version 6.07 (GraphPad software). Any p-value less than 0.05 was considered statistically significant. Specifically, * represents $P < 0.05$; ** represents $P < 0.01$; *** represents $P < 0.001$; **** represents $P < 0.0001$.

3.4. Results

3.4.1. Co-delivery of BMP2 mRNA with NS1 mRNA to hMSCs enhances BMP-2 expression

BMP2 mRNA and NS1 mRNA were co-delivered to hMSCs at a mass ratio of 3:1 based on our previous study (Wang et al., under submission). BMP-2 content in culture media collected every 12h was quantified (Fig. 1) Compared to BMP2 mRNA alone; co-transfection with NS1 mRNA increased the BMP-2 expression with significant difference from the early (12h-24h) to the later time (48h-60h). Following BMP/NS1

mRNAs transfection, the peak of BMP-2 expression started to peak at 24h and maintained up to 36h. While the highest amount of BMP-2 was obtained in the first 12h following BMP-2 mRNA transfection, then it decreased as function of time.

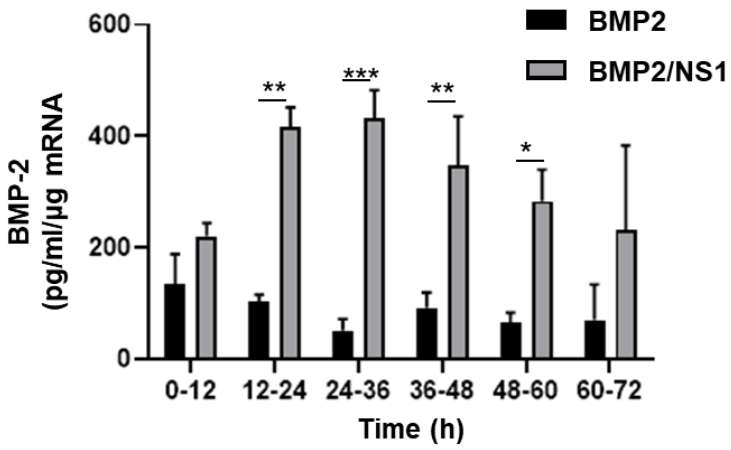

Fig.1. BMP-2 expressed from transfected hMSCs. The secreted BMP-2 from 1µg BMP2 mRNA (BMP2) and 0.75µg BMP2/0.25µg NS1 mRNAs (BMP2/NS1), formulated with Lipofectamine™ MessengerMax (LFM), transfected hMSCs was quantified by ELISA every 12h post-transfection.2way ANOVA, Sidak's multiple comparisons test, was used for statistical analysis.

3.4.2. Co-delivery of BMP2 mRNA with NS1 mRNA favors hMSCs osteogenic commitment

The osteogenic differentiation of hMSCs was evaluated by measuring osteoblastic genes expression and extracellular matrix (ECM) mineralization (Fig. 2). On day 1, 3, 7, 14 and 21 post-transfection, osteoblastic transcripts were quantified by RT-qPCR (Fig. 2A). In BMP2/NS1 group, the tendency of Runx2, ALP, OPN, OCN expression was higher than in BMP2 group throughout the measuring time albeit not significantly except for Runx2 on day 3. Twenty-eight days post-transfection, the deposited calcium was stained with Alizarin Red S (ARS). The ARS-stained calcium was further quantified by dissolving in 10% cetylpyridinium chloride solution (Fig. 2B). Compared to the NT group, the BMP2/NS1 group showed significantly higher ECM calcium, while the BMP2 group did not.

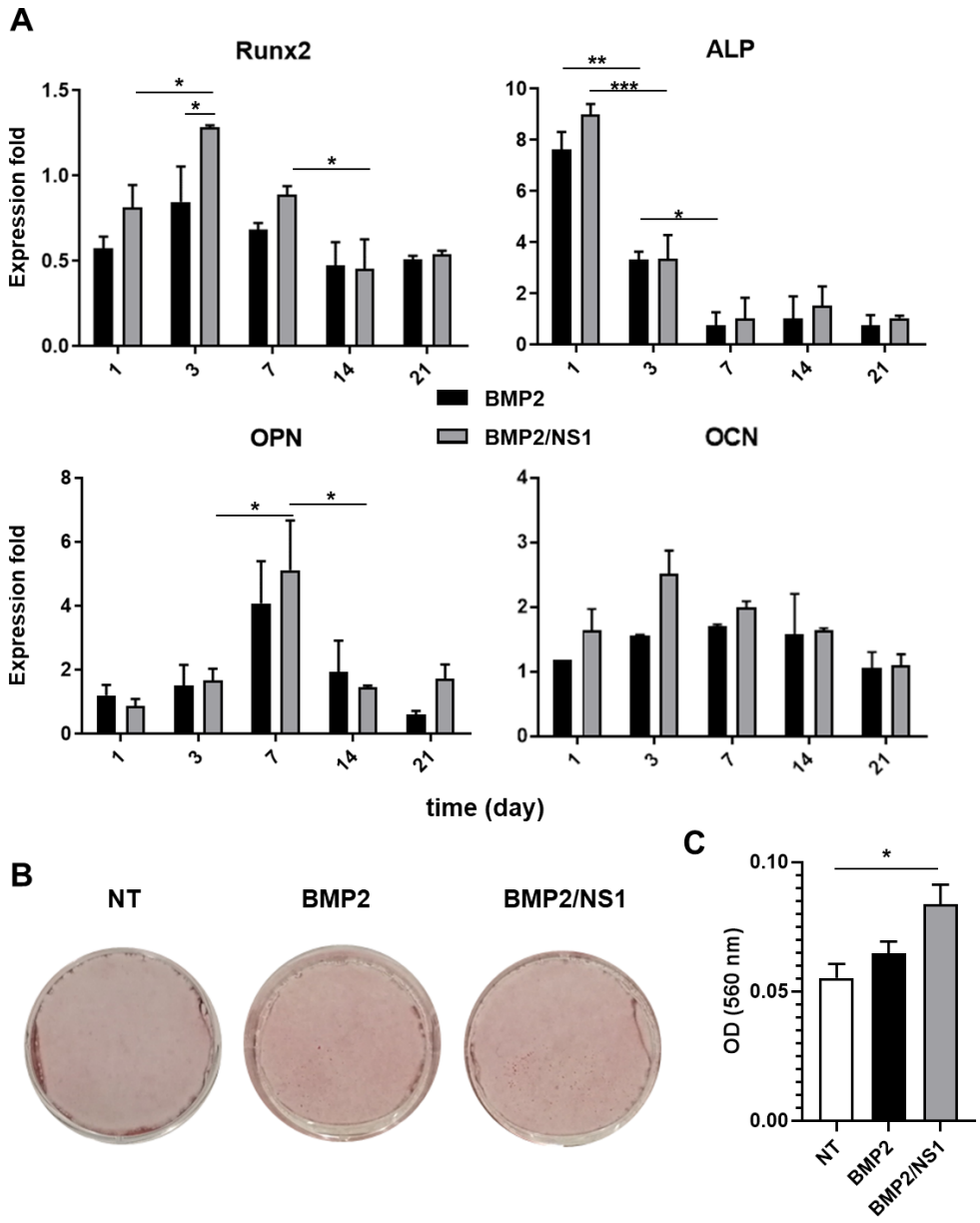

Fig. 2. hMSCs osteogenic commitment. hMSCs (P6-P8) were transfected either with 0.5 µg BMP2 mRNA or 0.375 µg BMP2/0.25 µg NS1 mRNAs, which formulated with LFM. (**A**) The expression of transcripts of osteoblastic genes was measured at day 1, day 3, day 7, day 14 and day 21 post-transfection by RT-qPCR, and normalized to non-treated cells (NT). $2^{\wedge-\Delta\ \Delta Ct}$ method was used for calculation. 2way ANOVA, Tukey's multiple comparisons test, was used for statistical analysis. (**B**) The calcification of extracellular matrix (ECM) was observed *via* ARS staining, 28 days post-transfection, and (**C**) quantified by dissolving the ARS-aggregates into 10% cetylpyridinium chloride (CPC) followed by an optical density (OD) assay at 560nm. Ordinary one-way ANOVA, Tukey's multiple comparisons test, was used for statistical analysis.

3.4.3. LPRs preparation and characterization

LPRs were prepared by a well-established two-step approach, comprising the complexation of polyplexes containing mRNA and the His-lPEI with a mRNA/His-lPEI weight ratio of 1/3, and then mixing the polyplexes with the liposomes (Lip100) at a mRNA/Lip100 weight ratio of 1/2 (Perche, Benvegnu et al. 2011); (Gonçalves, Berchel et al. 2014) (Fig. 3A). The complexation of mRNA was confirmed by an agarose gel electrophoretic mobility shift assay, in which no free mRNA migration was observed (data not shown). The LPRs had a mean hydrodynamic diameter of 208nm with the core morphology of mRNA/PTG1 complex surrounded by a unilamellar lipid bilayer structure of Lip100 (Fig. 3B). The LPRs were slightly positively charged as shown in Fig. 3C.

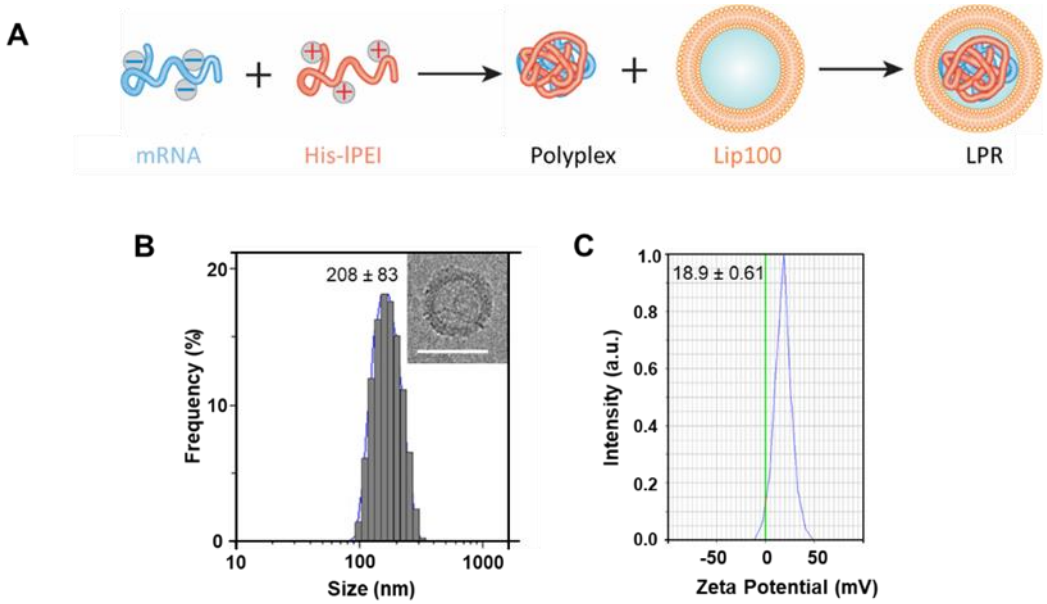

Fig. 3. LPR preparation and characterization. (**A**) Scheme of LPR nanoparticle formation. (**B, C**) The representative diagram of hydrodynamic diameter distribution (inset: TEM image with scale bar = 100 nm). and zeta potential of LPR made from GFP mRNA.

3.4.4. Preparation and characterization of collagen-based scaffolds

Three types of collagen-based scaffolds were produced by a freeze-drying approach using acetic acid as a porogen. They had a collagen/nanohydroxyapatite weight ratio

of either 1/0 (CoLL), 1/1 (CoLL-1nHA) or 1/3 (CoLL-3nHA). The porous structure was observed by the scanning electron microscopy (Fig. 4A). CoLL (Fig. 4A-a) and CoLL-1nHA (Fig. 4A-c) exhibited similar microstructure with connected macro- (>100μm) and micro-pores (<50μm). Whereas, CoLL-3nHA (Fig. 4A-e) was denser and devoid of micro-pores. The SEM images observed under the high magnification revealed embedded (Fig. 4. A-d) and exposed nHA particles (Fig. 4A-f). Two key parameters, i.e. pore size and porosity, of porous scaffold were quantified. As shown in Fig. 4B and C, CoLL, CoLL-1nHA and CoLL-3nHA had an average pore size/porosity of 168.7μm/ 91.26%, 151μm/ 89% and 165.9μm/ 76%, respectively. Compared to CoLL, both CoLL-1nHA and CoLL-3nHA demonstrated higher compressive strength in axial and radial orientations (Fig. 4D).

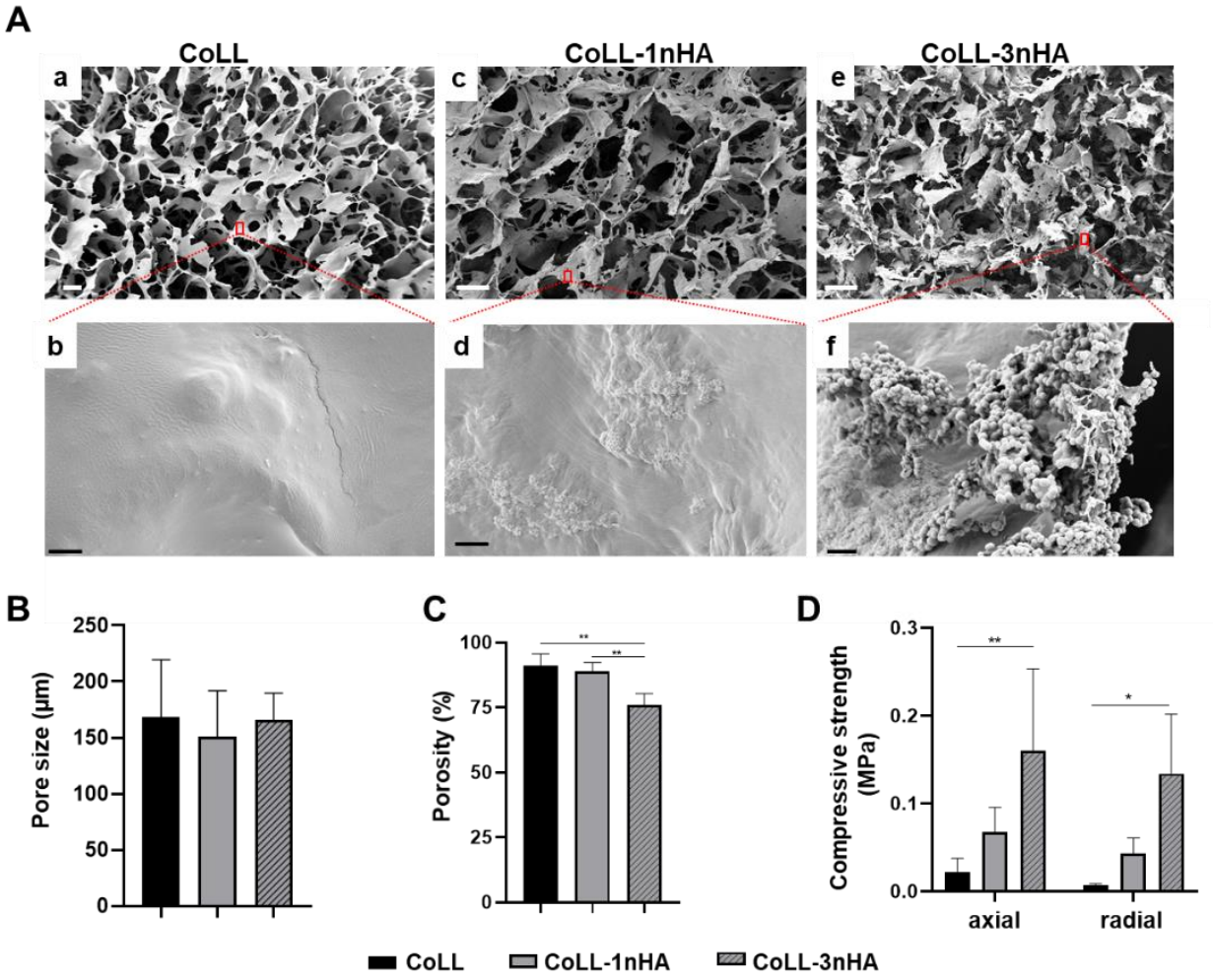

Fig. 4. Physical properties of Collagen scaffold and collagen-nanohydroxyapatite scaffolds. (**A**) The representative SEM microphotos of collagen scaffold (CoLL; **a, b**), collagen-nanohydroxyapatite scaffolds (mass ratio 1 to 1: CoLL-

1nHA - **c, d**; mass ratio 1 to 3: CoLL-3nHA - **e, f**). White scale bar: 100 µm; Black scale bar: 2µm. n=4. (**B**) shows the pore sizes of CoLL, CoLL-1nHA and CoLL-3nHA, which were calculated by ImageJ software based on SEM images. n=8. (**C**) The open porosities of CoLL, CoLL-1nHA and CoLL-3nHA were calculated by the liquid displacement method. n=4. Ordinary one-way ANOVA, Tukey's multiple comparisons test, was used for statistical analysis. (**D**) The scaffolds' compressive stregth. The axial and radial mechanical performaces of the three types of scaffold were tested, respectively. n=4. 2way ANOVA, Tukey's multiple comparisons test, was used for statistical analysis.

Then, we evaluated the cytocompatibility of those three scaffolds (Fig. 5A). XTT assay results done one post C2C12 murine cells seeding revealed that more cells were attached to CoLL-1nHA than CoLL-3nHA and CoLL. From day 1 to day 3, there was an intense cell proliferation in all three scaffolds. No significant cell viability difference was observed in cells seeded on those three scaffolds. Fig. 5B shows the visualized cell proliferation in CoLL-1nHA after labeling with green fluorescein. At day 1, few cells separated in the scaffold, and after one-week growth, the cells bridged together and filled the field.

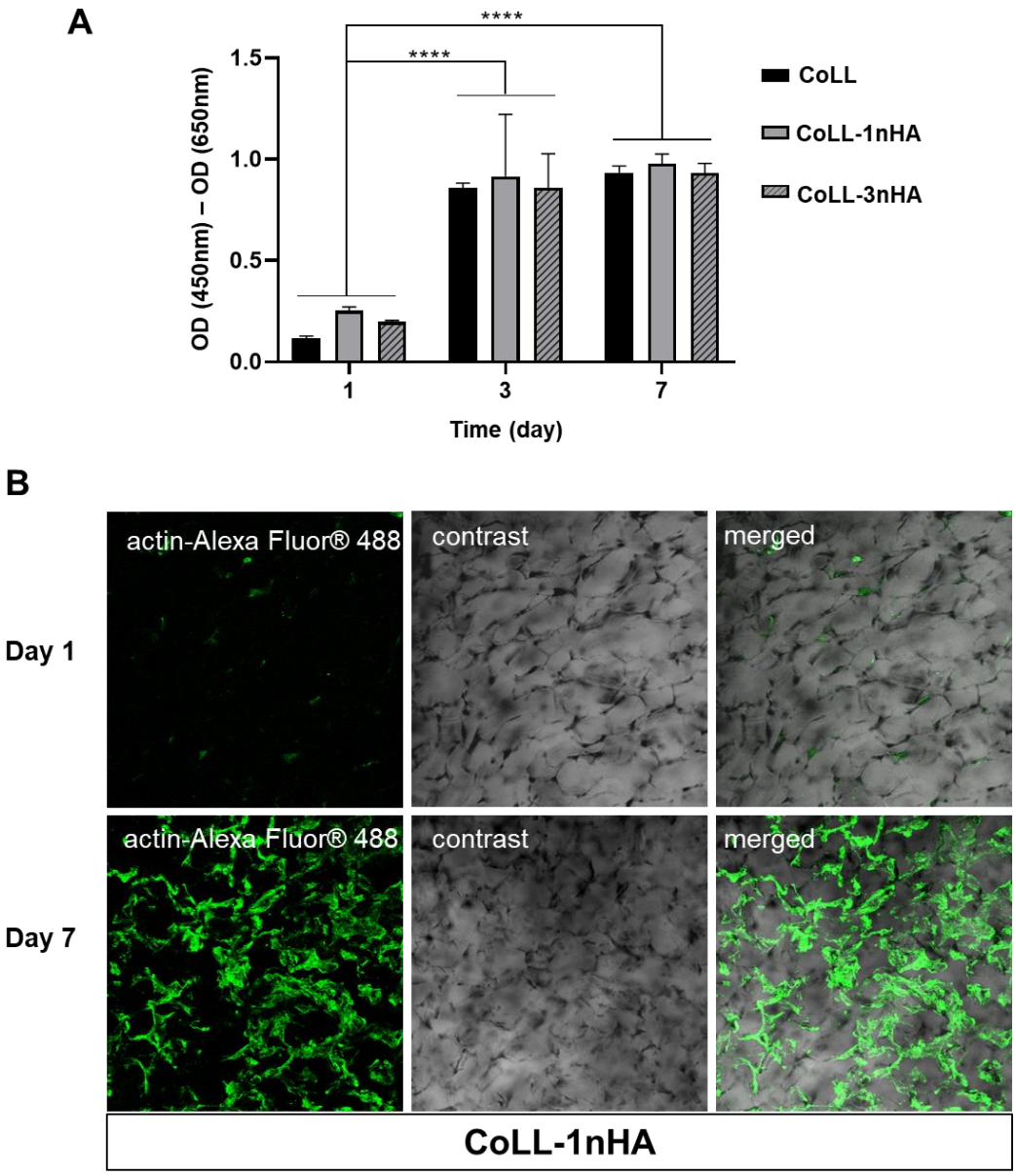

Fig. 5. Cell proliferation in collagen scaffold and collagen-nanohydroxyapatite scaffolds. 5x10^4 C2C12 cells were seeded into the CoLL, CoLL-1nHA and CoLL-3nHA scaffold, respectively. (A) Day 1, day 3, and day 7 post-seeding, cell growth condition in each scaffold was measured *via* XTT assay. 2way ANOVA, Tukey's multiple comparisons test, was used for statistical analysis. (B) Confocal laser scanning microscopy images of CoLL-1nHA-C2C12 constructs after being cultured for 1 and 7 days, in which cellular actin was labeled with anti-actin antibody and Alexa Fluor® 488 conjugated secondary antibody. X10 magnification.

3.4.5. Preparation and characterization of RAMs

To produce RAMs, LPRs containing 20μg mRNA were dropped into CoLL-1nHA and then freeze-dried (Fig. 6A-insert). The porous structure of RAM (Fig. 6A-top) and LPR spherical nanoparticles in RAM (Fig. 6A-bottom) were observed by SEM. The RAMs had similar porous structure (Fig. 6A-top) and pore size as CoLL-1nHA (Fig. 6B) with an increased mechanical strength (Fig. 6C). Compared to CoLL-1nHA, the axial compressive strength and radial compressive strength of RAM increased 6.3-fold and 1.7-fold, respectively.

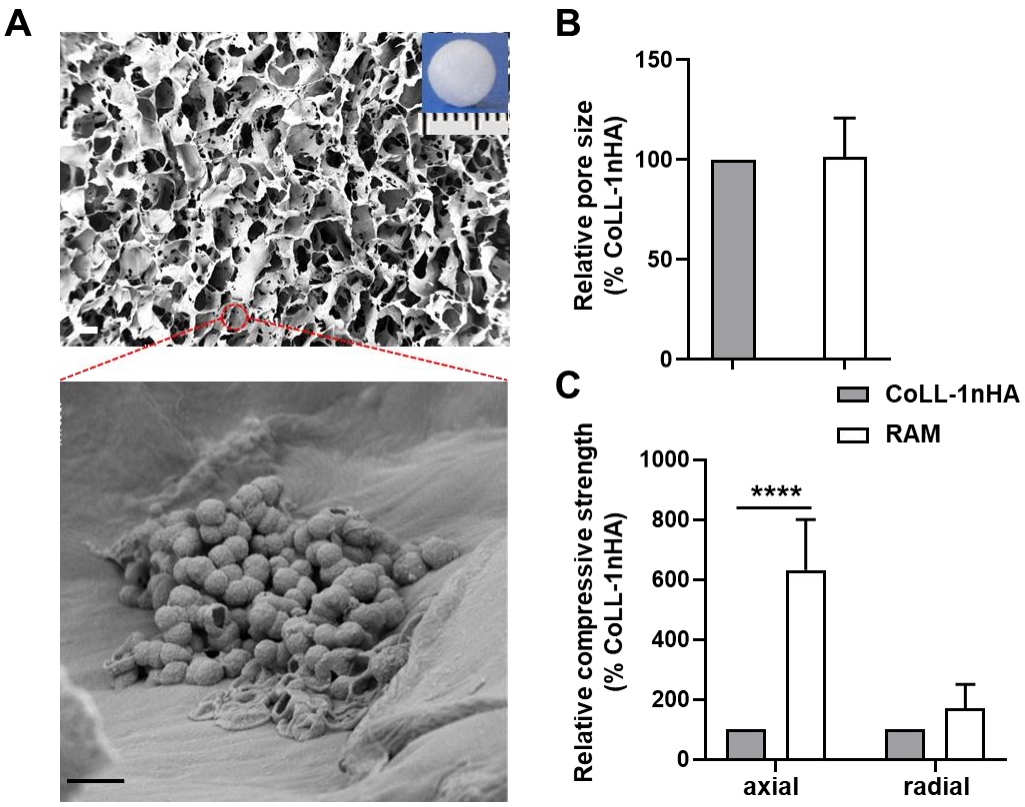

Fig. 6. Physical properties of RAM. (A) representative SEM images of RAM (upper, scale bar=100μm) and LPRs in RAM (lower, scale bar=1μm). The RAM was prepared based on CoLL-1nHA scaffold loaded with LPRs containing 20μg mRNA. (**B**) The pore sizes of RAMs were calculated based on SEM images, and normalized to the mean pore size of CoLL-1nHA. n=8. (**C**) the axial and radial compressive strengths of RAMs were measured, respectively, and normalized to the mean compressive strengths of CoLL-1nHA. n=4. 2way ANOVA, Sidak's multiple comparisons test, was used for statistical analysis.

Next, we assessed the LPRs loading efficiency and release kinetics (Fig. 7. A). The quantification of LPR in the container revealed that 26% of LPR was left unloaded suggesting that 74% of LPRs were absorbed by the CoLL-1nHA scaffold. The release of LPRs from RAMs was evaluated as function of time. There was a fast release in the first 120h (37%) followed by a slow release ending up to 46% during the rest of measuring time. The C2C12-BRE/Luc reporter cells, containing BMP-2 response elements fused with firefly luciferase gene (D. Logeart-Avramoglou 2006), were used to evaluate the activity of released LPRs (Fig. 7B-top). Four experimental groups were set for comparison, i.e. RAM containing 20μg BMP2 mRNA (RAM-BMP2), RAM containing 15μg BMP2/ 5μg NS1 mRNAs (RAM-BMP2/NS1), 1μg BMP2 mRNA formulated as LPR (BMP2), and 0.75μg BMP2/.25μg NS1 mRNAs formulated as LPR (BMP2/NS1) (Fig. 7B-bottom). Freshly prepared LPRs (BMP2 and BMP2/NS1) generated the maximum luciferase expression at 24h post-transfection, and lasted for 168h (7 days) with a gradual decrease. RAMs (RAM-BMP2 and RAM-BMP2/NS1) resulted in two-stage of luciferase expression: an upward stage from 24h to 72h followed by a downward stage from 72h to 336h (14 days). RAMs generated 2-fold longer luciferase expression than fresh LPRs, that up to 14 days. With the presence of NS1, BMP-2 mRNA translation was enhanced consistent with our previous founding (Wang et al., under submission): BMP2/NS1 group has 2.4-fold more underline area than the BMP2 group, and RAM-BMP2/NS1 group has 3-fold more area under the curve (AUC) than RAM-BMP2 group.

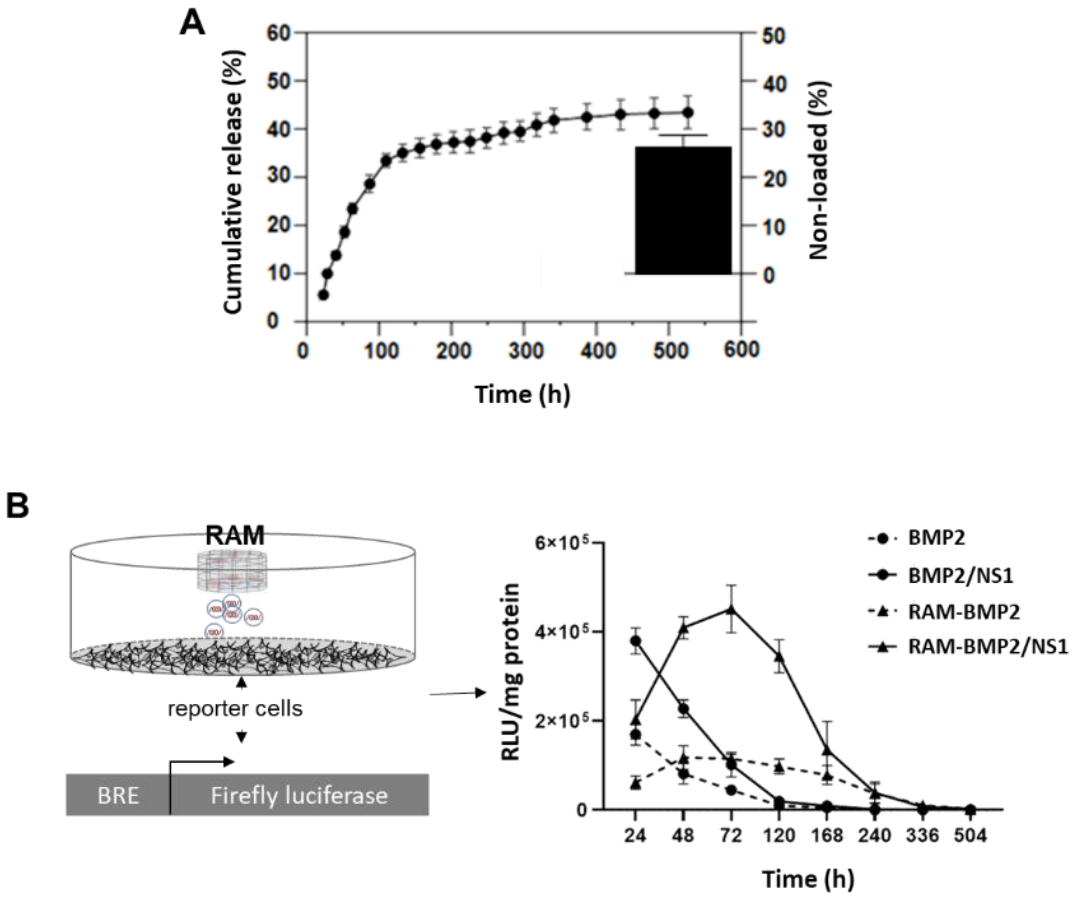

Fig. 7. LPRs release and activity. (A) the release kinetics of LPRs from RAM. The RAMs were incubated in TE buffer at 37℃, and the released mRNA were quantified after labeling with RiboGreen. The right column bar indicates the percentage of non-loaded LPRs. (B) the activity of released LPRs. (B-left) The RAMs containing 20μg BMP2 mRNA (RAM-BMP2) or 15μg BMP2/ 5μg NS1 mRNAs (RAM-BMP2/NS1) were incubated in wells culturing C2C12-BRE/Luc cells, which expression luciferase under BMP-2 stimulation (BMP-2 responses element, BRE). 1μg BMP2 mRNA (BMP2) and 0.75μg BMP2/0.25μg NS1 mRNA (BMP2/NS1), formulated into LPRs, were set as controls. (B-right) At indicated time points, the C2C12-BRE/Luc were harvested and lysed to luciferase expression assay.

3.5. Discussion

Delivery of mRNA for therapeutic purposes has gained remarkable progress (Sahin, Karikó et al. 2014), with extended application from vaccination to protein replacement

therapies, such as cardiovascular regenerative (Zangi, Lui et al. 2013). Using mRNA coding osteogenic proteins for bone regeneration is a young field that started from 2015 (Elangovan, Khorsand et al. 2015). Unlike previously reported studies using chemically modified mRNA, here we report non-modified mRNA-mediated *in vitro* and *in vivo* osteoinduction.

We previously developed a dual mRNAs platform, containing BMP2 mRNA and NS1 mRNA, for osteogenic purpose. NS1 works as an adjuvant to inhibit host cell immune response, which is comparable to pseudouridine modification. In line with our previous results, BMP2/NS1 mRNA transfected hMSCs yielded a large amount of BMP-2, significantly higher than single BMP2 mRNA transfected cells (Fig. 1). As a result, the dual mRNAs transfected hMSCs showed a higher level of osteogenesis (Fig. 2), however no significant difference between the BMP2/NS1 group and BMP2 group. This phenomenon could be caused by two reasons. First, the transient expression profile of administered mRNA. After 3 days, the BMP2/NS1 group and BMP2 group had similar BMP-2 expression. In contrast, the MSCs osteogenic differentiation needs 2 weeks of continuous stimulation. Second, it has been reported that hMSCs has low responsiveness to BMPs (Diefenderfer, Osyczka et al. 2003); (Osyczka, Diefenderfer et al. 2004). Thus, although the BMP2/NS1 group resulted in significantly higher BMP-2 than the BMP2 group in the first 3 days, no significant difference was induced in gene level of osteoblastic markers (except Runx2 at day 3) (Fig. 2A).

In clinical practice, bone grafts are critical in reconstructing massive bone loss or complex non-union defects (Yuan, Fernandes et al. 2010). According to a recent investigation from Zion market research, the global bone grafts and substitutes market was approximately $ 2,745 million in 2018 and is expected to generate around $ 4,235 million by 2026, registering a compound annual growth rate (CAGR) of 5.6% during the forecast period. With this demand, the aim of the BTE is to construct bone substitutes (BTE grafts) that as close as possible to the gold standard autografts through components, structure and function mimicking (Amini, Laurencin et al. 2012). RAM has emerged as an advanced approach for constructing bone grafts with the combination of BTE technology and mRNA-therapy technology (Elangovan, Khorsand et al. 2015); (Balmayor, Geiger et al. 2016).

Here, the collagen and nanohydroxyapatite (nHA), which represent the primary organic and inorganic compound in natural bone, were chosen to produce the basal porous scaffold (Fig. 4). Calf skin type I collagen scaffolds (CoLL) exhibited open pores and high level of interconnection (Fig. 4A-a and c), which were selected as basal material for further combination with nHA. As expected, the nHA reinforced collagen scaffold (CoLL-1nHA, CoLL-3nHA) had an increased mechanical strength in both axial and radial direction (Fig. 4D). The scaffolds showed more stress resistance in the axial direction than in redial direction. It was reported that the mechanical properties of a porous scaffold depend on the direction of the loading along the pore channels (Mao, Tang et al. 2019). During scaffolds freeze-drying, the aqueous solution was sublimated mainly through axial direction leading more pores aligned in the axial direction. More incorporation of nHA in CoLL-3nHA decreased the interconnection degree (in terms of porosity) (Fig. 4C), because of the elimination of micropores from the pore walls (Fig. 4A-e), and the non-embedded nHA to some extent, blocked the connection (Fig. 4A-f). It is known that the porosity, the permeability and the mechanical properties of the BTE scaffold are crucial parameters influencing host cell ingrowth, migration and proliferation (Karageorgiou and Kaplan 2005);(Amini, Laurencin et al. 2012). For instance, Lewandrowshi et al. found that the poly(propylene fumarate) scaffold has a higher porosity generating a greater and deeper bone ingrowth in rat tibias defect model (Lewandrowski, Gresser et al. 2000) due to higher level of vascularization and fluid permeability (Mastrogiacomo, Scaglione et al. 2006). Mechanical strong scaffolds tend to maintain their porous structure (pore spatial shape), and has the potential to modulate the cell fate by affecting cellular focal-adhesion structure and the cytoskeleton (Khatiwala, Peyton et al. 2006); (Engler, Sen et al. 2006). hMSCs grown on polyacrylamide gel with rigidity similar to collagenous osteoid precursors of bone resulted in polygonal shape with similar osteoblasts morphology as; however, when grown on matrix with rigidity similar to the brain, they exhibited branched, filopodia-rich morphology similar to primary neurons (Engler, Sen et al. 2006). In terms of biological performance, the addition of nHA did not show a significant influence on cell growth (Fig. 5A). Compared to CoLL and CoLL-3nHA, the CoLL-1nHA preserved slightly more cells, which could be caused by its high porosity (Fig. 4C); and the rough wall surface (Fig. 4A-d). This is line with Yuan et al. who showed that the surface roughness enhances the attachment, proliferation of anchorage-dependent bone forming cells (Yuan, Kurashina et al. 1999). Moreover, all scaffolds prepared in this

study underwent chemically crosslinking (at EDC: NHS: collagen carboxyl group molar ratio of 10: 4: 1), enabling them more resistance to enzyme degradation (S. Fig. 1). The outstanding physical and biological performances of CoLL-1nHA giving it values interesting candidate for preparing RAM.

We previously reported a lipopolyplex (LPR) formulation to delivery small interfering RNA (siRNA) *in vitro* (Gonçalves, Berchel et al. 2014). The Lip100/His-lPEI/siRNA formulated LPRs had an average size of 60 nm and were more efficient than formulations made with commercial vectors, i.e. JetPRIME™, INTERFERin® and Lipofectamine™2000. The formulation was then transferred to this study to complex and deliver mRNA. Although following the N/P ratio, the resulted LPR had larger size (208nm vs. 60nm), and less positive charge (+18.9mV vs. +84mV) (Fig. 3B, C). The size and global charge differences are likely due to the nucleic acid length (1381nt *vs* 23nt). By contrast, the size is similar to another type of LPR (235.7nm) from our lab, composed of Tri-mannosylated-lip100/ PEGylated histidinylated polylysine/ mRNA coding tumor or viral antigens, for *in vivo* vaccination (Van der Jeught, De Koker et al. 2018). During RAMs preparation, the LPRs had a good loading efficiency around 74% (Fig. 7A). Despite the similar size of LPR and scaffold pore (~200 nm), the LPR solution hydrated the freeze-dried scaffolds leading to their expansion favoring LPR loading. In addition, the distribution of LPR size indicates that some particles have a size lower than 200nm, which render them absorbed easily inside the scaffold.

Within the RAMs, the majority of LPR particles maintained a spherical shape, while some collapsed (Fig. 6A-bottom). Those collapsed form could correspond to liposomes lacking supportive polyplex cores. Optimizing the efficiency of polyplexes encapsulation could be one future axis of the lipopolyplex technology. Compared to CoLL-1nHA, the RAMs demonstrated enhanced compressive strength, especially in the axial direction (Fig. 6C). The LPRs were prepared in HEPES buffer containing 5% sucrose, thus after sublimation, the HEPES and sucrose molecules homogeneously deposit on pore walls, which may contribute to the mechanical changes as toughener. During rehydration, the RAM acted as a controller for LPRs release (Fig. 7A). After 24h of one-shot transfection, the protein expression continuously decreased (Fig. 7B). In contrast, the protein expression from the RAM groups was increased over 72h prior to decrease. Overall, mRNAs *in vitro* release from RAMs that lasted for 16 days gave rise to a prolonged protein expression period (2-fold) compared to direct cell

transfection. From the release, profile (Fig. 7B), we conclude that this phenomenon could be generated by multitransfection of cells thanks to continously released LPRs. On the other hand, the results revealed that the LPRs preserved their transfection capability after lyophilization.

3.6. Conclusion

In conclusion, we have demonstrated the non-modified dual mRNAs (BMP2/NS1 mRNAs) system was capable of inducing osteogenic differentiation of hMSCs. Lip100/His-lPEI based LPR could serve as mRNA delivery vector for the production of RAMs made with collagen-nanohydroxyapaptite scaffold. RAMs were able to mediate a high and prolonged BMP-2 expression as expected. Taken together, these results provided the preliminary basis for translating this technology (i.e. RAM containing the dual mRNAs) into *in vivo* application. Moreover, as an advanced combination of mRNA therapy and tissue engineering, the RAM technology, has broad potential applications as wound healing, as skin, cartilage and vertebral disc regeneration.

3.7. Acknowledgment

We are grateful to David Gosset from the P@CYFIC platform (CBM) for technical help in confocal laser scanning microscopy observation, Antony Delalande and Cyril Guimpied for mice surgery assistance, and Audrey Sauldubois from the Centre de Microscopie Electronique platform (Université d'Orléans) for TEM study. We also thank Sonia Georgeault from Plateforme IBiSA de Microscopie Electronique de l'Université de Tours for SEM observation. Region Centre Val de Loire and CNRS supported this work. Pinpin Wang was supported by a CSC grant from China.

3.7 Supplementary Data

S. Table 1. Primers for RT-qPCR

Gene		primer (5'->3')	length
Runx2 (NM_004348)	F	CCCAGTATGAGAGTAGGTGTCC	149
	R	GGGTAAGACTGGTCATAGGACC	
ALP (NM_001632)	F	CAACGAGGTCATCTCCGTGATG	129
	R	TACCAGTTGCGGTTCACCGTGT	
CoL1α1 (NM_000088)	F	GATTCCCTGGACCTAAAGGTGC	107
	R	AGCCTCTCCATCTTTGCCAGCA	
OPN (NM_000582)	F	CGAGGTGATAGTGTGGTTTATGG	128
	R	GCACCATTCAACTCCTCGCTTTC	
OCN (NM_199173)	F	CGCTACCTGTATCAATGGCTGG	123
	R	CTCCTGAAAGCCGATGTGGTCA	
GAPDH (NM_002046)	F	GTCTCCTCTGACTTCAACAGCG	131
	R	ACCACCCTGTTGCTGTAGCCAA	

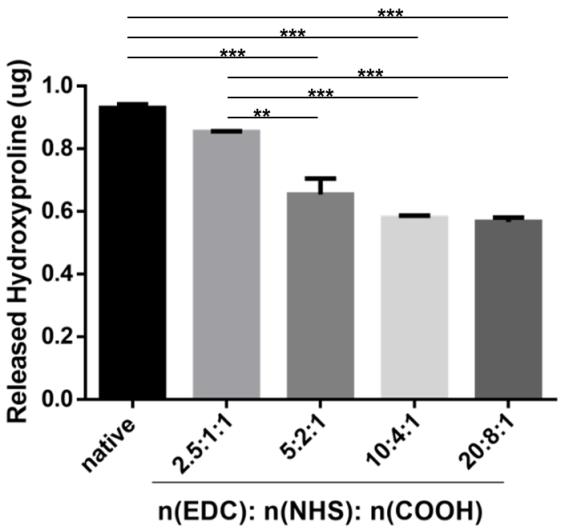

S. Fig. 1. Biodegradation resistance of collagen scaffolds. Collagen scaffolds were cross-linked with the indicated amount of EDC and NHS. The biodegradation resistance property was evaluated by collagenase I digestion (200U/ml). Released Hydroxyproline was quantified with an hydroxyproline assay kit (Sigma).

Part IV

Conclusions and perspectives

4.1. Conclusions

This last decade, we are witnessing the blooming of mRNA therapeutics. Many studies and first round of clinical trials indicated that those molecules hold a real promise as future biomedicines. Regenerative medicine is one of interesting application of mRNAs therapeutics. Indeed, they are the best choice to express growth factors, hormones or transcriptions factors as they have a transient nature and no risks of host genome integration.

To avoid the activation of immune RNA sensors inside the cells during exogenous mRNA administration, chemically modified nucleosides have been used to produce in vitro transcribed mRNA. This strategy has some limitations including the cost and the efficiency due to sequence and cell dependence.

The main purpose of my PhD work was to investigate the potentiality of BMP-2 mRNA for bone regeneration with a focus on assessing the ability of NS1 Influenza A protein to improve the translation of BMP-2 mRNA which is delivered in non-modified form.

In this thesis, we applied this strategy to the field of regenerative medicine, specifically, bone regeneration. The NS1 and BMP2 mRNAs were delivered to murine multipotent stem cells (C3H10T1/2) and human bone marrow-derived stem cells (HMSCs) for *in vitro* osteoinduction. Further, the dual mRNAs (BMP2/NS1), formulated as lipopolyplexes (LPRs), were used to modify a collagen-nanohydroxyapatite scaffold to prepare RNA activated matrix (RAM) for *in vivo* osteoinduction.

In summary, our results demonstrated that:

1. NS1 efficiently blocked cellular RNA sensors (e.g., IFNα/β, PKR, RIG-1, OAS1) in a dose dependent manner;

2. NS1 generally enhanced IVT mRNA translation regardless gene context and cell type;

3. The delivery of the dual mRNAs, at a BMP2/NS1 weight ratio of 3/1, to C3H10T1/2 and hMSCs, respectively, resulted in significant higher BMP-2 expression (8.5-fold) compared to delivery of some amount of BMP2 mRNA;

4. The delivery of the dual mRNAs induced osteogenic differentiation of C3H10T1/2 and hMSCs;

5. The RAMs had a long-lasting *in vitro* mRNA release profile, which leads to an enhanced and prolonged BMP-2 expression suggesting that released LPRs kept their mRNA delivery capacity.

This strategy could be a good alternative to modified nucleotides incorporation for suppressing IVT mRNA-induced innate immune response and maximizing the protein expression (Phua, Liu et al. 2017); (Liu, Chin et al. 2019). RAMs could be an off-the-shelf product for clinical orthopedic practice.

4.2. Perspectives

Three decades have passed since the first proof of IVT mRNA translation *in vivo* (Wolff, Malone et al. 1990). However, the application of mRNA for regeneration therapy is still in its infancy (Zangi, Lui et al. 2013); (Elangovan, Khorsand et al. 2015).

In our proof-of-concept research, we have shown the potential of delivering non-modified IVT mRNA for bone regeneration. However, more work needs to be done to advance the usage of IVT mRNA for bone regeneration. Below are some perspectives of this study.

For instance, one single transfection of mRNA did not induce significant osteogenic differentiation of MSCs; one-third of mRNA did not load into the CoLL-1nHA scaffold during RAM preparation and improper *in vivo* model for evaluation RAM function.

4.2.1 Improving IVT mRNA efficacy

4.2.1.1. Sequence engineering

Optimization of the sequence of 5'-and 3'-UTR and ORF is one approach to increase IVT mRNA stability and translation efficiency within cells (Zhang, De La Vega et al. 2018). Asrani and colleagues provided an experimental framework for a high throughput screening assay to simultaneously evaluate hundreds of UTRs for optimized protein expression (Asrani, Farelli et al. 2018). Translation efficiency enhancement resulting from sequence-engineering can even exceed nucleotides modification (pseudouridine) both *in vitro* and *in vivo* (Thess, Grund et al. 2015). However, to date, no universal UTRs can be translated across different genes and cell types. Substitution of rare codons with synonymous frequent codons improved protein synthesis (Gustafsson, Govindarajan et al. 2004) and mRNA half-life (Presnyak, Alhusaini et al. 2015). mRNAs containing rare codons or non-optimal codons and frequent codons or optimal codons has identical level of ribosomes engagement. But, the translocation of ribosome on non-optimized mRNAs is slower than that on optimized mRNAs, leading to a higher non-optimized mRNAs decay rate (Presnyak, Alhusaini et al. 2015). In our work, we did a basic attempt to generate mRNAs with different 3'-UTRs. The optimization of 5'-UTR and ORF sequence of the BMP2 and NS1 mRNAs could further improve their performance.

4.2.1.2. Secondary structure engineering

One of the features of mRNA is their propensity to form a secondary structure. In addition to the mRNA sequence, the mRNA secondary structure, such as stem-loops and circulation, can affect its stability and translation efficiency (Kozak 1989); (Wesselhoeft, Kowalski et al. 2018). For instance, compared to linear mRNA counterparts, the circular RNAs (circRNAs) lack of free ends that required for exonuclease-mediated degradation, enabling them to be resistant to degradation, and granting them extended lifespans (Chen and Yang 2015); (Enuka, Lauriola et al. 2015). Although endogenous circRNAs are reported as noncoding RNAs, exogenous circRNAs engineered with internal ribosome entry site (IRES) elements are translatable (Chen and Sarnow 1995); (Wang and Wang 2015). Wesselhoeft et al. recently demonstrated that circRNA yielded superior expression (i.e. higher and longer) *in vitro* and *in vivo* over linear mRNA, paralleled with a decreased induction of

TLRs (Wesselhoeft, Kowalski et al. 2018); (Wesselhoeft, Kowalski et al. 2019). Circularization of mRNA avoids TLR activation to the same extent as the inclusion of modified nucleotides in linear mRNA, demonstrating a new modality for therapeutic protein expression. Nevertheless, circRNAs application is labor intensive, as the mRNA circularization is complicated, and high purity is necessary (small amounts of contaminating linear RNA leading to robust cellular immune responses (Wesselhoeft, Kowalski et al. 2019)).

4.2.1.3. Self-replicating RNA

Bone regeneration requires continuous osteogenic stimulation. However, mRNA has an inherent transient expression property. Using self-replicating mRNA (RepRNA) could be a method to extent protein expression period (Ying, Zaks et al. 1999); (Geall, Verma et al. 2012). The RepRNA is built by replacing the virulence genes of RNA viruses containing positive-stranded RNA (e.g. alphaviruses, flaviviruses, measles viruses, and rhabdoviruses) with heterologous genes of interest (Fig. 1), and produced under a T7 or Sp6 promoter. After the transfection, replicase is expressed from the RepRNA to synthetize the minus RNA strand which serves as template to amplify the RepRNA and, for subgenomic RNA synthesis (Fig. 1B) (Strauss and Strauss 1994); (Lundstrom 2018). Yoshioka et al. synthesized Venezuelan equine encephalitis virus (VEEV) -based RepRNAs for fibroblasts reprograming (Yoshioka, Gros et al. 2013). Four reprogramming factors (i.e., OCT4, KLF4, and SOX2, with c-MYC or GLIS1) were integrated into one RepRNA construct. The proteins expressed from the RepRNA lasted for two weeks by a single-dose transfection.

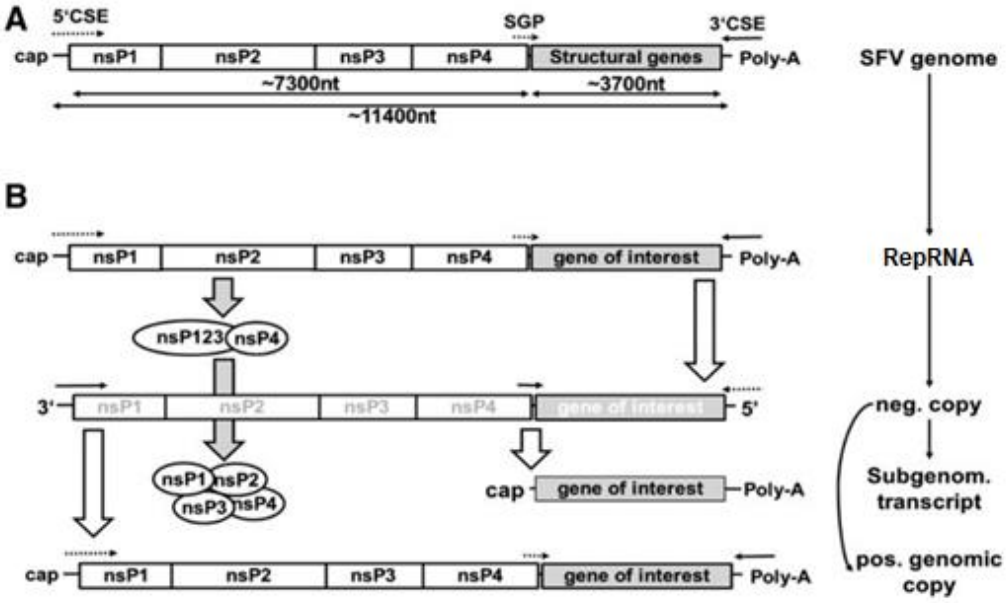

Fig. 1. RepRNA vector structure and amplification. (**A**) the genome structure of Semliki Forest virus (SFV) encoding non-structural proteins (nsP1-nsP4) and structural proteins (capsid and glycoproteins). CSE: conserved sequence elements; SGP: subgenomic promoter. (**B**) mechanism of self-replication: After transfection, the non-structural polyprotein (nsP1234) is translated from the RepRNA, which then autoproteolytically cleavage to the nsP123 and nsP4. nsP123 and nsP4 synthesize negative-stranded copies of the RepRNA. Later, the nsP123 polyprotein is cleaved to single proteins, and together to synthesize the RepRNA and the fragment containing gene of interest from its negative copies. Dotted arrow: inactive promoter; lined arrow: active promoter. Modified from (Beissert, Koste et al. 2017) with permission.

Previously, we developed a VEEV-based RepRNA coding hemagglutinin for vaccination purpose against influenza virus infection (Perche, Clemencon et al. 2019). Long-term BMP-2 protein expression from RepRNA (VEE-BMP2) (Fig. 2), would enhance ostoinduction. Moreover, as previously reported (Yoshioka, Gros et al. 2013), the polycistronic strategy is suitable for bone regeneration as well, as several factors work synergistically in this process (Hankenson, Gagne et al. 2015). For instance, the angiogenic VEGF and MSC recruitment stimulating SDF-1 can be integrated into one mRNA with BMP2.

However, it is worth to notice that, although RepRNA produces more proteins and for extended periods than mRNA, the dsRNAs produced during replication and other replication intermediates are potent inducers of antiviral responses which limit the repeated use of RepRNA (Pardi, Hogan et al. 2018). Additionally, the large size of RepRNA (9000–15000 nt) is a real challenge for its formulation as fewer delivery systems available (Geall, Verma et al. 2012). This task is tackled in our lab.

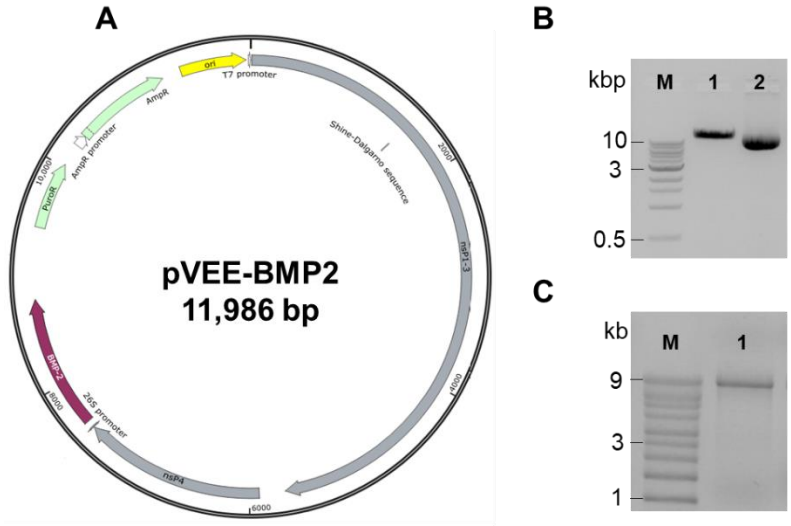

Fig. 2. Construction of self-replicating BMP2 mRNA. (**A**) plasmid structure of the self-replicating BMP2 (pVEE-BMP2): the BMP2 sequence was amplified from pCMV3-mBMP2-GFPSpark (Sino Biologicals), and inserted into vector, pT7-VEE-GFP (derived from Venezuelan equine encephalitis virus; the plasmid is a gift from Steven Dowdy), to replace GFP sequence. (**B**) the pVEE-BMP2 sequence was verified by agarose gel electrophoresis and sequencing (Eurofins). Lane 1: pVEE-BMP2 digested with XbaI; Lane 2: pVEE-BMP2. (**C**) denatured agarose gel electrophoresis of VEE-BMP2 mRNA. The mRNA was synthesized with T7 mMessage mMachine kit (Ambion) using XbaI linearized pVEE-BMP2 as template.

4.2.2 Expanding the potentiality of NS1

Under inflammation conditions, the pro-inflammatory cytokines, especially tumor necrosis factor alpha (TNFα), plays a major role in bone homeostasis regulation (Osta, Benedetti et al. 2014) (Fig. 3). In late 1980s, the TNFα was reported to affect bone formation *in vitro* (Bertolini, Nedwin et al. 1986); (Canalis 1987). Low dose transient

exposure to TNFα (24h) stimulated rat calvariae cell replication and collagen synthesis (Canalis 1987), while, chronic exposure to TNFα (≥48h) resulted in collagen degradation and bone resorption (Bertolini, Nedwin et al. 1986); (Canalis 1987). Later, more studies were performed to reveal the behind molecular mechanisms with cultured osteoprogenitors instead of bone tissue (Gilbert, He et al. 2002); (Kaneki, Guo et al. 2006). Challenging the rat calvaria osteoblast and M3T3-E1 cells with 10ng/ml TNFα for 24h resulted in 50%-70% reduction of Runx2 mRNA, and 2-fold reduction of Runx2 mRNA half-life (from 1.8h to 0.9h) (Gilbert, He et al. 2002). The Runx2 manipulation happens in protein level as well. Kaneki and colleagues discovered that TNFα stimulation upregulated the expression of Smad-specific E3 ubiquitin ligase 1 and 2 (Smurf1/2). Smurf1/2 ubiquitinated the Runx2 leading to its degradation (Kaneki, Guo et al. 2006). In addition, Smurf2 selectively interacts with and ubiquitinates Smads (preferably Smad1) (Zhang, Chang et al. 2001). Both the Runx2 and Smads are key components in BMPs signaling (Fig. 3).

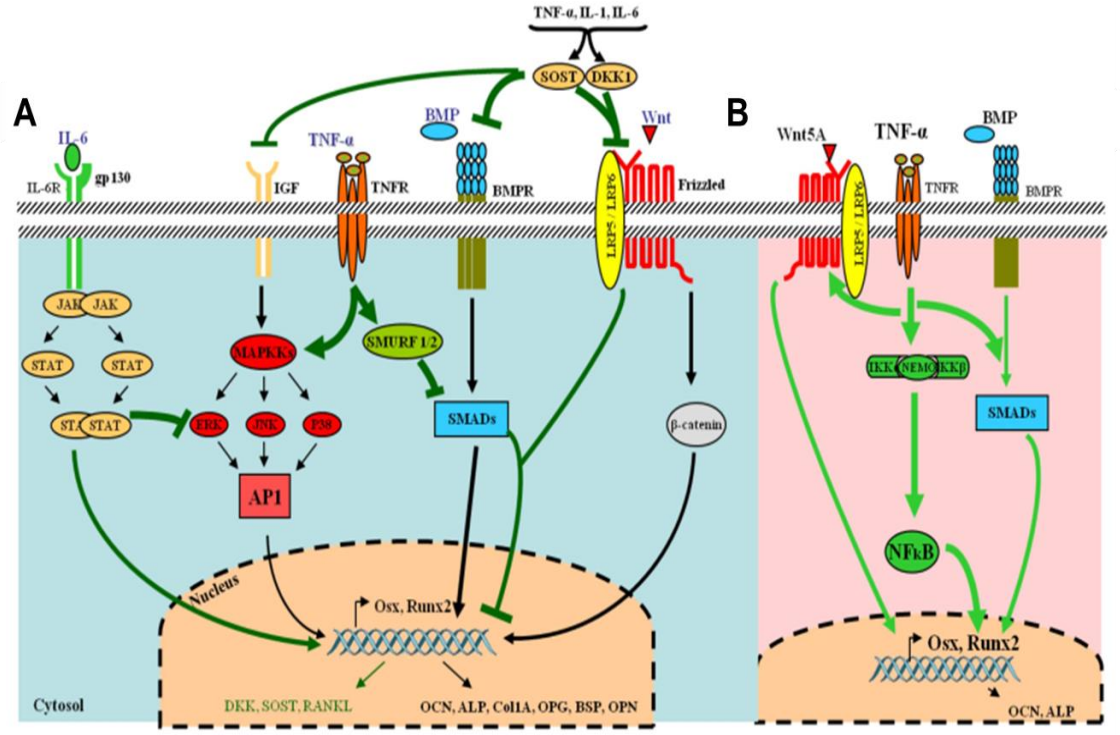

Fig. 3. The osteoblastogenesis paradoxical effects of TNFα. (**A**) Under inflammatory conditions, the release of pro-inflammatory cytokine of TNF-a leads to the inhibition of osteogenic differentiation via several mechanisms (represented in

green in the figure). TNF-a activates SMAD ubiquitination regulatory factor-1/2 (Smurf1/2) leading to the inhibition of SMADs. The pro-inflammatory cytokines also up-regulate dickkopf-related protein 1 (DKK-1) and sclerostin (SOST), which inhibit the Wnt–frizzled pathway, whereas many other osteoblast gene products are down-regulated. (**B**) TNF-a can also favor osteogenic differentiation *via* NF-kB by increasing expression of BMP-2, Osx, Runx2, OCN, and Wnt pathway. Abbreviation: BMPR, BMP receptor; AP-1, activator protein 1; ERK, extracellular signal-regulated kinase; FGF, fibroblast growth factor; IL-6R, IL-6 receptor; gp130, glycoprotein 130; JAK, janus kinase; JNK, JUN N-terminal kinase; p38, p38 MAPK; LRP5-6, low-density lipoprotein receptor-related protein 5 or 6; ALP, alkaline phosphatase; Osx, osterix (Sp7); OPG, osteoprotegerin; BSP, bone sialoprotein; OPN, osteopontin; OCN, osteocalcin. Adapted from (Osta, Benedetti et al. 2014) with permission.

The Smurf1/2 expression enhancement is directly associated with TNFα-mediated NF-κB (canonical) activation (Chang, Liu et al. 2013). Interestingly, it was shown that the NS1, from Influenza A/PR/8/34, suppresses NF-κB activation during viral infection (Wang, Li et al. 2000); (Gao, Song et al. 2012). Thus, the NS1 has another potential function in bone regeneration by inhibiting TNFα induced inflammation.

Our preliminary results suggest that simultaneous treatment of A549-NF-κB/luc cells, which stably express luciferase under NF-κB promoter, with TNFα and NS1 mRNA, NF-κB activation was suppressed by NS1 expression in a dose dependent manner (Fig. 4A). We observed the same results in hMSCs (Fig. 4B). However, we did not observe any NS1-mediated NF-κB inhibition in murine cell lines (i.e., C2C12 and C3H10T1/2) (data not shown), indicating this inflammation suppression function of NS1, from Influenza A/Texas/36/1994, is probably species dependent.

Nevertheless, with these results in hand, it is too early to conclude the osteogenic beneficial function from the NS1-NF-κB interaction. Several studies reported that TNFα favored osteogenic differentiation *via* the activation of NF-κB and a subsequent increase of BMP-2, ALP, or transcriptional coactivator with PDZ-binding motif (Hess, Ushmorov et al. 2009); (Cho, Shin et al. 2010). The stimulatory and inhibitory effects

could be result from the balance between TNFα concentration and cell type/cell differentiation stage (for review see (Osta, Benedetti et al. 2014)).

Still, it will be interesting to assess the effect of NS1 to halt or reduce inflammation in others pathologies as arthritis etc. Note that the transient nature of NS1 mRNA and the capacity of NS1 to reduce immune response renders this strategy quite interesting for local application.

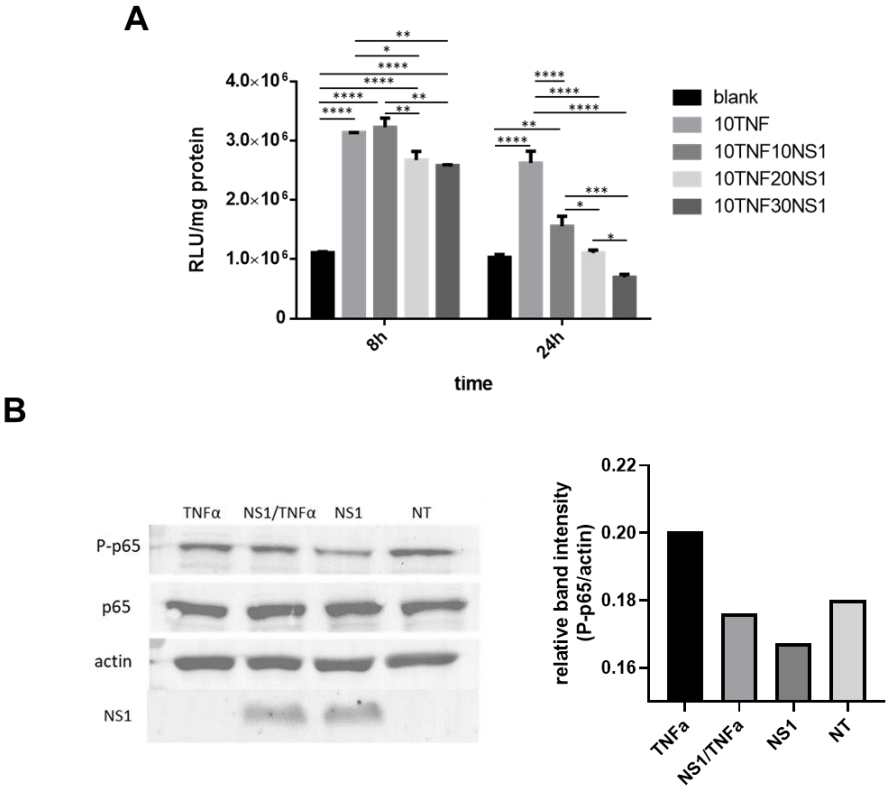

Fig. 4. NS1 inhibits NF-κB activation. (A) A549 cells, stably express luciferase under NF-κB promoter, were challenged with 10ng/ml TNFα (10TNF) at the presence of NS1 mRNA. Three NS1 mRNA concentrations were used: 10pg/cell (10NS1), 20pg/cell (20NS1), 30pg/cell (30NS1). Luciferase expression was measured at indicated time points. Statistical analysis was performed with 2way ANOVA, Tukey's multiple comparation test: *, P<0.05; **, P<0.01; ***, P<0.001; ****, P<0.0001. (**B**) hMSC, P7, were pre-transfected with NS1 mRNA for 12h, then treated with TNFα (20 ng/ml). After 30 min, cell lysate was prepared for measuring NF-κB activity by Western-blot.

.

References

1. Akay, G., M. A. Birch and M. A. Bokhari (2004). "Microcellular polyHIPE polymer supports osteoblast growth and bone formation in vitro." Biomaterials **25**(18): 3991-4000.
2. Alcami, A. and U. H. Koszinowski (2000). "Viral mechanisms of immune evasion." Immunol Today **21**(9): 447-455.
3. Alcamí, A., J. A. Symons and G. L. Smith (2000). "The Vaccinia Virus Soluble Alpha/Beta Interferon (IFN) Receptor Binds to the Cell Surface and Protects Cells from the Antiviral Effects of IFN." Journal of Virology **74**(23): 11230-11239.
4. Alexander, K. A., M. K. Chang, E. R. Maylin, T. Kohler, R. Muller, A. C. Wu, N. Van Rooijen, M. J. Sweet, D. A. Hume, L. J. Raggatt and A. R. Pettit (2011). "Osteal macrophages promote in vivo intramembranous bone healing in a mouse tibial injury model." J Bone Miner Res **26**(7): 1517-1532.
5. Alexopoulou, L., A. C. Holt, R. Medzhitov and R. A. Flavell (2001). "Recognition of double-stranded RNA and activation of NF-kappaB by Toll-like receptor 3." Nature **413**(6857): 732-738.
6. Amini, A. R., C. T. Laurencin and S. P. Nukavarapu (2012). "Bone tissue engineering: recent advances and challenges." Crit Rev Biomed Eng **40**(5): 363-408.
7. Amini, A. R., C. T. Laurencin and S. P. Nukavarapu (2012). "Differential analysis of peripheral blood- and bone marrow-derived endothelial progenitor cells for enhanced vascularization in bone tissue engineering." J Orthop Res **30**(9): 1507-1515.
8. Anastasina, M., N. Le May, A. Bugai, Y. Fu, S. Soderholm, L. Gaelings, T. Ohman, J. Tynell, S. Kyttanen, M. Barboric, T. A. Nyman, S. Matikainen, I. Julkunen, S. J. Butcher, J. M. Egly and D. E. Kainov (2016). "Influenza virus NS1 protein binds cellular DNA to block transcription of antiviral genes." Biochim Biophys Acta **1859**(11): 1440-1448.
9. Anderson, B. R., H. Muramatsu, S. R. Nallagatla, P. C. Bevilacqua, L. H. Sansing, D. Weissman and K. Kariko (2010). "Incorporation of pseudouridine into mRNA enhances translation by diminishing PKR activation." Nucleic Acids Res **38**(17): 5884-5892.
10. Anderson, J. M. (1992). "The bone-biomaterial interface. J. E. Davies, (ed.), University of Toronto Press, Toronto, Canada, 1991." Journal of Biomedical Materials Research **26**(10): 1395-1396.
11. Arnaud-Barbe, N., V. Cheynet-Sauvion, G. Oriol, B. Mandrand and F. Mallet (1998). "Transcription of RNA templates by T7 RNA polymerase." Nucleic Acids Res **26**(15): 3550-3554.
12. Arnsdorf, E. J., P. Tummala, R. Y. Kwon and C. R. Jacobs (2009). "Mechanically induced osteogenic differentiation--the role of RhoA, ROCKII and cytoskeletal dynamics." J Cell Sci **122**(Pt 4): 546-553.
13. Asrani, K. H., J. D. Farelli, M. R. Stahley, R. L. Miller, C. J. Cheng, R. R. Subramanian and J. M. Brown (2018). "Optimization of mRNA untranslated regions for improved expression of therapeutic mRNA." RNA Biol: 1-7.
14. Aye, S. S., R. Li, M. Boyd-Moss, B. Long, S. Pavuluri, K. Bruggeman, Y. Wang, C. R. Barrow, D. R. Nisbet and R. J. Williams (2018). "Scaffolds Formed via the Non-Equilibrium Supramolecular Assembly of the Synergistic ECM Peptides RGD and PHSRN Demonstrate Improved Cell Attachment in 3D." Polymers (Basel) **10**(7).
15. Ayllon, J., P. Domingues, R. Rajsbaum, L. Miorin, M. Schmolke, B. G. Hale and A. Garcia-Sastre (2014). "A single amino acid substitution in the novel H7N9 influenza A virus NS1 protein increases CPSF30 binding and virulence." J Virol **88**(20): 12146-12151.
16. Bab, I. and M. Chorev (2002). "Osteogenic growth peptide: from concept to drug design." Biopolymers **66**(1): 33-48.
17. Babendure, J. R., J. L. Babendure, J. H. Ding and R. Y. Tsien (2006). "Control of mammalian translation by mRNA structure near caps." RNA **12**(5): 851-861.
18. Badieyan, Z. S., T. Berezhanskyy, M. Utzinger, M. K. Aneja, D. Emrich, R. Erben, C. Schuler, P. Altpeter, M. Ferizi, G. Hasenpusch, C. Rudolph and C. Plank (2016). "Transcript-activated collagen matrix as sustained mRNA delivery system for bone regeneration." J Control Release **239**: 137-148.

19. Balmayor, E. R., J. P. Geiger, M. K. Aneja, T. Berezhanskyy, M. Utzinger, O. Mykhaylyk, C. Rudolph and C. Plank (2016). "Chemically modified RNA induces osteogenesis of stem cells and human tissue explants as well as accelerates bone healing in rats." Biomaterials **87**: 131-146.
20. Balmayor, E. R., J. P. Geiger, C. Koch, M. K. Aneja, M. van Griensven, C. Rudolph and C. Plank (2017). "Modified mRNA for BMP-2 in Combination with Biomaterials Serves as a Transcript-Activated Matrix for Effectively Inducing Osteogenic Pathways in Stem Cells." Stem Cells Dev **26**(1): 25-34.
21. Banerjee, A. K. (1980). "5'-terminal cap structure in eucaryotic messenger ribonucleic acids." Microbiol Rev **44**(2): 175-205.
22. Baron, R., L. Neff, D. Louvard and P. J. Courtoy (1985). "Cell-mediated extracellular acidification and bone resorption: evidence for a low pH in resorbing lacunae and localization of a 100-kD lysosomal membrane protein at the osteoclast ruffled border." J Cell Biol **101**(6): 2210-2222.
23. Bartos, M., T. Suchy and R. Foltan (2018). "Note on the use of different approaches to determine the pore sizes of tissue engineering scaffolds: what do we measure?" Biomed Eng Online **17**(1): 110.
24. Bashirullah, A., R. L. Cooperstock and H. D. Lipshitz (2001). "Spatial and temporal control of RNA stability." Proc Natl Acad Sci U S A **98**(13): 7025-7028.
25. Bassuk, J. A., T. Birkebak, J. D. Rothmier, J. M. Clark, A. Bradshaw, P. J. Muchowski, C. C. Howe, J. I. Clark and E. H. Sage (1999). "Disruption of the Sparc locus in mice alters the differentiation of lenticular epithelial cells and leads to cataract formation." Exp Eye Res **68**(3): 321-331.
26. Behravesh, E. and A. G. Mikos (2003). "Three-dimensional culture of differentiating marrow stromal osteoblasts in biomimetic poly(propylene fumarate-co-ethylene glycol)-based macroporous hydrogels." J Biomed Mater Res A **66**(3): 698-706.
27. Beissert, T., L. Koste, M. Perkovic, K. C. Walzer, S. Erbar, A. Selmi, M. Diken, S. Kreiter, O. Tureci and U. Sahin (2017). "Improvement of In Vivo Expression of Genes Delivered by Self-Amplifying RNA Using Vaccinia Virus Immune Evasion Proteins." Hum Gene Ther **28**(12): 1138-1146.
28. Bellahcene, A. and V. Castronovo (1997). "Expression of bone matrix proteins in human breast cancer: potential roles in microcalcification formation and in the genesis of bone metastases." Bull Cancer **84**(1): 17-24.
29. Bertolini, D. R., G. E. Nedwin, T. S. Bringman, D. D. Smith and G. R. Mundy (1986). "Stimulation of bone resorption and inhibition of bone formation in vitro by human tumour necrosis factors." Nature **319**(6053): 516.
30. Bertrand, E., C. Goncalves, L. Billiet, J. P. Gomez, C. Pichon, H. Cheradame, P. Midoux and P. Guegan (2011). "Histidinylated linear PEI: a new efficient non-toxic polymer for gene transfer." Chem Commun (Camb) **47**(46): 12547-12549.
31. Bianco, P., M. Riminucci, S. Gronthos and P. G. Robey (2001). "Bone marrow stromal stem cells: nature, biology, and potential applications." Stem Cells **19**(3): 180-192.
32. Bilezikian, J. P., L. G. Raisz and T. J. Martin (2008). Principles of bone biology. San Diego, Calif., Academic Press/Elsevier.
33. Blair, H. C., S. L. Teitelbaum, R. Ghiselli and S. Gluck (1989). "Osteoclastic bone resorption by a polarized vacuolar proton pump." Science **245**(4920): 855-857.
34. Bolander, M. E. (1992). "Regulation of fracture repair by growth factors." Proc Soc Exp Biol Med **200**(2): 165-170.
35. Bonewald, L. F. (2011). "The amazing osteocyte." J Bone Miner Res **26**(2): 229-238.
36. Bonucci, E. (1992). Calcification in biological systems. Boca Raton, CRC Press.
37. Borden, M., S. F. El-Amin, M. Attawia and C. T. Laurencin (2003). "Structural and human cellular assessment of a novel microsphere-based tissue engineered scaffold for bone repair." Biomaterials **24**(4): 597-609.
38. Bornholdt, Z. A. and B. V. Prasad (2006). "X-ray structure of influenza virus NS1 effector domain." Nat Struct Mol Biol **13**(6): 559-560.

39. Brisse, M. and H. Ly (2017). "Viral inhibitions of PACT-induced RIG-I activation." Oncotarget **8**(37): 60725-60726.
40. Buckwalter, J. A., Glimcher, M. J., Cooper, R. R., & Recker, R. R. (1995). "Bone biology. Part I: Structure, blood supply, cells, matrix, and mineralization." Journal of Bone and Joint Surgery - Series A **77**(8): 1256-1275.
41. Byrne, E. M., E. Farrell, L. A. McMahon, M. G. Haugh, F. J. O'Brien, V. A. Campbell, P. J. Prendergast and B. C. O'Connell (2008). "Gene expression by marrow stromal cells in a porous collagen-glycosaminoglycan scaffold is affected by pore size and mechanical stimulation." J Mater Sci Mater Med **19**(11): 3455-3463.
42. Cai, A., M. Jankowska-Anyszka, A. Centers, L. Chlebicka, J. Stepinski, R. Stolarski, E. Darzynkiewicz and R. E. Rhoads (1999). "Quantitative assessment of mRNA cap analogues as inhibitors of in vitro translation." Biochemistry **38**(26): 8538-8547.
43. Campana, V., G. Milano, E. Pagano, M. Barba, C. Cicione, G. Salonna, W. Lattanzi and G. Logroscino (2014). "Bone substitutes in orthopaedic surgery: from basic science to clinical practice." J Mater Sci Mater Med **25**(10): 2445-2461.
44. Canalis, E. (1987). "Effects of tumor necrosis factor on bone formation in vitro." Endocrinology **121**(5): 1596-1604.
45. Castillo, D., S. Montelongo, J. Pearson, J. L. Ong and T. Guda (2016). "Comparing mechanical properties of silk-coated and collagen-coated hydroxyapatite scaffolds." Frontiers in Bioengineering and Biotechnology.
46. Chahla, J., S. Mannava, M. E. Cinque, A. G. Geeslin, D. Codina and R. F. LaPrade (2017). "Bone Marrow Aspirate Concentrate Harvesting and Processing Technique." Arthrosc Tech **6**(2): e441-e445.
47. Chang, J., F. Liu, M. Lee, B. Wu, K. Ting, J. N. Zara, C. Soo, K. Al Hezaimi, W. Zou, X. Chen, D. J. Mooney and C. Y. Wang (2013). "NF-kappaB inhibits osteogenic differentiation of mesenchymal stem cells by promoting beta-catenin degradation." Proc Natl Acad Sci U S A **110**(23): 9469-9474.
48. Chang, P.-C., J. A. Cirelli, Q. Jin, Y.-J. Seol, J. V. Sugai, N. J. D'Silva, T. E. Danciu, L. A. Chandler, B. A. Sosnowski and W. V. Giannobile (2009). "Adenovirus encoding human platelet-derived growth factor-B delivered to alveolar bone defects exhibits safety and biodistribution profiles favorable for clinical use." Human gene therapy **20**(5): 486-496.
49. Chen, C.-y. and P. Sarnow (1995). "Initiation of protein synthesis by the eukaryotic translational apparatus on circular RNAs." Science **268**(5209): 415-417.
50. Chen, C. Y., R. Gherzi, S. E. Ong, E. L. Chan, R. Raijmakers, G. J. Pruijn, G. Stoecklin, C. Moroni, M. Mann and M. Karin (2001). "AU binding proteins recruit the exosome to degrade ARE-containing mRNAs." Cell **107**(4): 451-464.
51. Chen, K.-Y., C.-M. Chung, S.-M. Kuo, Y.-S. Chen and C.-H. Yao (2009). "Influence of Collagen I Nanospheres on the Growth and Osteogenic Difference of Rat Bone Marrow Stromal Cells." Journal of Medical and Biological Engineering **29**(6): 284-289.
52. Chen, L.-L. and L. Yang (2015). "Regulation of circRNA biogenesis." RNA biology **12**(4): 381-388.
53. Chen, P., J. Tao, S. Zhu, Y. Cai, Q. Mao, D. Yu, J. Dai and H. Ouyang (2015). "Radially oriented collagen scaffold with SDF-1 promotes osteochondral repair by facilitating cell homing." Biomaterials **39**: 114-123.
54. Chen, Z., Y. Li and R. M. Krug (1999). "Influenza A virus NS1 protein targets poly(A)-binding protein II of the cellular 3'-end processing machinery." EMBO J **18**(8): 2273-2283.
55. Chien, C. Y., R. Tejero, Y. Huang, D. E. Zimmerman, C. B. Rios, R. M. Krug and G. T. Montelione (1997). "A novel RNA-binding motif in influenza A virus non-structural protein 1." Nat Struct Biol **4**(11): 891-895.
56. Cho, H. H., K. K. Shin, Y. J. Kim, J. S. Song, J. M. Kim, Y. C. Bae, C. D. Kim and J. S. Jung (2010). "NF-κB activation stimulates osteogenic differentiation of mesenchymal stem cells derived from human adipose tissue by increasing TAZ expression." Journal of cellular physiology **223**(1): 168-177.

57. Claes, L., S. Recknagel and A. Ignatius (2012). "Fracture healing under healthy and inflammatory conditions." Nat Rev Rheumatol **8**(3): 133-143.
58. Coller, J. and R. Parker (2004). "Eukaryotic mRNA decapping." Annu Rev Biochem **73**: 861-890.
59. Contreras, R., H. Cheroutre, W. Degrave and W. Fiers (1982). "Simple, efficient in vitro synthesis of capped RNA useful for direct expression of cloned eukaryotic genes." Nucleic Acids Res **10**(20): 6353-6362.
60. Couttet, P., M. Fromont-Racine, D. Steel, R. Pictet and T. Grange (1997). "Messenger RNA deadenylylation precedes decapping in mammalian cells." Proc Natl Acad Sci U S A **94**(11): 5628-5633.
61. Csobonyeiova, M., S. Polak, R. Zamborsky and L. Danisovic (2017). "iPS cell technologies and their prospect for bone regeneration and disease modeling: A mini review." J Adv Res **8**(4): 321-327.
62. Cui, Z. K., J. A. Sun, J. J. Baljon, J. Fan, S. Kim, B. M. Wu, T. Aghaloo and M. Lee (2017). "Simultaneous delivery of hydrophobic small molecules and siRNA using Sterosomes to direct mesenchymal stem cell differentiation for bone repair." Acta Biomater **58**: 214-224.
63. Cunniffe, G. M., G. R. Dickson, S. Partap, K. T. Stanton and F. J. O'Brien (2010). "Development and characterisation of a collagen nano-hydroxyapatite composite scaffold for bone tissue engineering." J Mater Sci Mater Med **21**(8): 2293-2298.
64. D'Andrea, L. D., G. Iaccarino, R. Fattorusso, D. Sorriento, C. Carannante, D. Capasso, B. Trimarco and C. Pedone (2005). "Targeting angiogenesis: structural characterization and biological properties of a de novo engineered VEGF mimicking peptide." Proc Natl Acad Sci U S A **102**(40): 14215-14220.
65. D'Mello, S., K. Atluri, S. M. Geary, L. Hong, S. Elangovan and A. K. Salem (2017). "Bone Regeneration Using Gene-Activated Matrices." AAPS J **19**(1): 43-53.
66. D. Logeart-Avramoglou , M. B., K. Oudina, P. Ten Dijke, H. Petite (2006). "An assay for the determination of biologically active bone morphogenetic proteins using cells transfected with an inhibitor of differentiation promoter-luciferase construct." Analytical Biochemistry **349**: 78–86.
67. Daculsi, G., N. Passuti, S. Martin, C. Deudon, R. Z. Legeros and S. Raher (1990). "Macroporous calcium phosphate ceramic for long bone surgery in humans and dogs. Clinical and histological study." J Biomed Mater Res **24**(3): 379-396.
68. Dalby, M. J., N. Gadegaard, R. Tare, A. Andar, M. O. Riehle, P. Herzyk, C. D. Wilkinson and R. O. Oreffo (2007). "The control of human mesenchymal cell differentiation using nanoscale symmetry and disorder." Nat Mater **6**(12): 997-1003.
69. Dan, M., D. Zheng, L. L. Field and V. Bonnevie-Nielsen (2012). "Induction and activation of antiviral enzyme 2',5'-oligoadenylate synthetase by in vitro transcribed insulin mRNA and other cellular RNAs." Mol Biol Rep **39**(7): 7813-7822.
70. Denissen, H. W. and K. d. Groot (1979). "Immediate dental root implants from synthetic dense calcium hydroxylapatite." The Journal of Prosthetic Dentistry **42**(5): 551-556.
71. Devoldere, J., H. Dewitte, S. C. De Smedt and K. Remaut (2016). "Evading innate immunity in nonviral mRNA delivery: don't shoot the messenger." Drug Discov Today **21**(1): 11-25.
72. Diefenderfer, D. L., A. M. Osyczka, G. C. Reilly and P. S. Leboy (2003). "BMP Responsiveness in Human Mesenchymal Stem Cells." Connective Tissue Research **44**(1): 305-311.
73. Diehl, N. and H. Schaal (2013). "Make yourself at home: viral hijacking of the PI3K/Akt signaling pathway." Viruses **5**(12): 3192-3212.
74. Dimitriou, R., E. Tsiridis and P. V. Giannoudis (2005). "Current concepts of molecular aspects of bone healing." Injury **36**(12): 1392-1404.
75. Ducy, P., C. Desbois, B. Boyce, G. Pinero, B. Story, C. Dunstan, E. Smith, J. Bonadio, S. Goldstein, C. Gundberg, A. Bradley and G. Karsenty (1996). "Increased bone formation in osteocalcin-deficient mice." Nature **382**(6590): 448-452.
76. Ducy, P., M. Starbuck, M. Priemel, J. Shen, G. Pinero, V. Geoffroy, M. Amling and G. Karsenty (1999). "A Cbfa1-dependent genetic pathway controls bone formation beyond embryonic development." Genes Dev **13**(8): 1025-1036.

77. Dwek, J. R. (2010). "The periosteum: what is it, where is it, and what mimics it in its absence?" Skeletal Radiol **39**(4): 319-323.
78. Eastoe, J. E. and B. Eastoe (1954). "The organic constituents of mammalian compact bone." Biochem J **57**(3): 453-459.
79. Edmonds, M., M. H. Vaughan, Jr. and H. Nakazato (1971). "Polyadenylic acid sequences in the heterogeneous nuclear RNA and rapidly-labeled polyribosomal RNA of HeLa cells: possible evidence for a precursor relationship." Proc Natl Acad Sci U S A **68**(6): 1336-1340.
80. Ehrhardt, C. and S. Ludwig (2009). "A new player in a deadly game: influenza viruses and the PI3K/Akt signalling pathway." Cell Microbiol **11**(6): 863-871.
81. Ehrhardt, C., T. Wolff, S. Pleschka, O. Planz, W. Beermann, J. G. Bode, M. Schmolke and S. Ludwig (2007). "Influenza A virus NS1 protein activates the PI3K/Akt pathway to mediate antiapoptotic signaling responses." J Virol **81**(7): 3058-3067.
82. Einhorn, T. A. (1998). "The cell and molecular biology of fracture healing." Clin Orthop Relat Res(355 Suppl): S7-21.
83. Einhorn, T. A. and L. C. Gerstenfeld (2015). "Fracture healing: mechanisms and interventions." Nat Rev Rheumatol **11**(1): 45-54.
84. Elangovan, S., S. R. D'Mello, L. Hong, R. D. Ross, C. Allamargot, D. V. Dawson, C. M. Stanford, G. K. Johnson, D. R. Sumner and A. K. Salem (2014). "The enhancement of bone regeneration by gene activated matrix encoding for platelet derived growth factor." Biomaterials **35**(2): 737-747.
85. Elangovan, S., B. Khorsand, A. V. Do, L. Hong, A. Dewerth, M. Kormann, R. D. Ross, D. R. Sumner, C. Allamargot and A. K. Salem (2015). "Chemically modified RNA activated matrices enhance bone regeneration." J Control Release **218**: 22-28.
86. Elsdale, T. and J. Bard (1972). "Collagen substrata for studies on cell behavior." J Cell Biol **54**(3): 626-637.
87. Engler, A. J., S. Sen, H. L. Sweeney and D. E. Discher (2006). "Matrix elasticity directs stem cell lineage specification." Cell **126**(4): 677-689.
88. Enuka, Y., M. Lauriola, M. E. Feldman, A. Sas-Chen, I. Ulitsky and Y. Yarden (2015). "Circular RNAs are long-lived and display only minimal early alterations in response to a growth factor." Nucleic acids research **44**(3): 1370-1383.
89. Evans, C. H. and J. Huard (2015). "Gene therapy approaches to regenerating the musculoskeletal system." Nat Rev Rheumatol **11**(4): 234-242.
90. Fan, S., C. A. Macken, C. Li, M. Ozawa, H. Goto, N. F. Iswahyudi, C. A. Nidom, H. Chen, G. Neumann and Y. Kawaoka (2013). "Synergistic effect of the PDZ and p85beta-binding domains of the NS1 protein on virulence of an avian H5N1 influenza A virus." J Virol **87**(9): 4861-4871.
91. Fang, J., Y. Y. Zhu, E. Smiley, J. Bonadio, J. P. Rouleau, S. A. Goldstein, L. K. McCauley, B. L. Davidson and B. J. Roessler (1996). "Stimulation of new bone formation by direct transfer of osteogenic plasmid genes." Proc Natl Acad Sci U S A **93**(12): 5753-5758.
92. Farndale, R. W., T. Lisman, D. Bihan, S. Hamaia, C. S. Smerling, N. Pugh, A. Konitsiotis, B. Leitinger, P. G. de Groot, G. E. Jarvis and N. Raynal (2008). "Cell-collagen interactions: the use of peptide Toolkits to investigate collagen-receptor interactions." Biochem Soc Trans **36**(Pt 2): 241-250.
93. Fedorovich, N. E., R. T. Haverslag, W. J. Dhert and J. Alblas (2010). "The role of endothelial progenitor cells in prevascularized bone tissue engineering: development of heterogeneous constructs." Tissue Eng Part A **16**(7): 2355-2367.
94. Feng, W., X. Sun, N. Shi, M. Zhang, Z. Guan and M. Duan (2017). "Influenza a virus NS1 protein induced A20 contributes to viral replication by suppressing interferon-induced antiviral response." Biochem Biophys Res Commun **482**(4): 1107-1113.
95. Feng, Y. and M. Mrksich (2004). "The synergy peptide PHSRN and the adhesion peptide RGD mediate cell adhesion through a common mechanism." Biochemistry **43**(50): 15811-15821.
96. Ferreira, A. M., P. Gentile, V. Chiono and G. Ciardelli (2012). "Collagen for bone tissue regeneration." Acta Biomater **8**(9): 3191-3200.

97. Fietzek, P. P. and K. Kuhn (1976). "The primary structure of collagen." Int Rev Connect Tissue Res **7**: 1-60.
98. Finetti, F., A. Basile, D. Capasso, S. Di Gaetano, R. Di Stasi, M. Pascale, C. M. Turco, M. Ziche, L. Morbidelli and L. D. D'Andrea (2012). "Functional and pharmacological characterization of a VEGF mimetic peptide on reparative angiogenesis." Biochem Pharmacol **84**(3): 303-311.
99. Fisher, J. E., M. P. Caulfield, M. Sato, H. A. Quartuccio, R. J. Gould, V. M. Garsky, G. A. Rodan and M. Rosenblatt (1993). "Inhibition of osteoclastic bone resorption in vivo by echistatin, an "arginyl-glycyl-aspartyl" (RGD)-containing protein." Endocrinology **132**(3): 1411-1413.
100. Florencio-Silva, R., G. R. Sasso, E. Sasso-Cerri, M. J. Simoes and P. S. Cerri (2015). "Biology of Bone Tissue: Structure, Function, and Factors That Influence Bone Cells." Biomed Res Int **2015**: 421746.
101. Franceschi, R. T., S. Yang, R. B. Rutherford, P. H. Krebsbach, M. Zhao and D. Wang (2004). "Gene therapy approaches for bone regeneration." Cells Tissues Organs **176**(1-3): 95-108.
102. Freund, I., T. Eigenbrod, M. Helm and A. H. Dalpke (2019). "RNA Modifications Modulate Activation of Innate Toll-Like Receptors." Genes (Basel) **10**(2).
103. Friedenstein, A. J., S. Piatetzky, II and K. V. Petrakova (1966). "Osteogenesis in transplants of bone marrow cells." J Embryol Exp Morphol **16**(3): 381-390.
104. Frost, H. M. (1990). "Skeletal structural adaptations to mechanical usage (SATMU): 2. Redefining Wolff's law: the remodeling problem." Anat Rec **226**(4): 414-422.
105. Gabarin, N., H. Gavish, A. Muhlrad, Y. C. Chen, M. Namdar-Attar, R. A. Nissenson, M. Chorev and I. Bab (2001). "Mitogenic G(i) protein-MAP kinase signaling cascade in MC3T3-E1 osteogenic cells: activation by C-terminal pentapeptide of osteogenic growth peptide [OGP(10-14)] and attenuation of activation by cAMP." J Cell Biochem **81**(4): 594-603.
106. Gack, M. U., R. A. Albrecht, T. Urano, K. S. Inn, I. C. Huang, E. Carnero, M. Farzan, S. Inoue, J. U. Jung and A. Garcia-Sastre (2009). "Influenza A virus NS1 targets the ubiquitin ligase TRIM25 to evade recognition by the host viral RNA sensor RIG-I." Cell Host Microbe **5**(5): 439-449.
107. Gallie, D. R. (1998). "A tale of two termini: a functional interaction between the termini of an mRNA is a prerequisite for efficient translation initiation." Gene **216**(1): 1-11.
108. Gao, S., L. Song, J. Li, Z. Zhang, H. Peng, W. Jiang, Q. Wang, T. Kang, S. Chen and W. Huang (2012). "Influenza A virus-encoded NS1 virulence factor protein inhibits innate immune response by targeting IKK." Cell Microbiol **14**(12): 1849-1866.
109. Garcia, M. A., J. Gil, I. Ventoso, S. Guerra, E. Domingo, C. Rivas and M. Esteban (2006). "Impact of protein kinase PKR in cell biology: from antiviral to antiproliferative action." Microbiol Mol Biol Rev **70**(4): 1032-1060.
110. Geall, A. J., A. Verma, G. R. Otten, C. A. Shaw, A. Hekele, K. Banerjee, Y. Cu, C. W. Beard, L. A. Brito, T. Krucker, D. T. O'Hagan, M. Singh, P. W. Mason, N. M. Valiante, P. R. Dormitzer, S. W. Barnett, R. Rappuoli, J. B. Ulmer and C. W. Mandl (2012). "Nonviral delivery of self-amplifying RNA vaccines." Proc Natl Acad Sci U S A **109**(36): 14604-14609.
111. Ghayor, C. and F. E. Weber (2016). "Epigenetic Regulation of Bone Remodeling and Its Impacts in Osteoporosis." Int J Mol Sci **17**(9).
112. Gilbert, L., X. He, P. Farmer, J. Rubin, H. Drissi, A. J. van Wijnen, J. B. Lian, G. S. Stein and M. S. Nanes (2002). "Expression of the osteoblast differentiation factor RUNX2 (Cbfa1/AML3/Pebp2alpha A) is inhibited by tumor necrosis factor-alpha." J Biol Chem **277**(4): 2695-2701.
113. Glimcher, M. J., L. C. Bonar, M. D. Grynpas, W. J. Landis and A. H. Roufosse (1981). "Recent studies of bone mineral: Is the amorphous calcium phosphate theory valid?" Journal of Crystal Growth **53**(1): 100-119.
114. Globus, R. K., S. B. Doty, J. C. Lull, E. Holmuhamedov, M. J. Humphries and C. H. Damsky (1998). "Fibronectin is a survival factor for differentiated osteoblasts." J Cell Sci **111 (Pt 10)**: 1385-1393.

115. Gonçalves, C., M. Berchel, M.-P. Gosselin, V. Malard, H. Cheradame, P.-A. Jaffrès, P. Guégan, C. Pichon and P. Midoux (2014). "Lipopolyplexes comprising imidazole/imidazolium lipophosphoramidate, histidinylated polyethyleneimine and siRNA as efficient formulation for siRNA transfection." International journal of pharmaceutics **460**(1-2): 264-272.
116. Gotz, H. E., M. Muller, A. Emmel, U. Holzwarth, R. G. Erben and R. Stangl (2004). "Effect of surface finish on the osseointegration of laser-treated titanium alloy implants." Biomaterials **25**(18): 4057-4064.
117. Goubau, D., M. Schlee, S. Deddouche, A. J. Pruijssers, T. Zillinger, M. Goldeck, C. Schuberth, A. G. Van der Veen, T. Fujimura, J. Rehwinkel, J. A. Iskarpatyoti, W. Barchet, J. Ludwig, T. S. Dermody, G. Hartmann and C. Reis e Sousa (2014). "Antiviral immunity via RIG-I-mediated recognition of RNA bearing 5'-diphosphates." Nature **514**(7522): 372-375.
118. Granero-Molto, F., J. A. Weis, M. I. Miga, B. Landis, T. J. Myers, L. O'Rear, L. Longobardi, E. D. Jansen, D. P. Mortlock and A. Spagnoli (2009). "Regenerative effects of transplanted mesenchymal stem cells in fracture healing." Stem Cells **27**(8): 1887-1898.
119. Grier, A. E., S. Burleigh, J. Sahni, C. A. Clough, V. Cardot, D. C. Choe, M. C. Krutein, D. J. Rawlings, M. C. Jensen, A. M. Scharenberg and K. Jacoby (2016). "pEVL: A Linear Plasmid for Generating mRNA IVT Templates With Extended Encoded Poly(A) Sequences." Mol Ther Nucleic Acids **5**: e306.
120. Grudzien-Nogalska, E., J. Jemielity, J. Kowalska, E. Darzynkiewicz and R. E. Rhoads (2007). "Phosphorothioate cap analogs stabilize mRNA and increase translational efficiency in mammalian cells." RNA **13**(10): 1745-1755.
121. Guo, Z., L. M. Chen, H. Zeng, J. A. Gomez, J. Plowden, T. Fujita, J. M. Katz, R. O. Donis and S. Sambhara (2007). "NS1 protein of influenza A virus inhibits the function of intracytoplasmic pathogen sensor, RIG-I." Am J Respir Cell Mol Biol **36**(3): 263-269.
122. Gustafsson, C., S. Govindarajan and J. Minshull (2004). "Codon bias and heterologous protein expression." Trends in biotechnology **22**(7): 346-353.
123. Gutierrez-Sanchez, M., V. A. Escobar-Barrios, A. Pozos-Guillen and D. M. Escobar-Garcia (2019). "RGD-functionalization of PLA/starch scaffolds obtained by electrospinning and evaluated in vitro for potential bone regeneration." Mater Sci Eng C Mater Biol Appl **96**: 798-806.
124. Hale, B. G., D. Jackson, Y. H. Chen, R. A. Lamb and R. E. Randall (2006). "Influenza A virus NS1 protein binds p85beta and activates phosphatidylinositol-3-kinase signaling." Proc Natl Acad Sci U S A **103**(38): 14194-14199.
125. Hale, B. G., R. E. Randall, J. Ortin and D. Jackson (2008). "The multifunctional NS1 protein of influenza A viruses." J Gen Virol **89**(Pt 10): 2359-2376.
126. Hankenson, K. D., M. Dishowitz, C. Gray and M. Schenker (2011). "Angiogenesis in bone regeneration." Injury **42**(6): 556-561.
127. Hankenson, K. D., K. Gagne and M. Shaughnessy (2015). "Extracellular signaling molecules to promote fracture healing and bone regeneration." Adv Drug Deliv Rev **94**: 3-12.
128. Hanna, J., K. Saha, B. Pando, J. van Zon, C. J. Lengner, M. P. Creyghton, A. van Oudenaarden and R. Jaenisch (2009). "Direct cell reprogramming is a stochastic process amenable to acceleration." Nature **462**(7273): 595-601.
129. Harris, B. Z. and W. A. Lim (2001). "Mechanism and role of PDZ domains in signaling complex assembly." J Cell Sci **114**(Pt 18): 3219-3231.
130. Haugh, M. G., C. M. Murphy, R. C. McKiernan, C. Altenbuchner and F. J. O'Brien (2011). "Crosslinking and mechanical properties significantly influence cell attachment, proliferation, and migration within collagen glycosaminoglycan scaffolds." Tissue Eng Part A **17**(9-10): 1201-1208.
131. Heck, T., G. Faccio, M. Richter and L. Thony-Meyer (2013). "Enzyme-catalyzed protein crosslinking." Appl Microbiol Biotechnol **97**(2): 461-475.
132. Heil, F., H. Hemmi, H. Hochrein, F. Ampenberger, C. Kirschning, S. Akira, G. Lipford, H. Wagner and S. Bauer (2004). "Species-specific recognition of single-stranded RNA via toll-like receptor 7 and 8." Science **303**(5663): 1526-1529.

133. Herberg, S., C. Susin, M. Pelaez, R. N. Howie, R. Moreno de Freitas, J. Lee, J. J. Cray, Jr., M. H. Johnson, M. E. Elsalanty, M. W. Hamrick, C. M. Isales, U. M. Wikesjo and W. D. Hill (2014). "Low-dose bone morphogenetic protein-2/stromal cell-derived factor-1beta cotherapy induces bone regeneration in critical-size rat calvarial defects." Tissue Eng Part A **20**(9-10): 1444-1453.
134. Herrmann, M., S. Verrier and M. Alini (2015). "Strategies to Stimulate Mobilization and Homing of Endogenous Stem and Progenitor Cells for Bone Tissue Repair." Front Bioeng Biotechnol **3**: 79.
135. Hess, K., A. Ushmorov, J. Fiedler, R. E. Brenner and T. Wirth (2009). "TNFα promotes osteogenic differentiation of human mesenchymal stem cells by triggering the NF-κB signaling pathway." Bone **45**(2): 367-376.
136. Ho, M. H., L. T. Hou, C. Y. Tu, H. J. Hsieh, J. Y. Lai, W. J. Chen and D. M. Wang (2006). "Promotion of cell affinity of porous PLLA scaffolds by immobilization of RGD peptides via plasma treatment." Macromol Biosci **6**(1): 90-98.
137. Holtkamp, S., S. Kreiter, A. Selmi, P. Simon, M. Koslowski, C. Huber, O. Tureci and U. Sahin (2006). "Modification of antigen-encoding RNA increases stability, translational efficacy, and T-cell stimulatory capacity of dendritic cells." Blood **108**(13): 4009-4017.
138. Horikami, S. M., F. De Ferra and S. A. Moyer (1984). "Characterization of the infections of permissive and nonpermissive cells by host range mutants of vesicular stomatitis virus defective in RNA methylation." Virology **138**(1): 1-15.
139. Huang, C. Y., K. L. Hagar, L. E. Frost, Y. Sun and H. S. Cheung (2004). "Effects of cyclic compressive loading on chondrogenesis of rabbit bone-marrow derived mesenchymal stem cells." Stem Cells **22**(3): 313-323.
140. Huebsch, N., P. R. Arany, A. S. Mao, D. Shvartsman, O. A. Ali, S. A. Bencherif, J. Rivera-Feliciano and D. J. Mooney (2010). "Harnessing traction-mediated manipulation of the cell/matrix interface to control stem-cell fate." Nat Mater **9**(6): 518-526.
141. Hurst, S. M., T. S. Wilkinson, R. M. McLoughlin, S. Jones, S. Horiuchi, N. Yamamoto, S. Rose-John, G. M. Fuller, N. Topley and S. A. Jones (2001). "Il-6 and its soluble receptor orchestrate a temporal switch in the pattern of leukocyte recruitment seen during acute inflammation." Immunity **14**(6): 705-714.
142. Hutmacher, D. W. (2000). Scaffolds in tissue engineering bone and cartilage. The Biomaterials: Silver Jubilee Compendium. D. F. Williams. Oxford, Elsevier Science**:** 175-189.
143. Iijima, K., S. Ishikawa, K. Sasaki, M. Hashizume, M. Kawabe and H. Otsuka (2018). "Osteogenic Differentiation of Bone Marrow-Derived Mesenchymal Stem Cells in Electrospun Silica Nonwoven Fabrics." ACS Omega **3**(8): 10180-10187.
144. Iruela-Arispe, M. L., R. B. Vernon, H. Wu, R. Jaenisch and E. H. Sage (1996). "Type I collagen-deficient Mov-13 mice do not retain SPARC in the extracellular matrix: implications for fibroblast function." Dev Dyn **207**(2): 171-183.
145. Ito, H., M. Koefoed, P. Tiyapatanaputi, K. Gromov, J. J. Goater, J. Carmouche, X. Zhang, P. T. Rubery, J. Rabinowitz and R. J. Samulski (2005). "Remodeling of cortical bone allografts mediated by adherent rAAV-RANKL and VEGF gene therapy." Nature medicine **11**(3): 291.
146. Jabbari, E. (2013). "Osteogenic peptides in bone regeneration." Curr Pharm Des **19**(19): 3391-3402.
147. Jackson, R. J. (1993). "Cytoplasmic regulation of mRNA function: the importance of the 3' untranslated region." Cell **74**(1): 9-14.
148. Jager, M., M. Herten, U. Fochtmann, J. Fischer, P. Hernigou, C. Zilkens, C. Hendrich and R. Krauspe (2011). "Bridging the gap: bone marrow aspiration concentrate reduces autologous bone grafting in osseous defects." J Orthop Res **29**(2): 173-180.
149. Jansen, R. P. (2001). "mRNA localization: message on the move." Nat Rev Mol Cell Biol **2**(4): 247-256.

150. Jemielity, J., T. Fowler, J. Zuberek, J. Stepinski, M. Lewdorowicz, A. Niedzwiecka, R. Stolarski, E. Darzynkiewicz and R. E. Rhoads (2003). "Novel "anti-reverse" cap analogs with superior translational properties." RNA **9**(9): 1108-1122.
151. Jia, D., R. Rahbar, R. W. Chan, S. M. Lee, M. C. Chan, B. X. Wang, D. P. Baker, B. Sun, J. S. Peiris, J. M. Nicholls and E. N. Fish (2010). "Influenza virus non-structural protein 1 (NS1) disrupts interferon signaling." PLoS One **5**(11): e13927.
152. Jiang, W., Q. Wang, S. Chen, S. Gao, L. Song, P. Liu and W. Huang (2013). "Influenza A virus NS1 induces G0/G1 cell cycle arrest by inhibiting the expression and activity of RhoA protein." J Virol **87**(6): 3039-3052.
153. Jirikowski, G. F., P. P. Sanna, D. Maciejewski-Lenoir and F. E. Bloom (1992). "Reversal of diabetes insipidus in Brattleboro rats: intrahypothalamic injection of vasopressin mRNA." Science **255**(5047): 996-998.
154. Jones, E. and X. Yang (2011). "Mesenchymal stem cells and bone regeneration: current status." Injury **42**(6): 562-568.
155. Jureka, A. S., A. B. Kleinpeter, G. Cornilescu, C. C. Cornilescu and C. M. Petit (2015). "Structural Basis for a Novel Interaction between the NS1 Protein Derived from the 1918 Influenza Virus and RIG-I." Structure **23**(11): 2001-2010.
156. Kanczler, J. M., P. J. Ginty, L. White, N. M. Clarke, S. M. Howdle, K. M. Shakesheff and R. O. Oreffo (2010). "The effect of the delivery of vascular endothelial growth factor and bone morphogenic protein-2 to osteoprogenitor cell populations on bone formation." Biomaterials **31**(6): 1242-1250.
157. Kaneki, H., R. Guo, D. Chen, Z. Yao, E. M. Schwarz, Y. E. Zhang, B. F. Boyce and L. Xing (2006). "Tumor necrosis factor promotes Runx2 degradation through up-regulation of Smurf1 and Smurf2 in osteoblasts." J Biol Chem **281**(7): 4326-4333.
158. Karageorgiou, V. and D. Kaplan (2005). "Porosity of 3D biomaterial scaffolds and osteogenesis." Biomaterials **26**(27): 5474-5491.
159. Kariko, K., M. Buckstein, H. Ni and D. Weissman (2005). "Suppression of RNA recognition by Toll-like receptors: the impact of nucleoside modification and the evolutionary origin of RNA." Immunity **23**(2): 165-175.
160. Kariko, K., H. Muramatsu, J. Ludwig and D. Weissman (2011). "Generating the optimal mRNA for therapy: HPLC purification eliminates immune activation and improves translation of nucleoside-modified, protein-encoding mRNA." Nucleic Acids Res **39**(21): e142.
161. Kariko, K., H. Muramatsu, F. A. Welsh, J. Ludwig, H. Kato, S. Akira and D. Weissman (2008). "Incorporation of pseudouridine into mRNA yields superior nonimmunogenic vector with increased translational capacity and biological stability." Mol Ther **16**(11): 1833-1840.
162. Kariko, K., H. Ni, J. Capodici, M. Lamphier and D. Weissman (2004). "mRNA is an endogenous ligand for Toll-like receptor 3." J Biol Chem **279**(13): 12542-12550.
163. Kato, K., T. Kanaji, S. Russell, T. J. Kunicki, K. Furihata, S. Kanaji, P. Marchese, A. Reininger, Z. M. Ruggeri and J. Ware (2003). "The contribution of glycoprotein VI to stable platelet adhesion and thrombus formation illustrated by targeted gene deletion." Blood **102**(5): 1701-1707.
164. Katze, M. G., Y. He and M. Gale, Jr. (2002). "Viruses and interferon: a fight for supremacy." Nat Rev Immunol **2**(9): 675-687.
165. Keeney, M., J. J. van den Beucken, P. M. van der Kraan, J. A. Jansen and A. Pandit (2010). "The ability of a collagen/calcium phosphate scaffold to act as its own vector for gene delivery and to promote bone formation via transfection with VEGF165." Biomaterials **31**(10): 2893-2902.
166. Kesireddy, V. and F. K. Kasper (2016). "Approaches for building bioactive elements into synthetic scaffolds for bone tissue engineering." J Mater Chem B **4**(42): 6773-6786.
167. Khatiwala, C. B., S. R. Peyton, M. Metzke and A. J. Putnam (2007). "The regulation of osteogenesis by ECM rigidity in MC3T3-E1 cells requires MAPK activation." J Cell Physiol **211**(3): 661-672.

168. Khatiwala, C. B., S. R. Peyton and A. J. Putnam (2006). "Intrinsic mechanical properties of the extracellular matrix affect the behavior of pre-osteoblastic MC3T3-E1 cells." Am J Physiol Cell Physiol **290**(6): C1640-1650.
169. Khetan, S., M. Guvendiren, W. R. Legant, D. M. Cohen, C. S. Chen and J. A. Burdick (2013). "Degradation-mediated cellular traction directs stem cell fate in covalently crosslinked three-dimensional hydrogels." Nature Materials **12**: 458.
170. Khorsand, B., S. Elangovan, L. Hong, A. Dewerth, M. S. Kormann and A. K. Salem (2017). "A Comparative Study of the Bone Regenerative Effect of Chemically Modified RNA Encoding BMP-2 or BMP-9." AAPS J **19**(2): 438-446.
171. Khorsand, B., N. Nicholson, A. V. Do, J. E. Femino, J. A. Martin, E. Petersen, B. Guetschow, D. C. Fredericks and A. K. Salem (2017). "Regeneration of bone using nanoplex delivery of FGF-2 and BMP-2 genes in diaphyseal long bone radial defects in a diabetic rabbit model." J Control Release **248**: 53-59.
172. Kim, H. J., I. K. Park, J. H. Kim, C. S. Cho and M. S. Kim (2012). "Gas foaming fabrication of porous biphasic calcium phosphate for bone regeneration." Tissue Engineering and Regenerative Medicine **9**(2): 63-68.
173. Kim, I., S. A. McKenna, E. Viani Puglisi and J. D. Puglisi (2007). "Rapid purification of RNAs using fast performance liquid chromatography (FPLC)." RNA **13**(2): 289-294.
174. Kim, J., M. Guermah and R. G. Roeder (2010). "The human PAF1 complex acts in chromatin transcription elongation both independently and cooperatively with SII/TFIIS." Cell **140**(4): 491-503.
175. Klein, C., K. de Groot, W. Chen, Y. Li and X. Zhang (1994). "Osseous substance formation induced in porous calcium phosphate ceramics in soft tissues." Biomaterials **15**(1): 31-34.
176. Klemm, C., Y. Boergeling, S. Ludwig and C. Ehrhardt (2018). "Immunomodulatory Nonstructural Proteins of Influenza A Viruses." Trends Microbiol **26**(7): 624-636.
177. Knippenberg, M., M. N. Helder, B. Z. Doulabi, C. M. Semeins, P. I. Wuisman and J. Klein-Nulend (2005). "Adipose tissue-derived mesenchymal stem cells acquire bone cell-like responsiveness to fluid shear stress on osteogenic stimulation." Tissue Eng **11**(11-12): 1780-1788.
178. Kochs, G., A. Garcia-Sastre and L. Martinez-Sobrido (2007). "Multiple anti-interferon actions of the influenza A virus NS1 protein." J Virol **81**(13): 7011-7021.
179. Kok, K. H., P. Y. Lui, M. H. Ng, K. L. Siu, S. W. Au and D. Y. Jin (2011). "The double-stranded RNA-binding protein PACT functions as a cellular activator of RIG-I to facilitate innate antiviral response." Cell Host Microbe **9**(4): 299-309.
180. Konarska, M. M., R. A. Padgett and P. A. Sharp (1984). "Recognition of cap structure in splicing in vitro of mRNA precursors." Cell **38**(3): 731-736.
181. Kondo, N., A. Ogose, K. Tokunaga, H. Umezu, K. Arai, N. Kudo, M. Hoshino, H. Inoue, H. Irie, K. Kuroda, H. Mera and N. Endo (2006). "Osteoinduction with highly purified beta-tricalcium phosphate in dog dorsal muscles and the proliferation of osteoclasts before heterotopic bone formation." Biomaterials **27**(25): 4419-4427.
182. Kormann, M. S. D., G. Hasenpusch, M. K. Aneja, G. Nica, A. W. Flemmer, S. Herber-Jonat, M. Huppmann, L. E. Mays, M. Illenyi, A. Schams, M. Griese, I. Bittmann, R. Handgretinger, D. Hartl, J. Rosenecker and C. Rudolph (2011). "Expression of therapeutic proteins after delivery of chemically modified mRNA in mice." Nature Biotechnology **29**: 154.
183. Kozak, M. (1987). "An analysis of 5'-noncoding sequences from 699 vertebrate messenger RNAs." Nucleic Acids Res **15**(20): 8125-8148.
184. Kozak, M. (1989). "Circumstances and mechanisms of inhibition of translation by secondary structure in eucaryotic mRNAs." Mol Cell Biol **9**(11): 5134-5142.
185. Kozak, M. (2005). "Regulation of translation via mRNA structure in prokaryotes and eukaryotes." Gene **361**: 13-37.
186. Krane, S. M. (1982). "Collagenases and collagen degradation." J Invest Dermatol **79 Suppl 1**: 83s-86s.

187. Krebsbach, P. H., S. A. Kuznetsov, P. Bianco and P. G. Robey (1999). "Bone marrow stromal cells: characterization and clinical application." Crit Rev Oral Biol Med **10**(2): 165-181.
188. Krug, R. M. and A. García-Sastre (2013). The NS1 protein: A master regulator of host and viral functions. Textbook of Influenza**:** 114-132.
189. Kuo, S. M., S. J. Chang, I. Manousakas, L. C. Lin and T. W. Liu (2008). Preparation of Nano-Sized Collagen I and Collagen II Particles. 2008 2nd International Conference on Bioinformatics and Biomedical Engineering.
190. Kurashina, K., H. Kurita, Q. Wu, A. Ohtsuka and H. Kobayashi (2002). "Ectopic osteogenesis with biphasic ceramics of hydroxyapatite and tricalcium phosphate in rabbits." Biomaterials **23**(2): 407-412.
191. Kurdy, N. M., J. B. Weiss and A. Bate (1996). "Endothelial stimulating angiogenic factor in early fracture healing." Injury **27**(2): 143-145.
192. Kuznetsov, S. A., M. H. Mankani, S. Gronthos, K. Satomura, P. Bianco and P. G. Robey (2001). "Circulating skeletal stem cells." J Cell Biol **153**(5): 1133-1140.
193. Landis, W. J., M. J. Song, A. Leith, L. McEwen and B. F. McEwen (1993). "Mineral and organic matrix interaction in normally calcifying tendon visualized in three dimensions by high-voltage electron microscopic tomography and graphic image reconstruction." J Struct Biol **110**(1): 39-54.
194. Langberg, S. R. and B. Moss (1981). "Post-transcriptional modifications of mRNA. Purification and characterization of cap I and cap II RNA (nucleoside-2'-)-methyltransferases from HeLa cells." J Biol Chem **256**(19): 10054-10060.
195. Laurent, G. J. (1987). "Dynamic state of collagen: pathways of collagen degradation in vivo and their possible role in regulation of collagen mass." Am J Physiol **252**(1 Pt 1): C1-9.
196. Laurie, S. W. S., L. B. Kaban, J. B. Mulliken and J. E. Murray (1984). "Donor-Site Morbidity after Harvesting Rib and Iliac Bone." Plastic and Reconstructive Surgery **73**(6): 933-938.
197. Law, J. X., L. L. Liau, A. Saim, Y. Yang and R. Idrus (2017). "Electrospun Collagen Nanofibers and Their Applications in Skin Tissue Engineering." Tissue Eng Regen Med **14**(6): 699-718.
198. Lawrence, T. (2009). "The nuclear factor NF-kappaB pathway in inflammation." Cold Spring Harb Perspect Biol **1**(6): a001651.
199. Lee, F. Y., Y. W. Choi, F. F. Behrens, D. O. DeFouw and T. A. Einhorn (1998). "Programmed removal of chondrocytes during endochondral fracture healing." J Orthop Res **16**(1): 144-150.
200. Lee, J. W., J. Y. Kim and D. W. Cho (2010). "Solid Free-form Fabrication Technology and Its Application to Bone Tissue Engineering." Int J Stem Cells **3**(2): 85-95.
201. Lee, S. J., J. S. Choi, K. S. Park, G. Khang, Y. M. Lee and H. B. Lee (2004). "Response of MG63 osteoblast-like cells onto polycarbonate membrane surfaces with different micropore sizes." Biomaterials **25**(19): 4699-4707.
202. Lee, S. J., S. W. Kang, H. J. Do, I. Han, D. A. Shin, J. H. Kim and S. H. Lee (2010). "Enhancement of bone regeneration by gene delivery of BMP2/Runx2 bicistronic vector into adipose-derived stromal cells." Biomaterials **31**(21): 5652-5659.
203. LeGeros, R. Z. (2008). "Calcium phosphate-based osteoinductive materials." Chem Rev **108**(11): 4742-4753.
204. LeGeros, R. Z., S. Lin, R. Rohanizadeh, D. Mijares and J. P. LeGeros (2003). "Biphasic calcium phosphate bioceramics: preparation, properties and applications." J Mater Sci Mater Med **14**(3): 201-209.
205. Leibovich, S. J. and R. Ross (1975). "The role of the macrophage in wound repair. A study with hydrocortisone and antimacrophage serum." Am J Pathol **78**(1): 71-100.
206. Leitinger, B. and E. Hohenester (2007). "Mammalian collagen receptors." Matrix Biol **26**(3): 146-155.
207. Leven, R. M., A. S. Virdi and D. R. Sumner (2004). "Patterns of gene expression in rat bone marrow stromal cells cultured on titanium alloy discs of different roughness." J Biomed Mater Res A **70**(3): 391-401.

208. Lewandrowski, K. U., J. D. Gresser, S. Bondre, A. E. Silva, D. L. Wise and D. J. Trantolo (2000). "Developing porosity of poly(propylene glycol-co-fumaric acid) bone graft substitutes and the effect on osteointegration: a preliminary histology study in rats." J Biomater Sci Polym Ed **11**(8): 879-889.
209. Li, B., X. Luo and Y. Dong (2016). "Effects of Chemically Modified Messenger RNA on Protein Expression." Bioconjug Chem **27**(3): 849-853.
210. Li, S., J. Y. Min, R. M. Krug and G. C. Sen (2006). "Binding of the influenza A virus NS1 protein to PKR mediates the inhibition of its activation by either PACT or double-stranded RNA." Virology **349**(1): 13-21.
211. Li, W. J., C. T. Laurencin, E. J. Caterson, R. S. Tuan and F. K. Ko (2002). "Electrospun nanofibrous structure: a novel scaffold for tissue engineering." J Biomed Mater Res **60**(4): 613-621.
212. Li, Y., Z. Y. Chen, W. Wang, C. C. Baker and R. M. Krug (2001). "The 3'-end-processing factor CPSF is required for the splicing of single-intron pre-mRNAs in vivo." RNA **7**(6): 920-931.
213. Li, Y. J., N. N. Batra, L. You, S. C. Meier, I. A. Coe, C. E. Yellowley and C. R. Jacobs (2004). "Oscillatory fluid flow affects human marrow stromal cell proliferation and differentiation." J Orthop Res **22**(6): 1283-1289.
214. Li, Z., L. Kupcsik, S. J. Yao, M. Alini and M. J. Stoddart (2010). "Mechanical load modulates chondrogenesis of human mesenchymal stem cells through the TGF-beta pathway." J Cell Mol Med **14**(6A): 1338-1346.
215. Lin, A. S., T. H. Barrows, S. H. Cartmell and R. E. Guldberg (2003). "Microarchitectural and mechanical characterization of oriented porous polymer scaffolds." Biomaterials **24**(3): 481-489.
216. Lin, C.-Y., F. Perche, M. Ikegami, S. Uchida, K. Kataoka and K. Itaka (2016). "Messenger RNA-based therapeutics for brain diseases: An animal study for augmenting clearance of beta-amyloid by intracerebral administration of neprilysin mRNA loaded in polyplex nanomicelles." Journal of Controlled Release **235**: 268-275.
217. Liu, J., P. A. Lynch, C. Y. Chien, G. T. Montelione, R. M. Krug and H. M. Berman (1997). "Crystal structure of the unique RNA-binding domain of the influenza virus NS1 protein." Nat Struct Biol **4**(11): 896-899.
218. Liu, Y., Z. H. Chia, J. Liew, S. M. Or and K. K. L. Phua (2018). "Modulation of mRNA Translation and Cell Viability by Influenza A Virus Derived Nonstructural Protein 1." Nucleic Acid Ther **28**(3): 200-208.
219. Liu, Y., J. M. Chin, E. L. Choo and K. K. L. Phua (2019). "Messenger RNA translation enhancement by immune evasion proteins: a comparative study between EKB (vaccinia virus) and NS1 (influenza A virus)." Sci Rep **9**(1): 11972.
220. Lo, H. J., H. K. Huang and T. F. Donahue (1998). "RNA polymerase I-promoted HIS4 expression yields uncapped, polyadenylated mRNA that is unstable and inefficiently translated in Saccharomyces cerevisiae." Mol Cell Biol **18**(2): 665-675.
221. Loi, F., L. A. Cordova, J. Pajarinen, T. H. Lin, Z. Yao and S. B. Goodman (2016). "Inflammation, fracture and bone repair." Bone **86**: 119-130.
222. Loo, Y. M. and M. Gale, Jr. (2011). "Immune signaling by RIG-I-like receptors." Immunity **34**(5): 680-692.
223. Lopes, D., C. Martins-Cruz, M. B. Oliveira and J. F. Mano (2018). "Bone physiology as inspiration for tissue regenerative therapies." Biomaterials **185**: 240-275.
224. Lotfy, A., M. Salama, F. Zahran, E. Jones, A. Badawy and M. Sobh (2014). "Characterization of mesenchymal stem cells derived from rat bone marrow and adipose tissue: a comparative study." Int J Stem Cells **7**(2): 135-142.
225. Lucero, H. A. and H. M. Kagan (2006). "Lysyl oxidase: an oxidative enzyme and effector of cell function." Cell Mol Life Sci **63**(19-20): 2304-2316.
226. Lundstrom, K. (2018). "Self-Replicating RNA Viruses for RNA Therapeutics." Molecules **23**(12): 3310.

227. Lv, J., P. Xiu, J. Tan, Z. Jia, H. Cai and Z. Liu (2015). "Enhanced angiogenesis and osteogenesis in critical bone defects by the controlled release of BMP-2 and VEGF: implantation of electron beam melting-fabricated porous Ti6Al4V scaffolds incorporating growth factor-doped fibrin glue." Biomed Mater **10**(3): 035013.
228. Lynn, A. K., I. V. Yannas and W. Bonfield (2004). "Antigenicity and immunogenicity of collagen." J Biomed Mater Res B Appl Biomater **71**(2): 343-354.
229. Malone, R. W., P. L. Felgner and I. M. Verma (1989). "Cationic liposome-mediated RNA transfection." Proc Natl Acad Sci U S A **86**(16): 6077-6081.
230. Mao, M., Y. Tang, K. Zhao, Z. Duan and C. Wu (2019). "Fabrication of porous titanium scaffolds with centrosymmetric pore channels and improved radial fracture loading." Journal of materials science **54**(4): 3527-3535.
231. Marazzi, I., J. S. Ho, J. Kim, B. Manicassamy, S. Dewell, R. A. Albrecht, C. W. Seibert, U. Schaefer, K. L. Jeffrey, R. K. Prinjha, K. Lee, A. Garcia-Sastre, R. G. Roeder and A. Tarakhovsky (2012). "Suppression of the antiviral response by an influenza histone mimic." Nature **483**(7390): 428-433.
232. Mastrogiacomo, M., S. Scaglione, R. Martinetti, L. Dolcini, F. Beltrame, R. Cancedda and R. Quarto (2006). "Role of scaffold internal structure on in vivo bone formation in macroporous calcium phosphate bioceramics." Biomaterials **27**(17): 3230-3237.
233. Matsuo, H., H. Li, A. M. McGuire, C. M. Fletcher, A. C. Gingras, N. Sonenberg and G. Wagner (1997). "Structure of translation factor eIF4E bound to m7GDP and interaction with 4E-binding protein." Nat Struct Biol **4**(9): 717-724.
234. Mauney, J. R., V. Volloch and D. L. Kaplan (2005). "Role of adult mesenchymal stem cells in bone tissue engineering applications: current status and future prospects." Tissue Eng **11**(5-6): 787-802.
235. McCormick, C. and D. A. Khaperskyy (2017). "Translation inhibition and stress granules in the antiviral immune response." Nat Rev Immunol **17**(10): 647-660.
236. McKay, W. F., S. M. Peckham and J. M. Badura (2007). "A comprehensive clinical review of recombinant human bone morphogenetic protein-2 (INFUSE Bone Graft)." Int Orthop **31**(6): 729-734.
237. McKenna, S. A., I. Kim, E. V. Puglisi, D. A. Lindhout, C. E. Aitken, R. A. Marshall and J. D. Puglisi (2007). "Purification and characterization of transcribed RNAs using gel filtration chromatography." Nat Protoc **2**(12): 3270-3277.
238. McKibbin, B. (1978). "The biology of fracture healing in long bones." J Bone Joint Surg Br **60-B**(2): 150-162.
239. McMahon, L. A., V. A. Campbell and P. J. Prendergast (2008). "Involvement of stretch-activated ion channels in strain-regulated glycosaminoglycan synthesis in mesenchymal stem cell-seeded 3D scaffolds." J Biomech **41**(9): 2055-2059.
240. Melnyk, M., T. Henke, L. Claes and P. Augat (2008). "Revascularisation during fracture healing with soft tissue injury." Arch Orthop Trauma Surg **128**(10): 1159-1165.
241. Mendecki, J., S. Y. Lee and G. Brawerman (1972). "Characteristics of the polyadenylic acid segment associated with messenger ribonucleic acid in mouse sarcoma 180 ascites cells." Biochemistry **11**(5): 792-798.
242. Mevel, M., G. Breuzard, J. J. Yaouanc, J. C. Clement, P. Lehn, C. Pichon, P. A. Jaffres and P. Midoux (2008). "Synthesis and transfection activity of new cationic phosphoramidate lipids: high efficiency of an imidazolium derivative." Chembiochem **9**(9): 1462-1471.
243. Mevel, M., C. Neveu, C. Goncalves, J. J. Yaouanc, C. Pichon, P. A. Jaffres and P. Midoux (2008). "Novel neutral imidazole-lipophosphoramides for transfection assays." Chem Commun (Camb)(27): 3124-3126.
244. Mibayashi, M., L. Martinez-Sobrido, Y. M. Loo, W. B. Cardenas, M. Gale, Jr. and A. Garcia-Sastre (2007). "Inhibition of retinoic acid-inducible gene I-mediated induction of beta interferon by the NS1 protein of influenza A virus." J Virol **81**(2): 514-524.

245. Michaeli, D., G. R. Martin, J. Kettman, E. Benjamini, D. Y. Leung and B. A. Blatt (1969). "Localization of antigenic determinants in the polypeptide chains of collagen." Science **166**(3912): 1522-1524.
246. Michel, T., S. Golombek, H. Steinle, L. Hann, A. Velic, B. Macek, S. Krajewski, C. Schlensak, H. P. Wendel and M. Avci-Adali (2019). "Efficient reduction of synthetic mRNA induced immune activation by simultaneous delivery of B18R encoding mRNA." J Biol Eng **13**: 40.
247. Mignone, F., C. Gissi, S. Liuni and G. Pesole (2002). "Untranslated regions of mRNAs." Genome Biol **3**(3): REVIEWS0004.
248. Milligan, J. F., D. R. Groebe, G. W. Witherell and O. C. Uhlenbeck (1987). "Oligoribonucleotide synthesis using T7 RNA polymerase and synthetic DNA templates." Nucleic Acids Res **15**(21): 8783-8798.
249. Min, J. Y. and R. M. Krug (2006). "The primary function of RNA binding by the influenza A virus NS1 protein in infected cells: Inhibiting the 2'-5' oligo (A) synthetase/RNase L pathway." Proc Natl Acad Sci U S A **103**(18): 7100-7105.
250. Mobbs, R. J., M. Maharaj and P. J. Rao (2014). "Clinical outcomes and fusion rates following anterior lumbar interbody fusion with bone graft substitute i-FACTOR, an anorganic bone matrix/P-15 composite." J Neurosurg Spine **21**(6): 867-876.
251. Mockey, M., C. Goncalves, F. P. Dupuy, F. M. Lemoine, C. Pichon and P. Midoux (2006). "mRNA transfection of dendritic cells: synergistic effect of ARCA mRNA capping with Poly(A) chains in cis and in trans for a high protein expression level." Biochem Biophys Res Commun **340**(4): 1062-1068.
252. Morgan, E. F., G. L. Barnes and T. A. Einhorn (2013). Chapter 1 - The Bone Organ System: Form and Function. Osteoporosis (Fourth Edition). R. Marcus, D. Feldman, D. W. Dempster, M. Luckey and J. A. Cauley. San Diego, Academic Press**:** 3-20.
253. Mould, A. P., J. A. Askari and M. J. Humphries (2000). "Molecular basis of ligand recognition by integrin alpha 5beta 1. I. Specificity of ligand binding is determined by amino acid sequences in the second and third NH2-terminal repeats of the alpha subunit." J Biol Chem **275**(27): 20324-20336.
254. Moya, A., N. Larochette, M. Bourguignon, H. El-Hafci, E. Potier, H. Petite and D. Logeart-Avramoglou (2018). "Osteogenic potential of adipogenic predifferentiated human bone marrow-derived multipotent stromal cells for bone tissue-engineering." J Tissue Eng Regen Med **12**(3): e1511-e1524.
255. Mu, X., E. Greenwald, S. Ahmad and S. Hur (2018). "An origin of the immunogenicity of in vitro transcribed RNA." Nucleic Acids Res **46**(10): 5239-5249.
256. Mukherjee, D., M. Gao, J. P. O'Connor, R. Raijmakers, G. Pruijn, C. S. Lutz and J. Wilusz (2002). "The mammalian exosome mediates the efficient degradation of mRNAs that contain AU-rich elements." EMBO J **21**(1-2): 165-174.
257. Murphy, C. M. and F. J. O'Brien (2010). "Understanding the effect of mean pore size on cell activity in collagen-glycosaminoglycan scaffolds." Cell Adh Migr **4**(3): 377-381.
258. Muschler, G. F., C. Nakamoto and L. G. Griffith (2004). "Engineering principles of clinical cell-based tissue engineering." J Bone Joint Surg Am **86**(7): 1541-1558.
259. Myong, S., S. Cui, P. V. Cornish, A. Kirchhofer, M. U. Gack, J. U. Jung, K. P. Hopfner and T. Ha (2009). "Cytosolic viral sensor RIG-I is a 5'-triphosphate-dependent translocase on double-stranded RNA." Science **323**(5917): 1070-1074.
260. Nacheva, G. A. and A. Berzal-Herranz (2003). "Preventing nondesired RNA-primed RNA extension catalyzed by T7 RNA polymerase." Eur J Biochem **270**(7): 1458-1465.
261. Nagai, N., N. Kumasaka, T. Kawashima, H. Kaji, M. Nishizawa and T. Abe (2010). "Preparation and characterization of collagen microspheres for sustained release of VEGF." J Mater Sci Mater Med **21**(6): 1891-1898.
262. Naldini, L. (2015). "Gene therapy returns to centre stage." Nature **526**(7573): 351-360.

263. Nam, Y. S. and T. G. Park (1999). "Porous biodegradable polymeric scaffolds prepared by thermally induced phase separation." J Biomed Mater Res **47**(1): 8-17.
264. Nazarov, R., H. J. Jin and D. L. Kaplan (2004). "Porous 3-D scaffolds from regenerated silk fibroin." Biomacromolecules **5**(3): 718-726.
265. Nemeroff, M. E., S. M. Barabino, Y. Li, W. Keller and R. M. Krug (1998). "Influenza virus NS1 protein interacts with the cellular 30 kDa subunit of CPSF and inhibits 3'end formation of cellular pre-mRNAs." Mol Cell **1**(7): 991-1000.
266. Niu, X., Q. Feng, M. Wang, X. Guo and Q. Zheng (2009). "Porous nano-HA/collagen/PLLA scaffold containing chitosan microspheres for controlled delivery of synthetic peptide derived from BMP-2." J Control Release **134**(2): 111-117.
267. Noah, D. L., K. Y. Twu and R. M. Krug (2003). "Cellular antiviral responses against influenza A virus are countered at the posttranscriptional level by the viral NS1A protein via its binding to a cellular protein required for the 3' end processing of cellular pre-mRNAS." Virology **307**(2): 386-395.
268. Nukavarapu, S. P. and A. R. Amini (2011). "Optimal scaffold design and effective progenitor cell identification for the regeneration of vascularized bone." Conf Proc IEEE Eng Med Biol Soc **2011**: 2464-2467.
269. O'Keefe, R. J. and J. Mao (2011). "Bone tissue engineering and regeneration: from discovery to the clinic--an overview." Tissue Eng Part B Rev **17**(6): 389-392.
270. O'Leary, L. E., J. A. Fallas, E. L. Bakota, M. K. Kang and J. D. Hartgerink (2011). "Multi-hierarchical self-assembly of a collagen mimetic peptide from triple helix to nanofibre and hydrogel." Nat Chem **3**(10): 821-828.
271. Obenauer, J. C., J. Denson, P. K. Mehta, X. Su, S. Mukatira, D. B. Finkelstein, X. Xu, J. Wang, J. Ma, Y. Fan, K. M. Rakestraw, R. G. Webster, E. Hoffmann, S. Krauss, J. Zheng, Z. Zhang and C. W. Naeve (2006). "Large-scale sequence analysis of avian influenza isolates." Science **311**(5767): 1576-1580.
272. Offeddu, G. S., J. C. Ashworth, R. E. Cameron and M. L. Oyen (2015). "Multi-scale mechanical response of freeze-dried collagen scaffolds for tissue engineering applications." J Mech Behav Biomed Mater **42**: 19-25.
273. Olde Damink, L. H. H., P. J. Dijkstra, M. J. A. van Luyn, P. B. van Wachem, P. Nieuwenhuis and J. Feijen (1996). "Cross-linking of dermal sheep collagen using a water-soluble carbodiimide." Biomaterials **17**(8): 765-773.
274. Olszta, M. J., X. Cheng, S. S. Jee, R. Kumar, Y.-Y. Kim, M. J. Kaufman, E. P. Douglas and L. B. Gower (2007). "Bone structure and formation: A new perspective." Materials Science and Engineering: R: Reports **58**(3): 77-116.
275. Ono, I., T. Yamashita, H. Y. Jin, Y. Ito, H. Hamada, Y. Akasaka, M. Nakasu, T. Ogawa and K. Jimbow (2004). "Combination of porous hydroxyapatite and cationic liposomes as a vector for BMP-2 gene therapy." Biomaterials **25**(19): 4709-4718.
276. Opitz, B., A. Rejaibi, B. Dauber, J. Eckhard, M. Vinzing, B. Schmeck, S. Hippenstiel, N. Suttorp and T. Wolff (2007). "IFNbeta induction by influenza A virus is mediated by RIG-I which is regulated by the viral NS1 protein." Cell Microbiol **9**(4): 930-938.
277. Oshiumi, H., M. Matsumoto, S. Hatakeyama and T. Seya (2009). "Riplet/RNF135, a RING finger protein, ubiquitinates RIG-I to promote interferon-beta induction during the early phase of viral infection." J Biol Chem **284**(2): 807-817.
278. Osta, B., G. Benedetti and P. Miossec (2014). "Classical and Paradoxical Effects of TNF-alpha on Bone Homeostasis." Front Immunol **5**: 48.
279. Osyczka, A. M., D. L. Diefenderfer, G. Bhargave and P. S. Leboy (2004). "Different effects of BMP-2 on marrow stromal cells from human and rat bone." Cells Tissues Organs **176**(1-3): 109-119.
280. Pardi, N., M. J. Hogan, F. W. Porter and D. Weissman (2018). "mRNA vaccines - a new era in vaccinology." Nat Rev Drug Discov **17**(4): 261-279.

281. Parekh, S. H., K. Chatterjee, S. Lin-Gibson, N. M. Moore, M. T. Cicerone, M. F. Young and C. G. Simon, Jr. (2011). "Modulus-driven differentiation of marrow stromal cells in 3D scaffolds that is independent of myosin-based cytoskeletal tension." Biomaterials **32**(9): 2256-2264.
282. Pascolo, S. (2008). "Vaccination with messenger RNA (mRNA)." Handb Exp Pharmacol(183): 221-235.
283. Pek, Y. S., A. C. Wan and J. Y. Ying (2010). "The effect of matrix stiffness on mesenchymal stem cell differentiation in a 3D thixotropic gel." Biomaterials **31**(3): 385-391.
284. Peng, J., E. L. Murray and D. R. Schoenberg (2008). "In vivo and in vitro analysis of poly(A) length effects on mRNA translation." Methods Mol Biol **419**: 215-230.
285. Perche, F., T. Benvegnu, M. Berchel, L. Lebegue, C. Pichon, P.-A. Jaffrès and P. Midoux (2011). "Enhancement of dendritic cells transfection in vivo and of vaccination against B16F10 melanoma with mannosylated histidylated lipopolyplexes loaded with tumor antigen messenger RNA." Nanomedicine: Nanotechnology, Biology and Medicine **7**(4): 445-453.
286. Perche, F., T. Benvegnu, M. Berchel, L. Lebegue, C. Pichon, P. A. Jaffres and P. Midoux (2011). "Enhancement of dendritic cells transfection in vivo and of vaccination against B16F10 melanoma with mannosylated histidylated lipopolyplexes loaded with tumor antigen messenger RNA." Nanomedicine **7**(4): 445-453.
287. Perche, F., R. Clemencon, K. Schulze, T. Ebensen, C. A. Guzman and C. Pichon (2019). "Neutral Lipopolyplexes for In Vivo Delivery of Conventional and Replicative RNA Vaccine." Mol Ther Nucleic Acids **17**: 767-775.
288. Petite, H., V. Viateau, W. Bensaid, A. Meunier, C. de Pollak, M. Bourguignon, K. Oudina, L. Sedel and G. Guillemin (2000). "Tissue-engineered bone regeneration." Nat Biotechnol **18**(9): 959-963.
289. Peyton, S. R. and A. J. Putnam (2005). "Extracellular matrix rigidity governs smooth muscle cell motility in a biphasic fashion." J Cell Physiol **204**(1): 198-209.
290. Phua, K. K. L., Y. Liu and S. H. Sim (2017). "Non-linear enhancement of mRNA delivery efficiencies by influenza A derived NS1 protein engendering host gene inhibition property." Biomaterials **133**: 29-36.
291. Pountos, I. and P. V. Giannoudis (2016). "Is there a role of coral bone substitutes in bone repair?" Injury **47**(12): 2606-2613.
292. Presnyak, V., N. Alhusaini, Y. H. Chen, S. Martin, N. Morris, N. Kline, S. Olson, D. Weinberg, K. E. Baker, B. R. Graveley and J. Coller (2015). "Codon optimality is a major determinant of mRNA stability." Cell **160**(6): 1111-1124.
293. Qian, W., X. Wei, K. Guo, Y. Li, X. Lin, Z. Zou, H. Zhou and M. Jin (2017). "The C-Terminal Effector Domain of Non-Structural Protein 1 of Influenza A Virus Blocks IFN-beta Production by Targeting TNF Receptor-Associated Factor 3." Front Immunol **8**: 779.
294. Raftery, R. M., I. Mencia-Castano, S. Sperger, G. Chen, B. Cavanagh, G. A. Feichtinger, H. Redl, A. Hacobian and F. J. O'Brien (2018). "Delivery of the improved BMP-2-Advanced plasmid DNA within a gene-activated scaffold accelerates mesenchymal stem cell osteogenesis and critical size defect repair." J Control Release **283**: 20-31.
295. Rajsbaum, R., R. A. Albrecht, M. K. Wang, N. P. Maharaj, G. A. Versteeg, E. Nistal-Villan, A. Garcia-Sastre and M. U. Gack (2012). "Species-specific inhibition of RIG-I ubiquitination and IFN induction by the influenza A virus NS1 protein." PLoS Pathog **8**(11): e1003059.
296. Riddle, R. C., A. F. Taylor, D. C. Genetos and H. J. Donahue (2006). "MAP kinase and calcium signaling mediate fluid flow-induced human mesenchymal stem cell proliferation." Am J Physiol Cell Physiol **290**(3): C776-784.
297. Ripamonti, U. (1991). "The morphogenesis of bone in replicas of porous hydroxyapatite obtained from conversion of calcium carbonate exoskeletons of coral." J Bone Joint Surg Am **73**(5): 692-703.
298. Ripamonti, U. (1996). "Osteoinduction in porous hydroxyapatite implanted in heterotopic sites of different animal models." Biomaterials **17**(1): 31-35.

299. Rossler, B., J. Kreuter and D. Scherer (1995). "Collagen microparticles: preparation and properties." J Microencapsul **12**(1): 49-57.
300. Ruckle, A., E. Haasbach, I. Julkunen, O. Planz, C. Ehrhardt and S. Ludwig (2012). "The NS1 protein of influenza A virus blocks RIG-I-mediated activation of the noncanonical NF-kappaB pathway and p52/RelB-dependent gene expression in lung epithelial cells." J Virol **86**(18): 10211-10217.
301. Ruijtenberg, S. and S. van den Heuvel (2016). "Coordinating cell proliferation and differentiation: Antagonism between cell cycle regulators and cell type-specific gene expression." Cell Cycle **15**(2): 196-212.
302. Sachs, A. B., R. W. Davis and R. D. Kornberg (1987). "A single domain of yeast poly(A)-binding protein is necessary and sufficient for RNA binding and cell viability." Mol Cell Biol **7**(9): 3268-3276.
303. Sahin, U., K. Kariko and O. Tureci (2014). "mRNA-based therapeutics--developing a new class of drugs." Nat Rev Drug Discov **13**(10): 759-780.
304. Sahin, U., K. Karikó and Ö. Türeci (2014). "mRNA-based therapeutics—developing a new class of drugs." Nature reviews Drug discovery **13**(10): 759.
305. Saito, A., Y. Suzuki, S. Ogata, C. Ohtsuki and M. Tanihara (2003). "Activation of osteo-progenitor cells by a novel synthetic peptide derived from the bone morphogenetic protein-2 knuckle epitope." Biochim Biophys Acta **1651**(1-2): 60-67.
306. Scarborough, R. M., M. A. Naughton, W. Teng, J. W. Rose, D. R. Phillips, L. Nannizzi, A. Arfsten, A. M. Campbell and I. F. Charo (1993). "Design of potent and specific integrin antagonists. Peptide antagonists with high specificity for glycoprotein IIb-IIIa." J Biol Chem **268**(2): 1066-1073.
307. Schlake, T., A. Thess, M. Thran and I. Jordan (2018). "mRNA as novel technology for passive immunotherapy." Cell Mol Life Sci.
308. Schlee, M. and G. Hartmann (2010). "The chase for the RIG-I ligand--recent advances." Mol Ther **18**(7): 1254-1262.
309. Sheller, M. R., R. S. Crowther, J. H. Kinney, J. Yang, S. Di Jorio, T. Breunig, D. H. Carney and J. T. Ryaby (2004). "Repair of rabbit segmental defects with the thrombin peptide, TP508." J Orthop Res **22**(5): 1094-1099.
310. Shen, Z., G. Reznikoff, G. Dranoff and K. L. Rock (1997). "Cloned dendritic cells can present exogenous antigens on both MHC class I and class II molecules." J Immunol **158**(6): 2723-2730.
311. Sheridan, S. D., S. Gil, M. Wilgo and A. Pitt (2008). "Microporous membrane growth substrates for embryonic stem cell culture and differentiation." Methods Cell Biol **86**: 29-57.
312. Shi, S. and S. Gronthos (2003). "Perivascular niche of postnatal mesenchymal stem cells in human bone marrow and dental pulp." J Bone Miner Res **18**(4): 696-704.
313. Shimer, A. L., F. C. Oner and A. R. Vaccaro (2009). "Spinal reconstruction and bone morphogenetic proteins: open questions." Injury **40 Suppl 3**: S32-38.
314. Shin, M., H. Yoshimoto and J. P. Vacanti (2004). "In vivo bone tissue engineering using mesenchymal stem cells on a novel electrospun nanofibrous scaffold." Tissue Eng **10**(1-2): 33-41.
315. Steinmetz, N. J., E. A. Aisenbrey, K. K. Westbrook, H. J. Qi and S. J. Bryant (2015). "Mechanical loading regulates human MSC differentiation in a multi-layer hydrogel for osteochondral tissue engineering." Acta Biomater **21**: 142-153.
316. Stepinski, J., C. Waddell, R. Stolarski, E. Darzynkiewicz and R. E. Rhoads (2001). "Synthesis and properties of mRNAs containing the novel "anti-reverse" cap analogs 7-methyl(3'-O-methyl)GpppG and 7-methyl (3'-deoxy)GpppG." RNA **7**(10): 1486-1495.
317. Stevens, M. M. (2008). "Biomaterials for bone tissue engineering." Materials Today **11**(5): 18-25.
318. Story, B. J., W. R. Wagner, D. M. Gaisser, S. D. Cook and A. M. Rust-Dawicki (1998). "In vivo performance of a modified CSTi dental implant coating." Int J Oral Maxillofac Implants **13**(6): 749-757.

319. Strauss, J. H. and E. G. Strauss (1994). "The alphaviruses: gene expression, replication, and evolution." Microbiol Rev **58**(3): 491-562.
320. Strenkowska, M., J. Kowalska, M. Lukaszewicz, J. Zuberek, W. Su, R. E. Rhoads, E. Darzynkiewicz and J. Jemielity (2010). "Towards mRNA with superior translational activity: synthesis and properties of ARCA tetraphosphates with single phosphorothioate modifications." New J Chem **34**(5): 993-1007.
321. Sultana, N., A. Magadum, Y. Hadas, J. Kondrat, N. Singh, E. Youssef, D. Calderon, E. Chepurko, N. Dubois, R. J. Hajjar and L. Zangi (2017). "Optimizing Cardiac Delivery of Modified mRNA." Mol Ther **25**(6): 1306-1315.
322. Sumanasinghe, R. D., S. H. Bernacki and E. G. Loboa (2006). "Osteogenic differentiation of human mesenchymal stem cells in collagen matrices: effect of uniaxial cyclic tensile strain on bone morphogenetic protein (BMP-2) mRNA expression." Tissue Eng **12**(12): 3459-3465.
323. Suzuki, Y., M. Tanihara, K. Suzuki, A. Saitou, W. Sufan and Y. Nishimura (2000). "Alginate hydrogel linked with synthetic oligopeptide derived from BMP-2 allows ectopic osteoinduction in vivo." J. Biomed. Mater. Res. **50**: 405-409.
324. Svitkin, Y. V., Y. M. Cheng, T. Chakraborty, V. Presnyak, M. John and N. Sonenberg (2017). "N1-methyl-pseudouridine in mRNA enhances translation through eIF2alpha-dependent and independent mechanisms by increasing ribosome density." Nucleic Acids Res **45**(10): 6023-6036.
325. Takahashi, K., K. Tanabe, M. Ohnuki, M. Narita, T. Ichisaka, K. Tomoda and S. Yamanaka (2007). "Induction of pluripotent stem cells from adult human fibroblasts by defined factors." Cell **131**(5): 861-872.
326. Takahashi, K. and S. Yamanaka (2006). "Induction of pluripotent stem cells from mouse embryonic and adult fibroblast cultures by defined factors." Cell **126**(4): 663-676.
327. Takahata, M., E. M. Schwarz, T. Chen, R. J. O'Keefe and H. A. Awad (2012). "Delayed short-course treatment with teriparatide (PTH(1-34)) improves femoral allograft healing by enhancing intramembranous bone formation at the graft-host junction." J Bone Miner Res **27**(1): 26-37.
328. Talon, J., C. M. Horvath, R. Polley, C. F. Basler, T. Muster, P. Palese and A. Garcia-Sastre (2000). "Activation of interferon regulatory factor 3 is inhibited by the influenza A virus NS1 protein." J Virol **74**(17): 7989-7996.
329. Tavernier, G., O. Andries, J. Demeester, N. N. Sanders, S. C. De Smedt and J. Rejman (2011). "mRNA as gene therapeutic: how to control protein expression." J Control Release **150**(3): 238-247.
330. Tawaratsumida, K., V. Phan, E. R. Hrincius, A. A. High, R. Webby, V. Redecke and H. Hacker (2014). "Quantitative proteomic analysis of the influenza A virus nonstructural proteins NS1 and NS2 during natural cell infection identifies PACT as an NS1 target protein and antiviral host factor." J Virol **88**(16): 9038-9048.
331. Teixeira, B. N., P. Aprile, R. H. Mendonça, D. J. Kelly and R. M. d. S. M. Thiré (2019). "Evaluation of bone marrow stem cell response to PLA scaffolds manufactured by 3D printing and coated with polydopamine and type I collagen." Journal of Biomedical Materials Research Part B: Applied Biomaterials **107**(1): 37-49.
332. Teng, S., C. Liu, C. Krettek and M. Jagodzinski (2014). "The application of induced pluripotent stem cells for bone regeneration: current progress and prospects." Tissue Eng Part B Rev **20**(4): 328-339.
333. Termine, J. D. and A. S. Posner (1966). "Infrared analysis of rat bone: age dependency of amorphous and crystalline mineral fractions." Science **153**(3743): 1523-1525.
334. Thess, A., S. Grund, B. L. Mui, M. J. Hope, P. Baumhof, M. Fotin-Mleczek and T. Schlake (2015). "Sequence-engineered mRNA Without Chemical Nucleoside Modifications Enables an Effective Protein Therapy in Large Animals." Mol Ther **23**(9): 1456-1464.
335. Thomas, M., C. Kranjec, K. Nagasaka, G. Matlashewski and L. Banks (2011). "Analysis of the PDZ binding specificities of Influenza A virus NS1 proteins." Virol J **8**: 25.

336. Thua, T. H. L., D. P. Bui, D. T. Nguyen, D. N. Pham, Q. B. Le, P. H. Nguyen, N. V. Tran, P. Q. Le, W. D. Boeckx and A. De Mey (2015). "Autologous Bone Marrow Stem Cells combined with Allograft Cancellous Bone in Treatment of Nonunion." Biomedical Research and Therapy **2**(12).
337. Triana-Alonso, F. J., M. Dabrowski, J. Wadzack and K. H. Nierhaus (1995). "Self-coded 3'-extension of run-off transcripts produces aberrant products during in vitro transcription with T7 RNA polymerase." J Biol Chem **270**(11): 6298-6307.
338. Twu, K. Y., D. L. Noah, P. Rao, R. L. Kuo and R. M. Krug (2006). "The CPSF30 binding site on the NS1A protein of influenza A virus is a potential antiviral target." J Virol **80**(8): 3957-3965.
339. Uchida, S., K. Kataoka and K. Itaka (2015). "Screening of mRNA Chemical Modification to Maximize Protein Expression with Reduced Immunogenicity." Pharmaceutics **7**(3): 137-151.
340. Urist, M. R. and B. S. Strates (2009). "The classic: Bone morphogenetic protein." Clin Orthop Relat Res **467**(12): 3051-3062.
341. Van der Jeught, K., S. De Koker, L. Bialkowski, C. Heirman, P. Tjok Joe, F. Perche, S. Maenhout, S. Bevers, K. Broos, K. Deswarte, V. Malard, H. Hammad, P. Baril, T. Benvegnu, P. A. Jaffres, S. A. A. Kooijmans, R. Schiffelers, S. Lienenklaus, P. Midoux, C. Pichon, K. Breckpot and K. Thielemans (2018). "Dendritic Cell Targeting mRNA Lipopolyplexes Combine Strong Antitumor T-Cell Immunity with Improved Inflammatory Safety." ACS Nano **12**(10): 9815-9829.
342. van der Velden, A. W. and A. A. Thomas (1999). "The role of the 5' untranslated region of an mRNA in translation regulation during development." Int J Biochem Cell Biol **31**(1): 87-106.
343. Vanhaesebroeck, B., K. Ali, A. Bilancio, B. Geering and L. C. Foukas (2005). "Signalling by PI3K isoforms: insights from gene-targeted mice." Trends Biochem Sci **30**(4): 194-204.
344. Visser, R., G. A. Rico-Llanos, H. Pulkkinen and J. Becerra (2016). "Peptides for bone tissue engineering." J Control Release **244**(Pt A): 122-135.
345. Waltregny, D., A. Bellahcene, I. Van Riet, L. W. Fisher, M. Young, P. Fernandez, W. Dewe, J. de Leval and V. Castronovo (1998). "Prognostic value of bone sialoprotein expression in clinically localized human prostate cancer." J Natl Cancer Inst **90**(13): 1000-1008.
346. Wang, H., X. Li, E. Tomin, S. B. Doty, J. M. Lane, D. H. Carney and J. T. Ryaby (2005). "Thrombin peptide (TP508) promotes fracture repair by up-regulating inflammatory mediators, early growth factors, and increasing angiogenesis." J Orthop Res **23**(3): 671-679.
347. Wang, P., F. Perche, D. Logeart-Avramoglou and C. Pichon (2019). "RNA-based therapy for osteogenesis." Int J Pharm **569**: 118594.
348. Wang, V., G. Misra and B. Amsden (2008). "Immobilization of a bone and cartilage stimulating peptide to a synthetic bone graft." J Mater Sci Mater Med **19**(5): 2145-2155.
349. Wang, W., K. Riedel, P. Lynch, C. Y. Chien, G. T. Montelione and R. M. Krug (1999). "RNA binding by the novel helical domain of the influenza virus NS1 protein requires its dimer structure and a small number of specific basic amino acids." RNA **5**(2): 195-205.
350. Wang, X., B. Ding and B. Li (2013). "Biomimetic electrospun nanofibrous structures for tissue engineering." Mater Today (Kidlington) **16**(6): 229-241.
351. Wang, X., M. Li, H. Zheng, T. Muster, P. Palese, A. A. Beg and A. Garcia-Sastre (2000). "Influenza A virus NS1 protein prevents activation of NF-kappaB and induction of alpha/beta interferon." J Virol **74**(24): 11566-11573.
352. Wang, X., M. Li, H. Zheng, T. Muster, P. Palese, A. A. Beg and A. García-Sastre (2000). "Influenza A Virus NS1 Protein Prevents Activation of NF-κB and Induction of Alpha/Beta Interferon." Journal of Virology **74**(24): 11566-11573.
353. Wang, Y. and Z. Wang (2015). "Efficient backsplicing produces translatable circular mRNAs." Rna **21**(2): 172-179.
354. Ward, D. F., Jr., R. M. Salasznyk, R. F. Klees, J. Backiel, P. Agius, K. Bennett, A. Boskey and G. E. Plopper (2007). "Mechanical strain enhances extracellular matrix-induced gene focusing and promotes osteogenic differentiation of human mesenchymal stem cells through an extracellular-related kinase-dependent pathway." Stem Cells Dev **16**(3): 467-480.

355. Warren, L., P. D. Manos, T. Ahfeldt, Y. H. Loh, H. Li, F. Lau, W. Ebina, P. K. Mandal, Z. D. Smith, A. Meissner, G. Q. Daley, A. S. Brack, J. J. Collins, C. Cowan, T. M. Schlaeger and D. J. Rossi (2010). "Highly efficient reprogramming to pluripotency and directed differentiation of human cells with synthetic modified mRNA." Cell Stem Cell **7**(5): 618-630.
356. Weadock, K. S., E. J. Miller, L. D. Bellincampi, J. P. Zawadsky and M. G. Dunn (1995). "Physical crosslinking of collagen fibers: comparison of ultraviolet irradiation and dehydrothermal treatment." J Biomed Mater Res **29**(11): 1373-1379.
357. Wei, C. M., A. Gershowitz and B. Moss (1975). "Methylated nucleotides block 5' terminus of HeLa cell messenger RNA." Cell **4**(4): 379-386.
358. Weissman, D., N. Pardi, H. Muramatsu and K. Kariko (2013). "HPLC purification of in vitro transcribed long RNA." Methods Mol Biol **969**: 43-54.
359. Werme, K., M. Wigerius and M. Johansson (2008). "Tick-borne encephalitis virus NS5 associates with membrane protein scribble and impairs interferon-stimulated JAK-STAT signalling." Cell Microbiol **10**(3): 696-712.
360. Wernike, E., M. O. Montjovent, Y. Liu, D. Wismeijer, E. B. Hunziker, K. A. Siebenrock, W. Hofstetter and F. M. Klenke (2010). "VEGF incorporated into calcium phosphate ceramics promotes vascularisation and bone formation in vivo." Eur Cell Mater **19**: 30-40.
361. Wesselhoeft, R. A., P. S. Kowalski and D. G. Anderson (2018). "Engineering circular RNA for potent and stable translation in eukaryotic cells." Nat Commun **9**(1): 2629.
362. Wesselhoeft, R. A., P. S. Kowalski, F. C. Parker-Hale, Y. Huang, N. Bisaria and D. G. Anderson (2019). "RNA Circularization Diminishes Immunogenicity and Can Extend Translation Duration In Vivo." Mol Cell.
363. White, C. J. (1998). "Cranial implants."
364. Whitesides, G. M., J. P. Mathias and C. T. Seto (1991). "Molecular self-assembly and nanochemistry: a chemical strategy for the synthesis of nanostructures." Science **254**(5036): 1312-1319.
365. Williams, D. F. (2008). "On the mechanisms of biocompatibility." Biomaterials **29**(20): 2941-2953.
366. Wolff, J. A., R. W. Malone, P. Williams, W. Chong, G. Acsadi, A. Jani and P. L. Felgner (1990). "Direct gene transfer into mouse muscle in vivo." Science **247**(4949 Pt 1): 1465-1468.
367. Xing, Z., C. Lu, D. Hu, Y. Y. Yu, X. Wang, C. Colnot, M. Nakamura, Y. Wu, T. Miclau and R. S. Marcucio (2010). "Multiple roles for CCR2 during fracture healing." Dis Model Mech **3**(7-8): 451-458.
368. Yamasaki, H. and H. Sakai (1992). "Osteogenic response to porous hydroxyapatite ceramics under the skin of dogs." Biomaterials **13**(5): 308-312.
369. Yang, E., E. van Nimwegen, M. Zavolan, N. Rajewsky, M. Schroeder, M. Magnasco and J. E. Darnell, Jr. (2003). "Decay rates of human mRNAs: correlation with functional characteristics and sequence attributes." Genome Res **13**(8): 1863-1872.
370. Yannas, I. V., E. Lee, D. P. Orgill, E. M. Skrabut and G. F. Murphy (1989). "Synthesis and characterization of a model extracellular matrix that induces partial regeneration of adult mammalian skin." Proc Natl Acad Sci U S A **86**(3): 933-937.
371. Yasko, A. W., J. M. Lane, E. J. Fellinger, V. Rosen, J. M. Wozney and E. A. Wang (1992). "The healing of segmental bone defects, induced by recombinant human bone morphogenetic protein (rhBMP-2). A radiographic, histological, and biomechanical study in rats." J Bone Joint Surg Am **74**(5): 659-670.
372. Yin, C., J. A. Khan, G. V. Swapna, A. Ertekin, R. M. Krug, L. Tong and G. T. Montelione (2007). "Conserved surface features form the double-stranded RNA binding site of non-structural protein 1 (NS1) from influenza A and B viruses." J Biol Chem **282**(28): 20584-20592.
373. Ying, H., T. Z. Zaks, R.-F. Wang, K. R. Irvine, U. S. Kammula, F. M. Marincola, W. W. Leitner and N. P. Restifo (1999). "Cancer therapy using a self-replicating RNA vaccine." Nature medicine **5**(7): 823.

374. Yoon, J. J., S. H. Song, D. S. Lee and T. G. Park (2004). "Immobilization of cell adhesive RGD peptide onto the surface of highly porous biodegradable polymer scaffolds fabricated by a gas foaming/salt leaching method." Biomaterials **25**(25): 5613-5620.
375. Yoshioka, N., E. Gros, H. R. Li, S. Kumar, D. C. Deacon, C. Maron, A. R. Muotri, N. C. Chi, X. D. Fu, B. D. Yu and S. F. Dowdy (2013). "Efficient generation of human iPSCs by a synthetic self-replicative RNA." Cell Stem Cell **13**(2): 246-254.
376. Yu, H., P. J. Vandevord, W. Gong, B. Wu, Z. Song, H. W. Matthew, P. H. Wooley and S. Y. Yang (2008). "Promotion of osteogenesis in tissue-engineered bone by pre-seeding endothelial progenitor cells-derived endothelial cells." J Orthop Res **26**(8): 1147-1152.
377. Yu, Y., G. Jin, Y. Xue, D. Wang, X. Liu and J. Sun (2017). "Multifunctions of dual Zn/Mg ion co-implanted titanium on osteogenesis, angiogenesis and bacteria inhibition for dental implants." Acta Biomater **49**: 590-603.
378. Yuan, H., H. Fernandes, P. Habibovic, J. de Boer, A. M. Barradas, A. de Ruiter, W. R. Walsh, C. A. van Blitterswijk and J. D. de Bruijn (2010). "Osteoinductive ceramics as a synthetic alternative to autologous bone grafting." Proc Natl Acad Sci U S A **107**(31): 13614-13619.
379. Yuan, H., K. Kurashina, J. D. de Bruijn, Y. Li, K. De Groot and X. Zhang (1999). "A preliminary study on osteoinduction of two kinds of calcium phosphate ceramics." Biomaterials **20**(19): 1799-1806.
380. Yuan, H., K. Kurashina, J. D. de Bruijn, Y. Li, K. de Groot and X. Zhang (1999). "A preliminary study on osteoinduction of two kinds of calcium phosphate ceramics." Biomaterials **20**(19): 1799-1806.
381. Zangi, L., K. O. Lui, A. von Gise, Q. Ma, W. Ebina, L. M. Ptaszek, D. Später, H. Xu, M. Tabebordbar, R. Gorbatov, B. Sena, M. Nahrendorf, D. M. Briscoe, R. A. Li, A. J. Wagers, D. J. Rossi, W. T. Pu and K. R. Chien (2013). "Modified mRNA directs the fate of heart progenitor cells and induces vascular regeneration after myocardial infarction." Nature Biotechnology **31**(10): 898-907.
382. Zhang, D., X. Wu, J. Chen and K. Lin (2018). "The development of collagen based composite scaffolds for bone regeneration." Bioact Mater **3**(1): 129-138.
383. Zhang, H., C. Y. Lin and S. J. Hollister (2009). "The interaction between bone marrow stromal cells and RGD-modified three-dimensional porous polycaprolactone scaffolds." Biomaterials **30**(25): 4063-4069.
384. Zhang, W., R. E. De La Vega, M. J. Coenen, S. A. Muller, C. J. Peniche Silva, M. K. Aneja, C. Plank, M. van Griensven, C. H. Evans and E. R. Balmayor (2018). "An Improved, Chemically Modified RNA Encoding BMP-2 Enhances Osteogenesis In Vitro and In Vivo." Tissue Eng Part A.
385. Zhang, W., C. Zhu, Y. Wu, D. Ye, S. Wang, D. Zou, X. Zhang, D. L. Kaplan and X. Jiang (2014). "VEGF and BMP-2 promote bone regeneration by facilitating bone marrow stem cell homing and differentiation." Eur Cell Mater **27**: 1-11; discussion 11-12.
386. Zhang, Y., C. Chang, D. J. Gehling, A. Hemmati-Brivanlou and R. Derynck (2001). "Regulation of Smad degradation and activity by Smurf2, an E3 ubiquitin ligase." Proc Natl Acad Sci U S A **98**(3): 974-979.
387. Zheng, X. and P. C. Bevilacqua (2004). "Activation of the protein kinase PKR by short double-stranded RNAs with single-stranded tails." RNA **10**(12): 1934-1945.
388. Zohra, F. T., E. H. Chowdhury, S. Tada, T. Hoshiba and T. Akaike (2007). "Effective delivery with enhanced translational activity synergistically accelerates mRNA-based transfection." Biochem Biophys Res Commun **358**(1): 373-378.
389. Zuk, P. A., M. Zhu, P. Ashjian, D. A. De Ugarte, J. I. Huang, H. Mizuno, Z. C. Alfonso, J. K. Fraser, P. Benhaim and M. H. Hedrick (2002). "Human adipose tissue is a source of multipotent stem cells." Mol Biol Cell **13**(12): 4279-4295.

Annex- a published review

International Journal of Pharmaceutics 569 (2019) 118594

Contents lists available at ScienceDirect

International Journal of Pharmaceutics

journal homepage: www.elsevier.com/locate/ijpharm

RNA-based therapy for osteogenesis

Pinpin Wang[a], Federico Perche[a], Delphine Logeart-Avramoglou[b], Chantal Pichon[a,*]

[a] Centre de Biophysique Moléculaire UPR4301 CNRS, Rue Charles Sadron, Orléans Cedex 02, France
[b] Laboratory of Osteoarticular Biology, Bioengineering and Bioimaging, UMR CNRS 7052 INSERM U1271, 10, Avenue de Verdun, 75010 Paris, France

ARTICLE INFO

Keywords:
Osteogenesis
Gene therapy
RNA interference
mRNA
Protein replacement
Osteoporosis

ABSTRACT

Nucleic acid-based therapy has shown great promise in accelerating bone regeneration as well as other diseases. Nucleic acids used in gene therapy mainly are either plasmid DNA (pDNA) or RNAs. Although pDNA therapy has been extensively studied for decades with encouraging preclinical and clinical results, side effects, and low efficiency associated with nuclear trafficking are hard to bypass. Unlike pDNA, RNAs (mRNA, siRNA, miRNA) exert their function in the cytoplasm, thereby being more efficient in hard-to-transfect cells such as primary osteoblasts. RNA interference-based gene silencing represents a negative regulation which knockdown the expression of antagonists that impair osteogenesis process. In contrary, mRNA therapy for osteogenesis represents a positive regulation which delivers mRNA encoding growth factors to accelerate bone regeneration. This review presents a comprehensive summary of the mRNA and siRNA-based therapies and the targets for bone regeneration in case of bone defect and osteoporosis.

1. Introduction

Bone tissue has a self-healing capacity which is overwhelmed during traumatic events and bone pathologies. A constant homeostatic balance between bone formation by osteoblasts and bone resorption by osteoclasts is essential for bone tissue to restore fatigue microdamage and maintain bone mass and structure (Rodan and Martin, 2000). However, imbalances are associated with pathological or traumatic events. For instance, during some pathologies such as osteoporosis and osteonecrosis, osteoclasts are more active compared to osteoblasts resulting in low bone mass, poor bone strength, and micro-architectural deterioration of bone tissue (Roush, 2011; Genant et al., 1999). This imbalance increases the risk of bone fracture and subsequently delays bone healing, even leading to nonunion fractures (5–10% of cases) (Egermann et al., 2005). The occurrence of critical-sized defects following, for instance, either traumas or resection of osteosarcomas are additional challenges to the self-healing capacity of bone (Dimitriou et al., 2005).

Osteoporosis- and bone fractures are becoming a major health and economic burden with a progressively aging population. In the European Union, the estimated osteoporotic population was 27.5 million (22 million women and 5.5 million men) in 2010. The cost of osteoporosis-related incidents and fractures was estimated at 37 billion Euro in 2010, which is predicted to increase by 25% in 2025 (Svedbom et al., 2013).

Clinically, to reverse the loss of bone mass, there are two major pharmacological approaches based on either: 1) anabolic agents such as parathyroid hormone (PTH) to stimulate bone formation; or 2) anti-resorptive agents such as bisphosphonate, estrogens, and selective estrogen receptor modulators to prevent bone resorption (NIH Consensus Development Panel on Osteoporosis Prevention, Diagnosis, and Therapy, 2001). However, long-term administration of anabolic agents or antiresorptive agents is accompanied by adverse effects. For example, bisphosphonate-based therapy has been associated with jaw osteonecrosis and atypical fractures in long bone (Schilcher et al., 2011; Hollick and Reid, 2011). To restore bone defects, although the success rate has been significantly improved with the development of sophisticated surgical procedures, e.g. Ilizarov apparatus (Robert Rozbruch et al., 2006), Masquelet technique (Giannoudis et al., 2011), autografts still represent the gold standard treatment to treat massive bone loss (Goldberg and Stevenson, 1987; Giannoudis et al., 2011).

This last decade, it is admitted that there is a need to identify novel therapeutic strategies to enhance bone formation without side effects. Romosozumab, a monoclonal antibody targeting sclerostin, was developed as an anabolic and antiresorption drug to treat osteoporosis (Padhi et al., 2011; McClung et al., 2014; Cosman et al., 2016). Sclerostin is a negative regulator of bone formation by inhibiting Wnt/β-catenin pathway and a positive regulator of bone resorption by activating RANK/RANKL pathway (Suen and Qin, 2016). However, despite promising results in a recently finished phase three trial, some serious

* Corresponding author.
E-mail address: pichon@cnrs.fr (C. Pichon).

https://doi.org/10.1016/j.ijpharm.2019.118594
Received 30 April 2019; Received in revised form 2 August 2019; Accepted 3 August 2019
Available online 05 August 2019
0378-5173/

adverse events have been reported, such as hyperostosis and cardiovascular events (Cosman et al., 2016).

To repair bone defect, bone tissue engineering represents an attractive therapeutic alternative to bone grafts. Conventional bone tissue engineering constructs containing a biocompatible scaffold combined with osteogenic cells and/or recombinant osteogenic proteins are increasingly being used as bone graft substitutes (Amini et al., 2012). Although promising results showed bone reparation in clinical studies, many crucial hurdles remain such as side effects related to the supraphysiological dose of implanted osteogenic proteins (Shimer et al., 2009).

Gene therapy was proposed for bone regeneration many years ago. The goal of this approach is to either sustain or modulate the expression of therapeutic proteins. In vivo and ex vivo strategies have been performed mainly using viral vectors. The pDNA-based gene therapy for osteogenesis will not be covered in the present review, as it has been the focus of recent excellent published reviews (Evans and Huard, 2015; Im, 2013).

Combining RNAs, complexed within vectors, in scaffolds in the presence or absence of osteogenic cells is among the most advanced gene therapy solutions for bone healing. The scaffolds can be loaded with either messenger RNA (mRNA) encoding osteogenic factors, mimics of endogenous microRNA (miRNA), or siRNA to deplete negative regulators of bone formation (Elangovan et al., 2015; Khorsand et al., 2017a; Takayama et al., 2009a,b). In addition to local release from the scaffold, RNAs can be routed to the bone damaged area using a targeted delivery system (Zhang et al., 2015a,b; Sun et al., 2016). In this review, we will discuss the progress of mRNA and siRNA-based gene therapy for the treatment of either bone defects or loss bone mass. But to appreciate the goals of the various strategies, it is needed to give insights on how the bone homeostasis is maintained and what types of molecules are involved during bone regeneration.

2. Signaling pathways involved in bone homeostasis

Osteoblasts and osteoclasts are the two major cells involved in bone remodeling or bone defect-healing process. Their recruitment, proliferation, differentiation, activity and survival are tightly regulated by dozens of autocrine and paracrine factors through multiple signaling pathways such as Bone Morphogenetic Proteins (BMPs)/runt-related transcription factor 2 (Runx2) (Hankenson et al., 2015; Phimphilai et al., 2006), Wnt/β-catenin (Fischer et al., 2002; Rawadi et al., 2003), and receptor activator of nucleic factor-κB (RANK)/RANK ligand (RANKL) pathways (Wada et al., 2006; Zhuang et al., 2018) [Fig. 1].

Bone formation is generated by osteoblasts that promote bone matrix deposition and mineralization. Osteoblasts originate from mesenchymal stem cells (MSCs) that commit and differentiate under the control of various stimuli that influence osteogenesis. One of the key molecular switches in the commitment of mesenchymal progenitors to osteoblast lineage is the transcription factor cbfa/runx2, which has multiple upstream regulators and a wide variety of targets (Rutkovskiy et al., 2016). The Wnt and BMP signaling pathways are the major regulatory pathways involved in the regulation of Runx2. BMPs are cytokine members of the TGF-β family that are especially important for postnatal ossification (Hankenson et al., 2015). BMP signaling is initiated by the ligand binding to type I and type II BMP receptors which are serine/threonine kinase receptors complexing into transmembrane heterodimer. Upon binding of BMPs to their receptors, the activated receptors initiate two intracellular transduction pathways: the canonical Smad pathway and non-canonical mitogen-activated protein kinase (MAPK) pathway. In the canonical pathway, activated receptor recruit and phosphorylate Smad 1/5/8, which are translocated to the nucleus associated with Smad 4. The Smads complex together with Runx2 activates the expression of downstream osteogenic genes such as alkaline phosphatase (ALP), osteocalcin (OCN), osteopontin (OPN) (Chen et al., 2012b). The MAPK pathway is Smad independent and includes the activation of extracellular signal-regulated kinase 1/2 (ERK1/2), p38, and c-Jun NH2-terminal kinase (JNK1/2) resulting in Runx2 expression upregulation (Huang et al., 2014).

The BMP/Smad signaling cascade is tightly regulated by both intracellular (such as Smurf proteins) and extracellular processes. A family of secreted antagonists that negatively regulated the BMP/Smad signaling pathway includes Noggin (Smith and Harland, 1992), Gremlin (Hsu et al., 1998; Pearce et al., 1999), Chordin (Piccolo et al., 1996), crossveinless, USAG-1 and follistatin. Coexpressed with BMP-2, -4, and -7, the Noggin, Gremlin, and Chordin antagonists play key roles during development and skeletogenesis (Zimmerman et al., 1996; Merino et al., 1999; Scott et al., 2000; Fisher and Halpern, 1999). After secretion, these antagonists physically sequester BMPs, preventing ligand-receptor interactions.

Wnt/β-catenin signaling is another well-defined signaling pathway that promotes osteoblastic differentiation and activity. Wnt proteins constitute a family of secreted cysteine-rich glycosylated proteins. Activation of Wnt/β-catenin signaling pathway initiates from binding of the Wnt ligands with the complex of the 7-transmembrane domain spanning frizzled receptor and low-density lipoprotein receptor-related protein 5 and 6 (LRP5/6) coreceptors. Activation of the Wnt receptor complex triggers displacement of the multifunctional kinase GSK-3β from a regulatory APC/Axin/GSK-3β-complex, resulting in β-catenin stabilization and accumulation. The β-catenin translocates to the nucleus regulating osteogenic genes expression (Krishnan et al., 2006). Wnt signaling also reduces apoptosis of osteoblasts and osteocytes through mechanisms involvement of β-catenin and activation of PI3K/Akt (You et al., 2002; Longo et al., 2002).

Several antagonists are involved in Wnt/β-catenin signaling regulation. Among them, Dickkopf families (DKK1/2/4) bind to LRP5/6 complex leading to the LRP internalization and degradation (Mao et al., 2002). Also, the interaction of Wnts and frizzled receptors is inhibited by frizzled-related protein family (sFRP1/2/3) which sequester Wnts (Krishnan et al., 2006).

Bone resorption is mediated by osteoclasts, which are giant multinucleated cells derived from monocytes/macrophages. Osteoclasts resorb the bone tissue by dissolution of the inorganic phase through acidification of the isolated extracellular microenvironment followed by secretion of proteolytic enzymes. The osteoclast differentiation is locally regulated by RANK/RANKL signaling under the presence of macrophage colony-stimulating factor (M-SCF) (Wada et al., 2006). RANKL, a TNF-family molecule, either expressed on the surface of osteoblastic lineages or secreted from stromal or immune cells, interacts with RANK receptor in osteoclastic lineages. The RANK signaling transduction pathway is regulated by the adaptor proteins of TNF receptor-associated factor 1, 2, 3, 5 and 6 (TRAF 1, 2, 3, 5, 6) within which TRAD 6 is critical for RANK signaling (Koide et al., 2010). The TRAFs binds to RANK and transmits the RANK signal to downstream targets including nuclear factor-kappa B (NF-κB) pathway and MAPK pathway resulting in osteoclastic differentiation of macrophages cells, activation of bone resorption, and survival of osteoclasts. For example, ERKs and JNKs stimulate transcription factor Activating Protein-1, a dimer composed of c-Fos and c-Jun protein, together with activated NF-κB regulate the expression of nuclear factor of activated T cells c1 (NFATc1, also called NFAT2) leading to enhanced expression of osteoclastogenic genes. Proto-oncogene tyrosine-protein kinase Src (c-SRC) mediates RANK induced activation of the phosphatidylinositol 3-kinase (PI3K)/Akt signaling through binding to TRAF6 for anti-apoptosis (Nakashima et al., 2000). Osteoblasts also secrete a RANKL decoy receptor-osteoprotegerin (OPG) that competitively binds RANKL and, thus, inhibits osteoclast differentiation and survival (Hofbauer and Heufelder, 2001; Maxhimer et al., 2015).

RANKL induced-osteoclastogenesis stimulates semaphorin 4d (sema4d) expression from osteoclasts, which, in turn, regulates osteoblasts activity (Negishi-Koga et al., 2011). Sema4d is originally expressed as a transmembrane protein, then proteolytically cleaved into a

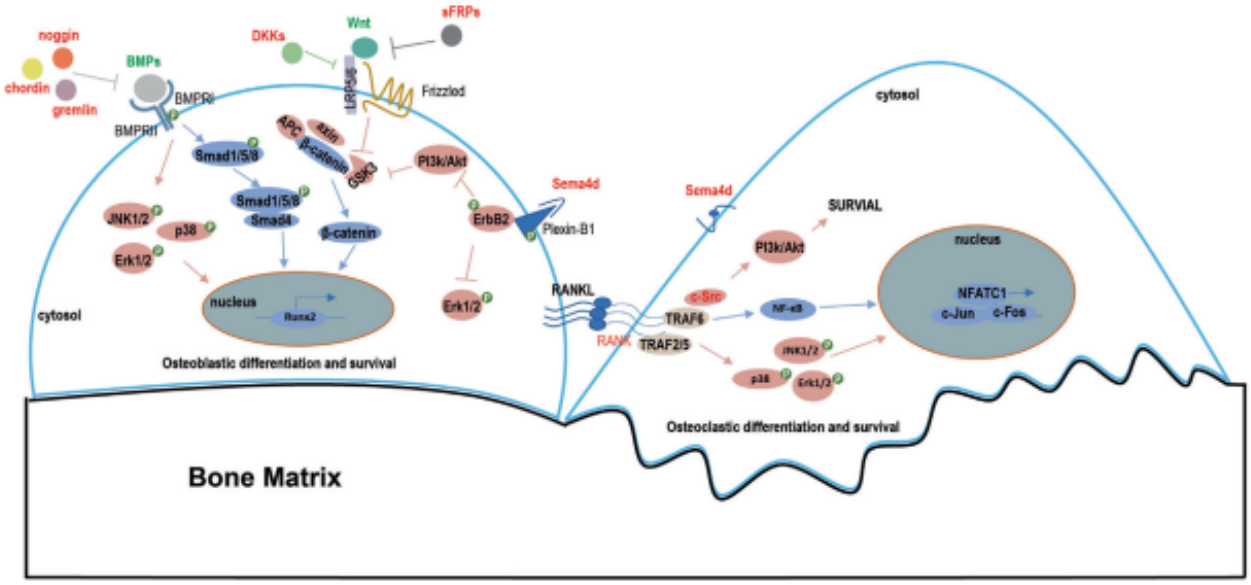

Fig. 1. Selective signaling pathways involved in bone homeostasis. During osteogenesis, BMPs and Wnts induce MSCs to differentiate into osteoblasts, which can be inhibited by extracellular antagonists such as noggin, chordin, gremlin, DKKs, and sFRPs. In the aspect of osteoclastogenesis, hematopoietic cells differentiate into osteoclasts under RANKL stimulation. The osteogenesis and osteoclastogenesis are mutually modulated. Osteoblastic lineages secreted RANKL increases osteoclastic generation and activity. The Sema4d expressed from osteoclasts inhibits osteoblasts activity. On the other hand, osteoclasts digest bone matrix resulting in osteogenic factors release.

soluble form (Suzuki et al., 2008). Binding of Sema4d to Plexin-B1, the Sema4d transmembrane receptor in osteoblast, inhibits Akt and Erk phosphorylation resulting in reduction of osteoblast mediated bone-formation.

The unraveling of the signaling pathways and identification of the regulators involved in bone formation and resorption enable to rationally design targeting therapeutics.

3. RNAi-based therapeutics for osteogenesis

Compared with conventional pharmacological inhibitors, siRNA offer several advantages such as high specificity and facile synthesis (Ozcan et al., 2015). siRNA can be designed to target a specific gene which is particularly useful to alter signaling pathways (Miller et al., 2003), even proteins inaccessible to conventional drugs (Filleur et al., 2003; Dorn et al., 2004).

In the following section, we focus on the therapeutic approach using siRNA mediated gene silencing to accelerate osteogenesis

3.1. siRNA mechanism of action

The RNA interference (RNAi) is a conserved mechanism regulating endogenous gene expression and defending against intracellular pathogens such as viruses (Agrawal et al., 2003). The term of RNAi was coined after the discovery that the injected dsRNA lead to specific silencing of genes highly homologous in sequence to the injected dsRNA in Caenorhabditis elegans (Fire, 1999). Soon after, Elbashir and colleagues revealed RNAi in mammalian cells (Elbashir et al., 2001a).

miRNAs are conserved small non-coding dsRNAs transcribed by genomes that exert RNAi functions through silencing the target mRNAs (Hannon, 2002). siRNAs are synthetic dsRNAs designed to silence a specific gene, which has 21–23 nucleotides with 3′ 2-nucleotides overhangs and 5′ phosphate groups (Elbashir et al., 2001b). The siRNAs can be exogenously introduced into cells in a final short form or long dsRNA form which cleaved by Dicer, an RNase III-like enzyme, in the cytoplasm to generate functional siRNAs. Interacting with AGO2-RISC enzyme complex, the sense strand of the siRNA is cleaved, and the anti-sense remains associated with the complex. The anti-sense guides the RISC complex binds to the targeting mRNA with full complementarity which then cleaved by AGO2. Fig. 2 exhibits the gene silencing process mediated by siRNA.

3.2. Silencing BMPs antagonists

a) noggin siRNA

Among the BMP antagonists, noggin is identified to be the most closely involved in the osteoinductive process of BMPs (Smith and Harland, 1992; Abe et al., 2000). Several studies demonstrated that increase noggin expression significantly impairs bone formation both *in vitro* and *in vivo* (Devlin et al., 2003; Xiao et al., 2002; Wu et al., 2003). These studies reinforce the crucial role of noggin as a negative regulator of bone formation. Wan and colleagues were the pioneers of this strategy. Retroviral particles encoding noggin siRNA were used for *in vitro* and *in vivo* experiments (Wan et al., 2007a,b). In vitro introduction of noggin siRNAs into MC3T3-E1 resulted in approximately 90% noggin transcripts reduction. Noggin elimination increased the Smad1/5 phosphorylation inducing BMP signaling, which promotes calcium deposition. In vivo strategy was based on primary calvarial osteoblasts transduced with noggin siRNA soaked into apatite-coated polylactic-co-glycolic acid scaffolds before implantation into a mice calvarial defect. After two weeks, the group of mice implanted with noggin down expressing cells demonstrated around 6-fold more bone content than the vehicle control group. Reducing noggin level enhances both intracellular and extracellular activities of BMPs, which is of benefit compared to BMPs administration requiring supraphysiological doses, always associates with some side effects (Shimer et al., 2009). Indeed, noggin expression was upregulated when recombinant BMP-2 was used to stimulate murine C2C12 myoblasts and mesenchymal stem cells (MSC), which in turn inhibits the osteogenic function of BMP-2 (Takayama et al., 2009a,b; Chen et al., 2012a). Studies from Takaoka's group demonstrated that noggin siRNA delivery abrogated rhBMP-2 induced noggin expression, resulting in accelerated osteoblastic differentiation of C2C12 cells *in vitro* and ectopic bone formation *in vivo* compared to rhBMP2 alone (Takayama et al., 2009a,b; Manaka et al., 2011a,b). Manaka and colleagues used a biodegradable hydrogel made from poly-D, L-lactic acid-*p*-dioxanone-polyethylene glycol block copolymer (PLA-DX-PEG) for *in vivo* noggin siRNA delivery. Implantation of

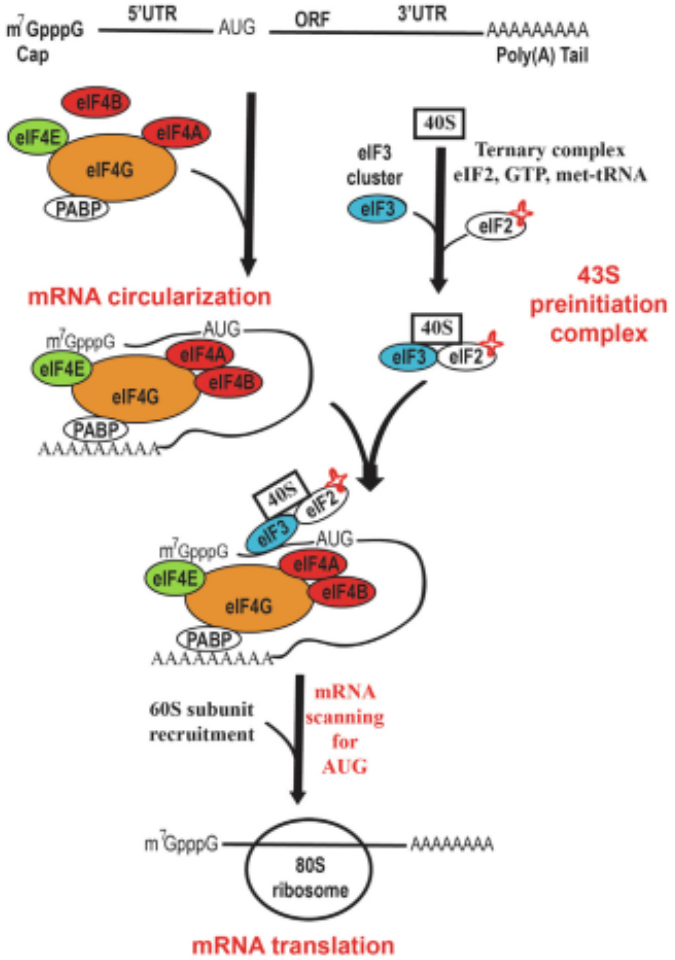

Fig. 2. Schematic mechanism of siRNA mediated RNA interference in mammalian cells. In cytoplasm, the Dicer enzyme cleaves long double-stranded RNA (dsRNA) to form active siRNA. The siRNA interacts with Argonaute 2 (AGO2) and the RNAi-induced silencing complex (RISC) leading to cleavage of the sense strand by AGO2. The target mRNA with complementary sequence to the antisense strand is recognized and cleaved. Reproduced from (de Fougerolles et al., 2007a,b) with permission.

PLA-DX-PEG hydrogel containing noggin siRNA and rhBMP2 into a mice dorsal muscle pouch successfully inhibited rhBMP2 induced noggin expression compared to hydrogel blend with rhBMP2 and control siRNA. The suppression effect lasts for up to 7 days with the peak occurring at day 2 (Manaka et al., 2011a,b).

The function of noggin silencing to benefit bone regeneration was improved when high efficient vector to deliver noggin siRNA was used (Choi et al., 2015; Inada et al., 2018). As an example, Cui and colleagues developed a sterosome vector composed of stearylamine (SA) and cholesterol (Chol) for delivering noggin siRNA to enhance the osteogenic differentiation of AMSCs (Cui et al., 2015). The freshly prepared SA/Chol/siRNA nanoparticles (NPs) exhibited high transfection efficiency (93%) comparable to commercial vector lipofectamine 2000® (96%). The value decreased to approximately 60% after incubating at 37℃ for two weeks, while it was highly reduced to 0.2 ± 0.1% for lipofectamine 2000® demonstrating that SA/Chol/siRNA NPs had excellent colloidal stability. Cells transfected with SA/Chol/noggin siRNA showed more than 45% noggin expression reduction significantly higher than that obtained using lipofectamine 2000® (~25%). In a mouse calvarial defect model, methacrylated glycol chitosan (MeGC) hydrogel, encapsulating AMSCs transfected with SA/Chol/noggin siRNA particles, was implanted into the defect site. Defects treated with SA/Chol/noggin siRNA were filled with ~20% regenerated bone tissue, which were ~15% and ~5% for groups using lipofectamine 2000/siRNA and control siRNA, respectively. This example points out the discrepancy that could be obtained between the *in vitro* and *in vivo* efficiency.

b) Chordin and gremlin siRNAs

Silencing chordin and gremlin could as well lead to enhanced osteogenesis *in vitro* and *in vivo*. The study from Kwong et al. firstly demonstrated that delivery of siRNA against chordin accelerates BMSCs osteogenic differentiation (Kwong et al., 2008). Comparing the expression of noggin, gremlin, chordin in bone marrow stem cells (BMSCs) isolated from patients with normal fracture healing and those with bone nonunion (BMSCs/N), Wang et al. found that chordin expression was the most upregulated (Wang et al., 2018a,b). Silencing chordin in BMSCs/N yielded more expression of osteogenic markers than gremlin and noggin silencing. Based on these observations, the authors defined chordin as the ideal target for inducing BMSc/N osteogenic differentiation. Several vehicles, i.e. polyspermine imidazole-4,5-imine (PSI), Polyethyleneimine of various size (800 and 25 kDa) and spermine, were tested to optimize chordin siRNA delivery. Results of *in vitro* osteogenic differentiation and *in vivo* bone regeneration demonstrated that PSI was the most potent vector followed by PEI 25KDa.

Interestingly, transfecting ST-2 stromal cells with gremlin siRNA using siLentFect® significantly enhanced the stimulatory effect of BMP-2 on alkaline phosphatase expression at all BMP-2 doses (0–10 nM) tested (Gazzerro et al., 2007). Such enhancement relied on increased Smad1/5/8 phosphorylation. Moreover, gremlin silencing enhanced Wnt3a signaling as well. A recent study showed gremlin knockdown by lipofectamine 2000®/gremlin-siRNA enhanced human MSCs osteogenic differentiation (Hu et al., 2017a). To date, no *in vivo* published studies using gremlin siRNA for bone formation.

3.3. Silencing osteoclasts stimulants and osteoblasts inhibitors

During osteoporosis, overactivation of osteoclasts results in the decreased bone mass and high-risk bone fracture that dramatically influence the quality of life. Osteoblast-osteoclast communication is mediated by several pairs of ligands and receptors, which are potential therapeutical targets to modulate bone regeneration. RANK/RANKL is known to be a critical signaling initiating osteoclast formation and activity. Silencing RANK gene with RANK siRNA successfully inhibited osteoclast differentiation of RAW264.7, a murine-macrophage osteoclast precursor cell line, *in vitro* (Wang and Grainger, 2010; Wang et al., 2012; Ma et al., 2014; Sezlev Bilecen et al., 2019). Transfecting RAW cells with DharmaFECT4/RANK-siRNA complexes, Wang and colleagues as pioneers, suppressed osteoclastic RAW cells as well as primary osteoclast precursors differentiation from mouse bone marrow cells. Two transfection strategies were tested for RANK silencing, which was one single transfection, and three successive transfections performed every other day. Both showed significant reduction of RANK expression and osteoclast formation, especially upon multiple transfections. In the study, osteoclast-mediated bone resorption was measured by seeding cells onto bovine bone slices. Results showed that the resorption pit numbers on bone slices were makedly curtailed in the RANK-siRNA treated groups.

Proto-oncogene tyrosine-protein kinase Src (c-Src) is a factor downstream RANK signaling controls bone metabolism by maintaining osteoclast function (Boyce et al., 1992; Lowe et al., 1993). c-Src knockdown mice showed increased bone formation leading to osteopetrosis (Frattini et al., 2000). Zhang et al. injected jetPEI®/Src-siRNA complexes into the proximal femur in a corticosteroid-induced osteoporosis rabbit model (Zheng et al., 2016). Src siRNA administration reduced Src mRNA level to ~50% in bone marrow cells of treated rabbits. Micro-computed tomography (μCT) analysis revealed that Src siRNA prevented bone loss in metaphyseal trabecular and maintained the bone mineral density similar to normal rabbit, whereas non-Src

Table 1
Summary of representative studies based on siRNA for *in vivo* osteogenesis.

Antagonist	Target	Vector	In vivo delivery	In vivo model	Ref.
Local delivery					
Chordin	BMP2	PSI; PEI800; PEI25KDa; spermine	Matrigel/transfected hBMSCs	Mouse tibial monocortical defect	Wang et al. (2018a,b)
		PEI-Et; PEI800; PEI25KDa	Matrigel/transfected hBMSCs	Mouse tibial monocortical defect	Wang et al. (2017a,b)
Noggin		retrovirus	Apatite coated PLGA scaffold/calvarial osteoblasts	Mouse Calvaria defect	Wan et al. (2007a,b)
		Lipofectamine 2000®	dorsal muscle injection followed by electroporation	Mouse ectopic bone formation-dorsal muscle	Takayama et al. (2009a,b)
		Naked siRNA	Paraspinal muscle injection followed by electroporation	Rabbit posterolateral spinal fusion	de Fougerolles et al. (2007a,b)
		Naked siRNA	PLA-DX-PEG hydrogel/siRNA	Mouse ectopic bone formation-dorsal muscle	Manaka et al. (2011a,b)
		Stereosomes	methacrylated glycol chitosan hydrogel/siRNA	Mouse Calvaria defect	Cui et al. (2015)
		PEI	PEG hydrogel/siRNA	rat calvarial defect	Nguyen et al. (2018)
		mPEG-bPEI-PAsp(DIP-BzA)	Fibrin hydrogel/transfected MC3T3-E1 cells	mouse calvarial defect	Huang et al. (2018a,b)
GNAS1	Runx2	ND98	PLGA fibrous membrane/siRNA/hADSCs	Mouse calvaria defect	Shin et al. (2016a,b)
		Ambion siPort®	Silk fibroin-chitosan scaffold/siRNA	Sheep ectopic bone formation-latissimus dorsi muscle	Rios et al. (2012)
Sema4d	Osteoclast-osteoblast communication	Asp8-Stearyl-R8	PLLA scaffold/siRNA	3 mm femoral cylindrical defects in ovariectomized rat	Zhang et al. (2016)
Src	Osteoclast-osteoblast communication	jetPEI®	intramedullary injected into proximal femur	corticosteroid-associated osteoporotic rabbit	Zhang et al. (2016)
Systemic delivery					
Sema4d	Osteoclast-osteoblast communication	Asp8-Stearyl-R8	IV	ovariectomized osteoporotic mouse	Zhang et al. (2015a,b)

PEI, polyethyleneimine; PSI, polyspermine imidazole-4,5-imine; PEI-Et, ethylene bis linked low-molecular-weight polyethyleneimine; GNAS1, guanine nucleotide-binding protein alpha-stimulating activity polypeptide 1; mPEG-bPEI-PAsp(DIP-BzA), monomethoxy-poly(ethylene glycol)-*b*-branched polyethyleneimine-*b*-poly[N-(N',N'-diisopropylaminoethyl)-co-benzylamino)aspartamide]; PLA-DX-PEG, poly-D, L-lactic acid-*p*-dioxanone-polyethylene glycol block co-polymer; ND98, five-tailed isomer of triethylenetetramine-laurylaminopropionate with a free internal amine, Cholesterol, and mPEG2000-C14 Glyceride; PLLA, poly-L-lactic acid; Asp8-Stearyl-R8, D-aspartic acid Octapeptide grafted Stearylated octaarginine; IV, intravenous; Sema4d, semaphorin 4d.

targeting siRNA groups and vehicle control group showed remarkably lower bone mineral densities.

Semaphorin 4d (Sema4d) is a recently uncovered molecule involved in osteoclast-osteoblast communication (Negishi-Koga et al., 2011). Sema4d secreted from osteoclasts reduced the osteoblastic differentiation of cocultured BMSCs, which was reversed by knockdown Sema4d in osteoclasts by Sema4d siRNA (Zhang et al., 2015a,b). The negative regulation property to osteoblast activity makes Sema4d a targeting candidate to increase osteogenesis. Intravenously delivery of Sema4d siRNA complexed with a bone targeting polymer, N-(2-hydroxypropyl) methacrylamide (HPMA) copolymers with D-aspartic acid octapeptide (D-Asp8), to murine osteopenia model resulted in improved bone mineral density, bone volume, and trabecular thickness (Zhang et al., 2015a,b). The Sema4d siRNA particles also worked to reverse periodontal disease induced alveolar bone loss (Zhang et al., 2014). A summary of studies using siRNA for in vivo bone regeneration is shown in Table 1.

3.4. Challenges and perspectives

siRNA-based therapeutics hold great promises as they can virtually silencing any genes, which may be inaccessible with conventional small molecules or protein drugs. In August 2018, FDA approved the first ever siRNA against transthyretin mRNA (Patisiran) responsible of hATTR (hereditary transthyretin-mediated amyloidosis), a life-threatening neurodegenerative rare inherited disease opens a real new type of pharmaceutics (Adams et al., 2017). Today, many advances in design of siRNA have permitted this landmark achievement. The first challenge is to design a rational siRNA sequence with high silencing efficiency, without off-target effects and immunogenicity. The off-target occurs when the siRNA has partial complementarity in the seed region with unintended genes. Moreover, siRNAs complementary to different regions of the target mRNA could result in diverse silencing efficiency. Today, there are siRNA design algorithms that can help to predict the silencing efficacy and reduced off-target effect (Chaudhary et al., 2011; Naito and Ui-Tei, 2013). siRNA is also known to active innate immune system in mammals (Sorensen et al., 2003). It results in the induction of interferon (IFN) and pro-inflammatory cytokines production. Duplexes of siRNA trigger PKR and TLR3/7/8, which can be reduced by chemical modifications, e.g., ribose 2′-OH group modification, locked and unlocked nucleic acids modification, and backbone phosphorothioate modification (Lam et al., 2015). Compare to the latter two, ribose 2′-OH group modification is the most popular and efficient way. Substitute 2′-OH of uridine with 2′-O-Me (2′-O-methyl) or 2′-F (2′-fluoro) was able to abrogate immune responses by blocking the recognition form TLRs (Cekaite et al., 2007). Locked and unlocked nucleic acids modification containing nucleic acid with a methylene bridge between the 2′-O and 4′-O of the ribose sugar (Veedu and Wengel, 2010), or nucleic acid lacking the C2′ and C3′-bond of the ribose ring (Laursen et al., 2010). Phosphorothioate modification is replacing one of the nonbridging phosphate oxygen atoms with a sulfur atom (Campbell et al., 1990). Despite less immune activation, the two modification mainly response to stabilize the RNA duplexes against nuclease.

The second challenge is the delivery of siRNA to the target sites efficiently and safely. siRNAs share the same types of non viral delivery systems with other nucleic acids, which are polymer-based vectors, lipid-based vectors, and inorganic vectors. Despite the progress made in improved transfection efficiency and reduced toxicity, delivering therapeutic siRNA for osteogenesis meets unique barrier. For optimal therapeutical effects, bone targeting vectors are needed. To date, three types of ligand moieties showed bone targeting ability, which are bisphosphonates, oligopeptides, and aptamers (oligonucleotides). $(Asp)_8$ (eight repeating sequences of aspartate) and $(AspSerSer)_6$ (six repetitive sequences of aspartate, serine and serine) are two representative targeting oligopeptides that showed high affinity to crystallized hydroxyapatite in bone-resorption surface, and lowly crystallized

hydroxyapatite as well as amorphous calcium phosphate in bone-formation surface, respectively (Zhang et al., 2012). Bisphosphonates, such as alendronate, could target both bone-formation and bone-resorption surface (Zhang et al., 2014). CH6 is a recently revealed aptamer targeting osteoblasts at cellular level, which is more efficient than $(AspSerSer)_6$ mediated bone target (Liang et al., 2015). Bone-specific delivery systems were obtained by conjugating those moieties to RNAs trapping vectors. More comprehensive discussion about siRNA delivery by bone targeting system could be found in a recently published review (Liu, 2016). Covalent Tetracyclines (TCs) conjugated poly (lactic-co-glycolic acid) (PLGA) copolymer (TC-PLGA) could be another bone targeting delivery system (Wang et al., 2015). TC is an antibiotic agent that has been found to be taken up by bone via its interaction with hydroxyapatite $Ca_{10}(PO_4)_6(OH)_2$ (Perrin, 1965). PLGA is an FDA approved biodegradable polymer that is wildly used to deliver therapeutic molecules including nucleic acids (Wang et al., 2012). In an ovariectomized osteoporosis rat model, TC-PLGA nanoparticles tend to accumulate in bone compared to PLGA alone (Wang et al., 2015). When loaded with simvastatin, TC-PLGA particles were more potent to enhance bone mineral density over PLGA. It could be worthwhile to exploit a similar strategy for siRNA delivery.

4. mRNA-based therapeutic for osteogenesis

4.1. Eukaryotic mRNA and in vitro transcription

mRNAs are the intermediate between the genetic information stored in DNA and proteins. DNA is first transcribed into mRNA in the nucleus, which thenexported and translated into proteins by the ribosomes in the cytoplasm. All mature eukaryotic mRNA consists of five moieties, which are the 5′ methylated guanosine cap (m^7Gp3N), the 5′ and 3′ untranslated region (5′-UTR and 3′-UTR), the open reading frame (ORF), and the 50–250 adenosine residues (poly(A) tail) (Jackson, 1993; Banerjee, 1980) (Fig. 3). ORF stores protein information in the codon sequence while the rest moieties responsible for the regulation of mRNA translocation, translation, and stability. Understanding the mechanisms behind mRNA translation and stability regulation has been useful to guide the design of *in vitro* transcribed (IVT) mRNA and increase the efficacy of mRNA therapy.

The 5′ m^7G cap is an evolutionarily conserved modification of eukaryotic mRNA with a N^7 methylated guanosine covalent to the first nucleotide of the pre-mRNA *via* a reversed 5′–5′ triphosphate linkage. Additional to N^7 methylation in 5′ m7G cap (m7GpppN, Cap 0), in higher eukaryotes, methylation also occurs at the 2′-O position of the +1 ribonucleotide ($m^7GpppNm$, Cap 1) and +2 ribonucleotide ($m^7GpppNmNm$, Cap 2), respectively (Wei et al., 1975);(Langberg and Moss, 1981). The cap structures and properties were revealed in the 1970s, due to the technical development for purifying mRNA based on the poly(A) structure (Edmonds et al., 1971; Mendecki et al., 1972). Majority of cellular mRNA translation is initiated in a cap-dependent manner. The cap acts as an anchor for recruiting eukaryotic translation initiation factor 4F complex (eIF4F complex), including eIF4E, eIF4G, and eIF4A, which is responsible for the recruitment of 43S complex of the small ribosomal subunit and associated translation factors to form the 48S pre-initiation complex (McCormick and Khaperskyy, 2017). mRNA lacks m^7G cap exhibited at least ten folds protein expression reduction (Horikami et al., 1984; Lo et al., 1998). Cap analogs, such as GpppG, m^7GpppG, and $m^7GpppGm$, are incorporated into RNAs during IVT (Konarska et al., 1984; Contreras et al., 1982). However, one-third of the IVT mRNA is improperly capped, thus poorly recognized by the translation initiation machinery (Matsuo et al., 1997; Cai et al., 1999). To address this problem, Jemielity group developed the anti-reverse cap analog (ARCA) in which the hydroxyl group in C2 or C3 position of the m^7G is removed or substituted with methoxy group (Stepinski et al., 2001; Jemielity et al., 2003). The ARCA-capped mRNA resulting in increased as well as prolonged protein expression (Mockey et al., 2006; Zohra et al., 2007). A further improvement in synthetic cap analogs has been achieved using sulfur to substitute nonbridging oxygen in either the α, β, or γ-position of the triphosphate. This substitution leads to an inhibition of pyrophosphatase Dcp1p/Dcp2p mediated mRNA decapping degradation (Grudzien-Nogalska et al., 2007). Another option is to replace the triphosphate with tetraphosphate to increase the affinity of the cap analog to the translation initiation factor eIF4E (Strenkowska et al., 2010).

5′ and 3′ UTRs play crucial roles in mRNA regulation of translocation (Jansen, 2001), translation (van der Velden and Thomas, 1999) and stabilization (Bashirullah et al., 2001). 5′-UTR regulates mRNA translation efficiency through its structure features, i.e., length, secondary structure, nucleotide sequence (Mignone et al., 2002). The best context for translation initiation is when the starting methionine codon (AUG) is in a Kozak sequence context ($GCC^A/_GCCAUGG$) with a purine at the −3 position and a guanine at the +4 position (Kozak, 1987, 2005). Yang et al. found that mRNAs with longer 3′-UTR (> 1Kb) decayed at a significantly faster rate than shorter 3′-UTR (Yang et al., 2003). Additionally, the exosome complex destructs transcripts bearing AU-rich motifs (Chen et al., 2001; Mukherjee et al., 2002), especially when the AU-rich motif is located in the 3′-UTR (Yang et al., 2003).

Poly (A) tail is also essential to improve mRNA intracellular stability and for successful translation initiation. Initiation of translation requires the formation of a pre-initiation complex (PIC) which is Poly(A) tail binds to polyadenylate-binding protein 1 (PABP) then interacts with eIF4G leading to mRNA circulation (Gallie, 1998). The length of the poly(A) tail is essential for mRNA stability. Eukaryotic mRNA undergoes progressive deadenylation leading to decapping followed by 5′–3′ exonucleolytic degradation (Coller and Parker, 2004). Transcripts with a short poly(A) tail are shown more vulnerable to decapping (Couttet et al., 1997). In parallel, translation efficient of administered IVT mRNA is positively correlated with poly(A) tail length (Mockey et al., 2006; Peng et al., 2008). The poly(A) tail could be either put on the template or added post IVT by enzymatic polyadenylation; the former strategy resulting in less polydisperse mRNA with higher translational activity (Grier et al., 2016).

In summary, the IVT mRNA should at least contains a cap structure, a poly(A) tail longer than 12 A residues which is the minimum poly(A)

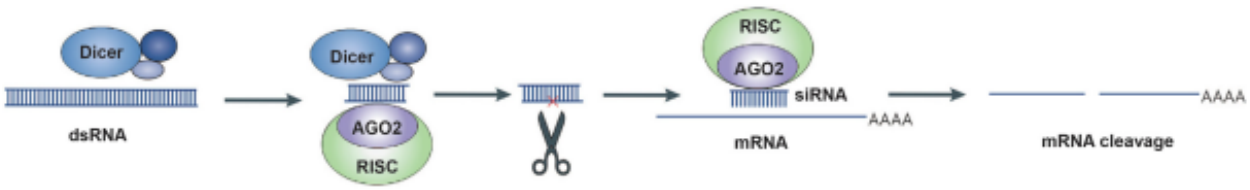

Fig. 3. Eukaryotic mRNA structure and translation initiation. Mature eukaryotic mRNA consists the 5′ methylated guanosine cap (m^7Gp3N), the 5′ and 3′ untranslated region (5′-UTR and 3′-UTR) flank the open reading frame (ORF), and the 50–250 adenosine residues (poly(A) tail). During translation, eukaryotic translation initiation factor 4E (eIF4E) binds to the m^7Gp3N cap, and polyadenylate-binding protein 1 (PABP1) binds to the 3′ poly(A) tail, followed by recruitment of eIF4G and eIF4A, leading to mRNA circularization. The translation initiation factor 4F complex (eIF4E, eIF4G, and eIF4A) recruits 43S preinitiation complex and associated translation factors to the 5′-UTR. Next, $tRNA^{met}$ recognizes the initiation codon (AUG), and large ribosome subunit (80S) locks the ORF and starts polypeptide synthesis.

length for PABP binding (Sachs et al., 1987). For optimal expression and stability, the 5′ and 3′ UTR with designed sequence can be added.

4.2. mRNA therapy and immunogenicity

Introducing exogenous mRNA into cells to express proteins of interest started three decades ago. In 1989, Malone and colleagues transfected tissue cultured NIH3T3 cells with IVT *P. pyralis* luciferase mRNA using a synthetic cationic lipid (Malone et al., 1989). The following year, Wolff and colleagues first demonstrated the feasibility of IVT mRNA mediated protein expression *in vivo* by direct injection of naked IVT mRNAs into mouse skeletal muscle (Wolff et al., 1990). In 1992, arginine vasopressin IVT mRNA was used to treat genetic mutation of vasopressin-induced diabetes insipidus in rat (Jirikowski et al., 1992). The diabetes insipidus was temporarily reversed for up to 5 days. Since then, extensive studies were focused on mRNA therapy (Tavernier et al., 2011; Schlake et al., 2018). Although mRNA design, synthesis, and delivery methods gained remarkable progress, the use of mRNA has been so far limited to vaccination because of its instability and immunogenicity (Pascolo, 2008; Schlake et al., 2018). After internalization, mRNA is mainly accumulated into endosomes, where the IVT mRNAs are recognized by Toll-like receptors (TLRs), specifically TLR3, 7, and 8, located in the endosome membrane (Kariko et al., 2005; Alexopoulou et al., 2001; Heil et al., 2004). TLR3 recognizes double-stranded RNA, and TLR7/8 recognize single-stranded RNA. The TLRs stimulation induces type I interferon (INFα/β) expression and associated anti-viral responses resulting in IVT mRNA translation suppression and degradation, and even host cell apoptosis (Kariko et al., 2004; Dan et al., 2012). The comprehensive immune responses induced by IVT mRNA is shown in Fig. 4.

In the last ten years, the discovery that incorporation of naturally modified nucleotides, such as pseudouridine, 5-methylcytidine, N6-methyladenosine, 5-methyluridine, or 2-thiouridine, suppressed IVT mRNA induced TLR3/7/8 activation in human DCs revitalized mRNA-based therapies (See Table 2) (Kariko et al., 2005; Freund et al., 2019) . Further, Kariko and colleagues compared the influence of each modified nucleotides in mRNA translation (Kariko et al., 2008). Interestingly, although pseudouridine is primarily found in tRNA, rRNA, and small nuclear RNA (Anderson et al., 2010), incorporation of pseudouridine into mRNA showed the highest translation enhancement *in vitro*, because pseudouridine incorporation changed the mRNA structure motifs which can active RNA-dependent protein kinase (PKR) leading to inhibition of translation initiation by eIF2α phosphorylation (Zheng and Bevilacqua, 2004). In addition to the nucleotides mentioned above, other modified nucleotides also exhibited the ability to increase mRNA translation and stability (Li et al., 2016). Svitkin and colleagues showed N1-methyl-pseudouridine modified luciferase mRNA yield 7.4-fold luciferase expression compared to non-modified mRNA, which was higher than the 5-methylcytidine modification and their combination. Also, they described the enhanced translation was partially contributed by suppressed eIF2α phosphorylation and increased ribosome pausing and density on the mRNA (Svitkin et al., 2017).

mRNA obtained by IVT is not uniform in length and structure. They can contain contaminants such as short RNAs generated from abortive transcription and double-stranded RNAs generated from RNA-primed transcription from RNA templates, self-complementary 3′ extension, transcription runoffs and, RNA-dependent RNA polymerase activity (Milligan et al., 1987; Triana-Alonso et al., 1995; Arnaud-Barbe et al., 1998; Nacheva and Berzal-Herranz, 2003; Mu et al., 2018). These contaminants are potent inducers of immune responses, and their removal requires mRNA purification after IVT (Kariko et al., 2008; Kariko et al., 2011). The purification is mostly done using chromatography to separate appropriately-sized mRNA from free nucleoside triphosphates, short RNA, and DNA template (Kim et al., 2007; McKenna et al., 2007). The elimination of double-stranded RNA requires high-performance liquid chromatography (HPLC) purification (Kariko et al., 2011; Weissman et al., 2013). These procedures are now used by most of mRNA-producing companies.

4.3. mRNA-based therapeutic for osteogenesis

mRNA as a potential therapeutic extended from vaccination to protein replacement therapy since modified mRNA was shown to facilitate exogenous mRNA-mediated *in vivo* protein expression with no or low immunogenicity (Kariko et al., 2008; Kormann et al., 2011). Zangi et al. injected modified RNA encoding human VEGF-A (vascular endothelial growth factor A) into mouse heart with myocardial infarction (Zangi et al., 2013). The VEGF-A expressed from modified mRNA significantly decreased the infarct size and enhanced the survival rate of recipients.

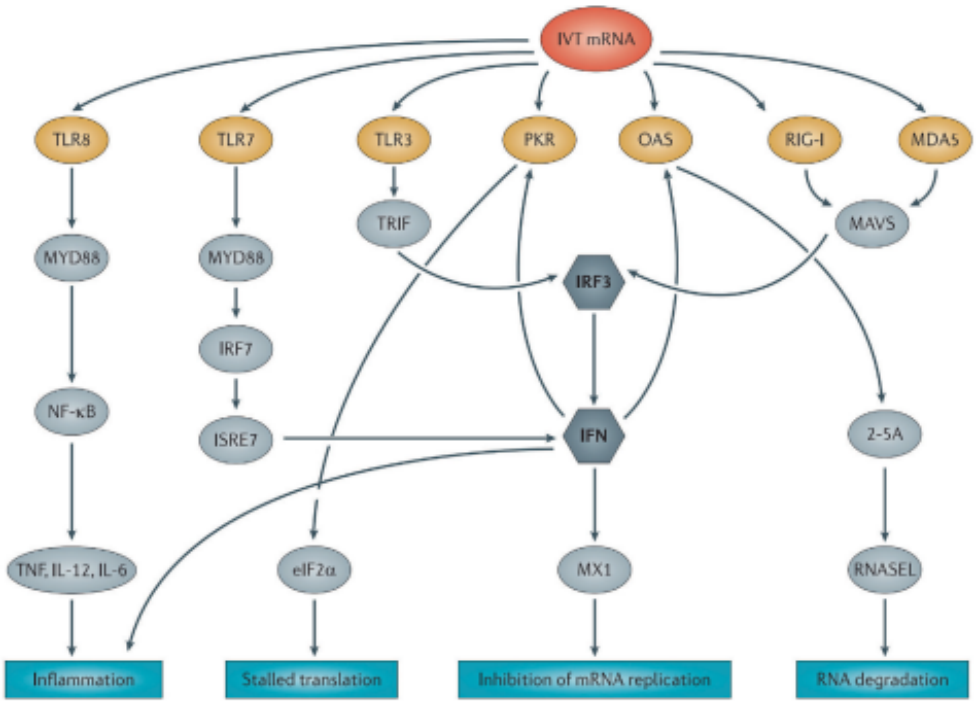

Fig. 4. Immune responses to synthetic mRNA. In vitro transcribed (IVT) mRNA is recognized by various endosomal innate immune receptors (toll-like receptor3/7/8 (TLR3/7/8)) and cytoplasmic innate immune receptors (RNA-activated protein kinase (PKR), retinoic acid-inducible gene I protein (RIG-I), melanoma differentiation associated protein 5 (MDA5) and 2′–5′-oligoadenylate synthase (OAS)). The activation of these RNA sensors results in IVT mRNA translation and replication inhibition, and degradation promotion. IFN, interferon; TNF, tumor necrosis factor; IL, interleukin; eIF2α, eukaryotic translation initiation factor 2α; RNASEL, ribonuclease L; IRF, interferon regulatory factor; ISRE7, interferon-stimulated response element; MAVS, mitochondrial antiviral signaling protein; MDA5, melanoma differentiation-associated protein 5; MYD88, myeloid differentiation primary response protein 88; MX1, myxovirus (influenza) resistance 1; NF-κB, nuclear factor-κB; TRIF, Toll-IL-1 receptor domain-containing adapter protein inducing IFNβ. Adapted from (Sahin et al., 2014) with permission.

Table 2
Summary of published studies using mRNA for *in vivo* bone regeneration.

Gene	Nucleotides modification in IVT mRNA	vector	Scaffold/cells	In vivo model	Ref.
BMP-2	$\Psi_{(1)}$* and $m5C_{(1)}$	Branched PEI (25 kDa)	Collagen sponge containing 25 μg mRNA polyplexes	Rat calvarial defect-5 mm diameter	Elangovan et al. (2015)
BMP-2	$s2U_{(0.25)}$ and $m5C_{(0.25)}$	Cationic lipid C12-EPE with helper lipids DOPE, cholesterol, and DMPE-PEG 2k	Fibrin gel loaded with 2.5 μg mRNA lipoplexes	Rat femur diaphysis transcortical bone defect-2 mm diameter	Balmayor et al. (2016)
BMP-2	$s2U_{(0.25)}$ and $m5C_{(0.25)}$	Cationic lipid C12-EPE with helper DPPC and cholesterol, and DMG-PEG2K	Collagen sponge containing 2.5 μg mRNA lipoplexes	Rat femur diaphysis transcortical bone defect-2 mm diameter	Badieyan et al. (2016)
BMP-2/9	$\Psi_{(1)}$ and $m5C_{(1)}$	Branched PEI (mol. wt. 25 kDa)	Freeze dried collagen scaffold containing 50 μg mRNA polyplexes	Rat calvarial defect-5 mm diameter	Khorsand et al. (2017a,b)
BMP-9	$\Psi_{(1)}$ and $m5C_{(1)}$	Branched PEI (mol. wt. 25 kDa)	Freeze dried collagen membrane containing 10 μg mRNA polyplexes	Rat calvarial defect-5 mm diameter	Khorsand et al. (2018)
BMP-2	$5IU_{(0.25)}5IC_{(0.075)}$	Cationic lipid C12-(2-3-2) with helper lipids DPPC, cholesterol, and DMG-PEG 2k	Vacuum dried collagen sponge containing 2.5 μg or 5 μg mRNA lipoplexes	Rat femoral segmental bone defect-5 mm diameter	Zhang et al. (2018)

* The subscripted value represents the proposition of modified nucleotides in the IVT mRNA.
Ψ, pseudouridine; m5C, 5-methylcytosine; 5 IU, 5-iodo-uridine; 5IC, 5-iodo-cytidine; s2U, 2-thiouridine; C12-EPE, oligo(alkyl amine) with ethylen-propylen-ethylen (EPE) backbone and five equivalents of 1,2-epoxydodecane; DOPC, 1,2-Dioleoyl-*sn*-Glycero-3-Phosphocholine; DPPC, 1,2-dipalmitoyl-*sn*-glycero-3-phosphocholine; DMG-PEG2K, 1,2-dimyristoyl-*rac*-glycero-3-methoxypolyethylene glycol-2000; DMPE-PEG2K, 1,2-distearoyl-*sn*-glycero-3-phosphoethanolamine-N-[amino(polyethylene glycol)-2000.

4.3.1. BMPs replacement therapy

For bone regeneration, recombinant BMPs have been used in therapy for over 40 years (Urist and Strates, 2009). As dominant osteoinductive factors, BMPs have been delivered into the site that needs bone regeneration in the form of recombinant protein (McKay et al., 2007) or plasmid encoding BMP gene used as naked or vectorized form (Fang et al., 1996; Khorsand et al., 2017b).. Elangovan et al. employed modified mRNA encoding BMP-2 to enhance bone regeneration *in vitro* and *in vivo* (Elangovan et al., 2015). Using IFNα as a marker, combined modification of pseudouridine and 5-methylcytidine almost entirely circumvented unmodified mRNA induced immune response. They compared the osteoblastic differentiation induction between the modified BMP2 mRNA and its pDNA counterpart. Bone Marrow-derived Stem Cells (BMSCs) transfected with polyethyleneimine branched PEI, mol. wt. 25 kDa)-complexed modified mRNA yielded three times more BMP2 in the cell culture medium than cells transfected with pDNA. The osteogenic differentiation markers expression, such as alkaline phosphatase (ALP), osteocalcin (OCN), were also higher in the modified mRNA group. As a result, implanting a collagen scaffold containing modified mRNA polyplexes into rat calvarial defects showed 3.94-fold higher BV/TV (mineralized bone volume as a fraction of the total tissue volume of interest) in defect site compared to empty scaffold control. This study, for the first time, verified the safety and efficacy of using modified mRNA coding an osteogenic factor for bone regeneration. It also demonstrated the potential of modified mRNA-loaded scaffold as a novel bone graft substitute. Similarly, BMP-2 mRNA bearing methylcytidine and 2-thiouridine modification exhibited greater bone formation capacity (Balmayor et al., 2016; Badieyan et al., 2016; Balmayor et al., 2017). Balmayor et al. prepared modified mRNA coding human BMP-2 by replacing 25% cytidine and 25% uridine with methylcytidine and 2-thiouridine. Adipo-derived mesenchymal stem cells (AMSCs) showed osteogenic differentiation once transfected with this modified BMP-2 mRNA through lipofection or magnetofection (Badieyan et al., 2016). Interestingly, AMSCs osteogenic differentiation was dose-dependent. For *in vivo* osteogenesis, liposomal formulation of modified BMP-2 mRNA mixed with a fibrin matrix was implanted into rat femur hole model. Two weeks post-operation, rats treated with modified BMP-2 mRNA obtained ~2-fold more callus tissue than fibrin matrix alone.

Most of studies on bone regeneration have been based on the use of BMP2 since it is considered as one of the most osteogenic factors. A recent study highlighted that BMP-9 could be also used as an alternative. The efficiency of modified mRNA coding BMP-2 or BMP-9 to induce *in vitro* osteogenesis and *in vivo* bone regeneration have been compared in a recent report (Khorsand et al., 2017a). BMSCs transfected with PEI-complexed modified BMP-9 had a significant increase in ALP gene expression and calcium deposition compared to modified BMP-2 mRNA, but not in Runx2 and OCN genes expression. Implanting collagen matrices containing modified BMP-9 mRNA or BMP-2 into rat calvarial defect resulted in a similar ratio of bone volume to tissue volume. However, modified BMP-9 groups had 2-fold more density in connective tissue than BMP-2 groups, which is consistent with the *in vitro* observation. Table 2 provides a summary of in vivo osteogenesis studies based on BMPs replacement therapy.

4.3.2. Reprogramming proteins replacement

Stem cells with osteogenic differentiation capacity have great applications in engineering bone substitutes with biocompatible scaffolds for bone regeneration (Amini et al., 2012). Mesenchymal stem cells are good candidates due to their bispecific differentiation toward osteogenic lineages. However, their limited proliferation in elder patients and multi-passage induced senescence limit their clinical applications (Jones and Yang, 2011). On the contrary, iPSCs (induced pluripotent stem cells) derived from somatic cells, typically fibroblast reprogramming, have the potential to circumvent this obstacle, with a lower rate of senescence after expansion, both *in vitro* and *in vivo* (Takahashi and Yamanaka, 2006; Takahashi et al., 2007). iPSCs showed osteogenic

differentiation under stimulation of osteogenic factors (Teng et al., 2014; Csobonyeiova et al., 2017).

Warren et al., reprogrammed fibroblasts to iPSCs by transfecting them with a mix of IVT mRNAs (both pseudouridine and 5-methylcytidine modified) coding for reprogramming transcription factors which are KLF4/c-MYC/OCT4/SOX2 (KMOS) or KLF4/c-MYC/OCT4/SOX2/LIN28 (KMOSL), respectively (Warren et al., 2010). The KMOSL mRNAs mix induced ESC-like colonies almost ten days earlier than the KMOS mRNAs mix, consistent with the previous report that LIN28 facilitated reprogramming (Yu et al., 2017; Hanna et al., 2009).

4.4. Challenges and perspectives

Advancing the use of mRNA for bone regeneration requires an increase of cost-benefit value over traditional approaches such as rhBMP2 and pDNA. Although the incorporation of modified nucleotides and HPLC purification of IVT mRNA improves its translation along with decreased activation of TLRs and PKR, the high cost remains a challenge. Optimization of the sequence of 5′- and 3′-UTR and ORF, is one reasonable approach to increase IVT mRNA stability and translation efficiency within cells (Zhang et al., 2018). Asrani and colleagues provided an experimental framework for a high throughput screening assay to simultaneously evaluate hundreds of UTRs for optimized protein expression (Asrani et al., 2018). Translation efficiency enhancement resulting from sequence-engineering can even exceed nucleotides modification (pseudouridine) both *in vitro* and *in vivo* (Thess et al., 2015). However, to date, no universal UTRs can be translated across different genes and cell types.

Applying mRNA for bone regeneration will benefit from continuous efforts in RNA design, particularly on circularization. Wesselhoeft et al. recently demonstrated that mRNA circularization yielded superior expression *in vivo* over linear mRNA, paralleled with decreased induction of TLRs (Wesselhoeft et al., 2019). Circularization of mRNA decreased TLR activation to the same extent as the inclusion of modified nucleotides in linear mRNA, demonstrating a new modality for therapeutic protein expression. Further advancement in the usage of mRNA for bone regeneration consists of sequence/structure optimization in osteogenic cells. Indeed, optimization of mRNA sequence has been mostly performed in dendritic cells or macrophages (Holtkamp et al., 2006; Uchida et al., 2015; Orlandini von Niessen et al., 2018), cancer cell lines (Trepotec et al., 2019; Wesselhoeft et al., 2018), fibroblasts (Hausburg et al., 2015; Ferizi et al., 2016), epithelial cells (Andries et al., 2015). However, rarely on clinically-relevant human mesenchymal stem cells (Hausburg et al., 2015). Based on the cell-type dependent effects of mRNA modifications on expression and immunogenicity (Uchida et al., 2015), incorporation of modified nucleotides should be tuned for MSCs.

Inspired by viruses impair host cells immune response, B18R protein, from Western vaccinia virus that binds to and neutralizes type I interferons, is frequently used as culture supplement after IVT mRNA transfection (Alcamí et al., 2000; Warren et al., 2010; Yoshioka et al., 2013). Unlike B18R, Influenza A virus non-structural protein 1 (NS1) is a multiple functional protein blocking several steps in immune responses. Recent study showed that co-transfection of NS1 mRNA withgene of interest, reduced immune response and increased protein expression (Phua et al., 2017). NS1 from A/Texas/36/91 strain exhibited better performance than pseudouridine modification.

Transient expression is the inherent property of mRNA. The one-shot high expression is sufficient for vaccination, but sometimes not for protein-replacement therapies. For instance, to reconstruct bone nonunion continuous expression of osteogenic factors is needed. Sustained release of mRNA complexes from a matrice resulting in cell multi-transfection and extended protein expression period. Hydrogels have been employed *in vitro* and *in vivo* as a therapeutic carrier to promote tissue formation. NHI3T3 cells encapsulated in fibrin hydrogel together with 1 μg pDNA coding firefly luciferase (fluc) expressed fluc for ten days with a less fluc decrease in first six days (des Rieux et al., 2009).

Alternatively, Yoshioka et al. synthesized a self-replicating mRNA (RepRNA) for long-term multiple protein expression (Yoshioka et al., 2013). The proteins expressed from the RepRNA lasted for two weeks by a single-dose transfection. However it is worth to notice that, although RepRNA produces more proteins and for extended periods than mRNA, the dsRNAs produced during replication and other replication intermediates are potent inducers of inflammation which limit the repeated use of RepRNA (Pardi et al., 2018). Additionally, the large size of RepRNA (9000–15000 nt) is a challenge for its formulation as fewer delivery systems available (Geall et al., 2012).

The polycistronic strategy suitable for bone regeneration as well, as several factors work synergistically in this process (Hankenson et al., 2015).

5. Conclusion

In this review we described applications of mRNA and siRNA for bone regeneration. While the preclinical efficacy of RNA for bone regeneration has been demonstrated (Balmayor et al., 2017; Ghadakzadeh et al., 2016), the road to clinical evaluation requiresmore efforts. It is still highly challenging to restore large bone defect or nonunion fractures. The estimation is about one million procedures that are occurring every year in Europe, and the market estimated around € 5 billion. Progress of RNAs design and delivery will undoubtedly benefit building therapeutic strategies for bone regeneration. The success of bone regeneration is highly dependent on osteogenic cells, their microenvironment, and the mechanical and structural properties of the extracellular matrix. Stem cells with osteogenic differentiation property showed a great therapeutic potential, however, the poor engraftment and low survival rate still impede their application. Currently developed CRISPR/Cas9 (clustered regularly interspaced short palindromic repeats/CRISPR associated protein 9) genome editing system gives a solution to enhance the stem cells performance (Zhang et al., 2017; Hille et al., 2018). Indeed, elevated inflammation in injured tissue is known to prevent stem cell differentiation. For instance, Brunger et al. have succeeded to remove IL-1 (interleukin 1) type I receptor gene from murine iPSCs by CRISPR/Cas9 system. The designed iPSCs demonstrated excellent resistance to IL-1 (interleukin 1) initiated inflammation and were successfully differentiated into chondrocytes (Brunger et al., 2017). Another issue related to the use of stem cells, is the multi-passage senescence. To address this, Hu and colleagues created immortalized BMSCs while maintaining MSC phenotype by targeting SV40T (simian virus SV40 large T antigen) into the Rosa26 locus (Hu et al., 2017a,b) using CRISPR/Cas9 gene editing system. The selection of the right 3D scaffold is crucial to restore and maintain the regeneration process. These last years, 3D-printed templates have been proposed to fabricate patient-specific bone grafts. Their preparation process is claimed to be easy, reproducible and can have specific micro-architecture with complex configuration (Zhang et al., 2019). Incorporation RNA therapeutics in such scaffold will allow creating patient specific bone grafts on demand.

Declaration of Competing Interest

The authors declare that they have no known competing financial interests or personal relationships that could have appeared to influence the work reported in this paper.

Acknowledgment

This work is supported by CNRS and University of Orléans. WANG Pinpin thanks the financial support from China Scholarship Council.

References

Abe, E., Yamamoto, M., Taguchi, Y., Lecka-Czernik, B., O'Brien, C.A., Economides, A.N., Stahl, N., Jilka, R.L., Manolagas, S.C., 2000. Essential requirement of BMPs-2/4 for both osteoblast and osteoclast formation in murine bone marrow cultures from adult mice: antagonism by noggin. J. Bone Miner. Res. 15, 663–673.

Adams, D., Suhr, O.B., Dyck, P.J., Litchy, W.J., Leahy, R.G., Chen, J., Gollob, J., Coelho, T., 2017. Trial design and rationale for APOLLO, a Phase 3, placebo-controlled study of patisiran in patients with hereditary ATTR amyloidosis with polyneuropathy. BMC Neurol. 17, 181.

Agrawal, N., Dasaradhi, P.V.N., Mohmmed, A., Malhotra, P., Bhatnagar, R.K., Mukherjee, S.K., 2003. RNA interference: biology, mechanism, and applications. Microbiol. Mol. Biol. Rev. 67, 657–685.

Alcamí, A., Symons, J.A., Smith, G.L., 2000. The vaccinia virus soluble alpha/beta interferon (IFN) receptor binds to the cell surface and protects cells from the antiviral effects of IFN. J. Virol. 74, 11230–11239.

Alexopoulou, L., Holt, A.C., Medzhitov, R., Flavell, R.A., 2001. Recognition of double-stranded RNA and activation of NF-kappaB by Toll-like receptor 3. Nature 413, 732–738.

Amini, A.R., Laurencin, C.T., Nukavarapu, S.P., 2012. Bone tissue engineering: recent advances and challenges. Crit. Rev. Biomed. Eng. 40, 363–408.

Anderson, B.R., Muramatsu, H., Nallagatla, S.R., Bevilacqua, P.C., Sansing, L.H., Weissman, D., Kariko, K., 2010. Incorporation of pseudouridine into mRNA enhances translation by diminishing PKR activation. Nucleic Acids Res. 38, 5884–5892.

Andries, O., Mc Cafferty, S., De Smedt, S.C., Weiss, R., Sanders, N.N., Kitada, T., 2015. N(1)-methylpseudouridine-incorporated mRNA outperforms pseudouridine-incorporated mRNA by providing enhanced protein expression and reduced immunogenicity in mammalian cell lines and mice. J. Controlled Release 217, 337–344.

Arnaud-Barbe, N., Cheynet-Sauvion, V., Oriol, G., Mandrand, B., Mallet, F., 1998. Transcription of RNA templates by T7 RNA polymerase. Nucleic Acids Res. 26, 3550–3554.

Asrani, K.H., Farelli, J.D., Stahley, M.R., Miller, R.L., Cheng, C.J., Subramanian, R.R., Brown, J.M., 2018. Optimization of mRNA untranslated regions for improved expression of therapeutic mRNA. RNA Biol. 1–7.

Badieyan, Z.S., Berezhanskyy, T., Utzinger, M., Aneja, M.K., Emrich, D., Erben, R., Schuler, C., Altpeter, P., Ferizi, M., Hasenpusch, G., Rudolph, C., Plank, C., 2016. Transcript-activated collagen matrix as sustained mRNA delivery system for bone regeneration. J. Controlled Release 239, 137–148.

Balmayor, E.R., Geiger, J.P., Aneja, M.K., Berezhanskyy, T., Utzinger, M., Mykhaylyk, O., Rudolph, C., Plank, C., 2016. Chemically modified RNA induces osteogenesis of stem cells and human tissue explants as well as accelerates bone healing in rats. Biomaterials 87, 131–146.

Balmayor, E.R., Geiger, J.P., Koch, C., Aneja, M.K., van Griensven, M., Rudolph, C., Plank, C., 2017. Modified mRNA for BMP-2 in combination with biomaterials serves as a transcript-activated matrix for effectively inducing osteogenic pathways in stem cells. Stem Cells Dev. 26, 25–34.

Banerjee, A.K., 1980. 5'-terminal cap structure in eucaryotic messenger ribonucleic acids. Microbiol. Rev. 44, 175–205.

Bashirullah, A., Cooperstock, R.L., Lipshitz, H.D., 2001. Spatial and temporal control of RNA stability. Proc. Natl. Acad. Sci. U.S.A. 98, 7025–7028.

Boyce, B.F., Yoneda, T., Lowe, C., Soriano, P., Mundy, G.R., 1992. Requirement of pp60c-src expression for osteoclasts to form ruffled borders and resorb bone in mice. J. Clin. Investig. 90, 1622–1627.

Brunger, J.M., Zutshi, A., Willard, V.P., Gersbach, C.A., Guilak, F., 2017. CRISPR/Cas9 editing of murine induced pluripotent stem cells for engineering inflammation-resistant tissues. Arthritis Rheumatol. 69, 1111–1121.

Cai, A., Jankowska-Anyszka, M., Centers, A., Chlebicka, L., Stepinski, J., Stolarski, R., Darzynkiewicz, E., Rhoads, R.E., 1999. Quantitative assessment of mRNA cap analogues as inhibitors of in vitro translation. Biochemistry 38, 8538–8547.

Campbell, J.M., Bacon, T.A., Wickstrom, E., 1990. Oligodeoxynucleoside phosphorothioate stability in subcellular extracts, culture media, sera and cerebrospinal fluid. J. Biochem. Bioph. Methods 20, 259–267.

Cekaite, L., Furset, G., Hovig, E., Sioud, M., 2007. Gene expression analysis in blood cells in response to unmodified and 2'-modified siRNAs reveals TLR-dependent and independent effects. J. Mol. Biol. 365, 90–108.

Chaudhary, A., Srivastava, S., Garg, S., 2011. Development of a software tool and criteria evaluation for efficient design of small interfering RNA. Biochem. Biophys. Res. Commun. 404, 313–320.

Chen, C., Uludag, H., Wang, Z., Jiang, H., 2012a. Noggin suppression decreases BMP-2-induced osteogenesis of human bone marrow-derived mesenchymal stem cells in vitro. J. Cell. Biochem. 113, 3672–3680.

Chen, C.Y., Gherzi, R., Ong, S.E., Chan, E.L., Raijmakers, R., Pruijn, G.J., Stoecklin, G., Moroni, C., Mann, M., Karin, M., 2001. AU binding proteins recruit the exosome to degrade ARE-containing mRNAs. Cell 107, 451–464.

Chen, G., Deng, C., Li, Y.P., 2012b. TGF-beta and BMP signaling in osteoblast differentiation and bone formation. Int. J. Biol. Sci. 8, 272–288.

Choi, B., Cui, Z.K., Kim, S., Fan, J., Wu, B.M., Lee, M., 2015. Glutamine-chitosan modified calcium phosphate nanoparticles for efficient siRNA delivery and osteogenic differentiation. J. Mater. Chem. B 3, 6448–6455.

Coller, J., Parker, R., 2004. Eukaryotic mRNA decapping. Annu. Rev. Biochem. 73, 861–890.

Contreras, R., Cheroutre, H., Degrave, W., Fiers, W., 1982. Simple, efficient in vitro synthesis of capped RNA useful for direct expression of cloned eukaryotic genes. Nucleic Acids Res. 10, 6353–6362.

Cosman, F., Crittenden, D.B., Adachi, J.D., Binkley, N., Czerwinski, E., Ferrari, S., Hofbauer, L.C., Lau, E., Lewiecki, E.M., Miyauchi, A., Zerbini, C.A., Milmont, C.E., Chen, L., Maddox, J., Meisner, P.D., Libanati, C., Grauer, A., 2016. Romosozumab treatment in postmenopausal women with osteoporosis. N. Engl. J. Med. 375, 1532–1543.

Couttet, P., Fromont-Racine, M., Steel, D., Pictet, R., Grange, T., 1997. Messenger RNA deadenylylation precedes decapping in mammalian cells. PNAS 94, 5628–5633.

Csobonyeiova, M., Polak, S., Zamborsky, R., Danisovic, L., 2017. iPS cell technologies and their prospect for bone regeneration and disease modeling: a mini review. J. Adv. Res. 8, 321–327.

Cui, Z.K., Fan, J., Kim, S., Bezouglaia, O., Fartash, A., Wu, B.M., Aghaloo, T., Lee, M., 2015. Delivery of siRNA via cationic Sterosomes to enhance osteogenic differentiation of mesenchymal stem cells. J. Controlled Release 217, 42–52.

Dan, M., Zheng, D., Field, L.L., Bonnevie-Nielsen, V., 2012. Induction and activation of antiviral enzyme 2',5'-oligoadenylate synthetase by in vitro transcribed insulin mRNA and other cellular RNAs. Mol. Biol. Rep. 39, 7813–7822.

de Fougerolles, A., Vornlocher, H.P., Maraganore, J., Lieberman, J., 2007a. Interfering with disease: a progress report on siRNA-based therapeutics. Nat. Rev. Drug Discov. 6, 443–453.

des Rieux, A., Shikanov, A., Shea, L.D., 2009. Fibrin hydrogels for non-viral vector delivery in vitro. J. Controlled Release 136, 148–154.

Devlin, R.D., Du, Z., Pereira, R.C., Kimble, R.B., Economides, A.N., Jorgetti, V., Canalis, E., 2003. Skeletal overexpression of noggin results in osteopenia and reduced bone formation. Endocrinology 144, 1972–1978.

Dimitriou, R., Tsiridis, E., Giannoudis, P.V., 2005. Current concepts of molecular aspects of bone healing. Injury 36, 1392–1404.

Dorn, G., Patel, S., Wotherspoon, G., Hemmings-Mieszczak, M., Barclay, J., Natt, F.J., Martin, P., Bevan, S., Fox, A., Ganju, P., Wishart, W., Hall, J., 2004. siRNA relieves chronic neuropathic pain. Nucleic Acids Res. 32, e49.

Edmonds, M., Vaughan Jr., M.H., Nakazato, H., 1971. Polyadenylic acid sequences in the heterogeneous nuclear RNA and rapidly-labeled polyribosomal RNA of HeLa cells: possible evidence for a precursor relationship. PNAS 68, 1336–1340.

Egermann, M., Schneider, E., Evans, C.H., Baltzer, A.W., 2005. The potential of gene therapy for fracture healing in osteoporosis. Osteoporos. Int. 16, S120–S128.

Elangovan, S., Khorsand, B., Do, A.V., Hong, L., Dewerth, A., Kormann, M., Ross, R.D., Sumner, D.R., Allamargot, C., Salem, A.K., 2015. Chemically modified RNA activated matrices enhance bone regeneration. J. Controlled Release 218, 22–28.

Elbashir, S.M., Harborth, J., Lendeckel, W., Yalcin, A., Weber, K., Tuschl, T., 2001a. Duplexes of 21-nucleotide RNAs mediate RNA interference in cultured mammalian cells. Nature 411, 494–498.

Elbashir, S.M., Lendeckel, W., Tuschl, T., 2001b. RNA interference is mediated by 21- and 22-nucleotide RNAs. Genes Dev. 15, 188–200.

Evans, C.H., Huard, J., 2015. Gene therapy approaches to regenerating the musculoskeletal system. Nat. Rev. Rheumatol. 11, 234–242.

Fang, J., Zhu, Y.Y., Smiley, E., Bonadio, J., Rouleau, J.P., Goldstein, S.A., McCauley, L.K., Davidson, B.L., Roessler, B.J., 1996. Stimulation of new bone formation by direct transfer of osteogenic plasmid genes. PNAS 93, 5753–5758.

Ferizi, M., Aneja, M.K., Balmayor, E.R., Badieyan, Z.S., Mykhaylyk, O., Rudolph, C., Plank, C., 2016. Human cellular CYBA UTR sequences increase mRNA translation without affecting the half-life of recombinant RNA transcripts. Sci. Rep. 6, 39149.

Filleur, S., Courtin, A., Ait-Si-Ali, S., Guglielmi, J., Merle, C., Harel-Bellan, A., Clezardin, P., Cabon, F., 2003. SiRNA-mediated inhibition of vascular endothelial growth factor severely limits tumor resistance to antiangiogenic thrombospondin-1 and slows tumor vascularization and growth. Cancer Res. 63, 3919–3922.

Fire, A., 1999. RNA-triggered gene silencing. Trends Genet. 15, 358–363.

Fischer, L., Boland, G., Tuan, R.S., 2002. Wnt-3A enhances bone morphogenetic protein-2-mediated chondrogenesis of murine C3H10T1/2 mesenchymal cells. J. Biol. Chem. 277, 30870–30878.

Fisher, S., Halpern, M.E., 1999. Patterning the zebrafish axial skeleton requires early chordin function. Nat. Genet. 23, 442–446.

Frattini, A., Orchard, P.J., Sobacchi, C., Giliani, S., Abinun, M., Mattsson, J.P., Keeling, D.J., Andersson, A.K., Wallbrandt, P., Zecca, L., Notarangelo, L.D., Vezzoni, P., Villa, A., 2000. Defects in TCIRG1 subunit of the vacuolar proton pump are responsible for a subset of human autosomal recessive osteopetrosis. Nat. Genet. 25, 343–346.

Freund, I., Eigenbrod, T., Helm, M., Dalpke, A.H., 2019. RNA modifications modulate activation of innate toll-like receptors. Genes (Basel) 10.

Gallie, D.R., 1998. A tale of two termini: a functional interaction between the termini of an mRNA is a prerequisite for efficient translation initiation. Gene 216, 1–11.

Gazzerro, E., Smerdel-Ramoya, A., Zanotti, S., Stadmeyer, L., Durant, D., Economides, A.N., Canalis, E., 2007. Conditional deletion of gremlin causes a transient increase in bone formation and bone mass. J. Biol. Chem. 282, 31549–31557.

Geall, A.J., Verma, A., Otten, G.R., Shaw, C.A., Hekele, A., Banerjee, K., Cu, Y., Beard, C.W., Brito, L.A., Krucker, T., O'Hagan, D.T., Singh, M., Mason, P.W., Valiante, N.M., Dormitzer, P.R., Barnett, S.W., Rappuoli, R., Ulmer, J.B., Mandl, C.W., 2012. Nonviral delivery of self-amplifying RNA vaccines. PNAS 109, 14604–14609.

Genant, H.K., Cooper, C., Poor, G., Reid, I., Ehrlich, G., Kanis, J., Nordin, B.E., Barrett-Connor, E., Black, D., Bonjour, J.P., Dawson-Hughes, B., Delmas, P.D., Dequeker, J., Ragi Eis, S., Gennari, C., Johnell, O., Johnston Jr., C.C., Lau, E.M., Liberman, U.A., Lindsay, R., Martin, T.J., Masri, B., Mautalen, C.A., Meunier, P.J., Khaltaev, N., et al., 1999. Interim report and recommendations of the world health organization task-force for osteoporosis. Osteoporos. Int. 10, 259–264.

Ghadakzadeh, S., Mekhail, M., Aoude, A., Hamdy, R., Tabrizian, M., 2016. Small players ruling the hard game: siRNA in bone regeneration. J. Bone Miner. Res. 31, 475–487.

Giannoudis, P.V., Faour, O., Goff, T., Kanakaris, N., Dimitriou, R., 2011. Masquelet technique for the treatment of bone defects: tips-tricks and future directions. Injury 42, 591–598.

Goldberg, V.M., Stevenson, S., 1987. Natural history of autografts and allografts. Clin.

Orthop. Relat. Res. 7–16.
Grier, A.E., Burleigh, S., Sahni, J., Clough, C.A., Cardot, V., Choe, D.C., Krutein, M.C., Rawlings, D.J., Jensen, M.C., Scharenberg, A.M., Jacoby, K., 2016. pEVL: a linear plasmid for generating mRNA IVT templates With extended encoded poly(A) sequences. Mol. Ther. Nucleic Acids 5, e306.
Grudzien-Nogalska, E., Jemielity, J., Kowalska, J., Darzynkiewicz, E., Rhoads, R.E., 2007. Phosphorothioate cap analogs stabilize mRNA and increase translational efficiency in mammalian cells. RNA 13, 1745–1755.
Hankenson, K.D., Gagne, K., Shaughnessy, M., 2015. Extracellular signaling molecules to promote fracture healing and bone regeneration. Adv. Drug Deliv. Rev. 94, 3–12.
Hanna, J., Saha, K., Pando, B., van Zon, J., Lengner, C.J., Creyghton, M.P., van Oudenaarden, A., Jaenisch, R., 2009. Direct cell reprogramming is a stochastic process amenable to acceleration. Nature 462, 595–601.
Hannon, G.J., 2002. RNA interference. Nature 418, 244–251.
Hausburg, F., Na, S., Voronina, N., Skorska, A., Muller, P., Steinhoff, G., David, R., 2015. Defining optimized properties of modified mRNA to enhance virus- and DNA- independent protein expression in adult stem cells and fibroblasts. Cell. Physiol. Biochem. 35, 1360–1371.
Heil, F., Hemmi, H., Hochrein, H., Ampenberger, F., Kirschning, C., Akira, S., Lipford, G., Wagner, H., Bauer, S., 2004. Species-specific recognition of single-stranded RNA via toll-like receptor 7 and 8. Science 303, 1526–1529.
Hille, F., Richter, H., Wong, S.P., Bratovic, M., Ressel, S., Charpentier, E., 2018. The biology of CRISPR-cas: backward and forward. Cell 172, 1239–1259.
Hofbauer, L.C., Heufelder, A.E., 2001. Role of receptor activator of nuclear factor-kappaB ligand and osteoprotegerin in bone cell biology. J. Mol. Med. (Berl.) 79, 243–253.
Hollick, R.J., Reid, D.M., 2011. Role of bisphosphonates in the management of postmenopausal osteoporosis: an update on recent safety anxieties. Menopause Int. 17, 66–72.
Holtkamp, S., Kreiter, S., Selmi, A., Simon, P., Koslowski, M., Huber, C., Tureci, O., Sahin, U., 2006. Modification of antigen-encoding RNA increases stability, translational efficacy, and T-cell stimulatory capacity of dendritic cells. Blood 108, 4009–4017.
Horikami, S.M., De Ferra, F., Moyer, S.A., 1984. Characterization of the infections of permissive and nonpermissive cells by host range mutants of vesicular stomatitis virus defective in RNA methylation. Virology 138, 1–15.
Hsu, D.R., Economides, A.N., Wang, X., Eimon, P.M., Harland, R.M., 1998. The Xenopus dorsalizing factor gremlin identifies a novel family of secreted proteins that antagonize BMP activities. Mol. Cell 1, 673–683.
Hu, K., Sun, H., Gui, B., Sui, C., 2017a. Gremlin-1 suppression increases BMP-2-induced osteogenesis of human mesenchymal stem cells. Mol. Med. Rep. 15, 2186–2194.
Hu, X., Li, L., Yu, X., Zhang, R., Yan, S., Zeng, Z., Shu, Y., Zhao, C., Wu, X., Lei, J., Li, Y., Zhang, W., Yang, C., Wu, K., Wu, Y., An, L., Huang, S., Ji, X., Gong, C., Yuan, C., Zhang, L., Liu, W., Huang, B., Feng, Y., Zhang, B., Haydon, R.C., Luu, H.H., Reid, R.R., Lee, M.J., Wolf, J.M., Yu, Z., He, T.C., 2017b. CRISPR/Cas9-mediated reversibly immortalized mouse bone marrow stromal stem cells (BMSCs) retain multipotent features of mesenchymal stem cells (MSCs). Oncotarget 8, 111847–111865.
Huang, J., Lin, C., Fang, J., Li, X., Wang, J., Deng, S., Zhang, S., Su, W., Feng, X., Chen, B., Cheng, D., Shuai, X., 2018a. pH-sensitive nanocarrier-mediated codelivery of simvastatin and noggin siRNA for synergistic enhancement of osteogenesis. ACS Appl. Mater. Interfaces 10, 28471–28482.
Huang, R.L., Yuan, Y., Tu, J., Zou, G.M., Li, Q., 2014. Opposing TNF-alpha/IL-1beta- and BMP-2-activated MAPK signaling pathways converge on Runx2 to regulate BMP-2-induced osteoblastic differentiation. Cell Death Dis. 5, e1187.
Im, G.I., 2013. Nonviral gene transfer strategies to promote bone regeneration. J. Biomed. Mater. Res. A 101, 3009–3018.
Inada, T., Tamura, A., Terauchi, M., Yamaguchi, S., Yui, N., 2018. A silencing-mediated enhancement of osteogenic differentiation by supramolecular ternary siRNA polyplexes comprising biocleavable cationic polyrotaxanes and anionic fusogenic peptides. Biomater. Sci. 6, 440–450.
Jackson, R.J., 1993. Cytoplasmic regulation of mRNA function: the importance of the 3' untranslated region. Cell 74, 9–14.
Jansen, R.P., 2001. mRNA localization: message on the move. Nat. Rev. Mol. Cell Biol. 2, 247–256.
Jemielity, J., Fowler, T., Zuberek, J., Stepinski, J., Lewdorowicz, M., Niedzwiecka, A., Stolarski, R., Darzynkiewicz, E., Rhoads, R.E., 2003. Novel "anti-reverse" cap analogs with superior translational properties. RNA 9, 1108–1122.
Jirikowski, G.F., Sanna, P.P., Maciejewski-Lenoir, D., Bloom, F.E., 1992. Reversal of diabetes insipidus in Brattleboro rats: intrahypothalamic injection of vasopressin mRNA. Science 255, 996–998.
Jones, E., Yang, X., 2011. Mesenchymal stem cells and bone regeneration: current status. Injury 42, 562–568.
Kariko, K., Buckstein, M., Ni, H., Weissman, D., 2005. Suppression of RNA recognition by toll-like receptors: the impact of nucleoside modification and the evolutionary origin of RNA. Immunity 23, 165–175.
Kariko, K., Muramatsu, H., Ludwig, J., Weissman, D., 2011. Generating the optimal mRNA for therapy: HPLC purification eliminates immune activation and improves translation of nucleoside-modified, protein-encoding mRNA. Nucleic Acids Res. 39, e142.
Kariko, K., Muramatsu, H., Welsh, F.A., Ludwig, J., Kato, H., Akira, S., Weissman, D., 2008. Incorporation of pseudouridine into mRNA yields superior nonimmunogenic vector with increased translational capacity and biological stability. Mol. Ther. 16, 1833–1840.
Kariko, K., Ni, H., Capodici, J., Lamphier, M., Weissman, D., 2004. mRNA is an endogenous ligand for toll-like receptor 3. J. Biol. Chem. 279, 12542–12550.
Khorsand, B., Elangovan, S., Hong, L., Dewerth, A., Kormann, M.S., Salem, A.K., 2017a. A comparative study of the bone regenerative effect of chemically modified RNA encoding BMP-2 or BMP-9. The AAPS journal 19, 438–446.
Khorsand, B., Nicholson, N., Do, A.V., Femino, J.E., Martin, J.A., Petersen, E., Guetschow, B., Fredericks, D.C., Salem, A.K., 2017b. Regeneration of bone using nanoplex delivery of FGF-2 and BMP-2 genes in diaphyseal long bone radial defects in a diabetic rabbit model. J. Controlled Release 248, 53–59.
Kim, I., McKenna, S.A., Viani Puglisi, E., Puglisi, J.D., 2007. Rapid purification of RNAs using fast performance liquid chromatography (FPLC). RNA 13, 289–294.
Koide, M., Kinugawa, S., Takahashi, N., Udagawa, N., 2010. Osteoclastic bone resorption induced by innate immune responses. Periodontology 2000 (54), 235–246.
Konarska, M.M., Padgett, R.A., Sharp, P.A., 1984. Recognition of cap structure in splicing in vitro of mRNA precursors. Cell 38, 731–736.
Kormann, M.S.D., Hasenpusch, G., Aneja, M.K., Nica, G., Flemmer, A.W., Herber-Jonat, S., Huppmann, M., Mays, L.E., Illenyi, M., Schams, A., Griese, M., Bittmann, I., Handgretinger, R., Hartl, D., Rosenecker, J., Rudolph, C., 2011. Expression of therapeutic proteins after delivery of chemically modified mRNA in mice. Nat. Biotechnol. 29, 154.
Kozak, M., 1987. An analysis of 5'-noncoding sequences from 699 vertebrate messenger RNAs. Nucleic Acids Res. 15, 8125–8148.
Kozak, M., 2005. Regulation of translation via mRNA structure in prokaryotes and eukaryotes. Gene 361, 13–37.
Krishnan, V., Bryant, H.U., Macdougald, O.A., 2006. Regulation of bone mass by Wnt signaling. J. Clin. Investig. 116, 1202–1209.
Kwong, F.N., Richardson, S.M., Evans, C.H., 2008. Chordin knockdown enhances the osteogenic differentiation of human mesenchymal stem cells. Arthritis Res. Ther. 10, R65.
Lam, J.K.W., Chow, M.Y.T., Zhang, Y., Leung, S.W.S., 2015. siRNA Versus miRNA as therapeutics for gene silencing. Mol. Ther. Nucleic Acids 4, e252.
Langberg, S.R., Moss, B., 1981. Post-transcriptional modifications of mRNA. Purification and characterization of cap I and cap II RNA (nucleoside-2'-)-methyltransferases from HeLa cells. J. Biol. Chem. 256, 10054–10060.
Laursen, M.B., Pakula, M.M., Gao, S., Fluiter, K., Mook, O.R., Baas, F., Langklaer, N., Wengel, S.L., Wengel, J., Kjems, J., Bramsen, J.B., 2010. Utilization of unlocked nucleic acid (UNA) to enhance siRNA performance in vitro and in vivo. Mol. BioSyst. 6, 862–870.
Li, B., Luo, X., Dong, Y., 2016. Effects of chemically modified messenger RNA on protein expression. Bioconjug. Chem. 27, 849–853.
Liang, C., Guo, B., Wu, H., Shao, N., Li, D., Liu, J., Dang, L., Wang, C., Li, H., Li, S., Lau, W.K., Cao, Y., Yang, Z., Lu, C., He, X., Au, D.W., Pan, X., Zhang, B.T., Lu, C., Zhang, H., Yue, K., Qian, A., Shang, P., Xu, J., Xiao, L., Bian, Z., Tan, W., Liang, Z., He, F., Zhang, L., Lu, A., Zhang, G., 2015. Aptamer-functionalized lipid nanoparticles targeting osteoblasts as a novel RNA interference-based bone anabolic strategy. Nat. Med. 21, 288–294.
Liu, X., 2016. Bone site-specific delivery of siRNA. J. Biomed. Res. 30 (4), 264–271.
Lo, H.J., Huang, H.K., Donahue, T.F., 1998. RNA polymerase I-promoted HIS4 expression yields uncapped, polyadenylated mRNA that is unstable and inefficiently translated in Saccharomyces cerevisiae. Mol. Cell. Biol. 18, 665–675.
Longo, K.A., Kennell, J.A., Ochocinska, M.J., Ross, S.E., Wright, W.S., MacDougald, O.A., 2002. Wnt signaling protects 3T3-L1 preadipocytes from apoptosis through induction of insulin-like growth factors. J. Biol. Chem. 277, 38239–38244.
Lowe, C., Yoneda, T., Boyce, B.F., Chen, H., Mundy, G.R., Soriano, P., 1993. Osteopetrosis in Src-deficient mice is due to an autonomous defect of osteoclasts. PNAS 90, 4485–4489.
Ma, Z., Yang, C., Song, W., Wang, Q., Kjems, J., Gao, S., 2014. Chitosan hydrogel as siRNA vector for prolonged gene silencing. J Nanobiotechnology 12, 23.
Malone, R.W., Felgner, P.L., Verma, I.M., 1989. Cationic liposome-mediated RNA transfection. PNAS 86, 6077–6081.
Manaka, T., Suzuki, A., Takayama, K., Imai, Y., Nakamura, H., Takaoka, K., 2011a. Local delivery of siRNA using a biodegradable polymer application to enhance BMP-induced bone formation. Biomaterials 32, 9642–9648.
Mao, B., Wu, W., Davidson, G., Marhold, J., Li, M., Mechler, B.M., Delius, H., Hoppe, D., Stannek, P., Walter, C., Glinka, A., Niehrs, C., 2002. Kremen proteins are Dickkopf receptors that regulate Wnt/beta-catenin signalling. Nature 417, 664–667.
Matsuo, H., Li, H., McGuire, A.M., Fletcher, C.M., Gingras, A.C., Sonenberg, N., Wagner, G., 1997. Structure of translation factor eIF4E bound to m7GDP and interaction with 4E-binding protein. Nat. Struct. Biol. 4, 717–724.
Maxhimer, J.B., Bradley, J.P., Lee, J.C., 2015. Signaling pathways in osteogenesis and osteoclastogenesis: lessons from cranial sutures and applications to regenerative medicine. Genes Dis. 2, 57–68.
McClung, M.R., Grauer, A., Boonen, S., Bolognese, M.A., Brown, J.P., Diez-Perez, A., Langdahl, B.L., Reginster, J.Y., Zanchetta, J.R., Wasserman, S.M., Katz, L., Maddox, J., Yang, Y.C., Libanati, C., Bone, H.G., 2014. Romosozumab in postmenopausal women with low bone mineral density. N. Engl. J. Med. 370, 412–420.
McCormick, C., Khaperskyy, D.A., 2017. Translation inhibition and stress granules in the antiviral immune response. Nat. Rev. Immunol. 17, 647–660.
McKay, W.F., Peckham, S.M., Badura, J.M., 2007. A comprehensive clinical review of recombinant human bone morphogenetic protein-2 (INFUSE Bone Graft). Int. Orthop. 31, 729–734.
McKenna, S.A., Kim, I., Puglisi, E.V., Lindhout, D.A., Aitken, C.E., Marshall, R.A., Puglisi, J.D., 2007. Purification and characterization of transcribed RNAs using gel filtration chromatography. Nat. Protoc. 2, 3270–3277.
Mendecki, J., Lee, S.Y., Brawerman, G., 1972. Characteristics of the polyadenylic acid segment associated with messenger ribonucleic acid in mouse sarcoma 180 ascites cells. Biochemistry 11, 792–798.
Merino, R., Rodriguez-Leon, J., Macias, D., Ganan, Y., Economides, A.N., Hurle, J.M., 1999. The BMP antagonist Gremlin regulates outgrowth, chondrogenesis and programmed cell death in the developing limb. Development 126, 5515–5522.
Mignone, F., Gissi, C., Liuni, S., Pesole, G., 2002. Untranslated regions of mRNAs. Genome

Biol. 3 REVIEWS0004.
Miller, V.M., Xia, H., Marrs, G.L., Gouvion, C.M., Lee, G., Davidson, B.L., Paulson, H.L., 2003. Allele-specific silencing of dominant disease genes. PNAS 100, 7195–7200.
Milligan, J.F., Groebe, D.R., Witherell, G.W., Uhlenbeck, O.C., 1987. Oligoribonucleotide synthesis using T7 RNA polymerase and synthetic DNA templates. Nucleic Acids Res. 15, 8783–8798.
Mockey, M., Goncalves, C., Dupuy, F.P., Lemoine, F.M., Pichon, C., Midoux, P., 2006. mRNA transfection of dendritic cells: synergistic effect of ARCA mRNA capping with Poly(A) chains in cis and in trans for a high protein expression level. Biochem. Biophys. Res. Commun. 340, 1062–1068.
Mu, X., Greenwald, E., Ahmad, S., Hur, S., 2018. An origin of the immunogenicity of in vitro transcribed RNA. Nucleic Acids Res. 46, 5239–5249.
Mukherjee, D., Gao, M., O'Connor, J.P., Raijmakers, R., Pruijn, G., Lutz, C.S., Wilusz, J., 2002. The mammalian exosome mediates the efficient degradation of mRNAs that contain AU-rich elements. EMBO J. 21, 165–174.
Nacheva, G.A., Berzal-Herranz, A., 2003. Preventing nondesired RNA-primed RNA extension catalyzed by T7 RNA polymerase. Eur. J. Biochem. 270, 1458–1465.
Naito, Y., Ui-Tei, K., 2013. Designing functional siRNA with reduced off-target effects. Methods Mol. Biol. 942, 57–68.
Nakashima, T., Kobayashi, Y., Yamasaki, S., Kawakami, A., Eguchi, K., Sasaki, H., Sakai, H., 2000. Protein expression and functional difference of membrane-bound and soluble receptor activator of NF-kappaB ligand: modulation of the expression by osteotropic factors and cytokines. Biochem. Biophys. Res. Commun. 275, 768–775.
Negishi-Koga, T., Shinohara, M., Komatsu, N., Bito, H., Kodama, T., Friedel, R.H., Takayanagi, H., 2011. Suppression of bone formation by osteoclastic expression of semaphorin 4D. Nat. Med. 17, 1473–1480.
Nguyen, M.K., Jeon, O., Dang, P.N., Huynh, C.T., Varghai, D., Riazi, H., McMillan, A., Herberg, S., Alsberg, E., 2018. RNA interfering molecule delivery from in situ forming biodegradable hydrogels for enhancement of bone formation in rat calvarial bone defects. Acta Biomater. 75, 105–114.
NIH Consensus Development Panel on Osteoporosis Prevention, Diagnosis, and Therapy, 2001. Osteoporosis prevention, diagnosis, and therapy. JAMA 285, 785–795.
Orlandini von Niessen, A.G., Poleganov, M.A., Rechner, C., Plaschke, A., Kranz, L.M., Fesser, S., Diken, M., Lower, M., Vallazza, B., Beissert, T., Bukur, V., Kuhn, A.N., Tureci, O., Sahin, U., 2018. Improving mRNA-based therapeutic gene delivery by expression-augmenting 3' UTRs identified by cellular library screening. Mol. Ther.
Ozcan, G., Ozpolat, B., Coleman, R.L., Sood, A.K., Lopez-Berestein, G., 2015. Preclinical and clinical development of siRNA-based therapeutics. Adv. Drug Deliv. Rev. 87, 108–119.
Padhi, D., Jang, G., Stouch, B., Fang, L., Posvar, E., 2011. Single-dose, placebo-controlled, randomized study of AMG 785, a sclerostin monoclonal antibody. J. Bone Miner. Res. 26, 19–26.
Pardi, N., Hogan, M.J., Porter, F.W., Weissman, D., 2018. mRNA vaccines – A new era in vaccinology. Nat. Rev. Drug Discov. 17, 261–279.
Pascolo, S., 2008. Vaccination with messenger RNA (mRNA). Handb. Exp. Pharmacol. 221–235.
Pearce, J.J., Penny, G., Rossant, J., 1999. A mouse cerberus/Dan-related gene family. Dev. Biol. 209, 98–110.
Peng, J., Murray, E.L., Schoenberg, D.R., 2008. In vivo and in vitro analysis of poly(A) length effects on mRNA translation. Methods Mol. Biol. 419, 215–230.
Perrin, D.D., 1965. Binding of tetracyclines to bone. Nature 208, 787–788.
Phimphilai, M., Zhao, Z., Boules, H., Roca, H., Franceschi, R.T., 2006. BMP signaling is required for RUNX2-dependent induction of the osteoblast phenotype. J. Bone Miner. Res. 21, 637–646.
Phua, K.K.L., Liu, Y., Sim, S.H., 2017. Non-linear enhancement of mRNA delivery efficiencies by influenza A derived NS1 protein engendering host gene inhibition property. Biomaterials 133, 29–36.
Piccolo, S., Sasai, Y., Lu, B., De Robertis, E.M., 1996. Dorsoventral patterning in Xenopus: inhibition of ventral signals by direct binding of chordin to BMP-4. Cell 86, 589–598.
Rawadi, G., Vayssiere, B., Dunn, F., Baron, R., Roman-Roman, S., 2003. BMP-2 controls alkaline phosphatase expression and osteoblast mineralization by a Wnt autocrine loop. J. Bone Miner. Res. 18, 1842–1853.
Rios, C.N., Skoracki, R.J., Mathur, A.B., 2012a. GNAS1 and PHD2 short-interfering RNA support bone regeneration in vitro and in an in vivo sheep model. Clin. Orthop. Relat. Res. 470, 2541–2553.
Robert Rozbruch, S., Weitzman, A.M., Tracey Watson, J., Freudigman, P., Katz, H.V., Ilizarov, S., 2006. Simultaneous treatment of tibial bone and soft-tissue defects with the Ilizarov method. J. Orthop. Trauma 20, 197–205.
Rodan, G.A., Martin, T.J., 2000. Therapeutic approaches to bone diseases. Science 289, 1508–1514.
Roush, K., 2011. Prevention and treatment of osteoporosis in postmenopausal women: a review. Am. J. Nurs. 111, 26–35 quiz 36-27.
Rutkovskiy, A., Stenslokken, K.O., Vaage, I.J., 2016. Osteoblast differentiation at a glance. Med. Sci. Monit. Basic Res. 22, 95–106.
Sachs, A.B., Davis, R.W., Kornberg, R.D., 1987. A single domain of yeast poly(A)-binding protein is necessary and sufficient for RNA binding and cell viability. Mol. Cell. Biol. 7, 3268–3276.
Sahin, U., Kariko, K., Tureci, O., 2014. mRNA-based therapeutics-developing a new class of drugs. Nat. Rev. Drug Discov. 13, 759–780.
Schilcher, J., Michaelsson, K., Aspenberg, P., 2011. Bisphosphonate use and atypical fractures of the femoral shaft. N. Engl. J. Med. 364, 1728–1737.
Schlake, T., Thess, A., Thran, M., Jordan, I., 2018. mRNA as novel technology for passive immunotherapy. Cell. Mol. Life Sci.
Scott, I.C., Steiglitz, B.M., Clark, T.G., Pappano, W.N., Greenspan, D.S., 2000. Spatiotemporal expression patterns of mammalian chordin during postgastrulation embryogenesis and in postnatal brain. Dev. Dyn. 217, 449–456.
Sezlev Bilecen, D., Uludag, H., Hasirci, V., 2019. Development of PEI-RANK siRNA complex loaded PLGA nanocapsules for the treatment of osteoporosis. Tissue Eng. Part A 25, 34–43.
Shimer, A.L., Oner, F.C., Vaccaro, A.R., 2009. Spinal reconstruction and bone morphogenetic proteins: open questions. Injury 40 (Suppl 3), S32–38.
Shin, J., Cho, J.H., Jin, Y., Yang, K., Lee, J.S., Park, H.J., Han, H.S., Lee, J., Jeon, H., Shin, H., Cho, S.W., 2016a. Mussel adhesion-inspired reverse transfection platform enhances osteogenic differentiation and bone formation of human adipose-derived stem cells. Small 12, 6266–6278.
Smith, W.C., Harland, R.M., 1992. Expression cloning of noggin, a new dorsalizing factor localized to the Spemann organizer in Xenopus embryos. Cell 70, 829–840.
Sorensen, D.R., Leirdal, M., Sioud, M., 2003. Gene silencing by systemic delivery of synthetic siRNAs in adult mice. J. Mol. Biol. 327, 761–766.
Stepinski, J., Waddell, C., Stolarski, R., Darzynkiewicz, E., Rhoads, R.E., 2001. Synthesis and properties of mRNAs containing the novel "anti-reverse" cap analogs 7-methyl (3'-O-methyl)GpppG and 7-methyl (3'-deoxy)GpppG. RNA 7, 1486–1495.
Strenkowska, M., Kowalska, J., Lukaszewicz, M., Zuberek, J., Su, W., Rhoads, R.E., Darzynkiewicz, E., Jemielity, J., 2010. Towards mRNA with superior translational activity: synthesis and properties of ARCA tetraphosphates with single phosphorothioate modifications. New J. Chem. 34, 993–1007.
Suen, P.K., Qin, L., 2016. Sclerostin, an emerging therapeutic target for treating osteoporosis and osteoporotic fracture: a general review. J. Orthop. Translat. 4, 1–13.
Sun, Y., Ye, X., Cai, M., Liu, X., Xiao, J., Zhang, C., Wang, Y., Yang, L., Liu, J., Li, S., Kang, C., Zhang, B., Zhang, Q., Wang, Z., Hong, A., Wang, X., 2016. Osteoblast-targeting-peptide modified nanoparticle for siRNA/microRNA delivery. ACS Nano 10, 5759–5768.
Suzuki, K., Kumanogoh, A., Kikutani, H., 2008. Semaphorins and their receptors in immune cell interactions. Nat. Immunol. 9, 17–23.
Svedbom, A., Hernlund, E., Ivergard, M., Compston, J., Cooper, C., Stenmark, J., McCloskey, E.V., Jonsson, B., Kanis, J.A., EU Review Panel of IOF, 2013. Osteoporosis in the European Union: a compendium of country-specific reports. Arch Osteoporos 8, 137.
Svitkin, Y.V., Cheng, Y.M., Chakraborty, T., Presnyak, V., John, M., Sonenberg, N., 2017. N1-methyl-pseudouridine in mRNA enhances translation through eIF2alpha-dependent and independent mechanisms by increasing ribosome density. Nucleic Acids Res. 45, 6023–6036.
Takahashi, K., Tanabe, K., Ohnuki, M., Narita, M., Ichisaka, T., Tomoda, K., Yamanaka, S., 2007. Induction of pluripotent stem cells from adult human fibroblasts by defined factors. Cell 131, 861–872.
Takahashi, K., Yamanaka, S., 2006. Induction of pluripotent stem cells from mouse embryonic and adult fibroblast cultures by defined factors. Cell 126, 663–676.
Takayama, K., Suzuki, A., Manaka, T., Taguchi, S., Hashimoto, Y., Imai, Y., Wakitani, S., Takaoka, K., 2009a. RNA interference for noggin enhances the biological activity of bone morphogenetic proteins in vivo and in vitro. J. Bone Miner. Metab. 27, 402–411.
Tavernier, G., Andries, O., Demeester, J., Sanders, N.N., De Smedt, S.C., Rejman, J., 2011 Mar 30. mRNA as gene therapeutic: how to control protein expression. J Control Release. 150 (3), 238–247.
Teng, S., Liu, C., Krettek, C., Jagodzinski, M., 2014. The application of induced pluripotent stem cells for bone regeneration: current progress and prospects. Tissue Eng. B Rev. 20, 328–339.
Thess, A., Grund, S., Mui, B.L., Hope, M.J., Baumhof, P., Fotin-Mleczek, M., Schlake, T., 2015. Sequence-engineered mRNA without chemical nucleoside modifications enables an effective protein therapy in large animals. Mol. Ther. 23, 1456–1464.
Trepotec, Z., Aneja, M.K., Geiger, J., Hasenpusch, G., Plank, C., Rudolph, C., 2019. Maximizing the translational yield of mrna therapeutics by minimizing 5'-UTRs. Tissue Eng. A 25, 69–79.
Triana-Alonso, F.J., Dabrowski, M., Wadzack, J., Nierhaus, K.H., 1995. Self-coded 3'-extension of run-off transcripts produces aberrant products during in vitro transcription with T7 RNA polymerase. J. Biol. Chem. 270, 6298–6307.
Uchida, S., Kataoka, K., Itaka, K., 2015. Screening of mRNA chemical modification to maximize protein expression with reduced immunogenicity. Pharmaceutics 7, 137–151.
Urist, M.R., Strates, B.S., 2009. The classic: bone morphogenetic protein. Clin. Orthop. Relat. Res. 467, 3051–3062.
van der Velden, A.W., Thomas, A.A., 1999. The role of the 5' untranslated region of an mRNA in translation regulation during development. Int. J. Biochem. Cell Biol. 31, 87–106.
Veedu, R.N., Wengel, J., 2010. Locked nucleic acids: promising nucleic acid analogs for therapeutic applications. Chem. Biodivers. 7, 536–542.
Wada, T., Nakashima, T., Hiroshi, N., Penninger, J.M., 2006. RANKL-RANK signaling in osteoclastogenesis and bone disease. Trends Mol. Med. 12, 17–25.
Wan, D.C., Pomerantz, J.H., Brunet, L.J., Kim, J.B., Chou, Y.F., Wu, B.M., Harland, R., Blau, H.M., Longaker, M.T., 2007a. Noggin suppression enhances in vitro osteogenesis and accelerates in vivo bone formation. J. Biol. Chem. 282, 26450–26459.
Wang, C., Xiao, F., Gan, Y., Yuan, W., Zhai, Z., Jin, T., Chen, X., Zhang, X., 2018a. Improving bone regeneration using chordin siRNA delivered by pH-responsive and non-toxic polyspermine imidazole-4,5-imine. Cell. Physiol. Biochem. 46, 133–147.
Wang, C., Yuan, W., Xiao, F., Gan, Y., Zhao, X., Zhai, Z., Zhao, X., Zhao, C., Cui, P., Jin, T., Chen, X., Zhang, X., 2017a. Biscarbamate cross-linked low-molecular-weight polyethylenimine for delivering anti-chordin sirna into human mesenchymal stem cells for improving bone regeneration. Front. Pharmacol. 8.
Wang, H., Liu, J., Tao, S., Chai, G., Wang, J., Hu, F.Q., Yuan, H., 2015. Tetracycline-grafted PLGA nanoparticles as bone-targeting drug delivery system. Int. J. Nanomed. 10, 5671–5685.
Wang, Y., Grainger, D.W., 2010. siRNA knock-down of RANK signaling to control

osteoclast-mediated bone resorption. Pharm. Res. 27, 1273–1284.
Wang, Y., Tran, K.K., Shen, H., Grainger, D.W., 2012. Selective local delivery of RANK siRNA to bone phagocytes using bone augmentation biomaterials. Biomaterials 33, 8540–8547.
Warren, L., Manos, P.D., Ahfeldt, T., Loh, Y.H., Li, H., Lau, F., Ebina, W., Mandal, P.K., Smith, Z.D., Meissner, A., Daley, G.Q., Brack, A.S., Collins, J.J., Cowan, C., Schlaeger, T.M., Rossi, D.J., 2010. Highly efficient reprogramming to pluripotency and directed differentiation of human cells with synthetic modified mRNA. Cell Stem Cell 7, 618–630.
Wei, C.M., Gershowitz, A., Moss, B., 1975. Methylated nucleotides block 5' terminus of HeLa cell messenger RNA. Cell 4, 379–386.
Weissman, D., Pardi, N., Muramatsu, H., Kariko, K., 2013. HPLC purification of in vitro transcribed long RNA. Methods Mol. Biol. 969, 43–54.
Wesselhoeft, R.A., Kowalski, P.S., Anderson, D.G., 2018. Engineering circular RNA for potent and stable translation in eukaryotic cells. Nat. Commun. 9, 2629.
Wesselhoeft, R.A., Kowalski, P.S., Parker-Hale, F.C., Huang, Y., Bisaria, N., Anderson, D.G., 2019. RNA circularization diminishes immunogenicity and can extend translation duration in vivo. Mol. Cell.
Wolff, J.A., Malone, R.W., Williams, P., Chong, W., Acsadi, G., Jani, A., Felgner, P.L., 1990. Direct gene transfer into mouse muscle in vivo. Science 247, 1465–1468.
Wu, X.-B., Li, Y., Schneider, A., Yu, W., Rajendren, G., Iqbal, J., Yamamoto, M., Alam, M., Brunet, L.J., Blair, H.C., Zaidi, M., Abe, E., 2003. Impaired osteoblastic differentiation, reduced bone formation, and severe osteoporosis in noggin-overexpressing mice. J. Clin. Investig. 112, 924–934.
Xiao, G., Gopalakrishnan, R., Jiang, D., Reith, E., Benson, M.D., Franceschi, R.T., 2002. Bone morphogenetic proteins, extracellular matrix, and mitogen-activated protein kinase signaling pathways are required for osteoblast-specific gene expression and differentiation in MC3T3-E1 cells. J. Bone Miner. Res. 17, 101–110.
Yang, E., van Nimwegen, E., Zavolan, M., Rajewsky, N., Schroeder, M., Magnasco, M., Darnell Jr., J.E., 2003. Decay rates of human mRNAs: correlation with functional characteristics and sequence attributes. Genome Res. 13, 1863–1872.
Yoshioka, N., Gros, E., Li, H.R., Kumar, S., Deacon, D.C., Maron, C., Muotri, A.R., Chi, N.C., Fu, X.D., Yu, B.D., Dowdy, S.F., 2013. Efficient generation of human iPSCs by a synthetic self-replicative RNA. Cell Stem Cell 13, 246–254.
You, Z., Saims, D., Chen, S., Zhang, Z., Guttridge, D.C., Guan, K.L., MacDougald, O.A., Brown, A.M., Evan, G., Kitajewski, J., Wang, C.Y., 2002. Wnt signaling promotes oncogenic transformation by inhibiting c-Myc-induced apoptosis. J. Cell Biol. 157, 429–440.
Yu, Y., Jin, G., Xue, Y., Wang, D., Liu, X., Sun, J., 2017. Multifunctions of dual Zn/Mg ion co-implanted titanium on osteogenesis, angiogenesis and bacteria inhibition for dental implants. Acta Biomater. 49, 590–603.
Zangi, L., Lui, K.O., von Gise, A., Ma, Q., Ebina, W., Ptaszek, L.M., Später, D., Xu, H., Tabebordbar, M., Gorbatov, R., Sena, B., Nahrendorf, M., Briscoe, D.M., Li, R.A., Wagers, A.J., Rossi, D.J., Pu, W.T., Chien, K.R., 2013. Modified mRNA directs the fate of heart progenitor cells and induces vascular regeneration after myocardial infarction. Nat. Biotechnol. 31, 898–907.
Zhang, G., Guo, B., Wu, H., Tang, T., Zhang, B.T., Zheng, L., He, Y., Yang, Z., Pan, X., Chow, H., To, K., Li, Y., Li, D., Wang, X., Wang, Y., Lee, K., Hou, Z., Dong, N., Li, G., Leung, K., Hung, L., He, F., Zhang, L., Qin, L., 2012. A delivery system targeting bone formation surfaces to facilitate RNAi-based anabolic therapy. Nat. Med. 18, 307–314.
Zhang, L., Yang, G., Johnson, B.N., Jia, X., 2019. Three-dimensional (3D) printed scaffold and material selection for bone repair. Acta Biomater. 84, 16–33.
Zhang, W., De La Vega, R.E., Coenen, M.J., Muller, S.A., Peniche Silva, C.J., Aneja, M.K., Plank, C., van Griensven, M., Evans, C.H., Balmayor, E.R., 2018. An improved, chemically modified RNA encoding BMP-2 enhances osteogenesis in vitro and in vivo. Tissue Eng. A.
Zhang, Y., Wei, L., Miron, R.J., Shi, B., Bian, Z., 2015a. Anabolic bone formation via a site-specific bone-targeting delivery system by interfering with semaphorin 4D expression. J. Bone Miner. Res. 30, 286–296.
Zhang, Y., Wei, L., Miron, R.J., Shi, B., Bian, Z., 2016. Bone scaffolds loaded with siRNA-Semaphorin4d for the treatment of osteoporosis related bone defects. Sci. Rep. 6, 26925.
Zhang, Y., Wei, L., Miron, R.J., Zhang, Q., Bian, Z., 2014. Prevention of alveolar bone loss in an osteoporotic animal model via interference of semaphorin 4d. J. Dent. Res. 93, 1095–1100.
Zhang, Z., Zhang, Y., Gao, F., Han, S., Cheah, K.S., Tse, H.F., Lian, Q., 2017. CRISPR/Cas9 genome-editing system in human stem cells: current status and future prospects. Mol. Ther. Nucleic Acids 9, 230–241.
Zheng, L.Z., Wang, X.L., Cao, H.J., Chen, S.H., Huang, L., Qin, L., 2016. Src siRNA prevents corticosteroid-associated osteoporosis in a rabbit model. Bone 83, 190–196.
Zheng, X., Bevilacqua, P.C., 2004. Activation of the protein kinase PKR by short double-stranded RNAs with single-stranded tails. RNA 10, 1934–1945.
Zhuang, Z., Yoshizawa-Smith, S., Glowacki, A., Maltos, K., Pacheco, C., Shehabeldin, M., Mulkeen, M., Myers, N., Chong, R., Verdelis, K., Garlet, G.P., Little, S., Sfeir, C., 2018. Induction of M2 macrophages prevents bone loss in murine periodontitis models. J. Dent Res 22034518805984.
Zimmerman, L.B., De Jesus-Escobar, J.M., Harland, R.M., 1996. The Spemann organizer signal noggin binds and inactivates bone morphogenetic protein 4. Cell 86, 599–606.
Zohra, F.T., Chowdhury, E.H., Tada, S., Hoshiba, T., Akaike, T., 2007. Effective delivery with enhanced translational activity synergistically accelerates mRNA-based transfection. Biochem. Biophys. Res. Commun. 358, 373–378.
de Fougerolles, A., Vornlocher, H.P., Maraganore, J., Lieberman, J., 2007b. Interfering with disease: a progress report on siRNA-based therapeutics. Nat. Rev. Drug Discov. 6 (6), 443–453.
Huang, J., Lin, C., Fang, J., Li, X., Wang, J., Deng, S., Zhang, S., Su, W., Feng, X., Chen, B., Cheng, D., Shuai, X., 2018b. pH-Sensitive nanocarrier-mediated codelivery of simvastatin and noggin siRNA for synergistic enhancement of osteogenesis. ACS Appl. Mater. Interfaces 10 (34), 28471–28482.
Manaka, T., Suzuki, A., Takayama, K., Imai, Y., Nakamura, H., Takaoka, K., 2011b. Local delivery of siRNA using a biodegradable polymer application to enhance BMP-induced bone formation. Biomaterials 32 (36), 9642–9648.
Rios, C.N., Skoracki, R.J., Mathur, A.B., 2012b. GNAS1 and PHD2 short-interfering RNA support bone regeneration in vitro and in an in vivo sheep model. Clin. Orthop. Relat. Res. 470 (9), 2541–2553.
Shin, J., Cho, J.H., Jin, Y., Yang, K., Lee, J.S., Park, H.J., Han, H.S., Lee, J., Jeon, H., Shin, H., Cho, S.W., 2016b. Mussel adhesion-inspired reverse transfection platform enhances osteogenic differentiation and bone formation of human adipose-derived stem cells. Small 12 (45), 6266–6278.
Takayama, K., Suzuki, A., Manaka, T., Taguchi, S., Hashimoto, Y., Imai, Y., Wakitani, S., Takaoka, K., 2009b. RNA interference for noggin enhances the biological activity of bone morphogenetic proteins in vivo and in vitro. J. Bone Miner. Metab. 27 (4), 402–411.
Wan, D.C., Pomerantz, J.H., Brunet, L.J., Kim, J.B., Chou, Y.F., Wu, B.M., Harland, R., Blau, H.M., Longaker, M.T., 2007b. Noggin suppression enhances in vitro osteogenesis and accelerates in vivo bone formation. J. Biol. Chem. 282 (36), 26450–26459.
Wang, C., Xiao, F., Gan, Y., Yuan, W., Zhai, Z., Jin, T., Chen, X., Zhang, X., 2018b. Improving bone regeneration using chordin siRNA delivered by pH-responsive and non-toxic polyspermine imidazole-4,5-imine. Cell. Physiol. Biochem. 46 (1), 133–147.
Wang, C., Yuan, W., Xiao, F., Gan, Y., Zhao, X., Zhai, Z., Zhao, X., Zhao, C., Cui, P., Jin, T., Chen, X., Zhang, X., 2017b. Biscarbamate cross-linked low-molecular-weight polyethylenimine for delivering anti-chordin sirna into human mesenchymal stem cells for improving bone regeneration. Front. Pharmacol. 8.
Zhang, Y., Wei, L., Miron, R.J., Shi, B., Bian, Z., 2015b. Anabolic bone formation via a site-specific bone-targeting delivery system by interfering with semaphorin 4D expression. J. Bone Miner. Res. 30 (2), 286–296.

Pinpin WANG

Evaluation de l'activité de NS1, une protéine non structurale dérivée du virus de l'influenza A pour une traduction améliorée de l'ARNm de BMP2 pour la régénération osseuse

L'utilisation de l'ARN messager (ARNm) codant une protéine de morphogenèse osseuse pour la régénération osseuse est une alternative prometteuse à l'ADN, aux protéines recombinantes et aux peptides. Cependant, l'ARNm synthétique transcrit *in vitro* (IVT mRNA) déclenche une réponse immunitaire en activant des senseurs qui entraînent sa dégradation et inhibe sa traduction. Par mimétisme avec les virus ARN qui inhibent les senseurs ARN, nous avons exploité NS1, une protéine non structurelle du virus de la grippe (A/Texas/36/1991) pour amplifier l'expression des IVT mRNA. La co-délivrance de l'ARNm de NS1 a entraîné une inhibition dose-dépendante des senseurs ARN qui est corrélée avec une traduction accrue 'un ARNm rapporteur dans plusieurs types cellulaires. La co-délivrance des ARNm de NS1 et de BMP-2, une protéine de morphogenèse osseuse dans les cellules souches pluripotentes murines (C3H10T1/2) a favorisé la différenciation ostéogénique, démontrée par une plus forte expression de marqueurs ostéoblastiques et une minéralisation plus dense. Dans une perspective clinique, nous avons utilisé des cellules souches mésenchymateuses dérivées de la moelle osseuse humaine (hMSC) pour l'ostéoinduction *in vitro*. La co-délivrance des ARNm de NS1 et de BMP2 a permis une meilleure différenciation ostéogénique de ces cellules, et une calcification extracellulaire plus dense comparé à l'ARNm BMP2 seul. Ensuite, nous avons fabriqué des matrices de collagène renforcées par de l'hydroxyapatite chargé avec les ARNm de NS1 et de BMP2 formulés en complexes ternaires liposome/polymère/ARNm (lipopolyplexes: LPR). Ces matrices activées en ARNm appelés RAM (RNA Activated Matrices) ont été évaluées pour leur capacité ostéoinductive vis-à-vis des hMSCs. L'imagerie par microscopie électronique et les tests mécaniques ont montré que, si l'incorporation des LPR n'influence pas la microstructure des matrices, elle augmente leur résistance à la compression. Nos résultats démontrent que la libération des ARNm des matrices se prolonge jusqu'à 16 jours ce qui a permis de doubler la période d'expression de BMP2 par rapport à la transfection directe des hMSCs. Enfin, les RAM ont été implantées à des souris et les analyses par radiographie et histologie, de leur effet osteoinductif *in vivo* sont en cours d'évaluation. L'ensemble de nos résultats montrent que la co-délivrance des ARNm de NS1 et de BMP-2 est une stratégie prometteuse et que la matrice RAM pourrait être un produit standard pour la chirurgie orthopédique.

Mots clés : délivrance d'ARNm, lipopolyplexe, senseurs ARN, protéines de morphogenèse osseuse, ostéogenèse, osteoinduction, matrice de collagène, hydroxyapatite

Evaluation of Influenza A derived nonstructural protein NS1 to enhance BMP2 mRNA translation for bone regeneration

Application of messenger RNA (mRNA) coding for an osteogenic factor for bone regeneration is a promising alternative to DNA, recombinant proteins and peptides. However, synthetic *in vitro* transcribed mRNA (IVT mRNA) triggers innate immune response resulting in mRNA degradation and translation inhibition. Inspired by the ability of viral immune evasion proteins to inhibit host cell responses against viral RNA, we applied the non-structural protein-1 (NS1) from Influenza A virus (A/Texas/36/1991) as an IVT mRNA enhancer. Dose-dependent blocking of RNA sensors by NS1 was correlated with an increase of reporter mRNA translation in several cell types. Dual delivery of BMP-2 mRNA coding for an osteogenic factor and NS1 mRNA in murine pluripotent stem cells (C3H10T1/2), promoted their osteogenic differentiation as evidenced by enhanced expression of osteoblastic markers (e.g. alkaline phosphatase, type I collagen, osteopontin, and osteocalcin), and extracellular mineralization. To be more clinically relevant, we then applied the dual mRNAs system to human bone marrow-derived mesenchymal stem cells (hMSCs) for *in vitro* osteoinduction. The dual mRNAs, improved osteoblastic genes expression and extracellular calcification over BMP2 mRNA alone. Then, the dual mRNAs were formulated as liposome/polymer/mRNA ternary complexes (lipopolyplexes: LPRs) and incorporated into the hydroxyapatite reinforced collagen scaffold to prepare RAMs (RNA Activated Matrices). Scanning electron microscopy imaging and mechanical tests demonstrated that while the mRNAs loading did not influence the scaffold's microstructure, the compressive strength was increased. The *in vitro* release of mRNAs from RAMs lasted for 16 days resulting to a doubling of the protein expression period compared to the direct transfection of cells. Finally, RAMs were subcutaneously implanted onto mice back for *in vivo* osteoinduction. The evaluation of *in vivo* bone formation by radiography and histology analyses is in progress. Overall, our results demonstrate that the co-delivery of NS1 and BMP-2 mRNAs is a promising strategy and RAM could be an off-the-shelf product for clinical orthopedic practice.

Keywords: mRNA delivery, RNA sensors, bone morphogenetic proteins, osteogenesis, lipopolyplex, collagen scaffold, hydroxyapatite

Centre de Biophysique Moléculaire (CBM, UPR 4301)
Rue Charles Sadron, 45071 Orléans